

Award Number: DAMD17-02-C-0073

TITLE: Overuse Injury Assessment Model

PRINCIPAL INVESTIGATOR: James H. Stuhmiller, Ph.D.
Weixin Shen, Ph.D.

CONTRACTING ORGANIZATION: L-3 Communications/Jaycor
San Diego, California 92121-1002

REPORT DATE: August 2007

TYPE OF REPORT: Final

PREPARED FOR: U.S. Army Medical Research and Materiel Command
Fort Detrick, Maryland 21702-5012

DISTRIBUTION STATEMENT: Approved for Public Release;
Distribution Unlimited

The views, opinions and/or findings contained in this report are those of the author(s) and should not be construed as an official Department of the Army position, policy or decision unless so designated by other documentation.

REPORT DOCUMENTATION PAGE				Form Approved OMB No. 0704-0188	
Public reporting burden for this collection of information is estimated to average 1 hour per response, including the time for reviewing instructions, searching existing data sources, gathering and maintaining the data needed, and completing and reviewing this collection of information. Send comments regarding this burden estimate or any other aspect of this collection of information, including suggestions for reducing this burden to Department of Defense, Washington Headquarters Services, Directorate for Information Operations and Reports (0704-0188), 1215 Jefferson Davis Highway, Suite 1204, Arlington, VA 22202-4302. Respondents should be aware that notwithstanding any other provision of law, no person shall be subject to any penalty for failing to comply with a collection of information if it does not display a currently valid OMB control number. PLEASE DO NOT RETURN YOUR FORM TO THE ABOVE ADDRESS.					
1. REPORT DATE (DD-MM-YYYY) 01-08-2007		2. REPORT TYPE Final		3. DATES COVERED (From - To) 22 FEB 2002 - 21 JUL 2007	
4. TITLE AND SUBTITLE Overuse Injury Assessment Model				5a. CONTRACT NUMBER	
				5b. GRANT NUMBER DAMD17-02-C-0073	
				5c. PROGRAM ELEMENT NUMBER	
6. AUTHOR(S) James H. Stuhmiller, Ph.D., Weixin Shen, Ph.D. E-Mail: James.Stuhmiller@L-3com.com				5d. PROJECT NUMBER	
				5e. TASK NUMBER	
				5f. WORK UNIT NUMBER	
7. PERFORMING ORGANIZATION NAME(S) AND ADDRESS(ES) L-3 Communications/Jaycor San Diego, California 92121-1002				8. PERFORMING ORGANIZATION REPORT NUMBER	
9. SPONSORING / MONITORING AGENCY NAME(S) AND ADDRESS(ES) U.S. Army Medical Research and Materiel Command Fort Detrick, Maryland 21702-5012				10. SPONSOR/MONITOR'S ACRONYM(S)	
				11. SPONSOR/MONITOR'S REPORT NUMBER(S)	
12. DISTRIBUTION / AVAILABILITY STATEMENT Approved for Public Release; Distribution Unlimited					
13. SUPPLEMENTARY NOTES					
14. ABSTRACT The research conducted under this contract has provided critical model, data, hardware, and software products to assist the MOMRP effort to provide research solutions to reduce injuries and improve performance outcomes during military training. This report summarizes those products in the following areas: Training, Overuse Injury, and Performance (TOP) modeling, Bone stress fracture research, Biomechanical modeling, and Mobile biomechanical measurements.					
15. SUBJECT TERMS Physical training, overuse injury, stress fracture, biomechanical, ambulatory measurements					
16. SECURITY CLASSIFICATION OF:			17. LIMITATION OF ABSTRACT	18. NUMBER OF PAGES	19a. NAME OF RESPONSIBLE PERSON
a. REPORT	b. ABSTRACT	c. THIS PAGE			19b. TELEPHONE NUMBER (include area code)
U	U	U	UU	276	USAMRMC
					Standard Form 298 (Rev. 8-98) Prescribed by ANSI Std. Z39.18

Contents

Page

1.	INTRODUCTION	1
2.	TRAINING, OVERUSE INJURY, AND PERFORMANCE MODELING	5
3.	BONE STRESS FRACTURE RESEARCH.....	9
4.	BIOMECHANICAL MODELING	11
5.	AMBULATORY BIOMECHANICAL MEASUREMENT	15

1. Introduction

Improving physical training to reduce the attrition rate of military recruits is a high priority goal of the U.S. military. At present almost 1 in 5 military recruits are lost to musculoskeletal injuries or poor performance during physical training. There is also concern that the increased reliance on reservists, which requires rapid train-up of these individuals, may result in even larger numbers of injuries. These problems are having serious deleterious effects on the number of deployable soldiers, in addition to the issue of medical costs. The high attrition rate is also anticipated to increase in future years due to the poor fitness levels and higher body mass index (BMI) values of today's youth. This research effort, sponsored by the Military Operational Medicine Research Program (MOMRP) of the US Army Medical Research and Materiel Command (USAMRMC), provided critical model, data, hardware, and software products to assist the MOMRP effort to provide research solutions to reduce injuries and improve performance outcomes during military training. It focused on the following topics that directly related to improving military physical training.

Training, Overuse Injury, and Performance (TOP) modeling. Mathematical models to predict overuse injuries and performance enhancement during Basic Combat Training (BCT) were developed. Through the collaboration with the U.S. Army Research Institute of Environmental Medicine (USARIEM) and other military research groups and organizations, a number of field study data were obtained from different military training programs that involved hundreds to thousands of subjects and reported details including training regimen, subject information, occurrence of injuries, and performance PT scores. Traditional statistical analysis of the data was first used to identify main risk factors to the negative training outcomes. Biomechanical and physiological considerations were then introduced in mathematical models using a dose-response concept that quantify each training activity into biomechanical and physiological doses corresponding to different performance and injury modalities in consideration. This approach allows combining different exercises during a training program for an objective comparison of different training regimens. It also makes it possible to study the effects of changing the activities and to understand the progression of performance and injuries during training.

Bone stress fracture research. Bone stress fracture is one of the most studied overuse injuries due to its high occurrence rate and the high cost in both lost days and medical expenses. However, the prediction of stress fracture during training remains elusive primarily due to the lack of data and the lack of understanding of the underlying physical or biological processes. We first focused on reviewing the existing research related to the

mechanisms of injury, and methodologies such as predictive models, risk factors, and the diagnostic techniques. It was recognized that (1) while fundamental understanding of bone adaptation and failure from the cellular level regulation of bone remodeling due to damage accumulation to its macroscopic quantification was still preliminary and controversial, it was generally accepted that bone strain is a fundamental variable at macroscopic level to both the damage accumulation and the regulation of the bone adaptation; and (2) few existing risk factors were significant predictors to stress fractures and accurate prediction of stress fractures requires accounting for individual bone geometry and material property and the exercise history. Efforts were then made to address both these issues:

1. Through collaboration with ARIEM, we obtained pQCT images of tibia from subjects going through training programs. Imaging analysis algorithms were developed to identify and segment endosteal and periosteal boundaries of the tibial cortex. Analyses were conducted to look for geometry and density changes during training and better individualized image based predictors to stress fractures or bone adaptation.
2. Finite element models of tibia were developed using individual geometry and bone density distributions reconstructed from pQCT images. By applying joint and muscle loads that are obtained from measurements or biomechanical model calculations, bone stresses and strains during various exercises can be obtained. The calculated bone stresses were then related to damage accumulation and bone adaptation to predict the likelihood of stress fracture injury if the subject goes through a specific training program.

Biomechanical modeling. The prediction of both performance and injury outcomes requires knowing the loads during exercises that come from solving a variety of biomechanical analysis problems using laboratory or field measurements of kinematics and kinetics as inputs. On the other hand, human biomechanical systems are highly complex nonlinear systems with a large number of interconnected and interacting elements leading to significant challenges to model development and integration. To address the issue, a versatile biomechanical modeling toolbox, NMS-dynamics, was developed to provide a suite of modeling components that can be assembled rapidly to address a majority of biomechanical problems. The toolbox was built upon Matlab and the SimMechanics software environment. It provides key segment, joint, and muscle elements and supports kinematical, inverse dynamic, and forward dynamic analysis. A number of assembled application models, such as a lower extremity inverse analysis model customized for USARIEM biomechanical laboratory and a head-neck forward analysis model were also developed.

Mobile biomechanical measurements. The predictive accuracy of training outcomes of the current generation of models is significantly limited by the lack of accuracy

in field data, especially the accurate logging of training amount and intensity. This issue needs to be addressed by providing ambulatory, unobtrusive instruments that are capable of acquiring biomechanical measurements at a resolution sufficient enough for distinguishing different exercise modalities and changes in locomotion patterns due to individual variations or changes in individual physical status. In this research, we developed a prototype instrument, M-TES DataLogger system, that integrated accelerometers and force sensors onto a commercial off-the-shelf (COTS) wireless sensor network (WSN) platform and implemented onboard data compression and fusion codes to record biomechanical data on a wearable data logger. Analysis algorithms were implemented in companion software M-TES Analyzer that estimates from measurements of the biomechanical parameters for walking, running, and jumping activities.

The chapters in this Part One final report summarize the methods and products developed, including publications, models, data, hardware, and software products, for each of these research areas. Technical details are given in Part Two through Part Five of the final reports.

2. Training, Overuse Injury, and Performance Modeling

TRAINING, OVERUSE INJURY, AND PERFORMANCE MODELING

Product

TOP Software version 1.1:
<http://216.55.166.75/Top1.1>

Publications

- B. L. Sih, Weixin Shen, and James H. Stuhmiller. "Overuse Injury Assessment Model," Jaycor Annual Report J3181-03-192, San Diego, CA. Apr. 2003.
- M. W. Woodmansee, B. L. Sih, Weixin Shen, and E. Niu. "Bone Overuse Injury Assessment Model," Jaycor Annual Report J3181-04-217, San Diego, CA. Feb. 2004.
- B. L. Sih and Weixin Shen. "Overuse Injury Assessment Model, Part I: Training, Overuse Injury, and Performance Modeling," L-3 Communications/Jaycor Annual Report J3181-06-296, San Diego, CA. Apr. 2006.
- Sih, Bryant L. and Shen, Weixin. "Overuse Injury Assessment Model: Training, Overuse Injury, and Performance Modeling," L-3 Communications/Jaycor Final Report No. J3181-07-336, San Diego, CA. Aug. 2007.
- Sih, Bryant L. "Overuse Injury Assessment Model—A biomechanical approach to the stress fracture problem," presented at Supplemental Military Conference, 2003 Annual Meeting of the American Society of Sports Medicine, San Francisco, CA. May 28, 2003.
- Sih, Bryant L. and Shen, Weixin. "Computational Modeling for Predicting Injuries and Physical Performance in Army Basic Combat Training—Model Development," presented at TOP Meeting, Natick, MA. Nov 16, 2006.

Background

The purpose of basic combat training (BCT) is to prepare recruits for the rigors of military life, including acquiring a high fitness level. Improving fitness is accomplished by overloading or stressing the body through exercise. However, training-related injuries affect about 25% of male recruits and about 50% of female recruits, a significant portion of which are severe enough to force recruits to withdraw from BCT. Additional attrition occurs when recruits fail to reach the desired fitness level (as measured by performance tests such as the military Physical Fitness Test or PFT). Overall, about 1 in 5 recruits fail to complete BCT. Thus, there is a need for guidance on minimizing injuries and maximizing performance in order to minimize personnel losses during BCT.

Method

The Training, Overuse Injury, and Performance (TOP) Model is a software framework for assessing the effects of physical training on performance and injury. This is accomplished by integrating biomechanical and physiological based injury and performance models to predict the training outcomes. The software interface is designed to allow users with different functional objectives to manage the program and acquire the results they desire in an efficient and user-friendly manner, from an easily accessible web-based program.

The TOP model uses a dose-response concept to quantify each training activity into biomechanical

cal and physiological loading doses. By summing the total number of doses an individual receives during training, a prediction about their performance and risk of injury can be calculated.

This modeling approach has many advantages over other approaches:

- Provides a better understanding of the influences that different training regimens have on performance and injury outcomes
- Gives insight into the progression of performance improvements and injury risk during training
- Incorporates statistical findings into a mechanistic modeling framework
- Allows easier incorporation of nonlinear relationships
- Dose-response approach allows different training regimens to be combined and compared
- Mechanistic model can be applied to more different situations compared to a statistical model developed by fitting inputs to outputs.

To provide the widest range of users to access the software, four different user types have been identified. Depending on the type of user, different levels of software functionality are available. The current version of TOP incorporates two of the four types of users:

Basic User: Interested in comparing their individual performance progress and injury likelihood during BCT to their peers. The output displays their individual scores and the average scores of their peers. Likely basics users are individual soldiers.

Mid-Level User: Focused with the performance and injury outcomes of a small group of individuals (2-30) involved in a training regimen. The output identifies individuals at high risk for performance failure or injury. Likely mid-level users are Drill Sergeants and fitness advisors.

Instructions
Each of the 4 buttons below leads to a window most of which require additional information. All buttons must be marked **Completed** before a training analysis can be performed.
The analysis will predict your final physical fitness test (PFT) score and the likelihood of injury.



The data input start page for a Basic User is designed for simplicity and consists of only 4 buttons.

The Mid-Level User interface is more complex but flexible, allowing users to change parameters such as the regimen workload. .



The TOP software prediction results for a Basic User, who is interested in their likelihood of failing basic combat training due to low fitness or injury.

Overuse Injury

Overuse Injury-Lower Body

10 ± 1% Chance of Injury (ave ± sd)


Plain

High Risk

Medium Risk

Low Risk

Info N/A



An overuse injury is an injury caused by repetitive motion. Common examples are tendonitis/bursitis/fasciitis, pain, and non-acute strains/sprains. A stress fracture is also an overuse injury but is considered separately. A lower body injury is considered from the waist down. The color and percentages given above is the predicted outcome for the group as a whole. Individual predictions can be found by clicking on the above tabs.

Good	5 out of 10 (50%)
Borderline	5 out of 10 (50%)
Poor	0 out of 10 (0%)
NA	0 out of 10 (0%)

Overuse Injury-Leg Stress Fracture

11 ± 1% Chance of Injury (ave ± sd)


Plain

High Risk

Medium Risk

Low Risk

Info N/A



A stress fracture is an overuse injury of the bone, caused by training harder than the bone is capable of handling. The most common stress fracture bone is the tibia or shin bone. The color and percentages given above is the predicted outcome for the group as a whole. Individual predictions can be found by clicking on the above tabs.

Good	2 out of 10 (20%)
Borderline	8 out of 10 (80%)
Poor	0 out of 10 (0%)
NA	0 out of 10 (0%)

The different results display for the Mid-Level user, which allows the easy identification of personnel who are at risk of injury. Performance predictions are presented in similar interface (not shown).

3. Bone Stress Fracture Research

BONE STRESS FRACTURE RESEARCH

Product

- Matlab algorithms for regional analysis of pQCT images
- Bone stress fracture prediction models : <http://216.55.166.75/stressfracture/>
- Patient-specific Finite Element Models of 17 tibias from the University of Connecticut study

Publications

Negus, Charles and Shen, Weixin. "Overuse Injury Assessment Model, Part III: Preliminary pQCT Analysis of Tibia Changes due to Physical Exercises," L-3 Communications/Jaycor Annual Report J3181-06-298, San Diego, CA. Apr. 2006

Evans, R.K., Negus, C.H., et al. "Regional bone changes in the tibia resulting from short term exercise regimens," For submission to the *J. Bone and Mineral Research*, 2007.

Evans, R.K., Negus, C.H., et al. "Regional changes in bone mineral density of the tibia following a 13-week aerobic training program" Presented at the 54th Annual Meeting of the ACSM, New Orleans, LA, May 29-June 6, 2007.

Negus, C.H., Evans, R.K., et al. "Using pQCT to assess regional bone changes resulting from short-term exercise interventions." To be presented at the 29th Annual Meeting of the ASBMR, Honolulu, Hawaii, 16-19 Sept 2007.

Background

Bone is a living tissue whose function and adaptation are mechanically mediated, and bone related diseases often have a mechanical pathogenesis. Effective diagnosis, intervention, and treatment of maladies such as stress fracture could greatly benefit from an understanding of the mechanical environment that results *in vivo* during normal and atypical physical activity. The mechanical stimulus is, however, both highly patient and location specific. The goal of the bone-related portion of the Overuse Injury Modeling project was to develop various computational methods, using principles from engineering, to perform patient-specific analysis of noninvasive, pQCT images and to then begin to assess the stress distribution in the tibia on a patient specific basis.

Methods

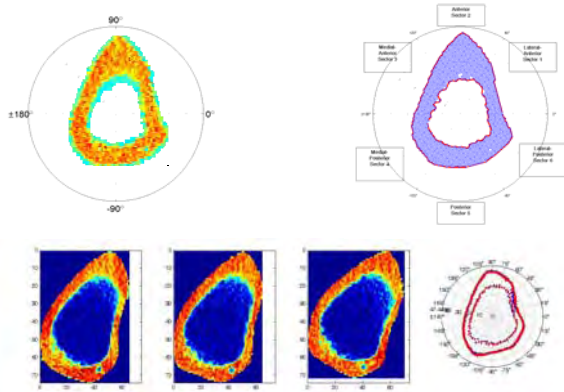
Analyze pQCT images received from USARIEM using novel Matlab software written for this study.

- Look at subtle regional changes which can not be detected using the vendors existing analysis software.
- Report results in peer reviewed journals and conferences.

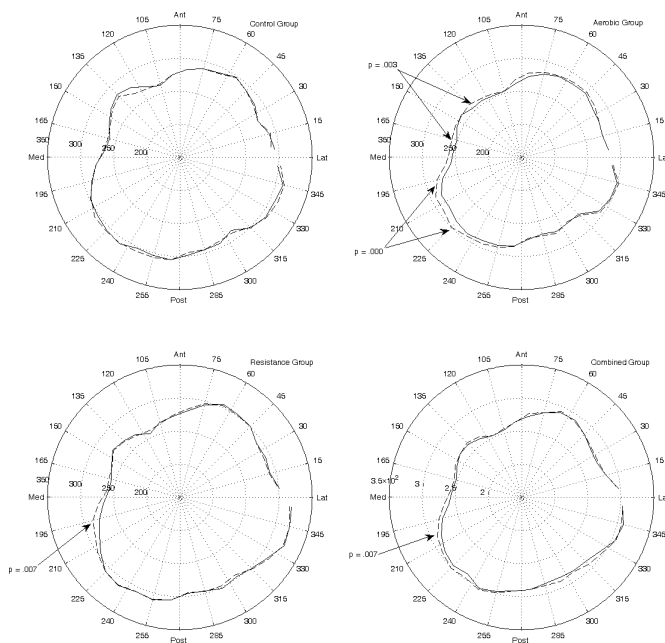
Extend pQCT analysis capability to a model generation capability.

- Use pQCT images to generate fully 3D, patient specific FEA.

Illustration

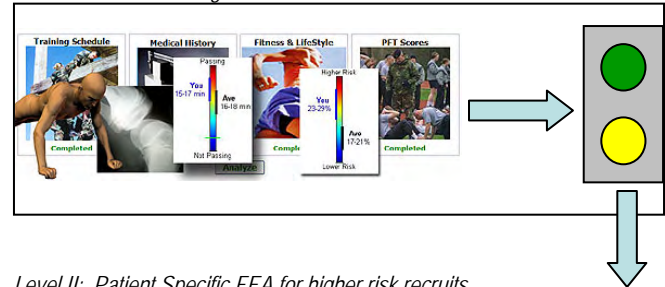


pQCT Analysis: Images are registered (top) and then pre, mid, and post are aligned (bottom).

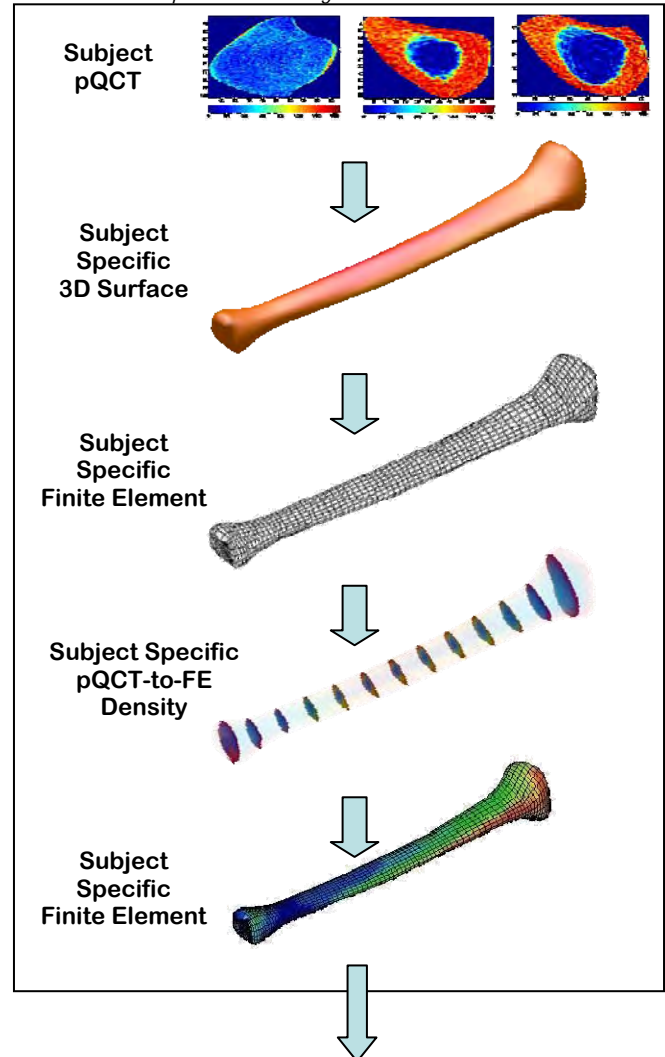


pQCT Results: University of Connecticut Study: Regional density changes found using image analysis

Level I: TOP Screening



Level II: Patient Specific FEA for higher risk recruits



Two level screening prior to BCT: Level I: TOP; Level II: Patient Specific FEA

4. Biomechanical Modeling

NMS-DYNAMICS

Product

NMS-Dynamics Analysis 1.0 desktop application

Publications

Overuse Injury Assessment Model, Part IV:
NMS-Dynamics, Kofi Amankwah, Weixin
Shen, Final Report, J3181-07-338, August 2007

Overuse Injury Assessment Model, Part II:
NMS-biodynamics—A Biomechanical Model-
ing Toolbox, Kofi Amankwah, Weixin Shen,
Annual Report J3181-06-297, April 2006

Background

The modeling, simulation, and analysis of the human neuromuscular system have become an increasingly important area of research. This has been driven by two factors: the basic desire to understand the fundamental mechanisms of the neuromuscular system, and by the increasing desire to improve health and reduce injuries to humans by optimizing products and physical training used by them. For the military, the desire to improve health and reduce injuries is a continual challenge. Military researchers face challenges to develop better equipment, improve training regimens, and design better methods to assess the health status of soldiers.

Biomechanical modeling has become an important part of understanding the human neuromuscular and skeletal systems. With modeling, the human body is represented with sets of mathematical relationships and related parameters. Utilizing computer simulations, models can simulate various scenarios to examine the impact

of these scenarios on body health and performance. In addition, by varying the model parameters during a simulation a better understanding can be gained of the underlying mechanisms of the neuromuscular system, and the influence of those mechanisms on the health and performance of the body. Accordingly, the advantages of modeling are that many more tests can be performed rapidly, with fewer resources, and with less risk to subjects. Biomechanical models however, must be developed and validated against experimental data to ensure their results are credible.

Method

The NeuroMuscular Skeletal Biodynamics (NMS-Biodynamics) toolbox is a software application for rapidly building human biomechanical models. The toolbox is a block programming language that allows users to develop biomechanical models by connecting blocks representing bones, joints, muscles, and passive tissues (e.g. ligaments). These models can be utilized to analyze experimental data and to simulate novel scenarios.

The toolbox can be applied in two manners. The toolbox can be utilized by users developing their own models. The user can then specify the block parameters and simulate the model under various conditions such as walking or running. This rapid development and simulation of biomechanical models enables the user to focus their time on answering their biomechanical questions and spend less time developing the model.

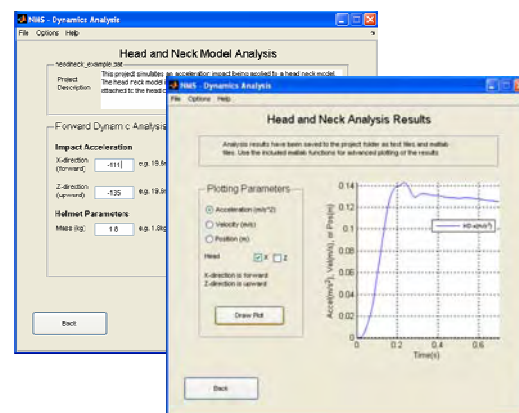
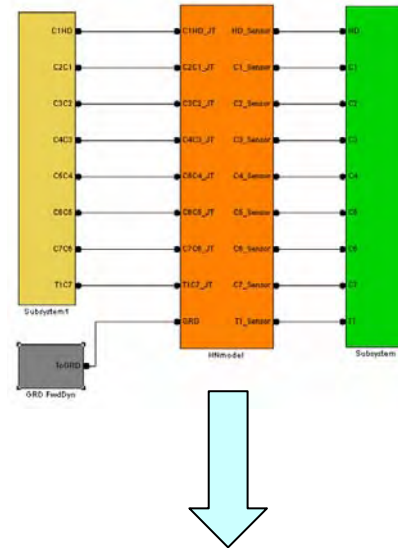
The second way the tool can be employed is custom application development for a customer, such as NMS-Dynamics Analysis 1.0. The developer can use the toolbox to build the underlying model for their customer and then build an interface for the customer to easily interact with the model. As a result, the customer does not spend time building a tool, but instead spends their time employing the tool to answer their particular question.

Toolbox features include:

- Modular design allows for rapid development of models
- Application develops the equations of motion for the user
- Built on the Matlab Simulink engine, which fully integrates with Matlab software
- Solves kinematic, inverse dynamic, forward dynamic, and muscle force sharing problems

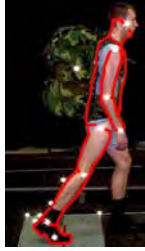
Illustration

NMS-Dynamics toolbox employed to build head neck model that accepts acceleration inputs at the T1 segment

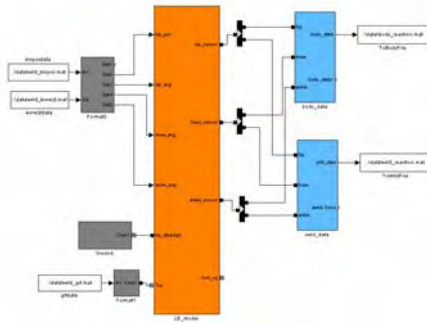
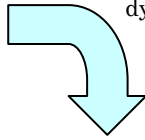


NMS-Dynamics Analysis 1.0 application provides a graphical user interface (GUI) to the model, which allows user to easily set up and simulate different acceleration impacts to the head neck model

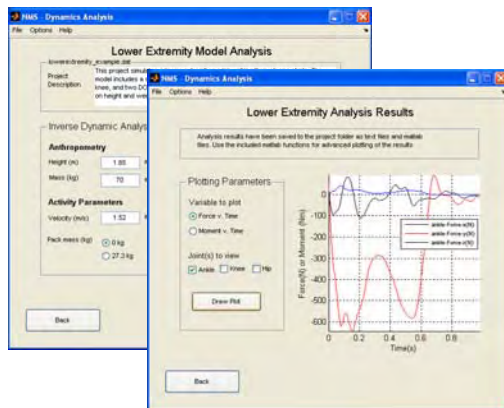
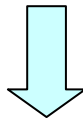
Developing a head neck model to simulate the effects of different impacts on the neck while wearing different helmets



Kinematic data recorded for a subject is utilized to develop an inverse dynamic model for walking



NMS-Dynamics toolbox used to build model and develop algorithm for scaling data to allow simulating subjects of different heights, weights, and walking speeds



NMS-Dynamics Analysis 1.0 application provides a GUI to the model, which allows user to easily set up and simulate the walking model for different subjects

From walking experiment to desktop application, using the experimental data to build a model and an interface to access the model

5. Ambulatory Biomechanical Measurement

MOBILE BIOMECHANICAL MEASURING SYSTEM

Product

- Mobile Training and Exercise System (M-TES) Data Logger 1.0
- M-TES Analyzer 1.0

Publications

Overuse Injury Assessment Model, Part V: Mobile Biomechanical Measuring System, Weixin Shen, Kofi Amankwah, Eugene Niu, Jonathan Zhang, Final Report J3181-07-339, August 2007

Background

Military physical training programs involve a number of activities to improve the health and performance of the soldier. A constant challenge is designing programs to maximize the individual's performance while minimizing the risk of a training injury. Currently some information about training regimens is manually recorded. However the inconsistency of these records and the insufficient information at the level of the individual make it difficult to accurately model the effects of a training regimen on an individual. The Mobile Training and Exercise System (M-TES) provides a method to address this problem.

The goal of developing the M-TES device is to provide the ability to wirelessly measure and record the activities of an individual in the field. The activities would include walking and running over different terrains and elevations, and jumping over obstacles. In addition the M-TES software would analyze the data to deter-

mine the activities performed and calculate biomechanical metrics for each activity.

Hardware Challenges

- Sampling the sensors sufficiently fast
- Having adequate bandwidth for transmitting data to the base station
- Providing scalability so that more or different sensors could be added to the system

Software Challenges

- Storing the data in an efficient manner
- Analyzing the data to properly reconstruct and classify the activities

Method

The M-TES hardware consists of two sensor units, a data logging base station, and a software program to analyze the recorded data. The two sensor units are worn on the ankles and each contains a biaxial accelerometer which measures accelerations in the vertical and forward directions. A force sensor is also attached to the sensor unit to measure the force under the heel of the foot. The data recorded by the sensor units are transmitted to the base station where they are stored. The base station employs flash memory to store the data until the data can be downloaded to a computer for analysis. The M-TES Analyzer program uses the data to reconstruct and classify the movements of the user, and calculate biomechanical metrics such as walking speed and stride length.

The current system utilizes motes (Mica2dot and Mica2, Crossbow Technologies, www.xbow.com).

Research Area: THIS WILL BE DETERMINED LATER

com) as the processor platform to acquire the measurements and to wirelessly transmit them to the base station. The nodes are capable of sampling frequency sufficient to capture the motions of the user. Bandwidth however, was limited and will be improved in the future. Nodes are designed to work with other nodes to form wireless sensor networks (WSNs), so scaling the system will be a straightforward process.

To store the data efficiently, a Fourier transform method is used to compress the data so that the full measurements can be reconstructed for later biomechanical analysis. This method allows for at least a 50% reduction in the storage space required.

To analyze the reconstructed data, the Analyzer program contains algorithms to classify the data into activities and then calculate biomechanical metrics for each of the activities. For example, the algorithms might determine the user was walking during a certain period of time and from that data determine the walking speed of the user.

Illustration

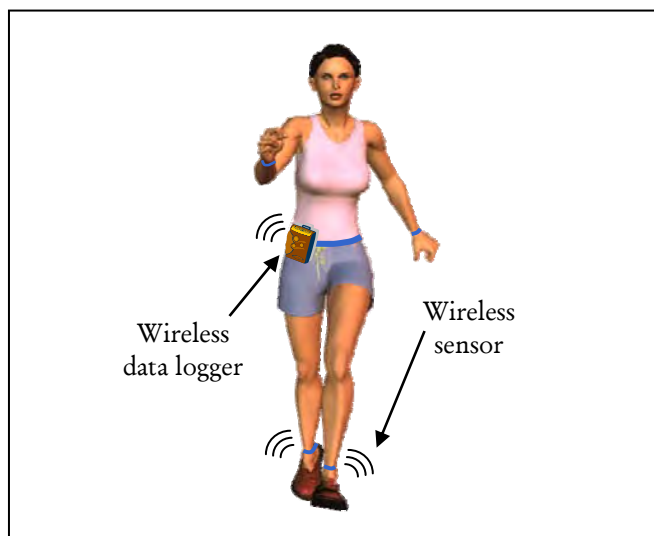
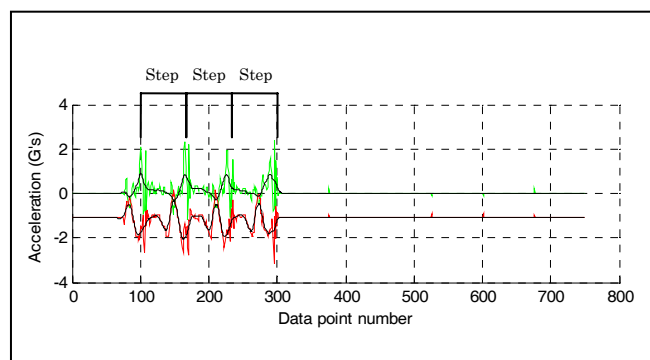


Illustration of a user wearing the M-TES device



M-TES hardware components



Example of raw and filtered acceleration data from one ankle sensor. The activity was classified as walking and each step has been highlighted.

REPORT DOCUMENTATION PAGE			<i>Form Approved</i> <i>OMB No. 0704-0188</i>		
Public reporting burden for this collection of information is estimated to average 1 hour per response, including the time for reviewing instructions, searching existing data sources, gathering and maintaining the data needed, and completing and reviewing this collection of information. Send comments regarding this burden estimate or any other aspect of this collection of information, including suggestions for reducing this burden to Department of Defense, Washington Headquarters Services, Directorate for Information Operations and Reports (0704-0188), 1215 Jefferson Davis Highway, Suite 1204, Arlington, VA 22202-4302. Respondents should be aware that notwithstanding any other provision of law, no person shall be subject to any penalty for failing to comply with a collection of information if it does not display a currently valid OMB control number. PLEASE DO NOT RETURN YOUR FORM TO THE ABOVE ADDRESS.					
1. REPORT DATE (DD-MM-YYYY) 08-20-2007		2. REPORT TYPE Final Report		3. DATES COVERED (From - To) Feb. 2002 - Feb. 2007	
4. TITLE AND SUBTITLE Overuse Injury Assessment Model, Part II: Training, Overuse Injury, and Performance Modeling			5a. CONTRACT NUMBER DAMD17-02-C0073		
			5b. GRANT NUMBER		
			5c. PROGRAM ELEMENT NUMBER		
6. AUTHOR(S) Bryant L. Sih Weixin Shen			5d. PROJECT NUMBER 3181		
			5e. TASK NUMBER		
			5f. WORK UNIT NUMBER		
7. PERFORMING ORGANIZATION NAME(S) AND ADDRESS(ES) L-3 Communications/Jaycor 3394 Carmel Mountain Road San Diego, CA 92121			8. PERFORMING ORGANIZATION REPORT NUMBER J3181-07-336		
9. SPONSORING / MONITORING AGENCY NAME(S) AND ADDRESS(ES) U.S. Army Medical Research Acquisition Activity Director 820 Chandler Street Fort Detrick, MD 21702-5014			10. SPONSOR/MONITOR'S ACRONYM(S) USAMRAA		
			11. SPONSOR/MONITOR'S REPORT NUMBER(S)		
12. DISTRIBUTION / AVAILABILITY STATEMENT					
13. SUPPLEMENTARY NOTES					
14. ABSTRACT One of the purposes of basic combat training (BCT) is to train recruits to a high fitness level. Unfortunately, about 1 in 5 recruits fail to complete BCT. Thus, there is a need for guidance on minimizing injuries and maximizing performance. This document describes the development of performance and injury prediction software for assessing the effects of training. Three performance and two injury models have been developed (push-up, sit-up, run, stress fracture, and overuse injury), all of which take into account initial physical fitness, anthropometry, and training regimen to predict changes during training. The models were optimized and validated with existing BCT datasets and were found to have similar accuracy as traditional statistical methods. We anticipate future development and additional data will improve accuracy across a wider range of training regimens than possible with statistical methods. The models were incorporated into a web-based software package to allow users to easily access the model predictions.					
15. SUBJECT TERMS Stress fracture, overuse injury, sit-ups, push-ups, running, basic combat training, modeling, optimization					
16. SECURITY CLASSIFICATION OF:			17. LIMITATION OF ABSTRACT UNLIMITED	18. NUMBER OF PAGES 81	19a. NAME OF RESPONSIBLE PERSON Blossom Widdar
a. REPORT UNCLASSIFIED	b. ABSTRACT UNCLASSIFIED	c. THIS PAGE UNCLASSIFIED			19b. TELEPHONE NUMBER (include area code) (301) 619-7143

Executive Summary

The purpose of basic combat training (BCT) is to prepare recruits for the rigors of military life, including acquiring a high fitness level. Improving fitness is accomplished by overloading or stressing the body through exercise. Unfortunately, about 1 in 5 recruits fail to complete BCT due to injury or low performance. Thus, there is a need for guidance on minimizing injuries and maximizing performance in order to minimize personnel losses during BCT.

The motivation for a novel prediction tool that can analyze different training regimens and populations stem from limitations of currently employed statistical methods. These include the inability to identify the relative importance of individual training activities and the difficulty in combining data from different sources. Plus, statistical methods are limited by the amount of available data. Most importantly, the results from statistically-based analyses are only applicable to the similar populations and training regimens, offering no guidance or predictability for different scenarios or the time course of injury rates and performance changes.

A better method is to develop mechanistic models that account for training activities and individual characteristics in a manner consistent with known physiological phenomenon (i.e., using biomechanical and biological principles). To simplify the model development while still capturing the overall exercise response, a dose-response framework was used to quantify training activities and predict outcome in a physiologically meaningful way. The inputs to the models are training regimen details and individual characteristics such as height and weight. These are used to estimate a “dose” based on known training enhancement principles and injury risk factors found in the literature. The “response” is also based on known principles found in the literature that relate training to injury risk and performance enhancement.

The models were optimized and validated with existing BCT datasets and were found to have similar accuracy as traditional statistical methods. The results support the development of dose-response models for predicting training performance outcomes. In most cases, the models performed similarly or better than a traditional statistical method. In situations where this was not the case, the difference was small and we anticipate that the Training, Overuse Injury, and Performance (TOP) model accuracy will uphold better against additional datasets. We also anticipate further improvements with better personnel and training measurements.

To facilitate the use of the performance and injury models, a web-based software program that incorporated the models was implemented. The objective of the software was

to demonstrate the feasibility of the models as a tool to help reduce injuries and maximize performance. The TOP software package is the result of this effort. This document describes development up to TOP 1.1, the version of the software completed in August 2007. The TOP package contains the three performance and two injury models (push-up, sit-up, run, stress fracture, and overuse injury).

Two user types were implemented— a *Basic User* or individual and a *Mid-Level User* or someone who is responsible for the fitness of small groups of people (10-20 people). Since the Basic and Mid-Level User have different requirements, different software interfaces have been designed to allow these users to enter data, run the TOP models, and view results easily in the context they desire. Additional user types to address the needs of Commanders, who are interested in the outcome from a large group of individuals, and researchers, who would be interested in accessing some of TOP 1.1's model algorithms directly, are planned for future TOP versions.

In addition, several subprograms were developed to increase the utility of the program for individual user's and researchers alike. This included body fat compliance and APFT score calculators as well as BCT background information. Also, password-protected access to the datasets used to derive the models was implemented.

In summary, the TOP models developed were found to have a similar accuracy to a statistical method commonly used in performance and injury prediction. In addition, software was designed and implemented that incorporated the models as a demonstration of the feasibility of the project in helping improve fitness and reduce injuries through the identification of high risk individuals and regimen optimization.

Contents

	<u>Page</u>
1. INTRODUCTION	1
2. PERFORMANCE & INJURY MODELS	3
2.1 MODEL DEVELOPMENT	3
2.1.1 <i>Modeling Approach</i>	3
2.1.2 <i>Run Model Overview</i>	4
2.1.3 <i>Upper-body Performance: Sit-ups & Push-ups Models (Initial version)</i>	7
2.1.4 <i>Stress Fracture</i>	13
2.1.5 <i>Lower-body Overuse Injury</i>	21
2.2 MODEL VALIDATION	28
2.2.1 <i>Run Performance</i>	28
2.2.2 <i>Sit-Up Performance</i>	29
2.2.3 <i>Push-up Performance</i>	30
2.2.4 <i>Stress Fracture</i>	31
2.2.5 <i>Lower-body Overuse Injury</i>	32
2.3 MODEL REFINEMENT	33
2.3.1 <i>Sit-Up Performance</i>	33
2.4 MODEL CONCLUSIONS	40
2.4.1 <i>Summary Tables</i>	41
3. SOFTWARE APPLICATION DEVELOPMENT.....	45
3.1 DEVELOPMENT APPROACH	45
3.2 DATABASE DEVELOPMENT	48
3.3 TOP IMPLEMENTATION.....	49
3.3.1 <i>Basic Level User</i>	50
3.3.2 <i>Mid-Level User</i>	58
3.4 DEVELOPERNET: DATA STORAGE & ACCESS	60
3.5 BASIC COMBAT TRAINING BACKGROUND INFORMATION SITE	62
4. CONCLUSIONS	69
4.1 KEY ACCOMPLISHMENTS	70
4.2 REPORTABLE OUTCOMES	70
5. LITERATURE	71
APPENDIX A. AVAILABLE DATASETS	75

Illustrations

	<u>Page</u>
1. The estimated number of sit-ups and push-ups performed each day during the U.S. Army Standardized Training Program.	9
2. Cumulative incidence of injury by cumulative miles of running for 2 army infantry basic training units during 12 weeks of training.	16
3. The cumulative stress fracture rate versus cumulative run distance for males and females of dataset G (see Appendix).....	17
4. The percent of males (left) and females (right) from dataset Group G that sustained a stress fracture when categorized by BMI.....	19
5. The cumulative overuse injury rate versus cumulative run distance for males and females of dataset G (see Appendix).....	24
6. The percent of males (left) and females (right) from dataset Group G that sustained a lower-body overuse injury when categorized by BMI.....	26
7. A free-body diagram of the sit-up.	34
8. The estimated saw-tooth angular velocity profile for performing a single sit-up at 120 reps/min.....	35
9. Free-body diagram to determine the mass and location relative to the hip for the head, arms and trunk (HAT).	36
10. The TOP web-site home page.....	45
11. The database schema to store training regimen data.	49
12. Basic Level User—Main Page.....	50
13. Basic Level User—Training Schedule sub-page.....	51
14. Basic Level User—Medical History sub-page.....	52
15. Basic Level User—Fitness and Lifestyle Background sub-section.	53
16. Basic Level User—Physical Fitness Scores sub-section.	54
17. Basic Level User—Results sub-section.	55
18. Printable report summarizing the Basic User model results.	56
19. Back page of the printable Basic User report.	57
20. The Subject selection page for the Mid-Level User.	58
21. The Regimen selection page for the Mid-Level User.....	58
22. The Analysis selection page for the Mid-Level User.	59
23. The Mid-Level User Results page.....	60
24. The DeveloperNet Main Page.	61
25. DeveloperNet Survey Data sub-window.	62
26. The injury section of the BCT Background web site.	63
27. The fitness testing section of the BCT Background web site.....	64

Tables

	<u>Page</u>
1. Performance model literature review summary.....	4
2. A comparison of the accuracy of a Test Index Cluster (TIC) analysis to that of the run performance model for male recruits undergoing basic combat training at various Army training sites.	6
3. A comparison of the accuracy of a Test Index Cluster (TIC) analysis to that of the run performance model for female recruits undergoing basic combat training at various Army training sites.....	6
4. The estimated number of sit-ups and push-ups performed for a single Conditioning Drill I and II bout used by the U.S.Army's Standardized Training regimen.	9
5. The optimum k_1 for males and females.	10
6. A comparison of the accuracy of a Test Index Cluster (TIC) analysis to that of the sit-up performance model for male recruits undergoing basic combat training at various Army training sites (Group G).	10
7. A comparison of the accuracy of a Test Index Cluster (TIC) analysis to that of the sit-up performance model for female recruits undergoing basic combat training at various Army training sites (Group G).	11
8. A comparison of the accuracy of a Test Index Cluster (TIC) analysis to that of the push-up performance model for male recruits undergoing basic combat training at various Army training sites (Group G).	12
9. A comparison of the accuracy of a Test Index Cluster (TIC) analysis to that of the push-up performance model for female recruits undergoing basic combat training at various Army training sites (Group G).	12
10. Risk factors for stress fractures: possible mechanisms and inter-relationships. (From Bennell et al. 1999).....	14
11. Consistently identified risk factors for overuse injuries occurring during military training.....	15
12. The best fit values for Equation (9) when applied to the male and female stress fracture versus dosage data from Group G.	18
13. Stress fracture scaling factors for Equation (13).	19
14. Stress fracture model accuracy for male recruits (Group G) undergoing basic combat training at various Army training sites.	20
15. Stress fracture model accuracy for female recruits (Group G) undergoing basic combat training at various Army training sites.	21
16. The best fit values for Equation (9) when applied to the male and female overuse injury versus dosage data from Group G.	24
17. Overuse injury scaling factors for Equation (15).	25
18. A comparison of the accuracy of a Test Index Cluster (TIC) analysis to that of the lower-body overuse injury model for male recruits undergoing basic combat training at various Army training sites (Group G).	27

19.	A comparison of the accuracy of a Test Index Cluster (TIC) analysis to that of the lower-body overuse injury model for female recruits undergoing basic combat training at various Army training sites (Group G).	27
20.	Run performance model and TIC validation results.	29
21.	Sit-up performance model and TIC validation results.	30
22.	Push-up performance model and TIC validation results.	31
23.	Stress fracture model validation results.	32
24.	Overuse injury model and TIC validation results.	33
25.	Estimates of the head, arms, and trunk (HAT) mass and distance from the hip joint.	37
26.	A comparison of the accuracy of a Test Index Cluster (TIC) analysis to that of the two sit-up performance models for male recruits undergoing basic combat training at various Army training sites (Group G).	38
27.	A comparison of the accuracy of a Test Index Cluster (TIC) analysis to that of the two sit-up performance models for female recruits undergoing basic combat training at various Army training sites (Group G).	39
28.	Sit-up results for the updated and original models.	39
29.	Performance and injury model algorithm summary tables.	41
30.	Performance model validation summary tables for both males and females.	42
31.	Injury model validation summary tables for both males and females.	43
32.	TOP Software release dates.	46
33.	TOP User Types.	47
34.	Stress fracture risk factor icons and information presented in the BCT Background Web Site.	65
35.	Overuse injury risk factor icons and information presented in the BCT Background Web Site.	66
36.	Acute injury risk factor icons and information presented in the BCT Background Web Site.	66
37.	Push-up performance factors presented in the BCT Background Web Site.	67
38.	Sit-up performance factors presented in the BCT Background Web Site.	67
39.	Run performance factors presented in the BCT Background Web Site.	68
40.	Summary of the datasets available for model development.	76

1. Introduction

The purpose of basic combat training (BCT) is to prepare recruits for the rigors of military life, including acquiring a high fitness level. Improving fitness is accomplished by overloading or stressing the body through exercise. However, training-related injuries affect about 25% of male recruits and about 50% of female recruits, a significant portion of which are severe enough to force recruits to withdraw from BCT. Additional attrition occurs when recruits fail to reach the desired fitness level (as measured by performance tests such as the military Physical Fitness Test or PFT). Overall, about 1 in 5 recruits fail to complete BCT. Thus, there is a need for guidance on minimizing injuries and maximizing performance in order to minimize personnel losses during BCT.

The primary goal of this project is to design and implement a framework for assessing the effects of physical training on performance and injury. To assess training effects, physiologically- and biomechanically-based models were combined with statistical methods to address the following objectives:

- Predict Army Physical Fitness (APFT) results
- Identify “high risk” individuals
- Guidance for modification of training regimens
- Compare training regimens

While these prediction models are required to assess training outcome, the use of the models by the military community is limited because of their complexity. To address this issue, the models (and some additional value-added features) were incorporated into a software package. The primary goals of the software package are:

- Efficient and user-friendly software interface for underlying complex models
- Allows users to easily manage software and view model prediction results
- Multiple interfaces to accommodate different user requirements

The Training, Overuse Injury, and Performance (TOP) software package is the result of the effort to assess physical training and create a tool to be a benefit to the military community. This document describes work up to TOP 1.1, the version of the software completed in July 2007.

2. Performance & Injury Models

2.1 Model Development

Any prediction tool developed requires input variables such as recruit's anthropometry and training regimen from which performance and injury output variables can be predicted. How the input variables are used to derive a prediction (i.e., an algorithm) depends on the modeling method chosen.

2.1.1 Modeling Approach

In general, there are two basic methods from which injury and performance prediction schemes can be derived, neither of which are appropriate from a practical point of view. A purely statistical approach derives statistical relationships between the input variables and observed outcomes from field data. However, as covered earlier, this method is only applicable to situations and populations from which the analyses were based, severely limiting the utility of this method. The other method is a physiologically-based computational model where the full pathway leading to the training outcomes is derived from known biological principles that directly account for effects of input variables. While this method has the potential to be more robust and accurate, it is impractical as a prediction tool—the algorithms are very complex, with too many input parameters to measure on a large group of subjects in the field.

The approach utilized in the TOP Model project is to incorporate simplified biomechanical and physiological models using input variables identified by the statistical model. This allows the limited use of computational modeling to increase the robustness and accuracy of a statistical approach. To accomplish this, two key modeling components are introduced: a *dosage* amount and a *response* model. The dosage is an intermediate variable that is more fundamentally related to training outcomes than those that can be easily identified or measured. For example, VO_2 or oxygen consumption is used as a dosage for the run performance model described in Sih and Shen (2006). This is the quantity that allows the model to account for different exercises based upon their “equivalent effects” (in terms of VO_2 or other dosage measures). The proposed response models are purposefully simple yet representative of the underlying mechanisms shown in the literature that led to the performance or injury outcomes.

There are several other advantages of a hybrid statistical-physiological approach. This includes allowing incremental improvement of model prediction by improving the underlying models or model parameters, better use of existing data (combining heterogeneous datasets), allowing extrapolation to different training regimens, and prediction of the time evolution of training outcomes. However, the method is more complex and less intuitively

tive than a traditional statistical approach and the overall accuracy depends on the size and quality of the data as well as how accurate the underlying mechanisms are modeled.

This approach was used to develop. The following section gives an overview of a previously described run performance model (Sih and Shen 2006) as well as details on the development of two additional performance models (sit-ups and push-ups). In addition, two injury models (stress fracture and overuse injury) were developed using the hybrid statistical-physiological approach.

2.1.1.1 Statistical Methods Overview

To compare model performance with a traditional statistical approach, the same Test Index Cluster (TIC) method as with the running model development was employed to determine the most statistically relevant variables from which to predict training outcome. The purpose of the TIC analysis is to identify relevant predictor variables and the most appropriate cutoff values with which to classify individuals into “high” and “low” risk groups. The procedure is as follows:

- Unpaired *t*-test to eliminate irrelevant variables
- Receiver-Operator Curve Analysis (ROC) to optimize variable cutoff values
- Logistic Regression to identify statistically significant variables
- Test Index Cluster Analysis to quantify the accuracy of identified variables in the prediction

Additional information on TIC analysis can be found in Allison et al. (2005) or statistical text books.

2.1.2 Run Model Overview

2.1.2.1 Literature Review

A performance model literature review was performed (Table 1). The previous literature review (Sih and Shen 2006) suggests that a “Banister-type” single-component model without fatigue. (See Sih and Shen 2006 for additional details.)

Table 1. Performance model literature review summary.

Source	Data Summary
(Morton et al. 1990)	“Banister” model. Uses exponential decay fitness and fatigue components with reasonable results.
(Busso 2003)	Banister model with a time varying fatigue component to account for increased fatigue from multiple training sessions. Appears more realistic than previous versions.

2.1.2.2 Methods

The performance model chosen is:

$$P = P_0 + (P_{\max} - P)g_1 \otimes W \quad (1)$$

where P is normalized performance, P_0 is initial or pretraining performance, P_{\max} is an individual's maximum P , g_1 is the performance enhancement component, W are daily training dosages, and \otimes is the convolution function. g_1 controls how training affects performance in the future whereas the convolution function allows multiple training bouts to contribute to performance.

A timed 2-mile run is part of the APFT that recruits must pass to complete BCT. To predict the runtime after training, Equation (1) was optimized using recruits who underwent Army BCT at various training centers. For running, performance P was defined as:

$$P = V_{\text{event}} / V_{\max} \quad (2)$$

where V_{event} is the final PFT run velocity and V_{\max} is the estimated World Record velocity for the final PFT run distance (2 miles). In addition, training dosage was defined as:

$$W = W_{\text{rate}} \times \text{duration} \times e^{bW_{\text{rate}}} \quad (3)$$

where the exponent accounts for high training loads where anaerobic process dominate. W_{rate} is bound by normalizing VO_2 using $\text{VO}_{2\max}$ and resting metabolic rate (RMR),

$$W_{\text{rate}} = (\text{VO}_2 - \text{RMR}) / (\text{VO}_{2\max} - \text{RMR}) \quad (4)$$

The final model parameters needed to compute P (Eq. (1)) are the coefficients in the performance enhancement component, g_1 , which is defined as:

$$g_1 = k_1 e^{-t/\tau_1} \quad (5)$$

where t is time (days), k_1 is a linear coefficient (unitless) and τ_1 is a time constant (days). This term dictates the amount of performance increase with training and the loss of the performance with time.

2.1.2.3 Results

Male Recruits

The initial prevalence (overall failure rate) was 4% for the males on the final PFT run. The TIC analysis identified only initial PFT runtime as a significant predictor, with a time of 20:17 or slower. Both the TIC and model predictions are comparable, with similar diagnostic accuracy (88% for TIC and 84% for the model) and positive post-test probabilities (Table 6).

Table 2. A comparison of the accuracy of a Test Index Cluster (TIC) analysis to that of the run performance model for male recruits undergoing basic combat training at various Army training sites.

TIC	Final PFT Run		MODEL	Final PFT Run	
	Fail	Pass		Fail	Pass
IST Run > 20:17	9	47	Pred Fail	10	67
IST Run < 20:17	11	428	Pred Pass	10	409

For the TIC, one item was identified: a runtime > 20:17 on the initial PFT run. A recruit with this item had a significantly greater chance of failing the final PFT (Sensitivity = 0.45; Specificity = 0.90; Positive pretest probability = 4%; Positive post-test probability = 16%; Negative post-test probability = 3%). For the performance model, accuracy was similar (Sensitivity = 0.50; Specificity = 0.86; Positive pretest probability = 4%; Positive post-test probability = 13%; Negative post-test probability = 2%).

Female Recruits

The initial prevalence (overall failure rate) was 8% for the females on the final PFT run. The TIC analysis identified only initial PFT runtime as a significant predictor, with a time of 22:55 or slower. Both the TIC and model predictions are comparable, with similar diagnostic accuracy (80% for TIC and 87% for the model) and positive post-test probabilities (Table 3).

Table 3. A comparison of the accuracy of a Test Index Cluster (TIC) analysis to that of the run performance model for female recruits undergoing basic combat training at various Army training sites.

TIC	Final PFT Run		MODEL	Final PFT Run	
	Fail	Pass		Fail	Pass
IST Run > 22:55	7	39	Pred Fail	4	18
IST Run < 22:55	14	202	Pred Pass	17	237

For the TIC, one item was identified: a runtime > 22:55 on the initial PFT run. A recruit with this item had a significantly greater chance of failing the final PFT (Sensitivity = 0.33; Specificity = 0.84; Positive pretest probability = 8%; Positive post-test probability = 15%; Negative post-test probability = 6%). For the performance model, accuracy was similar (Sensitivity = 0.19; Specificity = 0.93; Positive pretest probability = 8%; Positive post-test probability = 18%; Negative post-test probability = 7%).

2.1.2.4 Discussion

For both the male and female datasets, the run performance model prediction accuracy was comparable to a TIC analysis when subject height, weight, and gender as well as

initial PFT push-ups, sit-ups, and runtimes were used in literature-based regression equations to estimate the parameters for the above equations. Thus, the model gives reasonable results using parameters and values found in the literature and suggests that the model has the potential to predict PFT runtimes accurately. (See Sih and Shen 2006 for additional details.)

2.1.3 Upper-body Performance: Sit-ups & Push-ups Models (Initial version)

In addition to a run exercise, two upper-body performance tests are required to pass BCT in the U.S. Army Physical Fitness Test (PFT)—the maximal number of sit-ups and push-ups in two minutes. Other military branches may perform other upper-body tests such as crunches and pull-ups and models for these exercises will have to be developed at a later time. The PFT is usually administered three times—an initial (1st), mid-, and final (FPFT).

2.1.3.1 Literature Review

Unlike running, there is relatively little published on any upper-body performance enhancement during exercises such as sit-ups, push-ups and pull-ups. The few studies found suggested that initial strength is important (Flanagan et al. 2003) and that aerobic training does little to impact strength/power performances (Kraemer et al. 2001). In addition, it should be noted that males generally have 55% more upper body strength compared to women (Kraemer et al. 2001) and that initial body percent body fat and strength to fat-free mass ratio are good predictors of pull-up exercises (Flanagan et al. 2003).

2.1.3.2 Methods

The lack of information in the literature makes determining the key input variables and underlying mechanisms of sit-up and push-up performance difficult. Under ideal conditions, percent body fat and strength to fat-free mass ratio appear to be the best inputs to predictive sit-up and push-up models. However, neither of these can be accurately measured in the field, making their use impractical. Initial strength can be accounted for from 1st PFT sit-up and push-up tests and separate model parameters can be developed for each gender to account for male/female strength differences. Since the literature suggests that aerobic exercises such as marching and running are not appropriate, only upper body exercises such as those described in the U.S. Army's Conditioning Drill I and II are to be used as training inputs.

For the initial sit-up and push-up models, a similar response model formulation as the run model was used since many strength performance characteristics are similar to those seen for aerobic exercises—a decrease in training benefit from a fixed amount of exercise as fitness increases and the loss of fitness with disuse. The formulation is:

$$P = P_0 + P(g_1 \otimes W) \quad (6)$$

where P is normalized sit-up or push-up performance and P_0 is normalized initial or pre-training performance. g_1 is a time-dependent training enhancement constant and W is the daily training dosages, which are combined using \otimes , the convolution function—a summation function where the effect of training dosages decreases with time. Additional details on each of the model variables are discussed below.

Performance level P is a normalized exercise rate, defined as the percentage of the maximum number of sit-ups or push-ups per minute that can be performed:

$$P = \text{Rate}_{\text{event}} / \text{Rate}_{\text{max}} \quad (7)$$

This formulation allows performances of different durations to be predicted. Unable to find sit-ups records for the short time intervals seen in the PFT, rates at longer durations were investigated. The maximum number of sit-ups in an hour was set by Mark Pfeltz in 1985 and in 24 hours by Edmar Freitas in 2002. Both records were set at an approximately 77 sit-ups per minute rate. Unable to find any additional information, it was assumed that the maximum rate at the one to two minute duration to be 150 sit-ups per minute. For push-ups, there is anecdotal evidence that rates up to 200 per minute can be achieved. P_0 is the initial performance level, as measured by the 1st PFT divided by the maximal sit-up or push-up rate. No differences for gender was found or incorporated in the maximal rate for this model.

Training dosage W is defined as the number of sit-ups or push-ups per day performed during the training regimen and g_1 is defined as

$$g_1 = k_1 \exp(-t/\tau_1) \quad (8)$$

where k_1 is a training constant, which describes the increase in performance for a single training bout, τ_1 is a time constant (days), which describes the decrease in performance due to lack of exercise with time, and t is time in days. Being unable to find any training studies directly involving sit-ups or push-ups, we turn to a direct muscle strength study (Mulder et al. 2006) that found in 8 weeks a linear decrease of 16.8 ± 7.4 % in the muscle with bed rest. This suggests that τ_1 or the reduction in strength from disuse for muscle strength is approximately 100 days.

The only model parameter remaining that is needed to compute P is k_1 . Lacking information from the literature, k_1 was estimated by optimizing the sit-up and push-up outcomes from an acquired U.S. Army dataset (Group G, see Appendix). Males and females were analyzed separately. Unfortunately, the dataset lacked specific information on the NonStandardized Training Regimen used to train the recruits. However, Knapik et al.(2004) found a similar performance outcome between the Standardized and

NonStandardized regimens. Thus, the training regimen was assumed to be 8 weeks of Standardized Army BCT, which specifies the daily number of Conditioning Drill 1 and 2 repetitions to be performed. Table 4 lists the number of sit-ups and push-ups for each drill and Figure 1 shows the daily total number of each exercise or W estimated. Values for k_1 can be found in Table 5.

Table 4. The estimated number of sit-ups and push-ups performed for a single Conditioning Drill I and II bout used by the U.S. Army's Standardized Training regimen.

	# of Sit-ups	# of Push-ups
Conditioning Drill I	6	2
Conditioning Drill II	2	3

Note that the Conditioning Drills are often repeated multiple times during the exercise session.

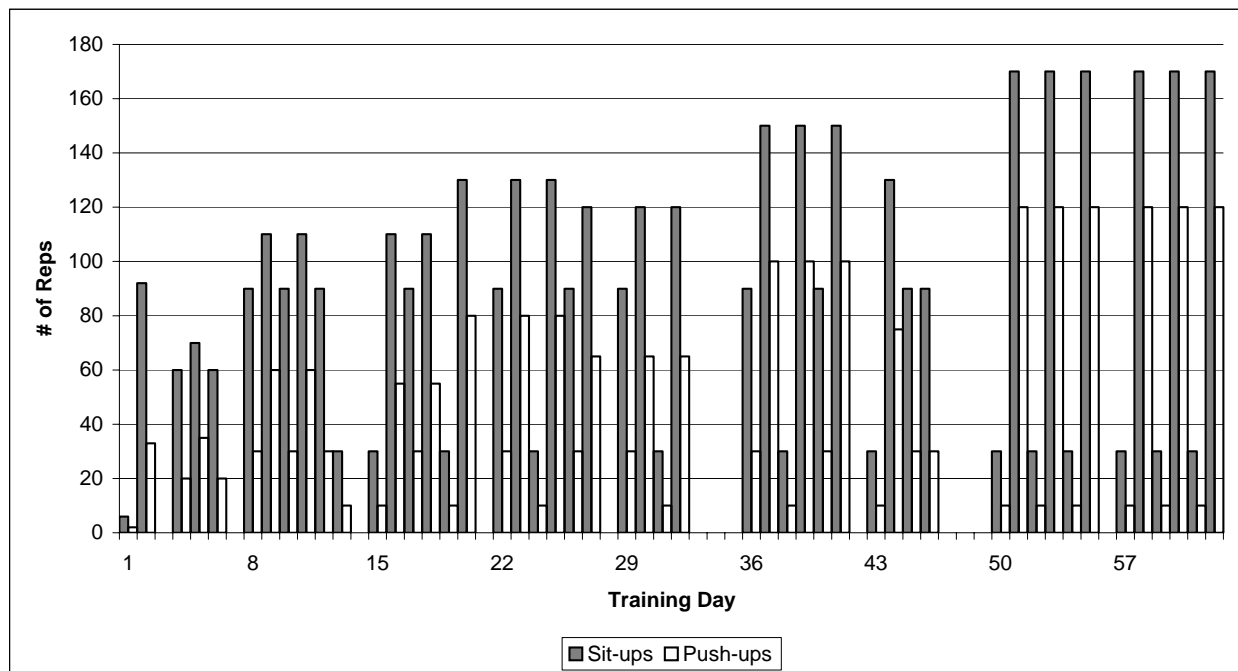


Figure 1. The estimated number of sit-ups and push-ups performed each day during the U.S. Army Standardized Training Program.

Values were estimated from the TRADOC Standardized Physical Training Guide (Army Accessions Command 2003).

Table 5. The optimum k_1 for males and females.

Using a constant τ_1 and the training dosage W , the best k_1 for males and females was found that resulted in the least squares error between the existing 1st and Final PFT performance results.

	Sit-ups ($\tau_1 = 100$ days)	Push-ups ($\tau_1 = 100$ days)
Male	$2.37\text{E-}5 \pm 1.41\text{E-}5$	$3.10\text{E-}5 \pm 1.73\text{E-}5$
Female	$2.68\text{E-}5 \pm 1.50\text{E-}5$	$2.67\text{E-}5 \pm 1.41\text{E-}5$

2.1.3.3 *Results*

To estimate model accuracy, model predictions were calculated using input values from dataset Group G (see Appendix), which contains data from approximately 681 male and 336 female recruits who underwent U.S. Army BCT circa 1997. Input variables for sit-ups were the 1st PFT sit-up count, gender, and daily sit-up number. Input variables for push-ups were the 1st PFT push-up count, gender, and daily push-up number. Accuracy was assessed by comparing model predictions to the observed Final PFT results. In addition, model predictions are compared to those derived from the statistically-based TIC procedure mentioned previously (See Section 2.1.1.1).

Sit-ups: Male Recruits

The initial prevalence (overall Final PFT failure rate) was 11% for the males on the final PFT sit-up exercise. The TIC analysis identified initial PFT sit-up number and previous activity level (self-rated questionnaire data) as significant predictors. Both the TIC and model predictions are comparable, with similar prognostic accuracy (74% for TIC and 75% for the model) and positive post-test probabilities (Table 6). Positive likelihood ratio (PLR) and 95% confidence interval for the TIC and model were 2.1 (1.4-3.0) and 1.7 (1.2-2.5), respectively.

Table 6. A comparison of the accuracy of a Test Index Cluster (TIC) analysis to that of the sit-up performance model for male recruits undergoing basic combat training at various Army training sites (Group G).

TIC	Final PFT Sit-Up		MODEL	Final PFT Sit-Up	
	Fail	Pass		Fail	Pass
Any one or more	17	118	Pred Fail	20	98
None	16	359	Pred Pass	37	380

For the TIC, two items were identified: a sit-up count < 57 on the initial PFT test and a self-reported fitness level of “about the same” or “somewhat less” than others. A recruit with either of these items had a significantly greater chance of failing the final PFT (Sensitivity =

0.75; Specificity = 0.51; Positive pretest probability = 6%; Positive post-test probability = 13%; Negative post-test probability = 4%). For the performance model, accuracy was similar (Sensitivity = 0.35; Specificity = 0.80; Positive pretest probability = 11%; Positive post-test probability = 17%; Negative post-test probability = 9%). Number of samples in TIC and model differ due to missing data.

Sit-ups: Female Recruits

The initial prevalence (overall Final PFT failure rate) was 21% for the females on the final PFT sit-up exercise. The TIC analysis identified initial PFT sit-up number and height as significant predictors. The TIC performed better than the model (prognostic accuracy of 81% for TIC and 66% for the model), including better positive post-test probabilities (Table 7). PLR and 95% confidence interval for the TIC and model were 1.9 (0.6-5.9) and 1.7 (1.2-2.3), respectively.

Table 7. A comparison of the accuracy of a Test Index Cluster (TIC) analysis to that of the sit-up performance model for female recruits undergoing basic combat training at various Army training sites (Group G).

TIC	Final PFT Sit-Up		MODEL	Final PFT Sit-Up	
	Fail	Pass		Fail	Pass
Any one or more	4	10	Pred Fail	30	69
None	41	208	Pred Pass	28	155

For the TIC, two items were identified: a sit-up count < 3 on the initial PFT test and a height > 1.52 m. A recruit with either of these items had a significantly greater chance of failing the final PFT (Sensitivity = 0.09; Specificity = 0.95; Positive pretest probability = 17%; Positive post-test probability = 29%; Negative post-test probability = 16%). For the performance model, accuracy was not as good (Sensitivity = 0.52; Specificity = 0.69; Positive pretest probability = 21%; Positive post-test probability = 30%; Negative post-test probability = 15%). Number of samples in TIC and model differ due to missing data.

Push-ups: Male Recruits

The initial prevalence (overall Final PFT failure rate) was 14% for the males on the final PFT push-up exercise. The TIC analysis identified initial PFT push-up number, previous activity level (self-rated questionnaire data), and age as significant predictors. Both the TIC and model predictions are comparable, with similar prognostic accuracy (75% for TIC and 73% for the model) and positive post-test probabilities (Table 8). PLR and 95% confidence interval for the TIC and model were 2.3 (1.7-3.2) and 1.9 (1.4-2.6), respectively.

Table 8. A comparison of the accuracy of a Test Index Cluster (TIC) analysis to that of the push-up performance model for male recruits undergoing basic combat training at various Army training sites (Group G).

TIC	Final PFT Push-Up	
	Fail	Pass
All Three	28	105
None	24	352

MODEL	Final PFT Push -Up	
	Fail	Pass
Pred Fail	32	100
Pred Pass	45	358

For the TIC, three items were identified: a sit-up count < 56 on the initial PFT test, a self-reported fitness level of “about the same” or “somewhat less” than others and an age of 24 years or younger. A recruit with all three of these items had a significantly greater chance of failing the final PFT (Sensitivity = 0.54; Specificity = 0.77; Positive pretest probability = 10%; Positive post-test probability = 21%; Negative post-test probability = 6%). For the performance model, accuracy was similar (Sensitivity = 0.42; Specificity = 0.78; Positive pretest probability = 14%; Positive post-test probability = 24%; Negative post-test probability = 11%). Number of samples in TIC and model differ due to missing data.

Push-ups: Female Recruits

The initial prevalence (overall Final PFT failure rate) was less than 5% for the females on the final PFT push-up exercise. The TIC analysis identified only height as a significant predictor. The TIC performed better than the model (prognostic accuracy of 85% for TIC and 73% for the model), including better positive post-test probabilities (Table 9). PLR and 95% confidence interval for the TIC and model were 6.4 (4.8-8.5) and 0.6 (0.2-2.1), respectively.

Table 9. A comparison of the accuracy of a Test Index Cluster (TIC) analysis to that of the push-up performance model for female recruits undergoing basic combat training at various Army training sites (Group G).

TIC	Final PFT Push-Up	
	Fail	Pass
Taller	3	41
Shorter	0	221

MODEL	Final PFT Push -Up	
	Fail	Pass
Pred Fail	2	62
Pred Pass	13	203

For the TIC, one item was identified: a height > 1.74 m. A recruit this item had a significantly greater chance of failing the final PFT (Sensitivity = 0.87; Specificity = 0.84; Positive pretest probability = 1%; Positive post-test probability = 8%; Negative post-test probability = 0%). For the performance model, accuracy was not as good (Sensitivity = 0.13; Specificity = 0.77; Positive pretest probability = 5%; Positive post-test probability = 3%; Negative post-test probability = 6%). Number of samples in TIC and model differ due to missing data.

2.1.3.4 *Discussion*

As expected, the accuracy of these models was lower than that seen for running due to the lack of information on these exercises in the literature. Because of similar performance characteristics to running, both the sit-up and push-up models were developed using a similar algorithm to that developed for the running model. However, unlike running, there was limited information available in the literature to estimate parameter values such as maximum exercise rates and other parameter constants. In addition, the training regimen lacked details to fully quantify the number of sit-ups and push-ups performed.

For both sit-ups and push-ups, the results were mixed with the model accuracy being similar to a TIC analysis for males but worse for females. The primary reason for the decrease in accuracy in the female push-up group is the small number of failures. In addition, height was identified (and used) by the TIC to predict outcome, a variable not previously identified as a significant factor during the literature review. Incorporation of height into the model may increase accuracy to the same level as the TIC or better. Also, the development of a strength-based model may yield increased accuracy. These changes were implemented in an updated sit-up model (see 2.3.1 Sit-Up Performance, page 33).

2.1.4 *Stress Fracture*

One of the most detrimental injuries in terms of attrition, military readiness, and medical cost is the lower leg stress fracture. The process leading to injury is complex, believed to be caused by damage accumulation due to excessive stress and strain on the bone from training.

Previously, an extensive literature review, analysis, and development of a model have been met with mixed results (Woodmansee et al. 2004). In the report, it was noted that much of the data published in the literature is conflicting, with only a few factors consistently identified as being correlated to stress fracture. This is likely due to the complicated nature of the injury, which is dependent on the quality of the bone, the physical condition of the muscle supporting the bone, the training regimen, and even the skill and motivation of the recruit. In theory, a thorough biomechanical analysis will help explain seemingly unrelated risk factors (i.e., the effect of various factors on the injury mechanism). However, the relatively small number of stress fractures (3-10% prevalence) and random nature of the injury make prediction difficult.

Previous modeling efforts in this area were unsuccessful primarily because the equations predicting stress fracture found in the literature were unstable. The models accounted for bone changes at the cellular level, which led to very different predictions with only a small change in model input values when applied to a whole bone. To address the

shortcomings of the models published in the literature, a simpler dose-response model was developed. This section describes the development of this model.

2.1.4.1 Literature Review

In the previous literature review (Woodmansee et al. 2004), multiple risk factors have been identified. Table 10 (Bennell et al. 1999) provides a good summary of possible risk factors and the theoretical biomechanical mechanism to injury. Of these risk factors, it is our opinion that bone geometry, fitness level, menstrual irregularities and training regiment appear to be the most consistently identified. See Table 11.

**Table 10. Risk factors for stress fractures: possible mechanisms and inter-relationships.
(From Bennell et al. 1999)**

Risk factor	Mechanisms and inter-relationships
Low bone density	Decreased bone strength
Small bone size	Decreased bone strength
Skeletal alignment	Elevated bone strain, unaccustomed bone strain, muscle fatigue
Body size and composition	Elevated bone strain, menstrual disturbances, muscle fatigue, low bone density
Bone turnover	Low bone density, elevated bone strain, inadequate repair of microdamage
Muscle flexibility and joint range	Elevated bone strain, unaccustomed bone strain, muscle fatigue
Muscle strength and endurance	Elevated bone strain, unaccustomed bone strain
Low calcium intake	Greater rate of bone turnover, low bone density, inadequate repair of microdamage
Nutritional factors	Altered body composition, low bone density, greater rate of bone turnover, reduced calcium absorption, menstrual disturbances, inadequate repair of microdamage
Menstrual disturbances	Low bone density, greater rate of bone remodeling, increased calcium excretion
Training	Elevated bone strain, unaccustomed bone strain, greater number of loading cycles, muscle fatigue, inadequate time for repair of microdamage, menstrual disturbances, altered body composition
Inappropriate surface	Elevated bone strain, unaccustomed bone strain, muscle fatigue
Inappropriate footwear	Elevated bone strain, unaccustomed bone strain, muscle fatigue
Higher external loading	Elevated bone strain, muscle fatigue
Genetic factors	Low bone density, greater rate of bone remodeling, psychological traits
Psychological traits	Excessive training, nutritional intake/eating disorders

Bone Geometry: Currently, most bone geometry studies utilized either DXA or X-ray to estimate bone dimensions. Most of the X-ray data comes from a single set of data gathered from Israeli recruits. In addition, the accuracy of sectional area measurements from DXA is unknown.

Fitness Level: Poor fitness or low levels of activity is likely a factor for military training. Caution must be used when referring to studies using athletes or habitual runners. These populations likely have a different fitness level than that seen in BCT.

Menstrual Irregularity: Menstrual irregularity is more common in female athletic populations, where it has been associated with stress fracture. This factor has also been seen in female recruits but the number of recruits with menstrual irregularity is small. The exact pathway of menstrual irregularity to stress fracture is not known.

Training Regimen: Numerous studies have associated training or changes in training regimens with stress fracture. Due to space constraints and the difficulty in monitoring BCT, none of these studies published sufficient information to quantify training.

Table 11. Consistently identified risk factors for overuse injuries occurring during military training.

Risk Factor	Reference
Bone Geometry (CSA, lcm, width, modulus)	(Beck et al. 1996; Giladi et al. 1987; Milgrom et al. 1988; Milgrom et al. 1989)
Fitness Level	(Lauder et al. 2000; Milgrom et al. 2000; Montgomery et al. 1989; Shaffer et al. 1999)
Menstrual Irregularity	(Bennell et al. 1999; Winfield et al. 1997)
Training Regimen	(Garcia et al. 1987; Popovich et al. 2000; Ross 1993; Scully and Besterman 1982)

Also of interest is a review by Jones et al. (1994) that noted no difference in overuse injury rate per cumulative run mileage, regardless of the time frame the running occurred (Figure 2). This suggests that the number of steps or loading cycles is a dominant factor in this type of injury and reflects the accumulation of damage with each step.

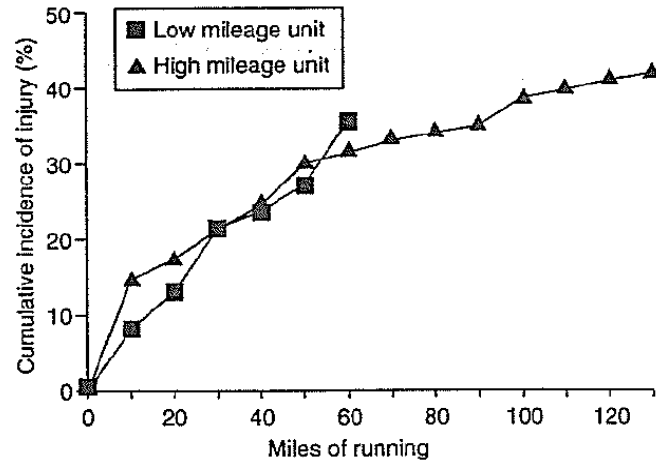


Figure 2. Cumulative incidence of injury by cumulative miles of running for 2 army infantry basic training units during 12 weeks of training.

Despite the differences in run distance, Final PFT runtimes were similar. (From Jones et al. 1994)

2.1.4.2 Methods

Direct measure of the four consistent risk factors identified in the literature is difficult in a large BCT population and, thus, the model was developed using less direct (and less accurate) estimates. For example, bone geometry, while important, cannot be measured directly to level of accuracy needed for stress fracture prediction. However, bone geometry is correlated to body mass, with heavy set individuals generally having bigger bones (Beck et al. 1996) and it is likely that the correlation also holds for Body Mass Index (BMI). Also, the accepted measure of aerobic fitness is oxygen consumption or VO_2 . Again, obtaining a direct VO_2 measurement from BCT recruits is impractical. However, BCT questionnaires routinely ask for a self-reported fitness level that can be used as a crude VO_2 estimate. As for the training regimen, ideally each individual's training would be quantified separately but a practical means to accomplish this has not been developed. Thus, we assume that all recruits perform the same training regimen—the one assigned in the training outline plan. For this initial model, we ignore the effects of menstrual irregularity on female stress fracture rates.

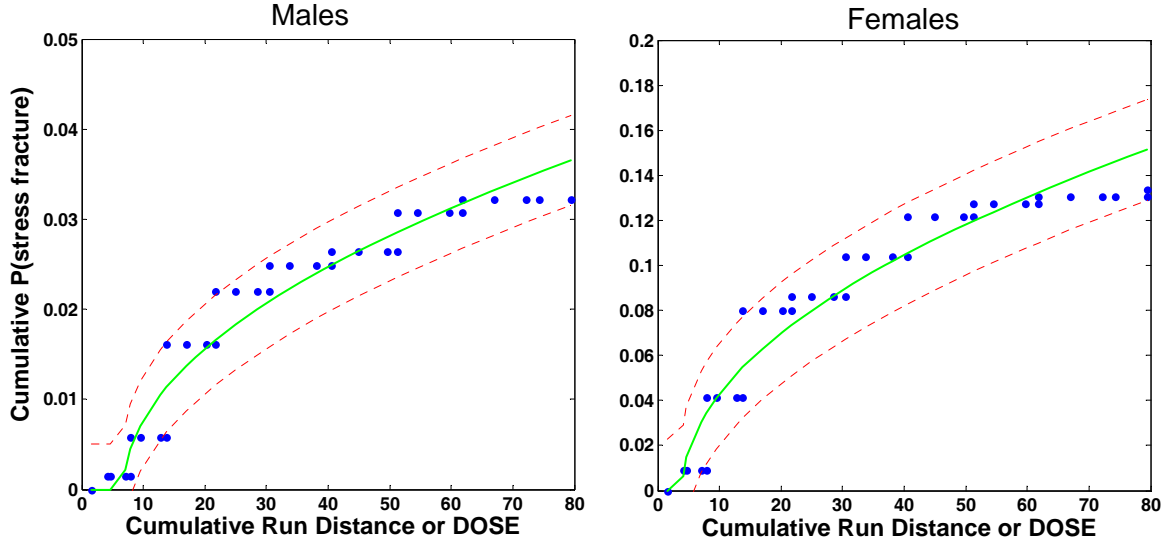


Figure 3. The cumulative stress fracture rate versus cumulative run distance for males and females of dataset G (see Appendix).

Lines represent the mean (solid) and 95% CI (dash).

To develop the response model, the observation by Jones et al. (1994) was applied to dataset Group G (see Appendix) by plotting the cumulative stress fracture incidence versus the cumulative distance run during training for males and females (Figure 3). Unfortunately, the dataset lacked the information to include marching but the effect is likely small due to the lower impact loads of marching. Under the assumption that these figures represent the average male or female probability of stress fracture, 1 km of running can be redefined as a dosage unit of “1.” Therefore, the figures also represent a cumulative “dose” versus cumulative injury (or chance of injury) stress fracture response model. Recruits more likely to be injured will have a larger dose per km run and those less likely will be able to run further before being subject to the same dosage as an average recruit. In developing an equation to represent injury response relationship, several key observations were incorporated. One is an initial offset to account for the lack of injuries during start of training. The second is that the injury rate increases rapidly initially and, third, that the injury rate continues to climb as the cumulative distance increases. These characteristics are all incorporated via the following equation:

$$P = A\sqrt{D - D_{\text{offset}}} \quad (9)$$

where P is the probability of stress fracture, D is the cumulative dose, D_{offset} is the dosage below which there are no stress fracture injuries, and A is a gender-based constant that adjusts the rapid initial and continued increase in injury likelihood with cumulative dosage.

The best values for A and D_{offset} were found for each gender using a least squares fit (Table 12).

Table 12. The best fit values for Equation (9) when applied to the male and female stress fracture versus dosage data from Group G.

	A	D_{offset}
Male	4.46E-3	6.3
Female	18.8E-3	6.8

Estimating training dosage can be difficult. Prior attempts at modeling stress fractures indicate that it is unfeasible to mimic the complex physiological and mechanical processes involved in the loading of bone. Nevertheless, from the literature it is apparent that some individuals are more susceptible to injury, which should be reflected in a higher dosage for the same distance run as an average individual. Identified factors include low physical conditioning, high or low BMI, and female gender (Table 11). Poor physical conditioning is likely contributing to fatigue, causing “bad form,” and a loss of coordination, which increases stress in the bone. Low BMI individuals (and female gender) have smaller bones, which are more easily damaged, and those with high BMI values put addition stress on tissues. To account for these factors, the following dosage definition was used:

$$D = \text{damage per unit training volume} \times \text{training volume} \quad (10)$$

Applying the cumulative distance concept:

$$D = (\text{damage/distance}) \times \text{cumulative distance} \times SF_{\text{gait}} \quad (11)$$

where “damage/distance” depends on an individual’s propensity for stress fracture and SF_{gait} weighs the effect of different gait (i.e., running has more affect on dose than marching). To account for physical conditioning and bone geometry in the damage/distance term, $VO_{2\text{max}}$ and BMI were used, respectively:

$$\text{damage/distance} = SF_{VO_2} (VO_{2\text{max}}) + SF_{\text{BMI}} (BMI - BMI_{\text{ideal}})^2 + SF_{\text{offset}} \quad (12)$$

Since $VO_{2\text{max}}$ was not measured in Group G, we estimate it based on self-reported questionnaire data provided. Assuming $VO_{2\text{max}}$ ranges from 45-85 ml/kg/min for males and 40-85 ml/kg/min for females (McArdle et al. 1991), a simple linear relationship between the questionnaire data and the $VO_{2\text{max}}$ range was computed where those that reported the highest fitness had the largest $VO_{2\text{max}}$ and vice versa. BMI (kg/m^2), which is weight / height², was provided in the dataset and the term $(BMI - BMI_{\text{ideal}})^2$ accounts for the

observed nonlinear trend. A plot of BMI and injury rate suggests that BMI_{ideal} is around 25 kg/m² and 22 kg/m² for males and females, respectively (Figure 4).

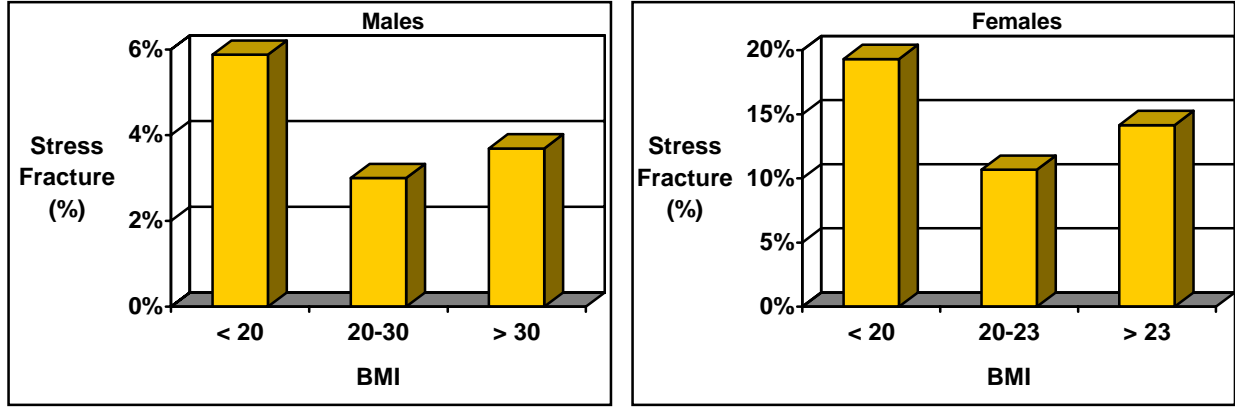


Figure 4. The percent of males (left) and females (right) from dataset Group G that sustained a stress fracture when categorized by BMI.

Note the nonlinear relationship seen for both genders.

To determine the three scaling factors (SF_{VO2max} , SF_{BMI} , and SF_{offset}) from Equation (12), an optimization scheme was employed. For each gender, Group G subjects were split into 5 different subgroups, depending on their questionnaire response and BMI values (high and low activity, high BMI, high and low aerobic activity). Since the stress fracture injury rate at the end of training, P , is known for each group, the response equation (Eqn. (9)) can be used to determine the corresponding dosage, D . Combining Equations (11) and (12) yields:

$$D = \left(SF_{VO_2} (VO_{2max}) + SF_{BMI} (BMI - BMI_{ideal})^2 + SF_{offset} \right) \times \text{cumulative distance} \times SF_{gait} \quad (13)$$

where the only unknowns are three scaling factors (SF_{VO2max} , SF_{BMI} , and SF_{offset}). Using least squares, the best fit values for the scaling factors was found that predicts the observed cumulative damage D for the seven sub-groups (Table 13). Using a standard Receiver-Operator Curve analysis, a cutoff value of 0.072 for males and 0.181 for females for P optimized the predictive capability of the model.

Table 13. Stress fracture scaling factors for Equation (13).

Determined by minimizing the error between the predicted and observed stress fracture rate for males and females of dataset Group G.

	SF_{VO_2}	SF_{BMI}	SF_{offset}
Male	-0.1319	0.029	9.87
Female	-0.0677	0.027	4.79

2.1.4.3 Results

To estimate model accuracy, model predictions were calculated using input values from dataset Group G (see Appendix), which contains data from approximately 681 male and 336 female recruits who underwent U.S. Army BCT circa 1997. Input variables included self-reported fitness level questionnaire answers, BMI, and gender. Accuracy was assessed by comparing model predictions to the observed stress fracture prevalence at the end of training. In addition, model predictions were to be compared to those derived from the statistically-based TIC procedure mentioned previously (See Section 2.1.1.1). However, no significant factors were found and a TIC was not performed.

Male Recruits

The initial prevalence (overall stress fracture rate) was 3% for the males. The model had a prognostic accuracy of 94% and a positive likelihood ratio (PLR) and 95% confidence interval of 3.2 (0.8-12.9).

Table 14. Stress fracture model accuracy for male recruits (Group G) undergoing basic combat training at various Army training sites.

Model	Observed	
	StFx	No StFx
Pred StFx	2	18
Pred No StFx	19	586

Sensitivity = 0.10; Specificity = 0.97; Positive pretest probability = 3%; Positive post-test probability = 10%; Negative post-test probability = 3%. A TIC analysis found no significant factors.

Female Recruits

The initial prevalence (overall stress fracture rate) was 13% for the females. The model had a prognostic accuracy of 73% and a PLR and 95% confidence interval of 3.2 (0.9-2.5).

Table 15. Stress fracture model accuracy for female recruits (Group G) undergoing basic combat training at various Army training sites.

Model	Observed	
	StFx	No StFx
Pred StFx	12	56
Pred No StFx	26	205

Sensitivity = 0.10; Specificity = 0.97; Positive pretest probability = 3%; Positive post-test probability = 10%; Negative post-test probability = 3%. A TIC analysis found no significant factors.

2.1.4.4 Discussion

Using concepts and factors identified in the literature, a dosage and response model for stress fracture prediction during training was developed. Factors incorporated into the dosage calculation include bone geometry (via BMI) and fitness level (from questionnaire answers). The response model is based on the observed relationship between running distance and injury likelihood, which reflects the accumulation of bone damage during cyclic loading. Thus, the dose-response algorithm accounts for the significant factors identified in the literature without overly complex physiologically-based equations, which were previously found to be unstable. In addition, a TIC analysis of the data found no statistically relevant variables, which highlights the potential of a model to be more robust than a traditional statistical approach.

There are a number of ways model accuracy can be improved. Current estimates of VO_2 from questionnaire data are unverified and a more direct method of measure VO_2 (or different measure of fitness) should be beneficial. Also, the assumed regimen for Group G does not contain any marching, and, thus, the model is unable to account for this mode of gait in the accumulation of damage and stress fracture prediction. In addition, the response model in its current form does not account for bone remodeling or the ability of bone to adapt to the additional stresses of BCT.

2.1.5 Lower-body Overuse Injury

In addition to stress fractures, the other common and detrimental injury during BCT is the soft tissue overuse injury of the lower body. This includes ailments such as tendinitis, bursitis, and fasciitis. The progression (and mechanism) of injury is similar to stress fracture—loading causes damage accumulation in the tissues which eventually leads to an injury.

2.1.5.1 Literature Review

Most research on soft tissue injury has been performed on the tendon, which is the structure connecting muscle to bone. Although there is a lack of understanding of the progression of overuse injury and the effect of loading, the general consensus is that loading has a short term effect of damaging the tendon but the long term effect is an adaptation and strengthening of the tissue (Archambault et al. 1995). In addition, researchers believe that adaptation depends on loading history but that data to support this hypothesis is difficult to acquire because of the limited loading history information available (Archambault et al. 1995).

Several attempts have been made to develop models to predict the changes in tendon structure and properties with loading. However, none appear capable of predicting injury in populations such as recruits undergoing BCT. This includes a model by Wren et al. (2000) that predicts changes in cross-sectional area, modulus, and strength of tendons from exercise, disuse, and remobilization. While the model is not injury-based and of limited use for this project, it predicts an adaptation time constant of three months, which suggests that damage accumulation rather than tissue adaptation is dominant in the time frame of BCT (2-3 months). A Paris Law-type damage model was developed by Adeeb et al. (2004), which is similar to those seen for stress fractures. However, these types of models were found to be unstable for stress fracture prediction when applied to large populations such as recruits undergoing BCT and are likely to be unstable in the prediction of soft tissue injuries as well. A third model was described in the literature—a damage model developed for when tendons exceed the elastic limit (Natali et al. 2005). Unfortunately, this is an acute injury situation and not associated with overuse injuries.

Like stress fracture, there are many risk factors associated with overuse injury. In general, these can be categorized into three groups: training regimen, anthropometry, and fitness level. Regimen factors include training conditions such surface and footwear (Jones 1983). However, the most common belief is that overuse injuries occur because of the sudden increase in exercise, which is often characterized by an increase in running distance per week as well as longer duration (amount per day) and higher frequency (number of days per week) workouts (Jones 1983; Jones et al. 1994). Note also that running mileage was a key factor (Figure 2) and used in the development of the stress fracture model. Anatomical factors include physical anomalies such as alignment issues, body weight, gender, and range of motion (Jones 1983; Krivickas 1997). It is thought that fitness level also plays an important role, with prior physical condition and/or injury, and technique being main factors (Jones 1983; Jones et al. 1994).

From the literature review, it is evident that most studies agree that overuse injuries are caused by a complex process that entails the accumulation of damage from excessive

loading. However, as noted by Krivickas (1997), the findings in the literature for some factors are inconsistent, correlations do not prove cause and effect, and results have not been evaluated for reliability and repeatability. Nevertheless, like stress fractures, training regimen, fitness level, and internal loading conditions (tissue geometry, body weight, etc.) are common identified risk factors that appear to be important. Also of note is the agreement that the sudden increase in training is a contributor to injury.

2.1.5.2 Methods

As with stress fractures, a thorough biomechanical model should be able to account for and bring together the seemingly unrelated risk factors but is too complex to be practical. Thus, a simpler model has been developed that accounts for the main overuse injury risk factors identified in the literature: training regimen, fitness level, and internal loading conditions. As before, the model consists of a dosage calculation to account for the identified risk factors and training amount, and a response model, which accounts for the initial increase in injury rate due to the sudden change in training and the long-term decrease in injury rate due to tissue strengthening.

Because of the similarities to stress fractures in terms of injury progression (damage accumulation), the same form of the response equation that was developed for stress fractures is used for overuse injuries, where the probability of injury P is based on the square root of the dosage (Eqn (9)). The square root gives an initial increase in injury probability due to the suddenness in training from BCT, and a leveling off of P as recruits become accustomed to the new training levels. As mentioned in the stress fracture section, there is also a damage offset, D_{offset} , which accounts for the initial portion of training where no injuries occur.

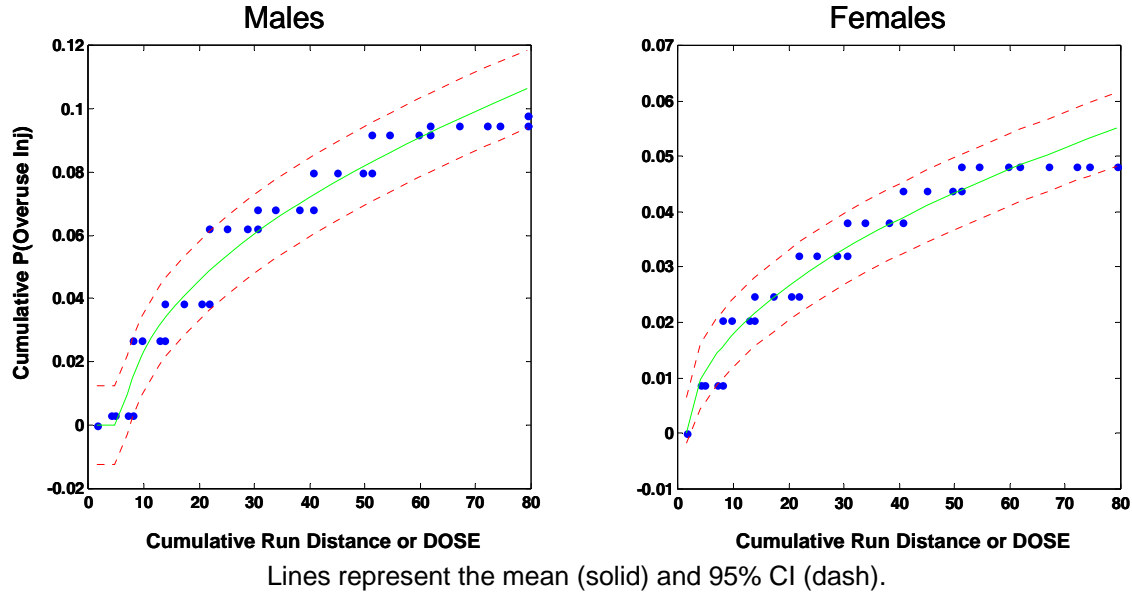


Figure 5. The cumulative overuse injury rate versus cumulative run distance for males and females of dataset G (see Appendix).

Using dataset Group G, a plot of cumulative overuse injury and cumulative distance run was plotted for both genders (Figure 5) and a least squares fitting technique was used to find the best parameter values (Table 16). Under the assumption that this curve represents the response of the average recruit, 1 km of running was again defined as a unit dosage of “1” and an algorithm to adjust dosage for different individuals and training regimens was sought.

Table 16. The best fit values for Equation (9) when applied to the male and female overuse injury versus dosage data from Group G.

	A	D_{offset}
Male	6.25E-3	1.7
Female	12.4E-3	6.4

The dosage component is again an overall damage equation identical to that of stress fractures (Eqn (11)). However, the damage/distance term is slightly different to reflect the difference between overuse injuries and stress fractures. Like the stress fracture model, this term incorporates known risk factors that affect an individual’s likelihood of injury by using VO_2 and BMI as estimates of fitness level and loading conditions. Unlike stress fractures, however, the effect of BMI on injury probability was found to be different, with high BMI being detrimental to males and low BMI being detrimental to females (Figure 6). The effect of BMI is likely two-fold. First, low BMI individuals will have smaller tissues, which

are more easily damaged with training, and high BMI individuals will be exposing their tissues to higher loads. Second, we hypothesize BMI also reflects pre-BCT training and may have a social aspect. Low BMI females (skinny) are less inclined to exercise compared to those that are heavier set. On the other hand, it is overweight males (high BMI) that are less likely to exercise on a regular basis. Both of these groups will not be as prepared for the sudden increase in exercise from BCT. Thus, the damage/distance component of Equation (11) becomes:

$$\text{damage/distance} = SF_{VO_2} (VO_{2\max}) + SF_{BMI} (BMI) + SF_{\text{offset}} \quad (14)$$

where $VO_{2\max}$ (ml/kg/min) is estimated from self-reported fitness level questionnaire responses and BMI (kg/m^2) is computed from weight and height. This is reflected in the equation for overuse injury damage:

$$D = (SF_{VO_2} (VO_{2\max}) + SF_{BMI} (BMI) + SF_{\text{offset}}) \times \text{cumulative distance} \times SF_{\text{gait}} \quad (15)$$

In a similar method to that used for the stress fracture model, recruits from Group G were broken down by gender into 6 subgroups depending on fitness level and BMI values to determine the three scaling factors ($SF_{VO_{2\max}}$, SF_{BMI} , and SF_{offset}) from Equation (15) (Table 17). Using a standard Receiver-Operator Curve analysis, a cutoff value of 0.071 for males and 0.2 for females for P optimized the predictive capability of the model for overuse injuries.

Table 17. Overuse injury scaling factors for Equation (15).

Determined by minimizing the error between the predicted and observed injury rate for males and females of dataset Group G.

	SF_{VO_2}	SF_{BMI}	SF_{offset}
Male	-0.0671	0.1851	0.7477
Female	-0.1448	-0.2589	16.01

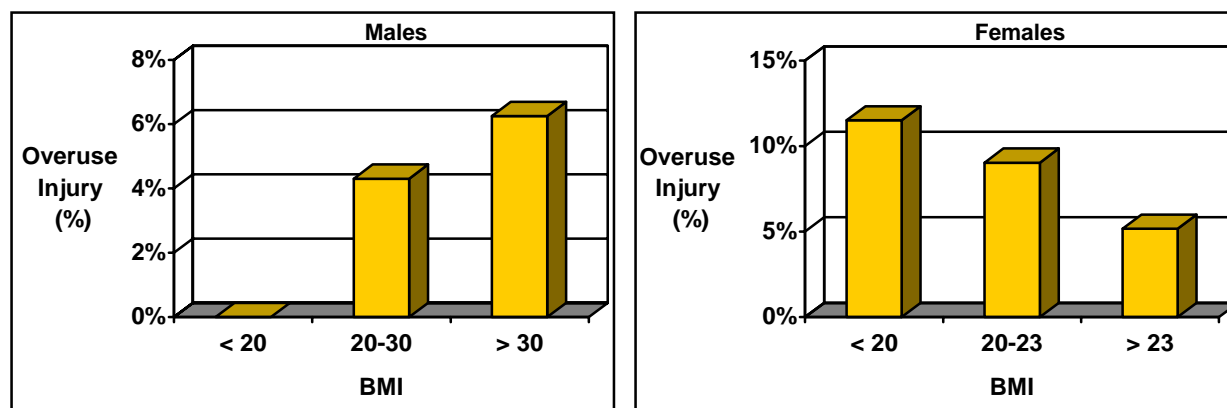


Figure 6. The percent of males (left) and females (right) from dataset Group G that sustained a lower-body overuse injury when categorized by BMI.

Note the opposing linear relationship seen for the genders.

2.1.5.3 Results

To estimate model accuracy, model predictions were calculated by reapplying input values from dataset Group G (see Appendix), which contains data from approximately 681 male and 336 female recruits who underwent U.S. Army BCT circa 1997. Input variables included self-reported fitness level questionnaire answers, BMI, and gender. Accuracy was assessed by comparing model predictions to the observed stress fracture prevalence at the end of training. In addition, model predictions were to be compared to those derived from the statistically-based TIC procedure mentioned previously (See Section 2.1.1.1).

Male Recruits

The initial prevalence (overall overuse injury rate) was 5% for the males undergoing the U.S. Army BCT. The TIC analysis identified a greater number of initial PFT push-ups as the only significant predictor. Although the TIC performed better, both the TIC and model predictions are comparable, with high prognostic accuracy (95% for TIC and 88% for the model) and positive post-test probabilities (Table 18). Positive likelihood ratio (PLR) and 95% confidence interval for the TIC and model were 4.2 (0.5-34.9) and 1.6 (0.6-4.1), respectively.

Table 18. A comparison of the accuracy of a Test Index Cluster (TIC) analysis to that of the lower-body overuse injury model for male recruits undergoing basic combat training at various Army training sites (Group G).

TIC	Observed		MODEL	Observed	
	OvrInj	NoOvrInj		OvrInj	NoOvrInj
> 77 1 st PFT Push-ups	1	5	Pred OvrInj	4	54
< 77 1 st PFT Push-ups	24	524	Pred No OvrInj	24	543

For the TIC, one item was identified: a push-up count > 77 on the initial PFT test. A recruit with this item had a significantly greater chance of sustaining an injury (Sensitivity = 0.04; Specificity = 0.99; Positive pretest probability = 5%; Positive post-test probability = 17%; Negative post-test probability = 4%). For the injury model, accuracy was similar but less accurate (Sensitivity = 0.14; Specificity = 0.91; Positive pretest probability = 4%; Positive post-test probability = 7%; Negative post-test probability = 4%). Number of samples in TIC and model differ due to missing data.

Female Recruits

The initial prevalence (overall overuse injury rate) was 9% for the females undergoing the U.S. Army BCT. The TIC analysis identified a small BMI as the only significant predictor. Both the TIC and model predictions are comparable, with similar prognostic accuracy (88% for TIC and 87% for the model) and positive post-test probabilities (Table 19). Positive likelihood ratio (PLR) and 95% confidence interval for the TIC and model were 2.7 (0.8-9.3) and 3.9 (1.3-11.5), respectively.

Table 19. A comparison of the accuracy of a Test Index Cluster (TIC) analysis to that of the lower-body overuse injury model for female recruits undergoing basic combat training at various Army training sites (Group G).

TIC	Observed		MODEL	Observed	
	OvrInj	NoOvrInj		OvrInj	NoOvrInj
< 19.4 BMI	3	11	Pred OvrInj	4	10
> 19.4 BMI	25	271	Pred No OvrInj	24	261

For the TIC, one item was identified: BMI < 19.4. A recruit with this item had a significantly greater chance of sustaining an injury (Sensitivity = 0.11; Specificity = 0.96; Positive pretest probability = 9%; Positive post-test probability = 21%; Negative post-test probability = 8%). For the injury model, accuracy was similar (Sensitivity = 0.14; Specificity = 0.96; Positive pretest probability = 9%; Positive post-test probability = 29%; Negative post-test probability = 8%). Number of samples in TIC and model differ due to missing data.

2.1.5.4 *Discussion*

Using the same concepts and equation form as that developed for stress fractures, a dosage and response model was created that predicts the likelihood of sustaining a lower-body overuse injury during training. The current model is based on the amount of damage sustained during running and incorporates several risk factors identified in the literature. Factors include fitness level (from questionnaire answers) as well as internal loading conditions and ability to adapt to the higher loading conditions of BCT (from BMI). The algorithms developed in this model are simpler but more stable than those in the literature, which should allow its application to a wider range of training regimens and populations.

Overall, the model performed with similar accuracy to the purely statistically-based TIC method. Of interest is that the TIC identified a higher number of push-ups in the 1st PFT as being predictive of overuse injury for males. The mechanism for this relationship is unclear and may be a Type I error—where a variable was erroneously found to be a factor because multiple variables were tested. Additional analysis of other datasets is needed to confirm push-up ability as a risk factor for overuse injuries.

As with the stress fracture model, model accuracy can be improved with more precise estimates of VO_2 , the incorporation of marching distances in the dosage estimate, and a tissue adaptation component.

2.2 Model Validation

Having developed three performance (run, sit-up, push-up) and two injury (stress fracture, overuse) models based on concepts and risk factors found in the literature, model parameters were estimated using a U.S. Army dataset (Group G). Model prediction accuracy was comparable to a standard statistical test (TIC) when predicting performance and injury outcomes to Group G—the dataset from which the model parameters were derived.

Also of interest is how the models perform on additional, novel datasets, i.e., model validation. This gives an estimate of how the model is expected to perform in the field, where the actual performance and injury outcome to a completely different training regimen and population is unknown. Because the validation situation is different than that from which the model parameters have been developed, a decrease in accuracy is expected. However, if the dosage algorithms and response models have captured the underlying physiological mechanisms adequately, the reduction in accuracy should be smaller than that seen using a pure statistical approach.

2.2.1 Run Performance

To validate the run performance model, input values from dataset Group F were entered into the model and the prediction was compared to the observed run performance

at the end of training. Group F (see Appendix) was composed of 181 males and 167 females that underwent U.S. Army BCT at Ft. Jackson, SC in 1998 using the Standardized Training regimen. Unfortunately, due to the lack of regimen data, the same regimen was used from which the model parameters were optimized. Thus, the model (incorrectly) assumes that both Group F and Group G used the same regimen.

The results (Table 20) show that the run performance model accuracy was comparable to that of the statistical analysis using the same input measures. Unfortunately, because the lack of data forced the exact same training regimen to be used in both model development and validation, it is difficult to conclusively demonstrate the models ability to predict performance with novel training regimens. Nevertheless, the results suggest that the modeling effort is “on the right track” and the predictions have the potential to be extrapolated to different regimens. As expected, however, accuracy was reduced when the model (and TIC) was applied to the new dataset. We anticipate the model accuracy to be better than the TIC if the true training regimen is known and the model algorithms are implemented correctly.

Table 20. Run performance model and TIC validation results.

		Men		Women	
		Group G (performance on derivation dataset)	Group F (performance on cross-validation)	Group G (performance on derivation dataset)	Group F (performance on cross-validation)
TIC	Prognostic Accuracy	80%	75%	88%	82%
	PLR (95% CI)	2.1 (1.1 to 4.1)	2.6 (1.4 to 4.7)	4.5 (2.6 to 7.9)	1.5 (0.4 to 5.6)
Model	Prognostic Accuracy	89%	83%	88%	80%
	PLR (95% CI)	2.3 (0.5 to 9.4)	3.5 (1.4 to 18)	2.6 (1.1 to 6.3)	1.9 (0.7 to 5.2)

A single factor was used for the TIC: 1st PFT run time (see Sih and Shen 2006). For the model, 1st PFT run time, height, weight, and regimen were factors.

2.2.2 Sit-Up Performance

As with running, the sit-up model was validated by applying the model to dataset Group F but with the same training regimen as Group G. For both males and females, the model accuracy increased when applied to the validation dataset. TIC accuracy also

increased to a lesser degree for females. Unfortunately, there was insufficient previous activity data to make a TIC prediction for the males. See Table 21.

Because model (and TIC) accuracy increased with the validation dataset, the results suggest that there measures or factors exist that can improve the results or possibly that the factor parameters (weightings) should be adjusted. For example, the TIC analysis found height to be important. Because TIC accuracy was not reduced when applied to the validation dataset, this supports the addition of height into the model as well. This requires an additional biomechanical term in the dosage to account for the “leverage” a tall recruit must overcome during sit-ups and was incorporated in a subsequent model (see 2.3.1 Sit-Up Performance, page 33). Unfortunately, no specific conclusions can be drawn from the male validation because of missing data.

Table 21. Sit-up performance model and TIC validation results.

		Men		Women	
		Group G (performance on derivation dataset)	Group F (performance on cross-validation)	Group G (performance on derivation dataset)	Group F (performance on cross-validation)
TIC	Prognostic Accuracy	74%	No Previous Activity Data	81%	84%
	PLR (95% CI)	2.1 (1.4 to 3.0)	---	1.9 (0.6-5.9)	5.8 (0.9-38.2)
Model	Prognostic Accuracy	75%	80%	66%	74%
	PLR (95% CI)	1.7 (1.2-2.5)	3.7 (2.1-6.2)	1.7 (1.2-2.3)	3.0 (2.0-4.7)

For males, two factors were used for the TIC: number of 1st PFT sit-ups and self-reported previous activity. For females, number of 1st PFT sit-ups and height were the two significant TIC factors. For the model, number of 1st PFT sit-ups, height, weight, and regimen were factors. See Section 2.1.2.

2.2.3 Push-up Performance

A similar result is seen with the push-up model validation (Table 22). Again, the model was validated by applying the model to dataset Group F but with the same training regimen as Group G. And as before, accuracy increased substantially in both the male and female validation datasets, with both genders having a prognostic accuracy greater than or equal to 85%. Because both sit-up and push-up model accuracy increased when applied to Group F and yet was well below accuracy levels seen in the running model, it calls into

question whether Group G is a valid dataset for sit-ups and push-ups. Additional datasets will need to be analyzed to see if these models continue to have inconsistent predictions.

Table 22. Push-up performance model and TIC validation results.

		Men		Women	
		Group G (performance on derivation dataset)	Group F (performance on cross- validation)	Group G (performance on derivation dataset)	Group F (performance on cross- validation)
TIC	Prognostic Accuracy	75%	No Previous Activity Data	85%	87%
	PLR (95% CI)	2.3 (1.7-3.2)	---	6.4 (4.8-8.5)	4.7 (1.1-20.6)
Model	Prognostic Accuracy	73%	86%	73%	85%
	PLR (95% CI)	1.9 (1.4-2.6)	4.4 (2.0-10.1)	0.6 (0.2-2.1)	3.4 (0.8-14.8)

For males, three factors were used for the TIC: number of 1st PFT push-ups, self-reported previous activity, and age. For females, only height was a significant TIC factor. For the model, number of 1st PFT push-ups, height and regimen were factors. See Section 2.1.2.

2.2.4 Stress Fracture

To validate the stress fracture model, input values from dataset Group A and C (see Appendix) were entered into the model and the prediction was compared to the observed injury rate at the end of training. Group C was composed of 1,286 males and Group A were 2,963 females undergoing U.S. Marine Corps BCT at San Diego and Parris Island, respectively. Unfortunately, both datasets only contained injury information for those that passed BCT—recruits with severe injuries or were unfit the pass the final PFT were not included in either dataset. Thus, because of limitations in the available datasets the validation accuracy results are not reflective of the incoming recruit population.

The results (Table 23) show that model accuracy drops when applied to the validation dataset but that the positive likelihood ratio becomes significantly greater than one. In addition, it should be noted that validation of the TIC method was not done because no significant factors were found in the original dataset (see Section 2.1.4). Thus, while the model's accuracy dropped with the validation dataset, it was able to create both a model and retain most the model's predictive capacity when applied to the novel dataset.

Table 23. Stress fracture model validation results.

		Men		Women	
		Group G (performance on derivation dataset)	Group C (performance on cross-validation)	Group G (performance on derivation dataset)	Group A (performance on cross-validation)
TIC	Prognostic Accuracy	NS	---	NS	---
	PLR (95% CI)	---	---	---	---
Model	Prognostic Accuracy	94%	82%	73%	72%
	PLR (95% CI)	3.2 (0.8-12.9)	2.5 (1.2-5.1)	1.5 (0.9-2.5)	1.8 (1.3-2.3)

No significant TIC factors were found for either gender. For the model, self-reported previous activity and number of days of aerobic exercise per week as well as BMI and regimen were factors. See Section 2.1.4.

2.2.5 Lower-body Overuse Injury

To validate the overuse injury model, input values from dataset Group A and C (see Appendix) were entered into the model and the prediction was compared to the observed injury rate at the end of training. These were the same validation groups as those used for the stress fracture model and, as before, only contain information on those that passed BCT. This is most reflective in the men, where none of those that passed BCT sustained an overuse injury (Table 24).

In general, the results are encouraging but not conclusive. The lack of a complete validation dataset hampered the attempt at showing the robustness of the model for the male group. However, the model did perform very similarly to the TIC when validating with the women datasets.

Table 24. Overuse injury model and TIC validation results.

		Men		Women	
		Group C (performance on derivation dataset)	Group G (performance on cross- validation)	Group A (performance on derivation dataset)	Group G (performance on cross- validation)
TIC	Prognostic Accuracy	95%	No 1 st Push-up measured	88%	75%
	PLR (95% CI)	4.2 (0.5-34.9)	---	2.7 (0.8-9.3)	1.6 (1.2-2.2)
Model	Prognostic Accuracy	88%	70%	87%	76%
	PLR (95% CI)	1.6 (0.6-4.1)	No inj reported	3.9 (1.3-11.5)	1.5 (1.0-2.1)

For males, one factor was used for the TIC: number of 1st PFT push-ups. For females, only BMI was a significant TIC factor. For the model, the self-reported activity level and number of aerobic days per week as well as BMI and regimen were used.

2.3 Model Refinement

From the knowledge gained from the previous model development, it is apparent that certain modifications may improve model accuracy. This section describes an update to the sit-up model. For sit-ups, the TIC analysis benefited from the inclusion of height as a factor, a variable not directly utilized in the performance model because it was not identified in the literature review. Thus, the sit-up performance model was modified to directly account for height.

2.3.1 Sit-Up Performance

The previous TIC analysis of female sit-ups (see page 11) suggests that height is an important factor where being tall is detrimental to passing the Final APFT Sit-Up. The inverse relationship between height and performance can be explained from a biomechanical perspective. Sit-ups require a torque to be produced about the hip to lift the head, arms, and trunk (HAT) and taller individuals have to exert a greater torque to perform the same movement as a shorter individual due to the added “leverage.”

2.3.1.1 Methods

For this model, several assumptions regarding torque, height, and weight are made:

- The maximum possible sit-up rate is determined, in part, by the maximum possible torque a person is capable of generating about the hip from the abdominal and hip flexor muscles

- The maximum possible torque (i.e., through perfect training) is the same for all people
- The maximum possible sit-up rate can be estimated from a biomechanical analysis involving the maximum possible torque, and the person's estimated HAT mass and center of mass location.

For the biomechanical analysis, we assume the upper-body can be modeled as a point mass and that the maximum angular acceleration (and torque) occurs when the body is horizontal (bottom of sit-up) as shown in Figure 7.

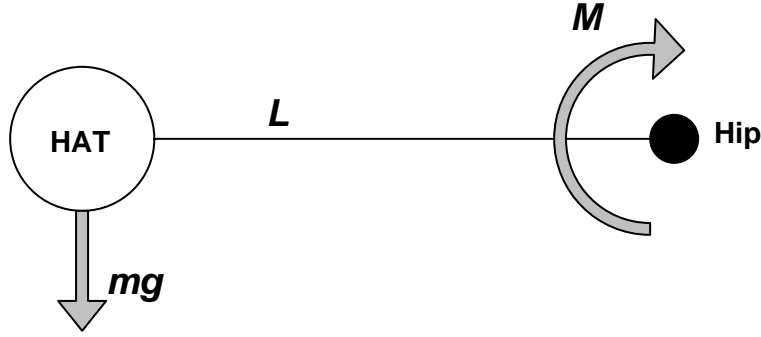


Figure 7. A free-body diagram of the sit-up.

The head, arms, and trunk (HAT) are subject to the force due to gravity (mg) and the torque (M) acting with moment arm, L .

From Figure 7, we can write the equation of motion to determine the angular acceleration (α , rad/s²) about the hip from the torque and HAT inertial properties.

$$M - mgL = m(\alpha L)L \quad (16)$$

where M is the torque produced about the hip, m is the mass of the HAT, L is the distance (m) from the HAT mass to the hip, and g is gravity (9.81 m/s²).

Based on the assumption that everyone is capable of generating the same maximum torque, it is possible to determine the angular acceleration of an individual as a function of HAT properties and the acceleration of another individual:

$$\begin{aligned} M - m_1 g L_1 &= m_1 \alpha_1 L_1^2 \\ M - m_2 g L_2 &= m_2 \alpha_2 L_2^2 \\ -m_1 g L_1 + m_2 g L_2 &= m_1 \alpha_1 L_1^2 - m_2 \alpha_2 L_2^2 \\ \alpha_2 &= \frac{m_1 \alpha_1 L_1^2 + m_1 g L_1 - m_2 g L_2}{m_2 L_2^2} \end{aligned} \quad (17)$$

where subscript “1” and “2” denote two different individuals. If we assume the individual “1” is the average person, then performance level P (see Equation (7)) can be redefined as a ratio of an individual’s predicted α_2 and α_1 , the acceleration for the average person.

$$P = \frac{\alpha_2}{\alpha_1} \quad (18)$$

Thus, the new P reflects an individual’s ability to perform relative to the average person based on HAT height and weight differences. Shorter, lighter individuals will have a theoretical higher level of attainable sit-up performance since the applied maximum torque will cause a greater acceleration and, hence, sit-up rate.

To use this equation, an average person’s α_1 and HAT properties (L_1, m_1) need to be estimated. In addition, an individual’s HAT properties (L_2, m_1) are also needed. To estimate α_1 , we note that the maximum sit-up rate was estimated to be 150 reps/min from World Record performances and assume the average person is capable of 120 reps/min or 2 sit-ups/s with ideal training. If a proper sit-up causes the HAT to follow a 90 degree arc, with a peak angular velocity at 45 degrees, and we assume a saw-tooth velocity profile, then the angular velocity vs. time plot can be represented as shown in Figure 8.

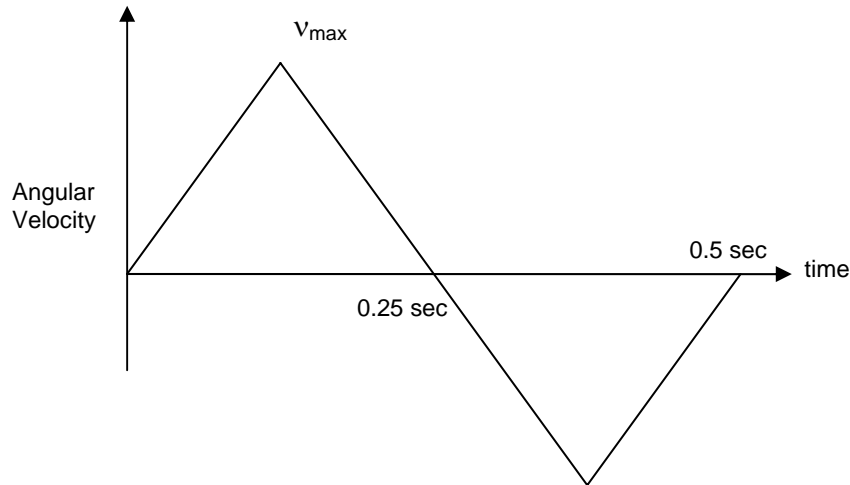


Figure 8. The estimated saw-tooth angular velocity profile for performing a single sit-up at 120 reps/min.

v_{\max} is the maximum angular velocity. Because of the assumed saw-tooth profile, angular acceleration α can be estimated from v_{\max} and the slope of the “saw-tooth.”

By definition, angular displacement, velocity, and time are related by:

$$D = \int V dt \quad (19)$$

where D (rad) is angular displacement, V (rad/s) is angular velocity, and t (s) is time. Thus, the estimated v_{\max} for the average person’s sit-up is:

$$\begin{aligned}\frac{\pi}{2} &= 0.5 \cdot v_{\max} \cdot 0.25 \text{ sec} \\ v_{\max} &= 4\pi\end{aligned}\tag{20}$$

And α_1 is estimated as:

$$\alpha_1 = \frac{dv}{dt} = \frac{v_{\max} - 0}{\frac{1}{8} \text{ sec}} = 32\pi \text{ rad} / \text{sec}^2\tag{21}$$

To estimate the HAT inertial properties (mass and distance to the hip joint), we turned to cadaveric studies where regressions were developed based on overall height (H) and body weight (m_{body}). See Figure 9 and Table 25. We assume that the average male is 1.753 m and weighs 75 kg. The average female is assumed to be 1.615 m and 60 kg. Using the same dosage (Equation (8)) and performance response (Equation (6)) as before, the model parameter k_1 was re-optimized to account for the new P estimation in order to compute P for sit-ups. Males and females were analyzed separately.

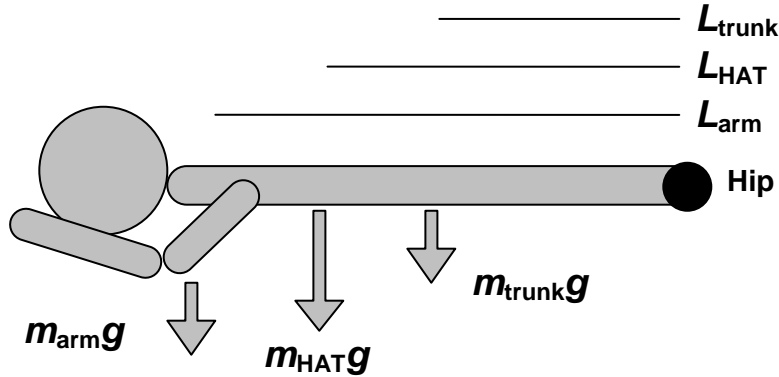


Figure 9. Free-body diagram to determine the mass and location relative to the hip for the head, arms and trunk (HAT).

Note: masses and distances for the arms and trunk were combined. It was assumed that the mass of the arms was located at the shoulder joint during the sit-up. The trunk includes the head. Arm and trunk masses and lengths were estimated from cadaveric studies.

Table 25. Estimates of the head, arms, and trunk (HAT) mass and distance from the hip joint.

From cadaveric studies (Clauser et al. 1969; Drillis 1958) and Figure 9.

Source: (Drillis 1958)		
	Stature or Total Height	H
	Floor-Hip Length	0.530 H
	Top of Head-Hip Length	(1-0.530)H = 0.47 H
	Hip-Shoulder Length	0.288 H
Source: (Clauser et al. 1969)		
	Trunk & Head Mass	$m_{\text{trunk}} = 0.5801 m_{\text{body}}$
	Trunk & Head Length	$L_{\text{trunk}} = 0.4079 \text{ Top of Head-Hip Length}$
	Arms Mass	$m_{\text{arms}} = 2 \times 0.0490 m_{\text{body}}$
	Arms Length	$L_{\text{arms}} = \text{Hip-Should Length}$
HAT (Head, Arms, Trunk) Properties		
	HAT Mass	$m_{\text{HAT}} = m_{\text{trunk}} + m_{\text{arms}}$
	HAT Length	$L_{\text{HAT}} = (m_{\text{trunk}} L_{\text{trunk}} + m_{\text{arms}} L_{\text{arms}}) / m_{\text{HAT}}$

2.3.1.2 Results

As before, to estimate model accuracy, model predictions were calculated using input values from dataset Group G (see Appendix), which contains data from approximately 681 male and 336 female recruits who underwent U.S. Army BCT circa 1997. Input variables for sit-ups were the 1st PFT sit-up count, gender, height, weight, and daily sit-up number. Accuracy was assessed by comparing model predictions to the observed Final PFT results. In addition, model predictions are compared to those derived from the statistically-based TIC procedure mentioned previously (see Statistical Methods Overview, pg. 4).

Sit-ups: Male Recruits

The initial prevalence (overall Final PFT failure rate) was 11% for the males on the final PFT sit-up exercise. The previously performed TIC analysis identified initial PFT sit-up number and previous activity level (self-rated questionnaire data) as significant predictors. Both the TIC and the previous model predictions had comparable prognostic accuracy (74% and 75%, respectively). The updated model prognostic accuracy was improved (88%). However, positive likelihood ratio (PLR) and 95% confidence interval was not as good, 1.3 (0.3-5.5). See Table 26 (and Table 6 for comparison).

Table 26. A comparison of the accuracy of a Test Index Cluster (TIC) analysis to that of the two sit-up performance models for male recruits undergoing basic combat training at various Army training sites (Group G).

TIC	Final PFT Sit-Up	
	Fail	Pass
Any one or more	17	118
None	16	359

MODEL	Final PFT Sit-Up	
	Fail	Pass
Pred Fail	20	98
Pred Pass	37	380

UPDATED MODEL	Final PFT Sit-Up	
	Fail	Pass
Pred Fail	2	14
Pred Pass	51	459

For the updated performance model, accuracy was similar but not as good compared to the previous analyses (Sensitivity = 0.04; Specificity = 0.97; Positive pretest probability = 10%; Positive post-test probability = 13%; Negative post-test probability = 10%). Number of samples in TIC and model differ due to missing data. See Table 6 as well.

Sit-ups: Female Recruits

The initial prevalence (overall Final PFT failure rate) was 21% for the females on the final PFT sit-up exercise. The previously performed TIC analysis identified initial PFT sit-up number and height as significant predictors. The TIC performed better than the previous model (prognostic accuracy of 81% and 66%, respectively). The updated model prognostic accuracy was improved substantially (78%). However, positive likelihood ratio (PLR) and 95% confidence interval was not as good, 2.4 (0.9-6.3). See Table 27 (and Table 7 for comparison).

Table 27. A comparison of the accuracy of a Test Index Cluster (TIC) analysis to that of the two sit-up performance models for female recruits undergoing basic combat training at various Army training sites (Group G).

TIC	Final PFT Sit-Up	
	Fail	Pass
Any one or more	17	118
None	16	359

MODEL	Final PFT Sit-Up	
	Fail	Pass
Pred Fail	20	98
Pred Pass	37	380

UPDATED MODEL	Final PFT Sit-Up	
	Fail	Pass
Pred Fail	6	10
Pred Pass	49	208

For the updated performance model, accuracy improved compared to the previous analyses (Sensitivity = 0.11; Specificity = 0.95; Positive pretest probability = 20%; Positive post-test probability = 38%; Negative post-test probability = 19%). Number of samples in TIC and model differ due to missing data. See Table 7 as well.

2.3.1.3 Validation

As before, the updated sit-up model was validated by applying the model to dataset Group F but with the same training regimen as Group G. For both males and females, the updated model accuracy increased slightly when applied to the validation dataset. See Table 28. Overall, the updated model performed very similarly between the two datasets, a feature not seen with the original model (or TIC).

Table 28. Sit-up results for the updated and original models.

		Men		Women	
		Group G (performance on derivation dataset)	Group F (performance on cross-validation)	Group G (performance on derivation dataset)	Group F (performance on cross-validation)
Updated Model	Prognostic Accuracy	88%	89%	78%	82%
	PLR (95% CI)	1.3 (0.3-5.5)	1.9 (0.3-14.3)	2.4 (0.9-6.3)	2.8 (0.8-10.1)
Model	Prognostic Accuracy	75%	80%	66%	74%
	PLR (95% CI)	1.7 (1.2-2.5)	3.7 (2.1-6.2)	1.7 (1.2-2.3)	3.0 (2.0-4.7)

2.4 Model Conclusions

In this report the development of four new models was described (sit-up and push-up performance; stress fracture and overuse injury) and validation results for the models as well as the running model developed previously were presented. While not conclusive, the results were generally favorable with the models having a similar accuracy as a pure statistically-based approach, especially when applied to a novel validation dataset.

Model development was based on developing a dose-response algorithm that took into account primary risk factors identified through statistical means and incorporating them into a simplified physiologically-based model. There are several advantages to this approach—risk factors can be integrated in a meaningful and often nonlinear way, biomechanical concepts are accounted for, and training regimen is incorporated directly. All these advantages should allow this approach to have similar accuracy to a statistical method with the added advantage of being able to predict outcomes to other populations and novel training regimens. In addition, the time course of performance and injury likelihood throughout training are a fundamental component of the model, a feature that would be very difficult to incorporate into a purely statistical model.

There were several issues with the datasets that were beyond the control of this project, which limited the ability to develop and validate the models. First, the datasets (acquired post hoc from other research studies) often collected different measures, making it difficult to find two datasets that contain the same input and output measures. Second, most of the datasets lack sufficient training regimen details to allow the models to develop algorithms and parameter values that are capable of predicting injury and performance across different regimens (i.e., many of the datasets contained no marching distances). Third, some of the datasets (U.S. Marine Corps) only contain measures from those that passed BCT, making it difficult to assess model performance at predicting the negative outcomes of injury and performance. We readily acknowledge that any data collected in the field on a large population such as that seen in BCT is a major undertaking, requiring many man-hours of preparation, data collection, and post-analysis. Steps were taken to incorporate the datasets including the use of questionnaire data to estimate VO_2 and making assumptions about the training regimen.

Clearly one of the key factors in improving model predictive accuracy is to acquire additional data that has more detailed training regimen measures. This would allow the models to better account for current and new performance factors, improve the model algorithms, and update the dosage calculations. In addition, an improved model from better regimen details should allow the model to extrapolate to different training regimens without the loss in accuracy currently seen.

2.4.1 Summary Tables

Table 29. Performance and injury model algorithm summary tables.

Includes response model formula, dosage calculation, and factors accounted for in the models.

Performance Models			
Response Model	$P = P_0 + (P_{\max} - P) g_1 \otimes W$		
Dosage	$W = W_{\text{rate}} \times \text{duration} \times \exp(b \times W_{\text{rate}})$		
Factors	Run	Sit-Up	Push-up
	Initial Runtime Height Weight Gender Regimen	Initial Sit-ups Gender Height Weight Regimen	Initial Push-ups Gender Regimen
Injury Models			
Response Model	$P_{\text{inj}} = A \times \text{sqrt}(D - D_{\text{offset}})$		
Dosage	$D = (\text{"damage"/dist}) \times \text{cumulative dist} \times SF_{\text{dist}}$		
Factors	Stress Fracture	Overuse Injury	
	Previous Activity Level Previous Aerobic Work BMI Gender Regimen	Previous Activity Level Previous Aerobic Work BMI Gender Regimen	

Table 30. Performance model validation summary tables for both males and females.

Performance Models—Males				
Prevalence		Run	Sit-Up	Push-up
		4%	11%	14%
TIC	Prognostic Accuracy	88%	74%	75%
	PLR (95% CI)	4.5 (2.6-7.9)	2.1 (1.4-3.0)	2.3 (1.7-3.2)
TOP/Updated TOP	Prognostic Accuracy	88%	75/88%	73%
	PLR (95% CI)	2.6 (1.1 to 6.3)	1.7 (1.2-2.5)/1.3 (0.3-5.5)	1.9 (1.4-2.6)
Performance Models—Females				
Prevalence		Run	Sit-Up	Push-up
		8%	21%	5%
TIC	Prognostic Accuracy	80%	81%	85%
	PLR (95% CI)	2.1 (1.1 to 4.1)	1.9 (0.6-5.9)	6.4 (4.8-8.5)
TOP/Updated TOP	Prognostic Accuracy	89%	66/78%	73%
	PLR (95% CI)	2.3 (0.5 to 9.4)	1.7 (1.2-2.3)/2.4 (0.9-6.3)	0.6 (0.2-2.1)

Tables include the TIC results for comparison.

Table 31. Injury model validation summary tables for both males and females.

Injury Models—Males			
Prevalence		Stress Fracture	Overuse Injury
		3%	4%
TIC	Prognostic Accuracy	---	95%
	PLR (95% CI)	---	4.2 (0.5-34.9)
TOP	Prognostic Accuracy	94%	88%
	PLR (95% CI)	3.2 (0.8-12.9)	1.6 (0.6-4.1)
Injury Models—Females			
Prevalence		Stress Fracture	Overuse Injury
		13%	9%
TIC	Prognostic Accuracy	---	88%
	PLR (95% CI)	---	2.7 (0.8-9.3)
TOP	Prognostic Accuracy	73%	87%
	PLR (95% CI)	1.5 (0.9-2.5)	3.9 (1.3-11.5)

Tables include the TIC results for comparison where possible.

3. Software Application Development

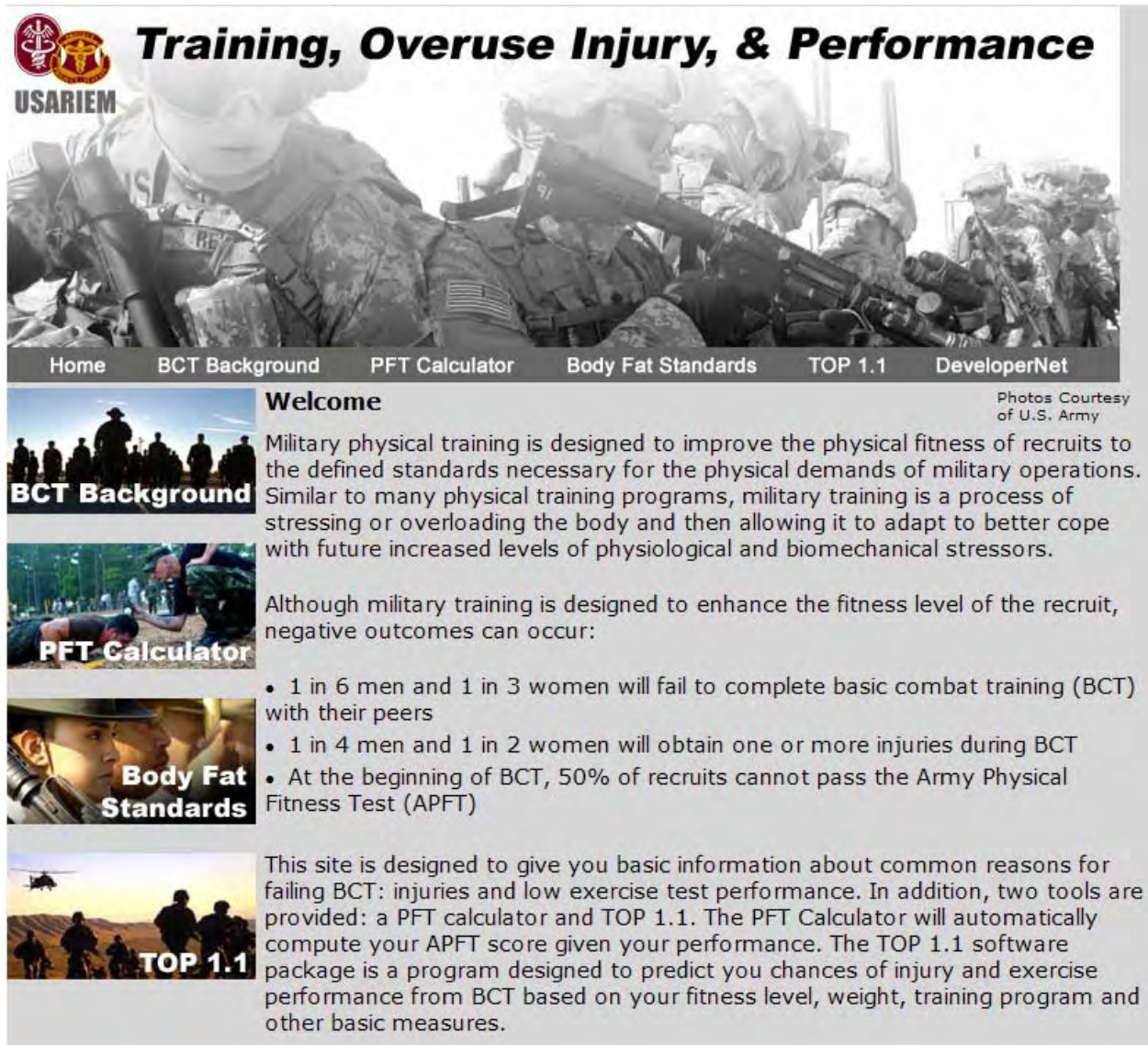


Figure 10. The TOP web-site home page.

The home pages serves as a gateway to TOP 1.1, the latest version of the software that incorporates the previously described performance and injury models, and other features such as a PFT Calculator.

3.1 Development Approach

In addition to developing the performance and injury models, a web-based software program was implemented using many of the features described in the conceptual mock-up from the previous report (Sih and Shen 2006). The objective of the software is to demon-

strate the feasibility of the model as a tool to help reduce injuries and maximize performance. Specifically, the goal is to develop software that will:

- Assess an individual's or group's injury risk in BCT
- Assess an individual's or group's poor performance risk in BCT
- Predict the time history of performance enhancement and injury risk
- Allow the evaluation of different training regimens

Also, additional features and updates were incorporated into TOP version 1.1, giving the program more utility and accuracy. Items include the inclusion of two additional information access web pages: a Basic Combat Training Education page and an access-limited DeveloperNet section where the data and documentation associated with the TOP project can be accessed. Both a PFT Score and a Body Fat Standards Calculator were also added. Rather than displaying as much information on the various aspects of BCT and the components of the TOP program, the Home Page only contains a brief description and is now used as a gateway to different sections of the program. (Figure 10)

Table 32. TOP Software release dates.

Version	Release Date
TOP 0.1α	Apr 2006
TOP 1.0	Nov 2006
TOP 1.1	Aug 2007

To provide the widest range of users to access the software, the original mockup was refined with four different user types defined, including goals, required model inputs, and desired outputs (Table 33). Depending on the type of user, we envision different levels of software functionality. Specifically, the users have been divided in the following manner:

Basic User: Interested in comparing their individual performance progress and injury likelihood during BCT to their peers. The output displays their individual scores and the average scores of their peers. This user can not change the training regimen, but can enter and modify their anthropometric data and physical fitness test (PFT) scores. Likely basics users are individual soldiers.

Mid-Level User: Focused with the performance and injury outcomes of a small group of individuals (2-30) involved in a training regimen. The output identifies individuals at high risk for performance failure or injury. This user can modify the properties of the individuals in the group and the training regimen. Likely mid-level users are drill sergeants and fitness advisors.

Table 33. TOP User Types.

Possible goals, needs, required inputs, and desired outputs from four potential users of a software package that incorporates the performance and injury models developed.

<i>Goals/Questions</i>	<i>Needs</i>	<i>Inputs</i>	<i>Outputs</i>
Basic User (Individual Soldier)			
Am I on track to pass FPFT?	Simple Personalized Prediction	Basic (Ht, wt, age, gender)	Relative Ranking
Might I be injured? What kind of injury?	Simple Interface (buttons, pictures)	Key Fitness/Inj/Anthro Measures	Graphs of progress & goals
How is my fitness relative to others right now?	Pre-fabricated Regimens	Simple History/Inj Questionnaire	
Mid-Level User (Drill Sgt/Fitness Trainer)			
Who is unfit, likely to not pass FPFT, need attention?	Simple Indiv Results for < 30 people	Basic (Ht, wt, age, gender)	Tables of indiv predictions (r/y/g)
As a group, are they on track to pass FPFT?	Limited Regimen Adjustment (sliders)	Key Fitness/Inj/Anthro Measures	Graphs of indiv progress & goals
Who is more likely to be injured?	Automated as much as possible	Pre-fabricated Regimens	
If I make them do "X", what happens to fitness? Injury?			
Group Level User (Company Commander)			
What % of recruits will pass FPFT?	Group Results for > 500 recruits	Same as Mid-Level	Summary Tables only
What % of recruits will be injured?	Limited Regimen Adjustment (sliders)		Graphs of pop. progress & goals
How will general regimen changes affect % passing?			
How will general regimen changes affect % injured?			
What regimen changes will maximize fitness, minimize injury?	Detailed Regimen Adjustment	Detailed Regimen Info	Graphs of pop. progress & goals
How much deviation from regimen "norm" is ok for fitness?	Optimization Scheme	Acceptable PFT, injury rates	
How much deviation from regimen "norm" is ok for injury?			
Researcher			
How does different regimens affect specific fitness measures?	Test different regimens	Detailed everything	Detailed outputs, CI's
How does different regimens affect specific injuries?	Test different populations	Access to model parameters	
How accurate are the predictions/models?	Detailed Regimen Adjustment		
What exercises are "equivalent"?	Detailed Recruit Info		

Group-Level User: Concerned with the average performance and injury outcomes of large groups of individuals involved in different training regimens. The output shows the average outcomes of the different training regimens, which allows the user to compare the metrics of each regimen. This user can change the training regimen and has access to many different groups of individuals and their average properties. Likely group-level users are Base Commanders and TRADOC (Training and Doctrine Command) personnel.

Research User: Interested in performance and injury outcomes from the individual level to the group level and the effect of training regimens on those outcomes. Additionally, these users may be interested in examining or modifying the underlying models that predict the training outcomes. The output provides the detailed results of the individuals and the groups. This user has the most access to the training regimens, properties of the individuals, and model parameters. Likely research users are individuals at military research laboratories.

3.2 Database Development

Another component that needs to be incorporated for a functional implementation of the models into a software package is a database schema. The schema is critical in that it needs to be able to store a wide variety of data for the models to use yet be flexible to allow users to modify and update data easily. Specifically, the schema must store user inputs and subject characteristics. In addition, the training regimen, which is time-based, must be stored in a manner that allows users to make broad changes (i.e., daily or weekly) yet provide a daily training schedule to the model.

To incorporate these characteristics, the database was partitioned into two separate sections—subject information and training regimen. The subject database is a typical schema consisting of a Subject ID, anthropometry values (gender, height, weight, etc.), previous injury history, questionnaire answers, and PFT scores. The training regimen schema is much more complex, with each event or exercise broken into separate movements, which are linked to the schedule through weekly and daily “multiplier” tables to allow users to increase or decrease the regimen easily (Figure 11). For each event, specific information such as the day, name, description, and number of repetitions are recorded. (There can be any number of events on a day.) The event is then broken into specific movements such as running or sit-ups and the specific parameters to describe the movement is stored (e.g., run distance or number of sit-ups). To control the amount of exercise done, the event is adjusted with three values: an event, day, and week multiplier. These values can be modified by individuals using the software and adjust the total amount of each movement done on each day. Thus, referring to Figure 11, the total number of sit-ups for an exercise on a given day is equal to the number sit-ups in the “Sit-Up Table” times the

number of reps for that event (NReps) times the Event, Day and Week Multipliers. The total number of sit-ups for the day is the sum of all sit-ups from the different events on that day.

Note also that a nonmodel feature was added to the software for added value: a body fat and height/height standards calculator calibrated for the U.S. Army. This data is also stored in the database. Subsequent software updates will incorporate standards calculators from other armed forces.

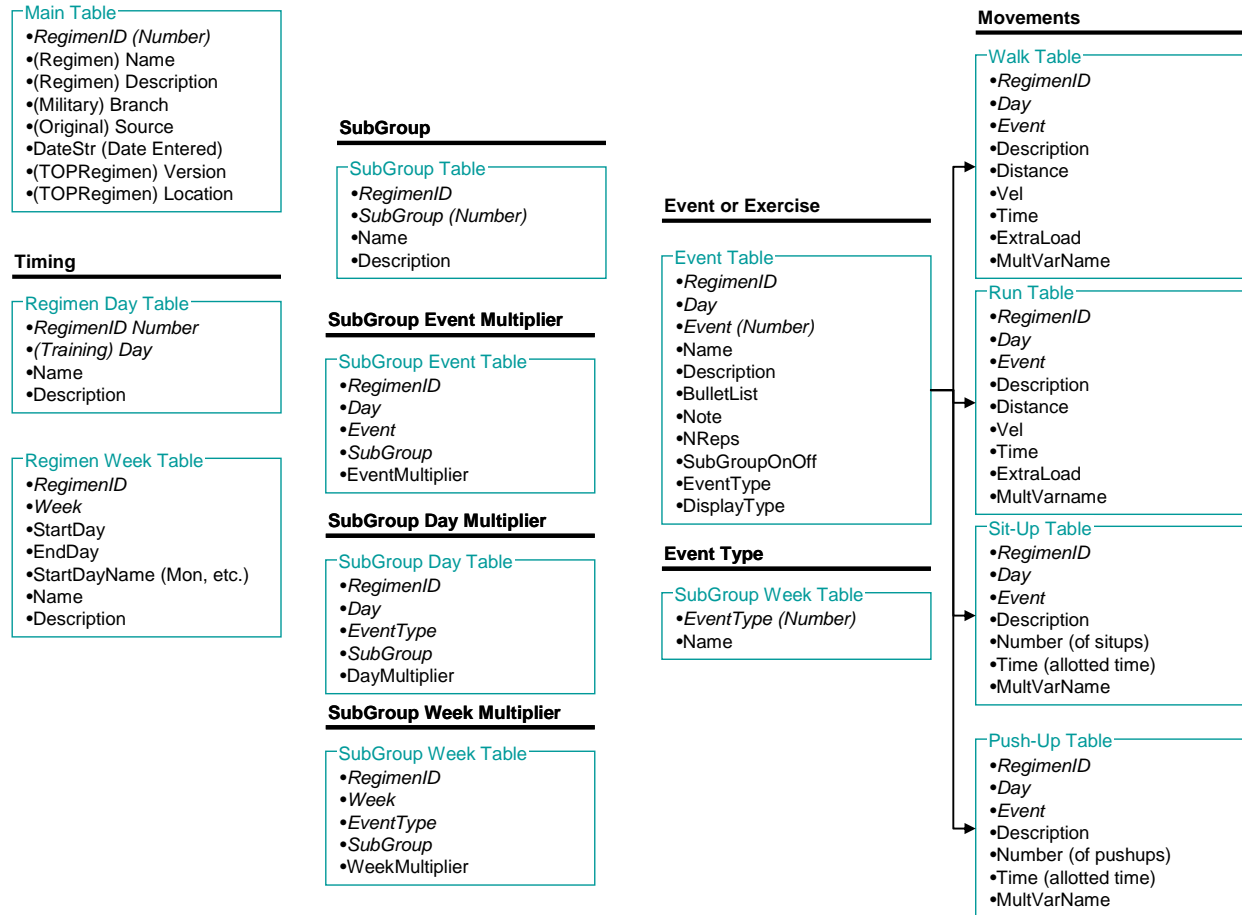


Figure 11. The database schema to store training regimen data.

To allow training dosages to be input into the models, each event or exercise is broken into movements. In addition, event, day and week “multiplier” values are stored and accessed via the software interface to allow users to make adjustments to the training regimen.

3.3 TOP Implementation

TOP 1.1 is the main component of the software where the previously described performance and injury models were implemented. The following figures are screen shots from TOP Software Version 1.1 to demonstrate some of the key features of the software,

including the graphical user interface, input screens, and model prediction reports. Two user types have been implemented: Basic and Mid-Level.

3.3.1 Basic Level User

The interface for the Basic Level User is designed to allow individuals to run the program with little or no instruction. Graphics are used where possible and instructions for each section are always in view.

Instructions

Each of the 4 buttons below leads to a window most of which require additional information. All buttons must be marked **Completed** before a training analysis can be performed.

The analysis will predict your final physical fitness test (PFT) score and the likelihood of injury.



Figure 12. Basic Level User—Main Page.

Basic Users can navigate to four different sections to input and/or modify data used for the model predictions.

Training Schedule							
						Finished	Cancel
Fort Jackson Basic Combat Training							
Note: Basic user can only view training schedule Click on a day for more exercise details							
	SUN	MON	TUE	WED	THU	FRI	SAT
week1	2006-09-17 Arrival/Processing	2006-09-18 Conditioning Drill 1	2006-09-19 Conditioning Drill 1 1 mi Timed Run	2006-09-20 Conditioning Drill 1 Conditioning Drill 2	2006-09-21 Conditioning Drill 1 Ability Group Run	2006-09-22 Conditioning Drill 1 Conditioning Drill 2	2006-09-23 Conditioning Drill 1 30:60's & 60:110's
week2	2006-09-24 No PT Schedule	2006-09-25 Conditioning Drill 1 Ability Group Run	2006-09-26 Conditioning Drill 1 Conditioning Drill 2	2006-09-27 Conditioning Drill 1 30:60's Conditioning Drill 1 Conditioning Drill 2	2006-09-28 Conditioning Drill 1	2006-09-29 No PT Schedule	2006-09-30 Conditioning Drill 1 1ST
week3	2006-10-01 Conditioning Drill 1 300-yard Shuttle Run Ability Group Run	2006-10-02 Conditioning Drill 1 Conditioning Drill 2	2006-10-03 Conditioning Drill 1 30:60's	2006-10-04 Conditioning Drill 1 Conditioning Drill 2	2006-10-05 Conditioning Drill 1 300-yard Shuttle Run Ability Group Run	2006-10-06 Conditioning Drill 1 Conditioning Drill 2	2006-10-07 No PT Schedule
week4	2006-10-08 Conditioning Drill 1 Ability Group Run	2006-10-09 Conditioning Drill 1 Conditioning Drill 2	2006-10-10 Conditioning Drill 1 300-yard Shuttle Run 60:110's	2006-10-11 Conditioning Drill 1 Conditioning Drill 2	2006-10-12 Conditioning Drill 1 Ability Group Run	2006-10-13 Conditioning Drill 1 Conditioning Drill 2	2006-10-14 No PT Schedule
week5	2006-10-15 Conditioning Drill 1 Ability Group Run	2006-10-16 Conditioning Drill 1 Conditioning Drill 2	2006-10-17 Conditioning Drill 1 300-yard Shuttle Run 60:110's	2006-10-18 Conditioning Drill 1 Conditioning Drill 2	2006-10-19 No PT Schedule	2006-10-20 APFT (diagnostic)	2006-10-21 No PT Schedule
week6	2006-10-22 Conditioning Drill 1 Ability Group Run	2006-10-23 Conditioning Drill 1 Conditioning Drill 2	2006-10-24 Conditioning Drill 1 300-yard Shuttle Run 60:110's	2006-10-25 Conditioning Drill 1 Conditioning Drill 2	2006-10-26 Conditioning Drill 1 Ability Group Run	2006-10-27 Conditioning Drill 1 Conditioning Drill 2	2006-10-28 No PT Schedule
week7	2006-10-29 Conditioning Drill 1 Ability Group Run	2006-10-30 Conditioning Drill 1 Conditioning Drill 2	2006-10-31 Conditioning Drill 1 1-mile Timed Confide	2006-11-01 Conditioning Drill 1	2006-11-02 No PT Schedule	2006-11-03 Final APFT	2006-11-04 No PT Schedule
week8	2006-11-05 Conditioning Drill 1 Ability Group Run	2006-11-06 Conditioning Drill 1 Conditioning Drill 2	2006-11-07 Conditioning Drill 1 60:110's	2006-11-08 Conditioning Drill 1 Conditioning Drill 2	2006-11-09 Conditioning Drill 1 Ability Group Run	2006-11-10 Conditioning Drill 1 Conditioning Drill 2	2006-11-11 No PT Schedule
week9	2006-11-12 Conditioning Drill 1 Ability Group Run	2006-11-13 Conditioning Drill 1 Conditioning Drill 2	2006-11-14 Conditioning Drill 1 60:110's	2006-11-15 Conditioning Drill 1 Conditioning Drill 2	2006-11-16 Conditioning Drill 1 Ability Group Run	2006-11-17 Conditioning Drill 1 Conditioning Drill 2	

Figure 13. Basic Level User—Training Schedule sub-page.

Basic Users can view the planned training regimen.

Medical History
Finished
Cancel


Instructions

Record your basic body measurements and previous injury history in the boxes below

Basic Information


Age (yrs): 22
Gender: Female
Height (inches): 67
Weight (pounds): 150

Body Measurement




Hip(inches):

Measure the hip circumference by placing the tape around the hips so that it passes over the greatest protrusion of the gluteal muscles (buttocks) as viewed from the side.




Forearm(inches):

Measure the forearm circumference by placing the tape around the forearm so that it passes over the thickest portion of the forearm.



Neck(inches):

Measure neck circumference at a point just below the larynx (Adam's Apple).



Wrist(inches):

Measure the wrist circumference by placing the tape around the area that is the thinnest.

Previous Injury Information

Date of Injury	Type	Body Part	
Last Week	Overuse Injury	Head	Edit Delete

Add new record

Figure 14. Basic Level User—Medical History sub-page.

Basic Users can input their basic body measures such as height and weight as well as specific measures required for calculation of the Body Fat Standard. Injury reporting is also stored in this section.

Finished

Cancel

Question

Answer

How do you rate your current physical fitness compared to other individuals of your gender and age?

Poor

During the 2 months prior to military training, what was the average number of times per week you exercised, played sports, or participated in strenuous labor?

4 times

Have you ever taken diet pills to lose weight?

Yes

Have you ever used laxatives to lose weight?

No

Have you ever caused yourself to vomit to lose weight?

No





Figure 15. Basic Level User—Fitness and Lifestyle Background sub-section.

Basic Users can answer specific questions that help the program adjust the models to each individual's exercise history. Additional questions can be added if required as models are refined.

Physical Fitness Scores

Finished
Cancel



Instructions
Record your Physical Fitness Test (PFT) results in the table below.

Date: The date of the PFT
Run Time: The time of the PFT run in min:sec formula
SU: The number of sit-ups or crunches done in the time allowed
PU: The number of push-ups or pull-ups done in the time allowed
Total Score: Your PFT score
PFT Type: Select the type of PFT performed

 clears the PFT results.

Recorded Physical Fitness Scores

Initial PFT

Date	Run Time	#SU	#PU	Total Score		
2006-08-09	00:20:20	50	48	229		

PFT

Date	Run Time	#SU	#PU	Total Score	

Final PFT

Date	Run Time	#SU	#PU	Total Score	

Enter additional PFT results:

Date:

Run Time (hh:mm:ss):

Pushups:

Run Score

Pushups Score

PFT Type:
Select One

Situps:

Situps Score

Total Score

Figure 16. Basic Level User—Physical Fitness Scores sub-section.
Basic Users can enter their PFT results. A PFT calculator has been added for convenience.

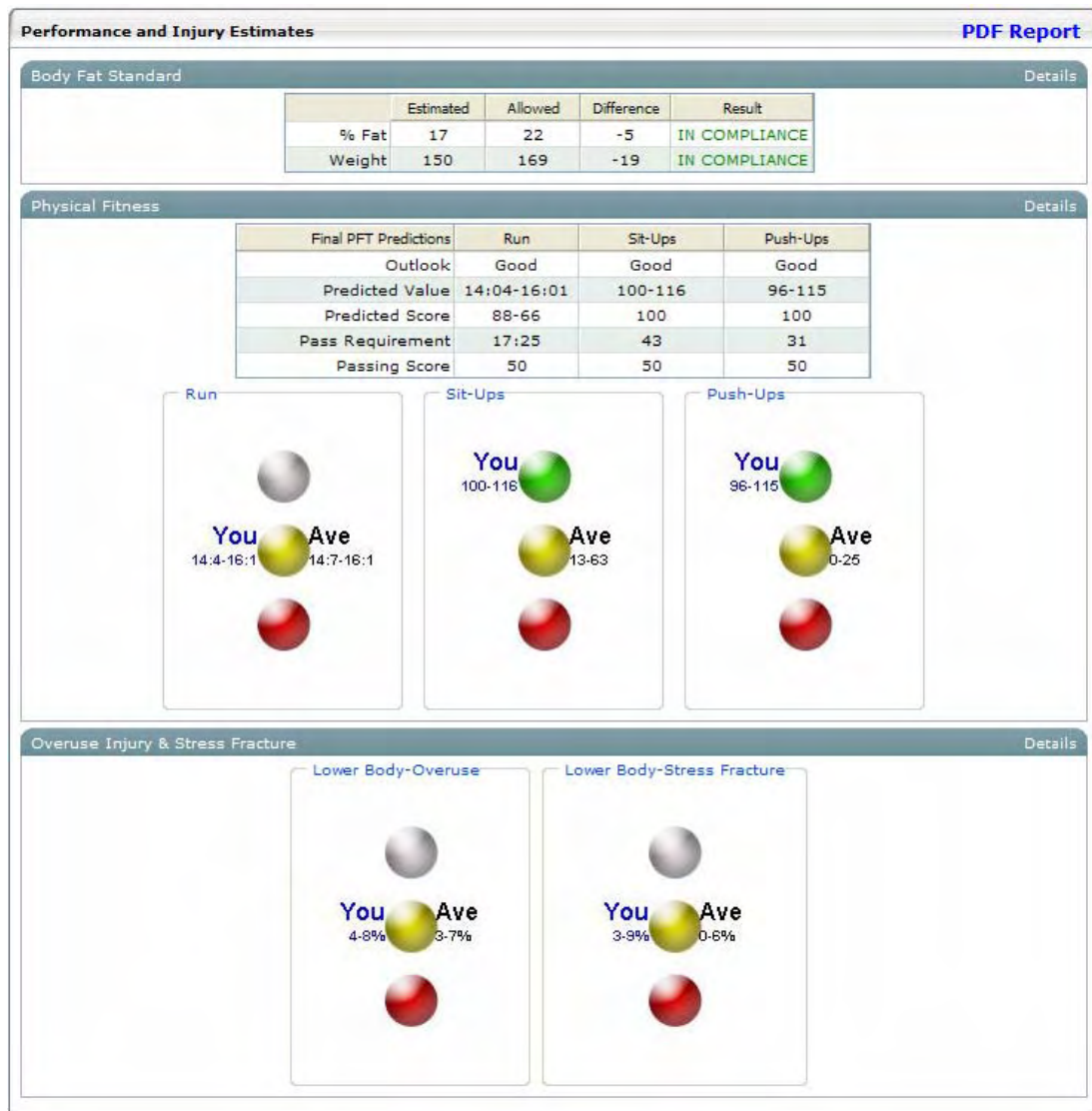


Figure 17. Basic Level User—Results sub-section.

Basic Users can view the model predictions and Body Fat Standards results. Emphasis was placed on simplicity and graphical displays.

TOP 1.1

Training, Overuse Injury & Performance Modeling

Analysis Report for:
Name: Smith, Joe
Username: Male1
GroupID: ABJA06-1001

Date: 06/29/2007

BASIC INFORMATION

Age (yrs): 22 Height (in): 67 Training Type: Army Basic Combat Training
Gender: Male Weight (lbs): 150 Location: Ft. Jackson, SC
Start Date: 2006-08-08

BODY FAT STANDARD

	Estimated	Allowed	Difference	Result
%Fat	17	22	5	IN COMPLIANCE
Weight	150	169	19	IN COMPLIANCE

PHYSICAL FITNESS

Final Physical Fitness Test

Your predicted performance on each of the final test events is based on your initial physical fitness test results (IPFT), planned training regimen, and fitness profile.

Final PFT Predictions	Run	Sit-Ups	Push-Ups
Out look	Good	Good	Good
Predicted	14:04-16:01	100-116	96-115
Predicted Score	88-66	100	100
Pass Requirement	17:25	43	31
Passing Score	50	50	50

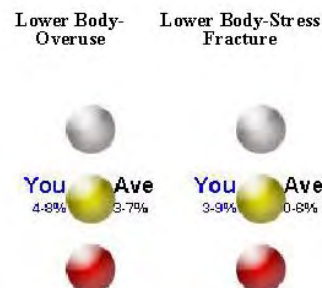


OVERUSE & STRESS FRACTURE INJURY

An overuse injury is an injury caused by repetitive motion. Common examples are tendonitis/bursitis/fasciitis, pain, and non-acute strains/sprains. A stress fracture is also an overuse injury but is considered separately.

Your chance of sustaining a lower body (legs & hip) overuse injury over the course of the planned training regimen. The percent likelihood of a typical (average) individual being injured from this training regimen is specified on the right.

A stress fracture is an overuse injury of the bone, caused by training harder than the bone is capable of handling. The most common stress fracture bone is the tibia or calf bone.



*These results are based on the average response of individuals similar to you undergoing the planned regimen. Your results may differ.

Figure 18. Printable report summarizing the Basic User model results.

TOP 1.1

Training, Overuse Injury & Performance Modeling

FREQUENTLY ASKED QUESTIONS

OVERVIEW

What is TOP 1.1?

TOP 1.1 is a tool designed to predict performance and injuries from training regimens or schedules.

How does it work?

TOP 1.1 uses your basic health information (height, weight, fitness level, etc.) in a computer simulation of your training plan. Using equations derived from scientific researchers, the program predicts your chances of injury and changes to your performance level.

PHYSICAL FITNESS

What is the Final Physical Fitness Test or Final PFT?

The Final PFT is the physical fitness test you must pass before graduating from training. The test is a three-event physical performance test used to assess muscular endurance and cardiorespiratory fitness. The three events are usually running, sit-ups, and push-ups. Passing scores are determined by your age, gender, and training program (basic combat training or an advanced training program).

What do the 'Final PFT Prediction' table results mean?

For each of the three events (and overall), a GOOD, BORDERLINE, or POOR grade is given. GOOD means you scored better than 95% of those in your age group. BORDERLINE is 50% and POOR is 5%. In addition, TOP 1.1 cannot predict your exact score for an event but gives a range for your likely scores.

What can I do to improve?

The regimen currently planned in order for you to pass the Final PFT may need to be modified. However, overtraining can lead to injuries and additional training should only be attempted with the guidance of a physical fitness advisor. Your fitness advisor can specify a different training program to be analyzed in TOP 1.1.

BODY FAT STANDARD

What is the Body Fat Standard?

The standard is a requirement that all enlisted personnel must meet in order to insure that everyone's fitness and percent body fat level meets acceptable standards. The criteria for compliance depend on the military branch.

What does 'Not In Compliance' mean?

In general, it means that your weight or percent body fat is too high. Dieting and exercise in a controlled manner is usually needed to bring your body fat standard measures back into compliance.

How is percent body fat estimated?

Key measurements such as height, weight, and neck circumference are used, comparing your values to similar individuals whose percent body fat is known.

Disclaimer

Exercise is not without its risks and this or any other exercise program may result in injury. To reduce the risk of injury in your case, consult a doctor before beginning this exercise program. The analysis presented is in no way intended as a substitute for medical consultation. As with any exercise program, if at any point during your workout you begin to feel faint, dizzy, or have physical discomfort, you should stop immediately and consult a physician.

Figure 19. Back page of the printable Basic User report.

3.3.2 Mid-Level User

The Mid-Level User interface contains fewer graphics and is more compact, allowing additional result details to be displayed after the model predictions have been made. Despite the compact interface, more features are accessible. Subjects are categorized into Groups, training regimens can be adjusted, and different analyses preformed. The results are also presented in a more compact form, allowing user's to quickly identify the overall status of the group as well as identify high risk individuals.

Instructions
This software will allow you to view and analyze the predicted effects of different training regimens on performance and injury of a small group of individuals. To use this software, choose (1) a group of subjects, (2) a training regimen, and (3) items to analyze. Click on each of the grey section bars to make your selections.

1. Subject Information: Select a group of individuals based on their Group ID. View individual performance and injury history.
2. Regimen Information: Change or customize the planned training regimen.
3. Analysis Selection: Specify the type of performance and injury outcomes to be predicted.
Additional instructions is given when each section is accessed.

Groups Regimen Analysis Result

View Groups New Group Load Group

Group ID	Number of People	Start date			
<input checked="" type="radio"/> ABJA06-1001	10	2006-07-24	Subject Details	View/Edit	Delete
<input type="radio"/> ABJA06-1006	0	2006-07-25	Subject Details	View/Edit	Delete

Figure 20. The Subject selection page for the Mid-Level User.

Subjects are categorized into Groups. Individual subject Medical History, Lifestyle & Fitness Questionnaire answers, and PFT Scores can be accessed as well.

Groups Regimen Analysis Result

Select Regimen New Regimen Load Regimen

Name	Start date			
<input checked="" type="radio"/> Jan Regimen	2006-07-26	Modify	Edit	Delete

Regimen Details

Week	March Mileage(%)	Run Mileage(%)	Conditioning Drills(%)
week1	<input type="text" value="100"/>	<input type="text" value="100"/>	<input type="text" value="100"/>
week2	<input type="text" value="100"/>	<input type="text" value="100"/>	<input type="text" value="100"/>
week3	<input type="text" value="100"/>	<input type="text" value="100"/>	<input type="text" value="100"/>
week4	<input type="text" value="100"/>	<input type="text" value="100"/>	<input type="text" value="100"/>
week5	<input type="text" value="100"/>	<input type="text" value="100"/>	<input type="text" value="100"/>
week6	<input type="text" value="100"/>	<input type="text" value="100"/>	<input type="text" value="100"/>
week7	<input type="text" value="100"/>	<input type="text" value="100"/>	<input type="text" value="100"/>
week8	<input type="text" value="100"/>	<input type="text" value="100"/>	<input type="text" value="100"/>
week9	<input type="text" value="100"/>	<input type="text" value="100"/>	<input type="text" value="100"/>

Confirm Modified Values Reset Values Cancel Save as regimen Variation

Figure 21. The Regimen selection page for the Mid-Level User.

Training regimen details can be viewed and edited from within the Mid-Level User program.

GroupsRegimenAnalysisResult

Performance

☒ FPFT Run

☒ FPFT Push-ups

☒ FPFT Sit-ups

☒ Select All

Overuse Injury

☒ Lower Body

☒ Leg Stress Fracture

Subjects

☒ Smith,Joe☒ Simpson,Bart☒ Jane,Mary☒ Select All

☒ Joe,GI☒ Smith,Jane☒ Simpson,Lisa

☒ Doe,John☒ Jane,GI

☒ Bob,Billy☒ Doe,Jane

Analysis Name:

Analyze

Figure 22. The Analysis selection page for the Mid-Level User.

The Mid-Level User has the flexibility to select the types of models to be run and which subjects to use.

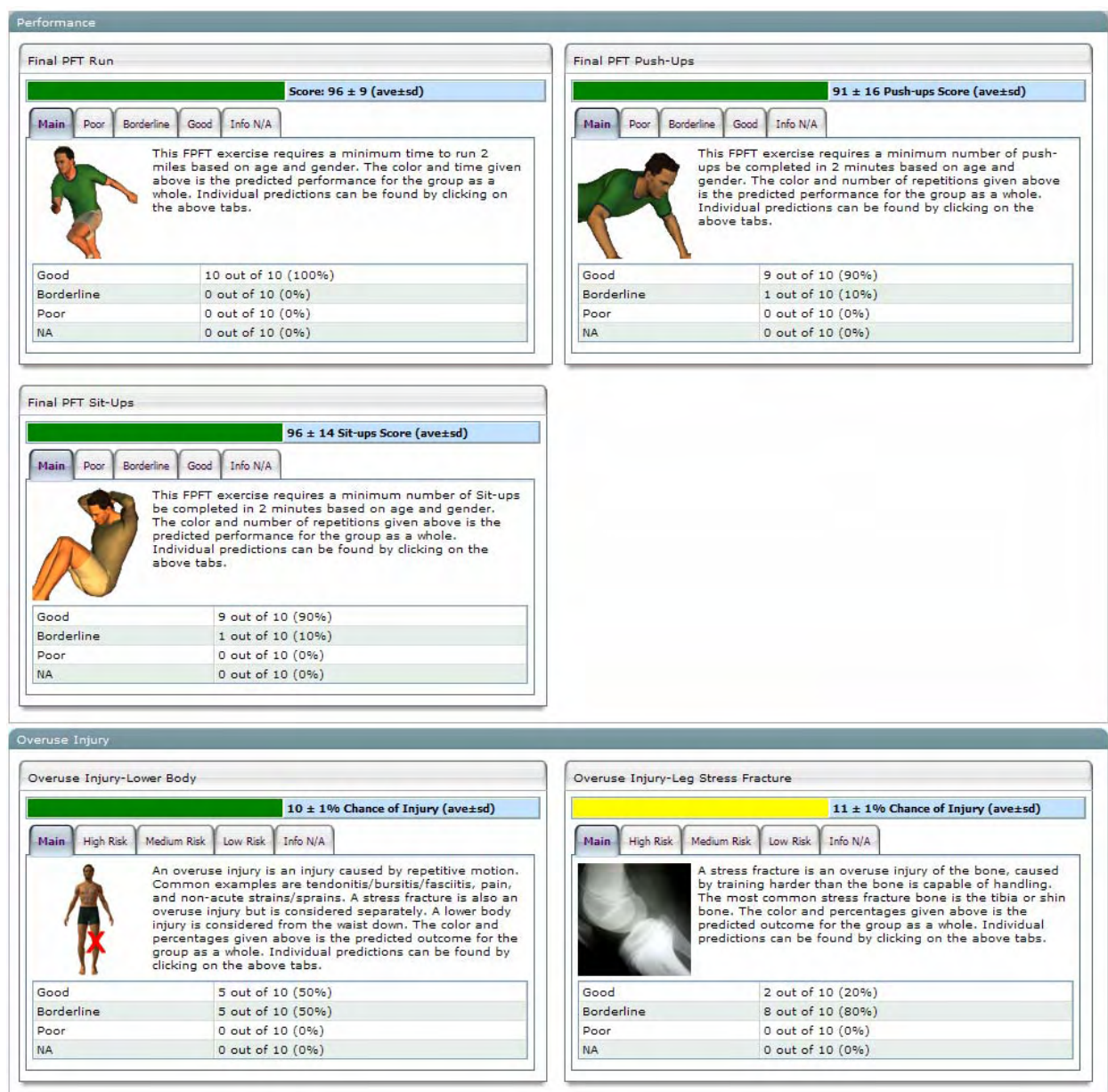


Figure 23. The Mid-Level User Results page.

Model results are categorized and individuals with different predicted outcomes are automatically characterized.

3.4 DeveloperNet: Data Storage & Access

The purpose of this section is to make available all of the datasets, documents, and presentations related to the TOP project. To accomplish this, the available data was organized into three sections: survey data, image data, and reports/presentation materials. Survey data contains raw data files from studies involving a large number of subjects. The information contained in the files differs between studies so each file also contains a short summary paragraph. These are the datasets used to optimize and validate the TOP models.

Image data is a depository for both raw and processed image files as well as statistical analyses files. Reports and presentation materials include annual reports, official military documents related to BCT, and slides of presentations involving the TOP Project. All files are downloadable but require a user login and password for security.



DeveloperNet

USARIEM

Home BCT Background PFT Calculator Body Fat Standards TOP 1.1 DeveloperNet

Access to all reference materials associated with the Training, Overuse, Injury Modeling effort, including raw data.

Survey Data	
Henderson Combat Medic Data 97	U.S. Army BCT & AIT data from recruits at Ft. Sam Houston undergoing AIT. Anthropometry, PFT, injury, and questionnaire data
MCRD-Parris Island 95	U.S. Marine Corps female BCT data from recruits at Parris Island, SC. Anthropometry, injury, and questionnaire data. No PFT results
MCRD-Parris Island 99	U.S. Marine Corps female BCT data from recruits at Parris Island, SC. PFT, injury, and questionnaire data. No anthropometry data
MCRD-San Diego 93	U.S. Marine Corps male BCT data from recruits at San Diego, CA. Anthropometry, injury, and questionnaire data. Limited PFT data
MCRD-San Diego 03	U.S. Marine Corps male BCT data from recruits at San Diego, CA. PFT data only
Recruit Assessment Program (RAP) Pilot Data 02	U.S. Army BCT data from male & female recruits at Ft. Jackson. Anthropometry, PFT, injury, and questionnaire data
Ft. Jackson Data 98	U.S. Army BCT data from male recruits at Ft. Jackson. Anthropometry, PFT, and laboratory exercise test results. No injury or questionnaire data
Israeli Defence Force 06	IDF BCT data from male & female recruits. Anthropometry, PFT, and stress fracture results. No additional injury data

Documentation	
TOP Reports, Presentation Materials and Notes	TOP annual reports plus model and software development slides and notes from various meetings
TOP References	Searchable database of research manuscripts used to develop the TOP models

Figure 24. The DeveloperNet Main Page.

The page contains two main sections—Survey Data and Documentation. An additional Image Data section is planned to allow access to bone image data that will be used to develop more advance versions of the stress fracture model.

Henderson Combat Medic Data 97

General Information

Branch: U.S. Army Program: BCT & AIT Year: 1997

Summary:

U.S. Army BCT & AIT data from recruits at Ft. Sam Houston undergoing AIT. Anthropometry, PFT, injury, and questionnaire data

Source: BAMC

Publications

"N. E. Henderson, J. J. Knapik, S. W. Shaffer, T. H. McKenzie, and G. M. Schneider. Injuries and inj

Supplemental Data

[Henderson_Combat_Medic_Data_97.sav](#)
Original SPSS data file
Format:SPSS

Comments

Subjects

	Males	Females
Number	682	337
Age	20 ± 3 yrs	19 ± 3 yrs
Height	1.74 ± 0.07 m	1.63 ± 0.06 m
Weight	73.2 ± 9.7 kg	61.5 ± 7.8 kg
BMI	24.1 ± 2.7 kg/m/m	23.1 ± 2.3 kg/m/m
Run:FailFinal PFT	21 (3.1 %)	22 (6.5 %)
Sit-Ups: Fail Final PFT	33 (4.8 %)	47 (13.9 %)
Push-Ups: Fails Final PFT	54 (7.9 %)	3 (0.9 %)
Stress Fracture	25 (3.7 %)	52 (15 %)

[Download Processed Data](#)
File: Henderson Combat Medic Data 97.xls
Format: Excel

Regimen (Weeks=9)

Location	"BCT: Various, AIT: Ft. Sam Houston"
Days	63
Total Run Distance	79.5 km
Total March Distance	NA
Total Days of Exercise	51
Source	None

[Download Processed Data](#)
File: Henderson Combat Medic Data 97 Regimen.xls
Format: Excel

Figure 25. DeveloperNet Survey Data sub-window.

This sub-window allows users to view background information, publications, comments and summary statistics of the dataset. Clicking on the links downloads the data.

3.5 Basic Combat Training Background Information Site

The purpose of the BCT Background web site is to inform new recruits about the causes of BCT attrition and how to minimize their risk of failing BCT in a simple, straight-forward manner. To accomplish this, icons and images are used as much as possible. Topics include risk factors for stress fractures, overuse injuries, and acute injuries as well as Physical Fitness Testing procedures and low performance factors.

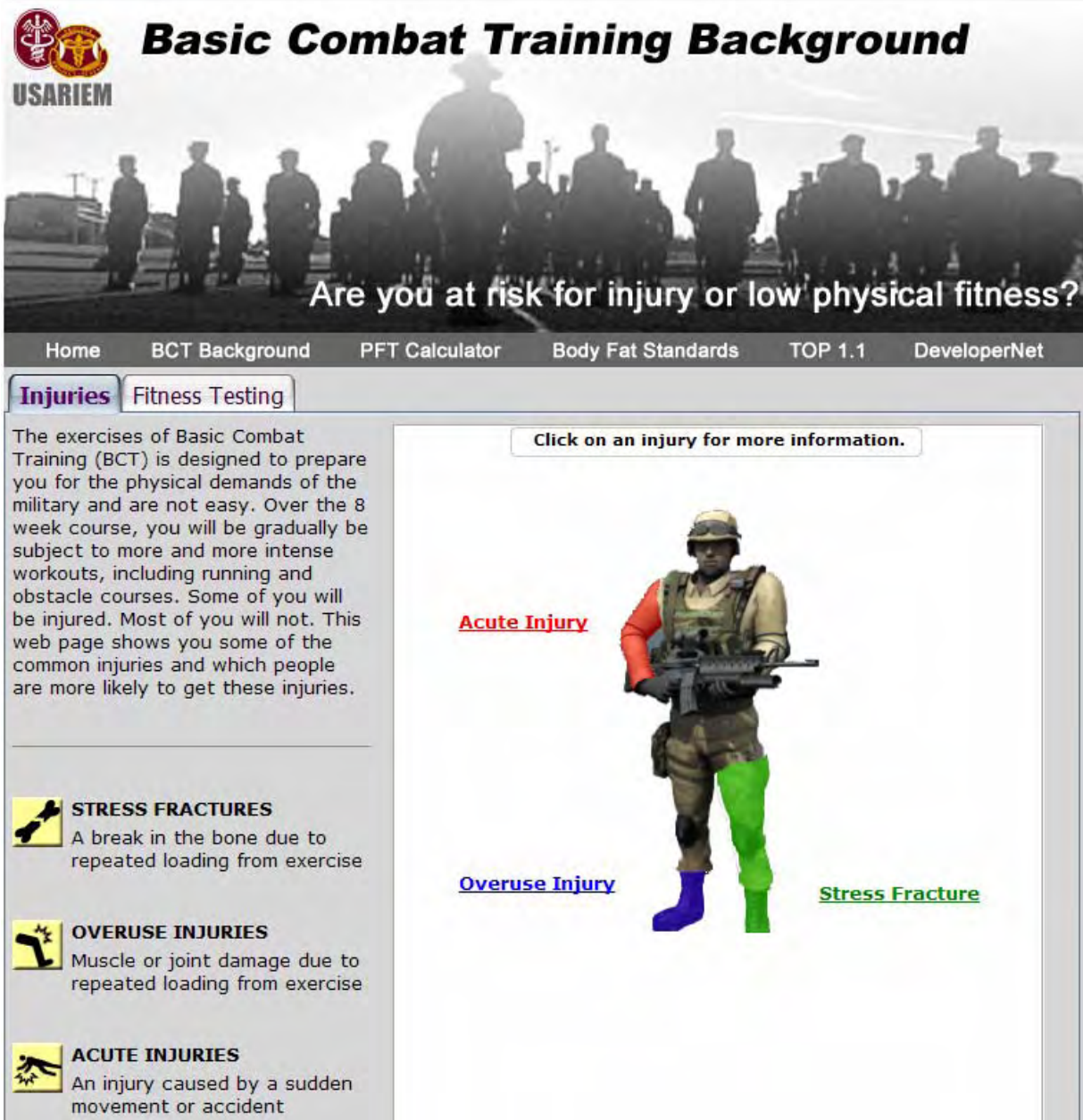


Figure 26. The injury section of the BCT Background web site.

This section features three classes of injuries—stress fractures overuse injuries, and acute injuries. Clicking on each type of injury leads to a sub-window that gives additional details about the injury as well as common risk factors.



Basic Combat Training Background



Are you at risk for injury or low physical fitness?

[Home](#) [BCT Background](#) [PFT Calculator](#) [Body Fat Standards](#) [TOP 1.1](#) [DeveloperNet](#)

[Injuries](#) [Fitness Testing](#)

In order to graduate from Basic Combat Training (BCT), you must pass the U.S. Army Physical Fitness Test (APFT), which consists of three exercises:

- Sit-ups: max number in 2 min
- Push-ups: max number in 2 min
- Run: fastest 2 mile runtime

The score given to each test depends on your gender and age. This web page shows you common characteristics of recruits fail to pass the APFT. While having the same traits does not guarantee failure, it does indicate that you may need to take your exercise training more seriously in order to pass the APFT.



SIT-UPS

This event measures the endurance of the abdominal and hip-flexor muscles.



PUSH-UPS

This event measures the endurance of the chest, shoulder, and triceps muscles.



RUN

This event tests the cardiorespiratory (aerobic) endurance and the endurance of the leg muscles.

[Sit-Ups](#) [Push-Ups](#) [Run](#)



[Pass/Fail Info](#) [Instructions](#) [Tips](#)



SIT-UPS

Number of reps required depends on gender and age

FAILURE RATE: **LOW**



1st PFT

LOW INITIAL APFT SCORE
A low sit-up score during the first or initial APFT is indicative of the amount of additional fitness needed to pass the final APFT at week 8. Those with lower initial APFT scores have a harder time passing the final APFT.



TECHNIQUE

Proper technique is important to prevent injury and/or disqualification

Figure 27. The fitness testing section of the BCT Background web site.

This section contains detailed information about each of the three exercises used in the U.S. Army Physical Fitness Test.

Table 34. Stress fracture risk factor icons and information presented in the BCT Background Web Site.







	Risk Level: Low Severity: High	
Definition	Caused by repeated loading of a bone through running and marching. The most commonly affected body part is the lower leg or tibia. Symptoms may include sharp pain while walking, swelling, and localized tenderness. Although uncommon (< 5 %), recovery from this injury requires 6-8 weeks of nonexercise and in many cases, prevents you from completing BCT.	
Risk Factors (Bennell et al. 1999; Ross and Woodward 1994; Taimela et al. 1990)		
 Over Training	In addition to your fitness level, it is believed that one of the major causes of stress fractures is the sudden increase in running and marching either during BCT and/or those that adopt an overly strenuous pre-BCT workout program.	
 Anthropometry	Those with anthropometric irregularities such as leg length discrepancies and low bone density are more likely to be injured.	
 Previous Injury	You are more likely to have another stress fracture if you have already had one before BCT.	
 Smoking	Those that smoke regularly are more likely to have a stress fracture.	
 Female	Females, in general, are more likely to have stress fractures. In addition, for females, if you have menstrual irregularities, you may be more prone to stress fractures.	

Table 35. Overuse injury risk factor icons and information presented in the BCT Background Web Site.






	Risk Level: Medium Severity: Medium	
Definition	Caused by repeating the same exercises too many times. This injury can occur on at any joint or muscle although most injuries occur in the foot region. This is a common injury (50-60%) with a wide range of symptoms, severity, and recovery time.	
Risk Factors (Almeida et al. 1999; Hartig and Henderson 1999; Jones et al. 1994; Jones and Knapik 1999; Ross and Woodward 1994)		
 Over Training	Performing a large number of the same or similar exercises without sufficient recovery can lead to overuse injuries.	
 Previous Injury	You are more likely to have another stress fracture if you have already had one before BCT.	
 Flexibility	Those with limited flexibility or those that are very flexible are more prone to overuse injuries.	
 Female	In general, females are more prone to overuse injuries.	

Table 36. Acute injury risk factor icons and information presented in the BCT Background Web Site.










	Risk Level: Low Severity: Low	
Definition	An injury due to a sudden mishap or accident. This type of injury is primarily random and can inflict injury on any part of the body. This is a rare injury (~2%) and the severity depends on the situation.	
Risk Factors		
 Fatigue	A likely cause of acute injuries is a lack of mental concentration due to fatigue.	
 Over Training	Over training can also increase the chances of an acute injury as muscles become tired and coordination decreases.	

Table 37. Push-up performance factors presented in the BCT Background Web Site.

		Failure Rate: Low
Information		Number of reps required depends on gender & age.
Risk Factors		
	Initial APFT	A low push-up score during the first or initial APFT is indicative of the amount of additional fitness needed to pass the final APFT at week 8. Those with lower initial APFT scores have a harder time passing the final APFT.
	Proper Technique	Proper technique is important to prevent injury and/or disqualification.





Official instructions and tips from (Headquarters Department of the Army 1998) are also presented.

Table 38. Sit-up performance factors presented in the BCT Background Web Site.

		Failure Rate: Low
Information		Number of reps required depends on gender & age.
Risk Factors		
	Initial APFT	A low sit-up score during the first or initial APFT is indicative of the amount of additional fitness needed to pass the final APFT at week 8. Those with lower initial APFT scores have a harder time passing the final APFT.
	Proper Technique	Proper technique is important to prevent injury and/or disqualification.

Official instructions and tips from (Headquarters Department of the Army 1998) are also presented.

Table 39. Run performance factors presented in the BCT Background Web Site.

	Failure Rate: Low
Information	Runtime required depends on gender & age.
Risk Factors	
 Initial APFT	A low run score during the first or initial APFT is indicative of the amount of additional fitness needed to pass the final APFT at week 8. Those with lower initial APFT scores have a harder time passing the final APFT.
 Ht, Wt, BMI	Those with a high body mass index (BMI) are considered heavy for their height and may not be a physically fit as those with an average BMI. In addition, a low BMI may indicate insufficient muscle strength to complete the run in the allotted time. Note that because BMI does not measure body fat or muscle content, it is not uncommon for low and high BMI individuals to pass the APFT.
 Proper Technique	Proper technique is important to prevent injury and/or disqualification.

Official instructions and tips from (Headquarters Department of the Army 1998) are also presented.

4. Conclusions

This report describes the development of the TOP Model, which is a set of models to predict injury and performance outcomes from a training regimen such as BCT. Several models were developed, including sit-up, push-up and run performance models as well as stress fracture and overuse injury models. They were developed and based on concepts found in the literature and through the analysis of acquired military datasets. In general, the models were found to have a similar accuracy to a statistical method commonly used in performance and injury prediction. In addition, software was designed and implemented that incorporated the models as a demonstration of the feasibility of the project in helping improve fitness and reduce injuries through the identification of high risk individuals and regimen optimization.

The primary limitation to the current version of the models developed is the lack of accuracy. While the models in their current form have a comparable accuracy to that of traditional statistical methods, the models were unable to consistently be an improvement over the statistical method during validation. There are several reasons for this. First, the datasets (acquired post hoc from other research studies) often collected different measures, making it difficult to find two datasets that contain the same input and output measures. Second, most of the datasets lack sufficient training regimen details to allow the models to develop algorithms and parameter values that are capable of predicting injury and performance across different regimens (i.e., many of the datasets contained no marching distances). Third, some of the datasets only contained measures from those that passed BCT, making it difficult to assess model performance at predicting the negative outcomes of injury and performance.

Clearly one of the key factors in improving model predictive accuracy is to acquire additional data that has more detailed training regimen measures. This would allow the models to better account for current and new performance factors, improve the model algorithms, and update the dosage calculations. In addition, an improved model from better regimen details should allow the model to extrapolate to different training regimens without the loss in accuracy currently seen.

There are several future tasks we hope to incorporate into the next version of the TOP model and software that will improve the utility of this effort. This includes acquiring additional field data that contains predictor variables, outcome measures, and detailed training regimen descriptors. Also, laboratory data that profiles the biomechanical loading for the various exercises used in training would enable better models to be developed. For software development, future tasks include implementing additional user types and upgrading the graphical user interface of the existing software based on potential user's feedback.

4.1 Key Accomplishments

Modeling

- Developed sit-up, push-up, and run performance models that predict final PFT outcomes
- Developed stress fracture and overuse injury models that predict the likelihood of injury during training

Software

- Implemented all performance and injury models (run, sit-up, push-up, stress fracture, and overuse injury)
- Developed and implemented a database schema to store subject information and training regimen details
- Identified four potential user types (basic, mid-level, group-level, and researcher) and their needs
- Created a fully functional web-based software package for two different user types (basic and mid-level), which incorporates all the performance and injury models currently developed.

4.2 Reportable Outcomes

We have:

- Demonstrated that a simplified dose-response method to account training regimen (and risk factors) is a feasible method of creating training prediction models
- Demonstrated the models' potential for similar or better accuracy than a traditional statistical prediction scheme by comparing the accuracy against different datasets
- Shown that a software package can be created that incorporates prediction models to allow users to quickly assess the training status of an individual or small group of trainees.

5. Literature

- Adeeb, S. M., Zec, M. L., Thornton, G. M., Frank, C. B., & Shrive, N. G. (2004). "A novel application of the principles of linear elastic fracture mechanics (LEFM) to the fatigue behavior of tendon tissue." J Biomech Eng **126**(5): 641-650.
- Allison, S. C., Knapik, J. J., Creedon Jr., J. F., and Sharp, M. A. (2005). "Development Of Test Item Clusters For Predicting Negative Outcomes In Basic Combat Training." U.S. Army Research Institute of Environmental Medicine, Natick, MA. Personal communication.
- Almeida, S. A., Williams, K. M., Shaffer, R. A., & Brodine, S. K. (1999). "Epidemiological patterns of musculoskeletal injuries and physical training." Med Sci Sports Exerc **31**(8): 1176-82.
- Archambault, J. M., Wiley, J. P., & Bray, R. C. (1995). "Exercise loading of tendons and the development of overuse injuries. A review of current literature." Sports Med **20**(2): 77-89.
- Army Accessions Command (2003). "Standardized Physical Training Guide BCT." .
- Beck, T. J., Ruff, C. B., Mourtada, F. A., Shaffer, R. A., Maxwell-Williams, K., Kao, G. L., Sartoris, D. J., & Brodine, S. (1996). "Dual-energy X-ray absorptiometry derived structural geometry for stress fracture prediction in male U.S. Marine Corps recruits." J Bone Miner Res **11**(5): 645-53.
- Bennell, K. L., Matheson, G., Meeuwisse, W., & Brukner, P. (1999). "Risk factors for stress fractures." Sports Med **28**(2): 91-122.
- Busso, T. (2003). "Variable dose-response relationship between exercise training and performance." Med Sci Sports Exerc **35**(7): 1188-1195.
- Clauser, C. E., McConville, J. T., & Young, J. W. (1969). "Weight, Volume, and Center of Mass of Segments of the Human Body." Aerospace Medical Research Laboratory, Aerospace Medical Division, Air Force Systems Command, Wright-Patterson Air Force Base, OH. AMRL-TR-69-70.
- Drillis, R. (1958). "Objective recording and biomechanics of pathological gait." Ann N Y Acad Sci **74**: 86-101.
- Flanagan, S. P., Vanderburgh, P. M., Borchers, S. G., & Kohstall, C. D. (2003). "Training college-age women to perform the pull-up exercise." Res Q Exerc Sport **74**(1): 52-59.
- Garcia, J. E., Grabhorn, L. L., & Franklin, K. J. (1987). "Factors associated with stress fractures in military recruits." Mil Med **152**(1): 45-8.

- Giladi, M., Milgrom, C., Simkin, A., Stein, M., Kashtan, H., Margulies, J., Rand, N., Chisin, R., Steinberg, R., Aharonson, Z., & et al. (1987). "Stress fractures and tibial bone width. A risk factor." J Bone Joint Surg Br **69**(2): 326-9.
- Hartig, D. E. & Henderson, J. M. (1999). "Increasing hamstring flexibility decreases lower extremity overuse injuries in military basic trainees." Am J Sports Med **27**(2): 173-6.
- Headquarters Department of the Army (1998). "Physical Fitness Training." Department of the Army, Washington, D.C. FM 21-20 C1.
- Jones, B. H. (1983). "Overuse injuries of the lower extremities associated with marching, jogging, and running: a review." Mil Med **148**(10): 783-7.
- Jones, B. H., Cowan, D. N., & Knapik, J. J. (1994). "Exercise, training and injuries." Sports Med **18**(3): 202-14.
- Jones, B. H. & Knapik, J. J. (1999). "Physical training and exercise-related injuries. Surveillance, research and injury prevention in military populations." Sports Med **27**(2): 111-25.
- Knapik, J. J., Darakjy, S., Scott, S., Hauret, K., Canada, S., Marin, R., Palkoska, F., VanCamp, S., Piskator, E., Rieger, W., & Jones, B. H. (2004). "Evaluation of Two Army Fitness Programs: The TRADOC Standardized Physical Training Program for Basic Combat Training and the Fitness Assessment Program." U.S. Army Center for Health Promotion and Preventative Medicine, Aberdeen Proving Ground, MD. USACHPPM Project No. 12-HF-5772B-04.
- Kraemer, W. J., Mazzetti, S. A., Nindl, B. C., Gotshalk, L. A., Volek, J. S., Bush, J. A., Marx, J. O., Dohi, K., Gomez, A. L., Miles, M., Fleck, S. J., Newton, R. U., & Hakkinen, K. (2001). "Effect of resistance training on women's strength/power and occupational performances." Med Sci Sports Exerc **33**(6): 1011-1025.
- Krivickas, L. S. (1997). "Anatomical factors associated with overuse sports injuries." Sports Med **24**(2): 132-46.
- Lauder, T. D., Dixit, S., Pezzin, L. E., Williams, M. V., Campbell, C. S., & Davis, G. D. (2000). "The relation between stress fractures and bone mineral density: evidence from active-duty Army women." Arch Phys Med Rehabil **81**(1): 73-9.
- McArdle, W. D., Katch, F. I., & Katch, V. L. (1991). Exercise Physiology: Energy, Nutrition, and Human Performance Malvern, PA, Lea & Febiger.
- Milgrom, C., Giladi, M., Simkin, A., Rand, N., Kedem, R., Kashtan, H., & Stein, M. (1988). "An analysis of the biomechanical mechanism of tibial stress fractures among Israeli infantry recruits. A prospective study." Clin Orthop(231): 216-21.
- Milgrom, C., Giladi, M., Simkin, A., Rand, N., Kedem, R., Kashtan, H., Stein, M., & Gomori, M. (1989). "The area moment of inertia of the tibia: a risk factor for stress fractures." J Biomech **22**(11-12): 1243-1248.

- Milgrom, C., Simkin, A., Eldad, A., Nyska, M., & Finestone, A. (2000). "Using bone's adaptation ability to lower the incidence of stress fractures." Am J Sports Med **28**(2): 245-51.
- Montgomery, L. C., Nelson, F. R., Norton, J. P., & Deuster, P. A. (1989). "Orthopedic history and examination in the etiology of overuse injuries." Med Sci Sports Exerc **21**(3): 237-43.
- Morton, R. H., Fitz-Clarke, J. R., & Banister, E. W. (1990). "Modeling human performance in running." J Appl Physiol **69**(3): 1171-7.
- Mulder, E. R., Stegeman, D. F., Gerrits, K. H., Paalman, M. I., Rittweger, J., Felsenberg, D., & de Haan, A. (2006). "Strength, size and activation of knee extensors followed during 8 weeks of horizontal bed rest and the influence of a countermeasure." Eur J Appl Physiol **97**(6): 706-715.
- Natali, A. N., Pavan, P. G., Carniel, E. L., Lucisano, M. E., & Taglialavoro, G. (2005). "Anisotropic elasto-damage constitutive model for the biomechanical analysis of tendons." Med Eng Phys **27**(3): 209-214.
- Popovich, R. M., Gardner, J. W., Potter, R., Knapik, J. J., & Jones, B. H. (2000). "Effect of rest from running on overuse injuries in army basic training." Am J Prev Med **18**(3 Suppl): 147-55.
- Ross, J. (1993). "A review of lower limb overuse injuries during basic military training. Part 2: Prevention of overuse injuries." Mil Med **158**(6): 415-20.
- Ross, J. & Woodward, A. (1994). "Risk factors for injury during basic military training. Is there a social element to injury pathogenesis?" J Occup Med **36**(10): 1120-6.
- Scully, T. J. & Besterman, G. (1982). "Stress fracture--a preventable training injury." Mil Med **147**(4): 285-7.
- Shaffer, R. A., Brodine, S. K., Almeida, S. A., Williams, K. M., & Ronaghy, S. (1999). "Use of simple measures of physical activity to predict stress fractures in young men undergoing a rigorous physical training program." Am J Epidemiol **149**(3): 236-42.
- Sih, B. L. & Shen, W. (2006). "Overuse Injury Assessment Model, Part I: Training, Overuse Injury, and Performance Modeling." L-3 Communications/Jaycor, San Diego, CA. J3181-06-296.
- Taimela, S., Kujala, U. M., & Osterman, K. (1990). "Stress injury proneness: a prospective study during a physical training program." Int J Sports Med **11**(2): 162-5.
- Winfield, A. C., Moore, J., Bracker, M., & Johnson, C. W. (1997). "Risk factors associated with stress reactions in female Marines." Mil Med **162**(10): 698-702.

- Woodmansee, M. W., Sih, B. L., Shen, W., & Niu, E. (2004). "Bone Overuse Injury Assessment Model: Annual Report." Simulation, Engineering, and Testing Group, Jaycor, Inc., San Diego, CA. J3181-04-217.
- Wren, T. A., Beaupre, G. S., & Carter, D. R. (2000). "Tendon and ligament adaptation to exercise, immobilization, and remobilization." J Rehabil Res Dev **37**(2): 217-24.

Appendix A. Available Datasets

The project currently has eight different datasets containing subject information ranging from fitness test scores to injury and anthropometry measures. Some datasets also contain questionnaire responses on initial fitness level, hormone regulation and previous injuries. Unfortunately, only limited information on the training regimen that the recruits from these datasets participated in is known. Table 40 summarizes the information contained in each dataset. The IDF or Israeli Defense Force dataset was recently acquired and has not yet been assessed for its ability to contribute to this effort (Group H).

The primary dataset used for the development of the performance and injury models is Group G (Table 40), which is composed of 681 males and 336 females that underwent U.S. Army BCT circa 1997. As shown in Table 40, this dataset was chosen because it is the most complete of the eight datasets currently acquired, containing input measures such as anthropometry, questionnaire data, and 1st PFT results as well as performance and injury outcome records from BCT. Validation datasets included Group A and Group C, two U.S. Marine Corps datasets as well as Group F, another U.S. Army dataset, none of which were complete.

Table 40. Summary table of the datasets available for model development.

GROUP	A	B	C	D	E	F	G	H	I
Dataset Info									
Location & Year	MCRD-PI 1995	MCRD-PI 1999	MCRD-SD 1993	MCRD-SD 2003	MCRD-SD 2005	Ft Jackson 1998	Ft S Ht Tx ~1997	IDF 2006	Ft. Jackson 2002-04
Source	NHRC	NHRC	NHRC	MCRD-SD	MCRD-SD	ARIEM	BAMC	IDF	CHPPM
Nsubjects	2963	821	1286	3782	572	350	1019	197	1902
Fitness Testing									
IST Data		✓		✓	✓	✓	✓	✓	✓
Mid-PFT Data									
Other Fit Tests						✓		✓	
FPFT Data				✓	✓	✓	✓	✓	✓
Injury Status									
Stress Fracture	✓	✓	✓				✓	✓	✓
Overuse Injuries	✓	✓	✓				✓		✓
Mishap/Acute Injuries	✓	✓	✓				✓		✓
Questionnaire									
Init Fit Level	✓	✓	✓				✓	✓	✓
H Regulation	✓	✓	✓				✓	✓	✓
Prev Injuries	✓	✓	✓				✓	✓	✓
Anthropometry									
Gender	F	F	M	M	M	M	M, F	M, F	✓
Ht, Wt, Age	✓	✓	✓		✓	✓	✓	✓	✓
Detailed Anthro	✓		✓			✓		✓	
Training Regimen									
Ndays	83	83	82	85	85	63	63/70	112	---
Regimen	BCT	BCT	BCT	BCT	BCT	BCT	BCT/AIT	BCT	---
Reg Details	Good	---	OK	Poor	---	---	Poor	OK	---



communications

Applied Technologies

OVERUSE INJURY ASSESSMENT MODEL

Part III: Bone Stress Fracture Research

FINAL REPORT

Report No. J3181-07-337
for period February 22, 2002 – February 21, 2007
under Contract No. DAMD17-02-C-0073

Prepared by:

Charles H. Negus, Ph.D.
Weixin Shen, Ph.D.

L-3 Communications/Jaycor
3394 Carmel Mountain Road
San Diego, California 92121-1002

Prepared for:

Commander
U.S. Army Medical Research and Materiel Command
504 Scott Street
Fort Detrick, Maryland 21702-5012

August 2007

REPORT DOCUMENTATION PAGE				Form Approved OMB No. 0704-0188	
Public reporting burden for this collection of information is estimated to average 1 hour per response, including the time for reviewing instructions, searching existing data sources, gathering and maintaining the data needed, and completing and reviewing this collection of information. Send comments regarding this burden estimate or any other aspect of this collection of information, including suggestions for reducing this burden to Department of Defense, Washington Headquarters Services, Directorate for Information Operations and Reports (0704-0188), 1215 Jefferson Davis Highway, Suite 1204, Arlington, VA 22202-4302. Respondents should be aware that notwithstanding any other provision of law, no person shall be subject to any penalty for failing to comply with a collection of information if it does not display a currently valid OMB control number. PLEASE DO NOT RETURN YOUR FORM TO THE ABOVE ADDRESS.					
1. REPORT DATE (DD-MM-YYYY) 08-20-2007		2. REPORT TYPE Final Report		3. DATES COVERED (From - To) Feb. 2002 - Feb. 2007	
4. TITLE AND SUBTITLE Overuse Injury Assessment Model, Part III: Bone Stress Fracture Research				5a. CONTRACT NUMBER DAMD17-02-C0073	
				5b. GRANT NUMBER	
				5c. PROGRAM ELEMENT NUMBER	
6. AUTHOR(S) Charles H. Negus Weixin Shen				5d. PROJECT NUMBER 3181	
				5e. TASK NUMBER	
				5f. WORK UNIT NUMBER	
7. PERFORMING ORGANIZATION NAME(S) AND ADDRESS(ES) L-3 Communications/Jaycor 3394 Carmel Mountain Road San Diego, CA 92121				8. PERFORMING ORGANIZATION REPORT NUMBER J3181-07-337	
9. SPONSORING / MONITORING AGENCY NAME(S) AND ADDRESS(ES) U.S. Army Medical Research Acquisition Activity Director 820 Chandler Street Fort Detrick, MD 21702-5014				10. SPONSOR/MONITOR'S ACRONYM(S) USAMRAA	
				11. SPONSOR/MONITOR'S REPORT NUMBER(S)	
12. DISTRIBUTION / AVAILABILITY STATEMENT					
13. SUPPLEMENTARY NOTES					
14. ABSTRACT Bone is a living tissue whose function and adaptation are mechanically mediated, and bone related diseases often have a mechanical pathogenesis. Effective diagnosis, intervention, and treatment of maladies such as stress fracture could greatly benefit from an understanding of the mechanical environment that results <i>in vivo</i> during normal and atypical physical activity. The mechanical stimulus is, however, both highly patient and location specific. The goal of the bone-related portion of the Overuse Injury Modeling project was to develop various computational methods, using principles from engineering, to perform patient-specific analysis of pQCT images and to then begin to assess the stress distribution in the tibia on a patient specific basis.					
15. SUBJECT TERMS Bone, stress fracture, finite element analysis, pQCT, computational modeling					
16. SECURITY CLASSIFICATION OF:			17. LIMITATION OF ABSTRACT	18. NUMBER OF PAGES	19a. NAME OF RESPONSIBLE PERSON
a. REPORT UNCLASSIFIED	b. ABSTRACT UNCLASSIFIED	c. THIS PAGE UNCLASSIFIED			Blossom Widder
			UNLIMITED	77	19b. TELEPHONE NUMBER (include area code) (301) 619-7143

Executive Summary

This report describes three efforts related to preventing stress fractures in the military through the development of techniques intended for patient-specific analysis and modeling of subject tibias.

The first section of this report describes our effort to conduct a detailed analysis of pQCT images taken of the tibias of 59 volunteers from the University of Connecticut. The purpose of this study was to use pQCT to evaluate the subtle changes to bone morphology expected in a healthy adult female undergoing a rigorous short term exercise intervention. To this end, analysis software was written for the purpose in Matlab. The University of Connecticut cohort was chosen to be a similar age to military recruits, and the duration of the training intervention was intended to be typical of military indoctrination. A further goal was to identify trends between type of exercise and the tibial location where changes occurred. In order to make meaningful comparisons between images taken Pre training with those taken Mid or Post training, and across subjects, all image sets first underwent a rotation and registration procedure using software written for the purpose. Following rotation and registration, the software was used to make detailed, regional analyses of the tibias. It was found that trabecular density (Tb.Dn) in the ultra-distal tibia was the first measure to reflect bone changes brought on by increased physical activity. This early trabecular modeling is consistent with its faster remodeling rate compared to cortical bone, a fact owed to its greater surface area (Guo 2001). Further results suggest that impact-producing aerobic exercises are the most effective at producing such changes. That aerobic exercise seems necessary to produce observable changes is not surprising giving the state of knowledge of bone cell mechanobiology.

The second section of this report describes a study in which a larger set of pQCT images was collected from recruits in the Israeli Defense Force. As with the University of Connecticut study, pQCT images were collected prior to basic combat training. Rather than conducting a “Pre-Post” type analysis, the image analysis software written for the University of Connecticut study was used to conduct a study of morphological differences between male and female recruits. This study determined that while women have higher cortical density than men, they have less bone area. Higher density bone tends to be more brittle, and thus more prone to stress fracture. Additionally, the tibias of females in this study had moments of inertia roughly half that of men, indicating similar loads may yield higher bending stresses in women than in men.

These two studies demonstrated that pQCT gives reliable and repeatable measurements of bone mineralization and yields accurate geometric measurements. Further, it inherently takes into account some factors such as genetics, diet, and hormones. These

observations led to the third effort described in this report: using pQCT to generate Patient Specific Finite Element models of the tibia. The procedure involved taking measurements at three slice planes (4%, 38%, 66%) and then scaling a generic tibia to match these dimensions. Next, the tibia model material properties are predicted per element based on the density values in the pQCT images. Applied loading conditions are also derived on a patient-specific basis from an inverse dynamics biomechanical model. The results of a pilot study using this procedure on a subset of the University of Connecticut cohort are presented.

Contents

	<u>Page</u>
1. INTRODUCTION	1
2. REGIONAL BONE CHANGES IN THE TIBIA RESULTING FROM SHORT TERM EXERCISE REGIMENS	3
2.1 INTRODUCTION	3
2.2 MATERIALS AND METHODS	4
2.2.1 <i>Subjects</i>	4
2.2.2 <i>Exercise Regimens</i>	5
2.2.3 <i>pQCT Collection</i>	5
2.2.4 <i>Data Analysis</i>	7
2.2.5 <i>Statistical Methods</i>	9
2.3 RESULTS	10
2.3.1 <i>Density measures</i>	10
2.3.2 <i>Areal Measures</i>	10
2.3.3 <i>BMC Measures</i>	10
2.3.4 <i>Strength Indices</i>	10
2.4 DISCUSSION	20
3. ISRAELI DEFENSE FORCE COHORT ANALYSIS	23
3.1 INTRODUCTION	23
3.2 METHODS	23
3.3 RESULTS	24
3.3.1 <i>Measures at 4% of Tibial Length</i>	24
3.3.2 <i>Measures at 38% of Tibial Length</i>	24
3.3.3 <i>Measures at 66% of Tibial Length</i>	24
3.3.4 <i>Geometric Measures</i>	24
3.4 DISCUSSION	33
4. PATIENT SPECIFIC STRESS ANALYSIS	35
4.1 BACKGROUND	35
4.1.1 <i>Introduction: Mechanobiology in bone related diseases</i>	35
4.1.2 <i>Current challenges to patient-specific computational modeling</i>	39
4.2 OUR APPROACH TO PATIENT SPECIFIC FE MODELING	40
4.2.1 <i>pQCT to 3D Model procedure</i>	40
4.3 FUTURE IMPROVEMENTS	43
4.4 SUMMARY	44
5. REFERENCES	45
APPENDIX A. PQCT IMAGE ANALYSIS UTILITIES	49
APPENDIX B. SAMPLE PATIENT SPECIFIC FEA RESULTS	51

Illustrations

	<u>Page</u>
1. ANALYSIS SECTOR DEFINITIONS.	8
2. AVERAGE REGIONAL TB.DN, 4% (MG/CM ³). PRE (SOLID), MID (DASHED), AND POST (DOTTED) TRAINING.	17
3. AVERAGE REGIONAL TRABECULAR [BMC], 4% (MG/MM). PRE(SOLID), MID (DASHED), AND POST (DOTTED) TRAINING.	18
4. CORTICAL THICKNESS, CT.TH, 66%, MM. PRE (SOLID), AND POST (DASHED) TRAINING.	19
5. NORMALIZED CANAL RADIUS, CA. RD , 66%. PRE (SOLID), AND POST (DASHED) TRAINING.	20
6. REGIONAL TRABECULAR DENSITY AT 4% OF TIBIAL LENGTH.	25
7. REGIONAL TRABECULAR AREA AT 4% OF TIBIAL LENGTH.	25
8. REGIONAL CORTICAL DENSITY AT 38% OF TIBIAL LENGTH.	26
9. REGIONAL CORTICAL AREA AT 38% OF TIBIAL LENGTH.	26
10. REGIONAL NORMALIZED CANAL RADIUS AT 38% OF TIBIAL LENGTH.	27
11. REGIONAL CORTICAL THICKNESS AT 38% OF TIBIAL LENGTH.	27
12. REGIONAL CORTICAL DENSITY AT 66% OF TIBIAL LENGTH.	28
13. REGIONAL CORTICAL AREA AT 66% OF TIBIAL LENGTH.	28
14. REGIONAL NORMALIZED CANAL RADIUS AT 66% OF TIBIAL LENGTH.	29
15. REGIONAL CORTICAL THICKNESS AT 66% OF TIBIAL LENGTH.	29
16. CROSS SECTIONAL MOMENTS OF INERTIA MEASURED ABOUT THE MEDIAL-LATERAL (ML), ANTERIOR-POSTERIOR (AP), AND POLAR AXES AT 38% OF TIBIAL LENGTH.	30
17. CROSS SECTIONAL MOMENTS OF INERTIA MEASURED ABOUT THE MEDIAL-LATERAL (ML), ANTERIOR-POSTERIOR (AP), AND POLAR AXES AT 66% OF TIBIAL LENGTH.	30
18. BONE STRENGTH INDEX MEASURED ABOUT THE MEDIAL-LATERAL (ML), ANTERIOR-POSTERIOR (AP), AND POLAR AXES AT 38% OF TIBIAL LENGTH.	31
19. BONE STRENGTH INDEX MEASURED ABOUT THE MEDIAL-LATERAL (ML), ANTERIOR-POSTERIOR (AP), AND POLAR AXES AT 66% OF TIBIAL LENGTH.	31
20. DIAPHYSEAL WIDTH MEASURED ALONG THE MEDIAL-LATERAL (ML) AND ANTERIOR-POSTERIOR (AP) AXES AT 38% OF TIBIAL LENGTH.	32
21. DIAPHYSEAL WIDTH MEASURED ALONG THE MEDIAL-LATERAL (ML) AND ANTERIOR-POSTERIOR (AP) AXES AT 66% OF TIBIAL LENGTH.	32
22. A MODEL OF STRAIN AMPLIFICATION FROM THE ORGAN LEVEL (A) TO TISSUE-LEVEL STRAIN RATE (B) TO THE OSTEOCYTE RESIDING IN THE LACUNAR-CANALICULAR SYSTEM (C1, C2). IMAGE COURTESY OF MELISSA KNOTHE-TATE, CASE WESTERN RESERVE UNIVERSITY.	36
23. VARIATIONS IN SHAPE AND DENSITY DISTRIBUTION FROM 16 FEMALE PARTICIPANTS, AGE 18-35, OF THE UNIVERSITY OF CONNECTICUT STUDY (SEE CHAPTER 2). IMAGES WERE TAKEN BY PQCT AT 38% OF TIBIAL LENGTH. THESE MORPHOLOGICAL VARIATIONS, COMBINED WITH INDIVIDUAL ANTHROPOMETRICS AND PHYSICAL ACTIVITY, WILL LEAD TO A HIGHLY PATIENT AND LOCATION SPECIFIC STRESS/STRAIN PROFILE.	38

24.	DIAPHYSEAL BOUNDARIES (GREEN AND BLUE TRACES) IMPORTED INTO A GENERIC TIBIAL MODEL OF THE EPIPHYSES WITH THE DIAPHYSIS MISSING. THE PATIENT’S OWN PQCT IMAGES ARE USED TO MODEL THE HIGH STRESS DIAPHYSEAL REGION.	41
25.	A FINITE ELEMENT MESH OF A TIBIA GENERATED IN TRUEGRID.....	42
26.	A SEMI-TRANSPARENT VIEW OF THE FINAL FINITE ELEMENT MODEL OF A SUBJECT. THE EXTERIOR SHAPE OF THE BONE AND THE DENSITY DISTRIBUTION HAVE BEEN DERIVED FROM THREE PQCT IMAGES TAKEN FROM THE SUBJECT.	43
27.	A TWO-LEVEL PROTOCOL FOR ASSESSING STRESS FRACTURE RISK IN RECRUITS.	44
28.	SUBJECT 02: TOP (FROM LEFT): PQCT IMAGES, FEA MODEL AT 38% (ABOVE) AND 66% (BELOW), PREDICTED 3D GEOMETRY, PREDICTED 3D DENSITY. BOTTOM (FROM LEFT): PREDICTED PRINCIPAL STRESS DISTRIBUTION FOR A 3BW LOAD, PREDICTED PRINCIPAL STRESS DISTRIBUTION FOR A 1000N LOAD.	55
29.	SUBJECT 04: TOP (FROM LEFT): PQCT IMAGES, FEA MODEL AT 38% (ABOVE) AND 66% (BELOW), PREDICTED 3D GEOMETRY, PREDICTED 3D DENSITY. BOTTOM (FROM LEFT): PREDICTED PRINCIPAL STRESS DISTRIBUTION FOR A 3BW LOAD, PREDICTED PRINCIPAL STRESS DISTRIBUTION FOR A 1000N LOAD.	56
30.	SUBJECT 06: TOP (FROM LEFT): PQCT IMAGES, FEA MODEL AT 38% (ABOVE) AND 66% (BELOW), PREDICTED 3D GEOMETRY, PREDICTED 3D DENSITY. BOTTOM (FROM LEFT): PREDICTED PRINCIPAL STRESS DISTRIBUTION FOR A 3BW LOAD, PREDICTED PRINCIPAL STRESS DISTRIBUTION FOR A 1000N LOAD.	57
31.	SUBJECT 13: TOP (FROM LEFT): PQCT IMAGES, FEA MODEL AT 38% (ABOVE) AND 66% (BELOW), PREDICTED 3D GEOMETRY, PREDICTED 3D DENSITY. BOTTOM (FROM LEFT): PREDICTED PRINCIPAL STRESS DISTRIBUTION FOR A 3BW LOAD, PREDICTED PRINCIPAL STRESS DISTRIBUTION FOR A 1000N LOAD.	58
32.	SUBJECT 14: TOP (FROM LEFT): PQCT IMAGES, FEA MODEL AT 38% (ABOVE) AND 66% (BELOW), PREDICTED 3D GEOMETRY, PREDICTED 3D DENSITY. BOTTOM (FROM LEFT): PREDICTED PRINCIPAL STRESS DISTRIBUTION FOR A 3BW LOAD, PREDICTED PRINCIPAL STRESS DISTRIBUTION FOR A 1000N LOAD.	59
33.	SUBJECT 18: TOP (FROM LEFT): PQCT IMAGES, FEA MODEL AT 38% (ABOVE) AND 66% (BELOW), PREDICTED 3D GEOMETRY, PREDICTED 3D DENSITY. BOTTOM (FROM LEFT): PREDICTED PRINCIPAL STRESS DISTRIBUTION FOR A 3BW LOAD, PREDICTED PRINCIPAL STRESS DISTRIBUTION FOR A 1000N LOAD.	60
34.	SUBJECT 30: TOP (FROM LEFT): PQCT IMAGES, FEA MODEL AT 38% (ABOVE) AND 66% (BELOW), PREDICTED 3D GEOMETRY, PREDICTED 3D DENSITY. BOTTOM (FROM LEFT): PREDICTED PRINCIPAL STRESS DISTRIBUTION FOR A 3BW LOAD, PREDICTED PRINCIPAL STRESS DISTRIBUTION FOR A 1000N LOAD.	61
35.	SUBJECT 33: TOP (FROM LEFT): PQCT IMAGES, FEA MODEL AT 38% (ABOVE) AND 66% (BELOW), PREDICTED 3D GEOMETRY, PREDICTED 3D DENSITY. BOTTOM (FROM LEFT): PREDICTED PRINCIPAL STRESS DISTRIBUTION FOR A 3BW LOAD, PREDICTED PRINCIPAL STRESS DISTRIBUTION FOR A 1000N LOAD.	62
36.	SUBJECT 41: TOP (FROM LEFT): PQCT IMAGES, FEA MODEL AT 38% (ABOVE) AND 66% (BELOW), PREDICTED 3D GEOMETRY, PREDICTED 3D DENSITY. BOTTOM (FROM LEFT): PREDICTED PRINCIPAL STRESS DISTRIBUTION FOR A 3BW LOAD, PREDICTED PRINCIPAL STRESS DISTRIBUTION FOR A 1000N LOAD.	63
37.	SUBJECT 42: TOP (FROM LEFT): PQCT IMAGES, FEA MODEL AT 38% (ABOVE) AND 66% (BELOW), PREDICTED 3D GEOMETRY, PREDICTED 3D DENSITY. BOTTOM (FROM LEFT): PREDICTED PRINCIPAL STRESS DISTRIBUTION FOR A 3BW LOAD, PREDICTED PRINCIPAL STRESS DISTRIBUTION FOR A 1000N LOAD.	64

38.	SUBJECT 48: TOP (FROM LEFT): PQCT IMAGES, FEA MODEL AT 38% (ABOVE) AND 66% (BELOW), PREDICTED 3D GEOMETRY, PREDICTED 3D DENSITY. BOTTOM (FROM LEFT): PREDICTED PRINCIPAL STRESS DISTRIBUTION FOR A 3BW LOAD, PREDICTED PRINCIPAL STRESS DISTRIBUTION FOR A 1000N LOAD.....	65
39.	SUBJECT 49: TOP (FROM LEFT): PQCT IMAGES, FEA MODEL AT 38% (ABOVE) AND 66% (BELOW), PREDICTED 3D GEOMETRY, PREDICTED 3D DENSITY. BOTTOM (FROM LEFT): PREDICTED PRINCIPAL STRESS DISTRIBUTION FOR A 3BW LOAD, PREDICTED PRINCIPAL STRESS DISTRIBUTION FOR A 1000N LOAD.....	66
40.	SUBJECT 52: TOP (FROM LEFT): PQCT IMAGES, FEA MODEL AT 38% (ABOVE) AND 66% (BELOW), PREDICTED 3D GEOMETRY, PREDICTED 3D DENSITY. BOTTOM (FROM LEFT): PREDICTED PRINCIPAL STRESS DISTRIBUTION FOR A 3BW LOAD, PREDICTED PRINCIPAL STRESS DISTRIBUTION FOR A 1000N LOAD.....	67
41.	SUBJECT 54: TOP (FROM LEFT): PQCT IMAGES, FEA MODEL AT 38% (ABOVE) AND 66% (BELOW), PREDICTED 3D GEOMETRY, PREDICTED 3D DENSITY. BOTTOM (FROM LEFT): PREDICTED PRINCIPAL STRESS DISTRIBUTION FOR A 3BW LOAD, PREDICTED PRINCIPAL STRESS DISTRIBUTION FOR A 1000N LOAD.....	68
42.	SUBJECT 58: TOP (FROM LEFT): PQCT IMAGES, FEA MODEL AT 38% (ABOVE) AND 66% (BELOW), PREDICTED 3D GEOMETRY, PREDICTED 3D DENSITY. BOTTOM (FROM LEFT): PREDICTED PRINCIPAL STRESS DISTRIBUTION FOR A 3BW LOAD, PREDICTED PRINCIPAL STRESS DISTRIBUTION FOR A 1000N LOAD.....	69
43.	SUBJECT 60: TOP (FROM LEFT): PQCT IMAGES, FEA MODEL AT 38% (ABOVE) AND 66% (BELOW), PREDICTED 3D GEOMETRY, PREDICTED 3D DENSITY. BOTTOM (FROM LEFT): PREDICTED PRINCIPAL STRESS DISTRIBUTION FOR A 3BW LOAD, PREDICTED PRINCIPAL STRESS DISTRIBUTION FOR A 1000N LOAD.....	70
44.	SUBJECT 80: TOP (FROM LEFT): PQCT IMAGES, FEA MODEL AT 38% (ABOVE) AND 66% (BELOW), PREDICTED 3D GEOMETRY, PREDICTED 3D DENSITY. BOTTOM (FROM LEFT): PREDICTED PRINCIPAL STRESS DISTRIBUTION FOR A 3BW LOAD, PREDICTED PRINCIPAL STRESS DISTRIBUTION FOR A 1000N LOAD.....	71

Tables

	<u>Page</u>
1. SUBJECT PRESTUDY CHARACTERISTICS.....	5
2. AEROBIC GROUP EXERCISE REGIMEN.....	6
3. RESISTANCE GROUP EXERCISE REGIMEN	6
4. SPECIFIC EXERCISE REGIMEN- RESISTANCE GROUP	7
5. REGIONAL TRABECULAR DENSITY (MEAN, SD), MEAN CHANGES, AND P-VALUE (LSD) WHERE SIGNIFICANT, 4%.....	12
6. REGIONAL TRABECULAR AREA (MEAN, SD), MEAN CHANGES, AND P-VALUE (LSD) WHERE SIGNIFICANT, 4%	12
7. REGIONAL BONE MINERAL CONTENT (MEAN, SD), MEAN CHANGES, AND P-VALUE (LSD) WHERE SIGNIFICANT, 4%.....	13
8. REGIONAL CORTICAL DENSITY (MEAN, SD) AND MEAN CHANGES, 38%.	13
9. REGIONAL CORTICAL AREA (MEAN AND SD) AND MEAN CHANGES, 38%.....	14
10. REGIONAL BONE MINERAL CONTENT (MEAN, SD) AND MEAN CHANGES, 38%.	14
11. REGIONAL CORTICAL DENSITY (MEAN, SD) AND MEAN CHANGES, 66%.	15
12. REGIONAL CORTICAL AREA (MEAN, SD) AND MEAN CHANGES, 66%.	16
13. REGIONAL BONE MINERAL CONTENT (MEAN, SD) AND MEAN CHANGES, 66%.	16

1. Introduction

Bone is a living tissue whose function and adaptation are mechanically mediated, and bone related diseases often have a mechanical pathogenesis. Effective diagnosis, intervention, and treatment of maladies such as stress fracture could greatly benefit from an understanding of the mechanical environment that results *in vivo* during normal and atypical physical activity. The mechanical stimulus is, however, both highly patient and location specific. The goal of the bone-related portion of the Overuse Injury Modeling project was to develop various computational methods, using principles from engineering, to perform patient-specific analysis of pQCT images and to then begin to assess the stress distribution in the tibia on a patient specific basis.

This report is divided into three sections. The first section (Chapter 2) describes research and analysis of data collected from a USARIEM sponsored study conducted with volunteers from the University of Connecticut. This chapter is substantially a reprint of a manuscript submitted to the Journal of Bone and Mineral Research which describes the study in detail. Summaries of the Matlab codes used to conduct the analysis are included in the Appendix as a supplement to this.

The second section (Chapter 3) describes a similarly structured study involving a cohort from the Israeli Defense Forces. This study, however, only analyzed baseline pQCT images collected from 91 recruits during induction to Basic Combat Training. The goal of this study was to quantify differences in bone morphology between men and women.

The third section (Chapter 4) describes our efforts to develop modeling software which can generate and analyze a fully three-dimensional model tibia given only a few pQCT scans of an individual. The model is then used as input to a finite element analysis which estimates *in vivo* stresses and strains in the bone given the subjects body weight. This process is referred to as Patient Specific Finite Element Analysis.

Since stress fracture occurrence is a highly patient-specific phenomenon, their prevention will largely have to be patient-specific as well. The analysis and modeling techniques developed in the course of this research will contribute to diagnostic capabilities that will be practical enough for widespread military use.

2. Regional Bone Changes in the Tibia Resulting from Short Term Exercise Regimens

2.1 Introduction

Controlled studies intending to show the beneficial effects of exercise intervention on bone strength in humans present two primary difficulties. First, a physical regimen must be of sufficient intensity and duration when compared with the normal baseline activities of a subject to produce a mechanical stimulus of sufficient magnitude and duration to result in adaptation. Secondly, a noninvasive diagnostic technique must be used which has adequate resolution to reliably observe what are likely to be in adults, subtle changes in bone morphology.

These observable “subtle changes” are of two types: changes in volumetric bone mineral density (vBMD) and changes in geometric or architectural changes such as cortical thickness (**Ct.Th**), cortical area (**Ct.Ar**), or cross-sectional moment of inertia (**I** or **J**). Most of these changes are expected to be local, both in terms of longitudinal location (e.g., epiphyseal vs diaphyseal) and in terms of cross-sectional region (e.g., anterior vs posterior) with different regimens leading to differing localized effects.

Exercise intervention studies have not, however, been primarily concerned with quantifying localized effects, instead demonstrating, among various cohorts, the osteogenic effect of exercise and physical activity (Chilibeck et al. 1995; Schoutens et al. 1989). In a 1999 review of the literature on the effect of exercise interventions on bone loss in pre- and post-menopausal women (most of which relied on DXA measurements). Wolff et al. (1999) found that exercise training programs reversed or prevented bone loss in the femoral neck and lumbar spine. Vainionpaa et al. (2007) used QCT to measure the bone geometry in 65 adult women before and after an exercise intervention, finding that impact-exercises resulted in a significantly higher femoral circumference at mid diaphysis. Additionally, a number of animal studies have demonstrated the importance of dynamic bone loading for instigating an osteogenic response (Judex and Zernicke 2000; Mosley and Lanyon 1998; Robling et al. 2002; Rubin and Lanyon 1984; Umemura et al. 1997). While two dimensional imaging techniques such as DXA may show long term bone adaptations, it lacks the resolution to detect the subtle changes occurring in the short term (3 months or less).

Peripheral Quantitative Computed Tomography (pQCT) has been validated and used extensively to make assessments of whole cross-sectional properties (Sievanen et al. 1998; Fujita 2002). Geometric indices based on such measurements are useful as they have been shown to correlate with fracture risk (Tommasini et al. 2005). pQCT has also recently been used to measure bone quality changes resulting from exercise intervention among children

(Heinonen et al. 2000; Johannsen et al. 2003; Macdonald et al. 2007; Specker and Binkley 2003). These results confirm similar findings from DXA studies of habitual physical activity (Rautava et al. 2007; Tobias et al. 2007).

pQCT also presents the opportunity for more refined, regional analysis of changes to bone morphology in the long bones of the lower extremities. This is particularly true if the images acquired by pQCT are exported and analyzed a posteriori with specialized software. Some recent research has employed pQCT to conduct a regional analysis of bone cross-sections. pQCT has been used to examine regional variations in the cortical bone of animals (Nonaka et al. 2006) and humans (Lai et al. 2005a) and trabecular bone in humans (Lai et al. 2005b). The study by Lai et al. (2005a) of postmenopausal women found that the posterior cortex had a significantly higher cortical density than the anterior cortex, suggesting that the posterior cortex may be adapted for compressive loading and the anterior cortex is adapted to the tensile loading which are predominant loading modes during gait. Lai et al. (2005b) used pQCT and microCT to compare trabecular BMD in four quadrants of the ultradistal tibia. They found that both pQCT and microCT showed significantly lower trabecular BMD in the anterior than in the posterior region. In an exercise and hormone replacement therapy intervention study of postmenopausal women, Cheng et al. (2002) used QCT with the program Bonalyse 1.3 to calculate the polar distribution of mass in the diaphysis of the tibia and femur. They found that HRT and high-impact exercise resulted in a significant positive increase in bone mass in the proximal tibia, primarily in the antero-posterior direction. Ruffing et al. (2006) used pQCT to perform a statistical analysis correlating lifestyle factors with bone mass and size for a large cohort of military cadets.

The usefulness of pQCT to detect early, regional changes in bone from an exercise intervention is not well studied. The purpose of this study was to use pQCT to evaluate the subtle changes to bone morphology expected in a healthy adult female undergoing a rigorous short term exercise intervention. The cohort was chosen to be a similar age to military recruits, and the duration of the intervention was intended to be typical of military indoctrination. A further goal was to identify trends between type of exercise and the tibial location where changes occurred.

2.2 Materials and Methods

2.2.1 Subjects

Seventy-one subjects initially signed up for the study and 14 dropped after pre-testing. The remaining 57 were divided into four exercise regimen groups: Control, Aerobic, Resistance, Combined (Aerobic and Resistance). Their mean age, height, and weight are given in Table 1.

Table 1. Subject Prestudy Characteristics.

	<i>n</i>	<i>Age (yr)</i>	<i>Height (in)</i>	<i>Weight (kg)</i>
Control	10	19.7 ± 1.42	65.10 ± 2.77	65.98 ± 8.19
Aerobic	14	21.07 ± 1.90	65.14 ± 2.38	64.99 ± 6.78
Resistance	18	20.44 ± 2.12	65.00 ± 3.20	65.15 ± 8.14
Combined	17	20.06 ± 1.56	64.82 ± 2.81	65.55 ± 12.12

2.2.2 Exercise Regimens

Subjects in the Aerobic training group performed aerobic or running based exercises on three alternating days a week. On nontesting weeks, Mondays were used for 20-30 minute running at 70 to 85% of maximum heart rate. On Wednesdays, subjects conducted interval runs, totaling about 2 miles, comprised of 400m, 800m, 1200m, or 1600m segments at near maximum heart rate (see Table 2). On nontesting Fridays, subjects performed 30 minutes of running or similar aerobic exercise at 80-85% maximum heart rate. All sessions included 5-10 minute warm-up and warm-down periods. Heart rates were monitored using Polar heart rate monitors (Polar Electro Oy, Finland, model #S610).

Subjects in the Resistance exercise training group performed nonlinear, periodized resistance training in which the load and repetition varied on a weekly basis (see Table 3). The exercises and load ranges performed were selected specifically to impact lower body bone remodeling (See Table 4). “Light” days involved 12 RM loads, “Moderate” days involved 8-10RM loads, and “heavy” days involved 6-7 RM loads.

Subjects in the Combined exercise training group performed both the aerobic and the resistance exercise training regimens on the same day and during the same session. The resistance regimen was performed prior to the aerobic regimen.

2.2.3 pQCT Collection

Images were collected using a Norland-Stratek XCT-3000. The left tibia was imaged in 55 subjects, the right in the remaining two. Before each image, a scout scan was conducted to determine the location of the endplate of the distal tibia. A reference line was placed at this location and the overall tibial length for each subject was entered. Prior to data collection, a hydroxyapatite standard phantom was used to ensure measured values were within manufacturers limits. Images were collected at slice levels of 4%, 38% and 66% of tibial length. A slice depth of 2.2 mm was used at a voxel resolution of 0.4 mm/voxel.

Table 2. Aerobic Group Exercise Regimen

		Week 2	Week 3	Week 4	Week 5	Week 6	Week 7	Week 8	Week 9	Week 10	Week 11	Week 12	Week 13
M	Testing	Testing	20-30 Min @ 75%	30 Min @ 75%	30 Min @ 75%	30 Min @ 75%	30 Min @ 75%	30 Min @ 75%	30 Min @ 75%	30 Min @ 75%	30 Min @ 75%	Testing	Testing
W	Testing	Testing	20-30 Min @ 75%	30 Min @ 75%	1 Mile	1.5 Mile	2 Mile	2 Mile	2 Mile	2 Mile	3 Mile	Testing	Testing
F	Testing	2 Mi	20-30 Min @ 75%	30 Min @ 80- 85%	30 Min @ 80- 85%	30 Min @ 80- 85%	30 Min @ 80- 85%	30 Min @ 80- 85%	30 Min @ 80- 85%	30 Min @ 80- 85%	2 Mile	Testing	Testing

Table 3. Resistance Group Exercise Regimen

	Week 1	Week 2	Week 3	Week 4	Week 5	Week 6	Week 7	Week 8	Week 9	Week 10	Week 11	Week 12	Week 13
M	Testing	Testing	Light	Moderate	Heavy	Moderate	Testing	Heavy	Moderate	Light	Heavy	Testing	Testing
W	Testing	Testing	Moderate	Light	Moderate	Heavy	Testing	Light	Heavy	Heavy	Moderate	Testing	Testing
F	Testing	Testing	Heavy	Moderate	Light	Moderate	Moderate	Heavy	Moderate	Moderate	Light	Testing	Testing

Table 4. Specific Exercise Regimen- Resistance Group

Monday	Wednesday	Friday
Squat	Leg Press*	Squat
Stiff Leg Deadlift	Stiff Leg Deadlift	Stiff Leg Deadlift
Bench	Incline Bench	Bench
Pulldown	Seated Row	Pulldown
Upright Row	Shoulder Press	Upright Row
Calf Exercises	Calf Exercises	Calf Exercises
Abdominal Work	Abdominal Work	Abdominal Work

Images were collected, at each slice level, during pre-training testing (“Pre” images), at week 7 (“Mid” training) and at week 13 (“Post” training). Thus there were nine images (4%, 38%, and 66% at Pre, Mid, and Post training) comprising each subject “image set”.

2.2.4 Data Analysis

At the conclusion of the 13 week study, all image sets were analyzed using Matlab codes written for the purpose by the authors.

In order to make meaningful comparisons between images taken Pre training with those taken Mid or Post training, and across subjects, all image sets first underwent a rotation and registration procedure.

For each subject, the 4% slice was centered on the tibial perimeter, but the 38% and 66% slices were centered on the intramedullary canal so that the canal radius and cortical wall thickness could be accurately calculated in each sector. The crest of the tibia at 66% was then assumed to point in the anterior direction, and the 38% and 4% slices were rotated accordingly by the same angle as at 66%. The images of two subjects which were collected from their right legs were inverted so that they could be compared with the left tibias of the other subjects. Alignment was checked for each subject by overlaying plots of the periosteal boundaries for each subject and minimizing the difference in boundaries.

Six 60° polar sectors were defined for analysis: Lateral Anterior, Anterior, Medial Anterior, Medial Posterior, Posterior, and Lateral Posterior (see Figure 1).

The tibia was isolated in each image and each voxel within the tibia was classified based on its vBMD value as being either trabecular (100-600 mg/cm³), transitional (600-800 mg/cm³), or cortical (800-1500mg/cm³). Histograms for each image indicated there were relatively few pixels in the transitional regime which is in keeping with the known separation between cortical and trabecular BMD values. For this reason, voxels in the transitional

regime were assumed to be largely partial-volume artifacts, and not included in the final analysis.

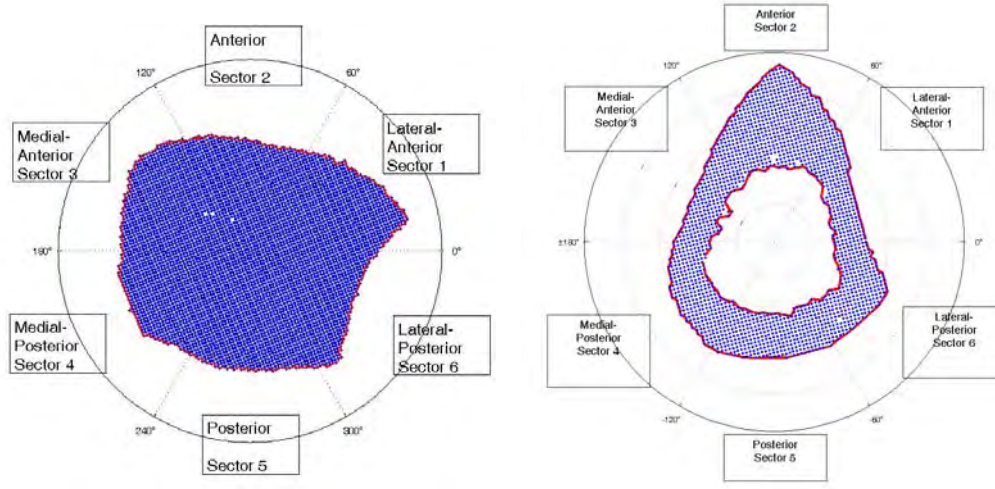


Figure 1. Analysis Sector definitions.

Shown is a 4% slice (left) and a 66% slice. The crest of the tibia at 66% was rotated to point in the anterior direction for each subject. This is the left tibia, looking proximally.

Because a variety of methods for calculating geometric and density parameters from pQCT have been reported in the literature, and because this analysis was not based on parameters calculated from the native, proprietary pQCT software such as BonAlyse, we present a detailed description of how each quantity was calculated.

For each tibia image, the following calculations were made:

- **AP, ML** (Anterior-Posterior and Medial-Lateral width: 4%, 38%, and 66%): Calculated from the coordinates of the voxels at the greatest directional extent.
- **I_{AP}, I_{ML}, J** (Cross sectional moments of inertia: 38% and 66%): Moments of inertia calculated about the anterior-posterior and medial-lateral axes respectively. The polar moment of inertia $J = I_{AP} + I_{ML}$. Moments of inertia were calculated using only those voxels in the cortical threshold range.
- **Ct.Ar** (Cortical area, for 38% and 66% only): The areal sum of the voxels in the cortical range. This was calculated for each polar sector (e.g., Ct.Ar_{Lat-Ant}) and for the whole tibial cross section (Ct.Ar_{Tot}).
- **Tb.Ar** (Trabecular area, for 4% only): The areal sum of the voxels in the trabecular range. Though calculated at 38% and 66%, there were too few voxels in this range for a meaningful analysis.

- **Ct.Dn** (Cortical density, for 38% and 66% only): The average of all voxels falling within the cortical thresholds. These were calculated for each polar sector and for the whole tibial cross section.
- **Tb.Dn** (Trabecular density, for 4% only): The average of all voxels falling within the trabecular thresholds. These were calculated for each polar sector and for the whole tibial cross section.
- **BMC** (Bone Mineral Content): Calculated by multiplying, for a given sector or region of interest, the **Ct.Dn** or **Tb.Dn** by **Ct.Ar** or **Tb.Ar**, respectively and then by the slice thickness (2.2 mm).
- **BSI** (Bone Strength Index, for 38% and 66% only): A measure of bending stiffness, $BSI = (Ct.Dn_{Tot})(I)$.
- **SI_{AP}, SI_{ML}** (Slenderness Index, 38% and 66% only): The ratio of the AP and ML section modulus to the product of tibial length, L and body weight, BW (Selker and Carter 1989; Tommasini et al. 2005). So for example, the SI about the anterior-posterior axis would be,

$$SI_{AP} = \frac{1}{\frac{\left[\frac{J}{AP/2} \right]}{[(L)(BW)]}} \quad (0.1)$$

- **Ct.Th** (Cortical thickness, 38% and 66% only): The average radial distance between the periosteal boundary and the endosteal boundary, calculated in 10° sector increments but averaged over 60° polar sectors.
- **Ca.|Rd|** (Normalized canal radius, 38% and 66%): The radial distance to the endosteal boundary divided by the radial distance to the periosteal boundary. Calculated in 10° sector increments but averaged over 60° polar sectors.

2.2.5 Statistical Methods

Trabecular remodeling was assessed solely using the 4% site, which contains but a thin cortical shell.. The number of trabecular voxels at the 38% and 66% were, in most cases, between 5-10% of the number at the 4% site.

The 38% and 66% sites were both used to assess changes in cortical bone.

2.3 Results

2.3.1 Density measures

Significant increases in Tb.Dn were observed in the medial sectors at the 4% site (Table 5 and Figure 2). Significant changes in Ct.Dn were not seen at either the 38% (Table 8) or 66% (Table 11) sites.

2.3.2 Areal Measures

A significant increase in Tb.Ar was only observed in the Lateral-Anterior sector of the Aerobic group (Table 6). No significant change was seen Ct.Ar at 38% (Table 9) or 66% (Table 12).

At the diaphyseal locations, Ct.Ar is closely related to the cortical thickness Ct.Th (shown in Figure 4 for 66%) and normalized medullary canal radius Ca.|Rd| (shown in Figure 5 for 66%) since these quantities are all a function of the number of voxels in the cortical threshold range. The Anterior sector of the Control group at 66% underwent a significant -3.75% ($p = .00006$) change in cortical thickness with a concomitant (though insignificant) -1.36% change in Ct.Ar. and .96% increase in Ct.Dn. Since the normalized canal radius Ca.|Rd| remained essentially unchanged, this suggests the decrease in cortical thickness was due primarily to endosteal resorption.

2.3.3 BMC Measures

The aerobic group had significant increases in BMC in the medial-anterior and lateral-anterior sectors at 4%, while the resistance group had modest, but not statistically significant increases in the Medial sectors (Table 7 and Figure 3).

2.3.4 Strength Indices

There were no significant changes found in I_{ML} , I_{AP} , J , BSI , or SI .

For the sectors at the 4% site that experienced a significant change in Tb.Dn, a regression analysis was conducted to see if the amount of change correlated with anthropometric or geometric parameters:

1. SI_{AVG} ($SI_{AP-38\%}$, $SI_{ML-38\%}$, $SI_{AP-66\%}$, $SI_{ML-66\%}$)
2. SI_{ML} ($SI_{ML-38\%}$, $SI_{ML-66\%}$)
3. SI_{AP} ($SI_{AP-38\%}$, $SI_{ML-38\%}$)
4. I_{ML} ($I_{ML-38\%}$, $I_{AP-66\%}$)
5. I_{AP} ($I_{AP-38\%}$, $I_{AP-66\%}$)
6. J ($J-38\%$, $J-66\%$)

7. **ML** (ML-38%, ML-66%)

8. **AP** (AP-38%, AP-66%)

9. **BW**

In each case, parameters were averaged among the quantities in parentheses and among pre, mid, and post values. None of the regions with significant changes in Tb.Dn correlated with any of these anthropometric/geometric parameters.

Table 5. Regional trabecular density (mean, SD), mean changes, and p-value (LSD) where significant, 4%.

	<i>Control</i>				<i>Aerobic</i>				<i>Resistance</i>				<i>Combined</i>			
	<i>Pre</i>	<i>Mid</i>	<i>Post</i>	<i>Avg.Pre-Post % Change</i>	<i>Pre</i>	<i>Mid</i>	<i>Post</i>	<i>Avg.Pre-Post % Change</i>	<i>Pre</i>	<i>Mid</i>	<i>Post</i>	<i>Avg.Pre-Post % Change</i>	<i>Pre</i>	<i>Mid</i>	<i>Post</i>	<i>Avg.Pre-Post % Change</i>
<i>4% Tb.Dn</i>																
Lat-Ant	290.2 15.9	289.2 15.7	289.2 14.0	-0.31	281.6 48.1	282.3 48.0	283.4 45.8	0.88	296.6 39.9	296.7 38.4	295.5 39.1	-0.33	284.6 31.2	285.6 28.9	284.8 29.7	0.13
Ant	278.1 16.3	276.1 17.1	278.0 17.0	-0.04	267.5 48.2	267.0 47.6	270.7 48.9	1.21	279.5 37.9	280.5 37.2	280.7 37.4	0.48	269.5 27.8	270.9 27.1	270.9 27.5	0.53
Med-Ant	272.0 22.0	271.1 18.7	269.4 18.3	-0.87	255.6 37.1	259.0 36.5	260.0 37.5	1.75 (p=.003)	264.9 37.6	265.4 40.1	265.1 37.7	0.10	258.6 22.4	261.1 21.0	260.9 19.6	1.00
Med-Post	297.0 25.3	297.3 28.8	297.6 27.1	0.17	279.2 30.5	285.8 31.6	288.0 31.8	3.16 (p=.000)	290.7 45.1	295.4 45.7	295.4 44.7	1.68 (p=.007)	282.9 33.0	287.8 32.8	288.7 31.0	2.18 (p=.00068)
Post	299.9 25.0	299.3 25.0	299.7 27.6	-0.09	280.0 40.7	282.3 41.0	282.1 41.0	0.75	302.9 46.2	301.3 44.2	302.1 46.1	-0.24	291.6 32.4	294.3 29.7	293.8 30.5	0.89
Lat-Post	301.9 33.1	304.1 31.9	304.6 31.2	0.98	286.5 51.5	290.2 51.9	287.9 49.4	0.66	312.4 52.3	314.1 52.1	311.9 52.7	-0.13	297.2 63.1	300.9 33.6	299.2 34.6	0.77
All	289.9 13.4	289.5 13.3	289.7 13.6	-0.03	275.1 39.6	277.8 39.7	278.7 38.8	1.40 (p=.0004)	291.2 39.8	292.2 39.8	291.8 39.4	0.26	280.7 26.3	283.4 24.8	283.0 24.5	0.92 (p=.0095)

Table 6. Regional trabecular area (mean, SD), mean changes, and p-value (LSD) where significant, 4%.

	<i>Control</i>				<i>Aerobic</i>				<i>Resistance</i>				<i>Combined</i>			
	<i>Pre</i>	<i>Mid</i>	<i>Post</i>	<i>Avg.Pre-Post % Change</i>	<i>Pre</i>	<i>Mid</i>	<i>Post</i>	<i>Avg.Pre-Post % Change</i>	<i>Pre</i>	<i>Mid</i>	<i>Post</i>	<i>Avg.Pre-Post % Change</i>	<i>Pre</i>	<i>Mid</i>	<i>Post</i>	<i>Avg.Pre-Post % Change</i>
<i>4% Tb.Ar</i>																
Lat-Ant	167.0 19.2	165.6 18.3	163.2 20.5	-2.28	160.9 18.7	161.2 16.2	166.4 16.4	3.68 (p=.0022)	157.3 29.6	161.9 33.7	159.9 31.7	1.48	158.4 18.6	158.1 19.2	158.7 21.0	0.03
Ant	141.0 18.1	143.0 20.1	138.9 18.3	-1.46	132.4 16.0	135.8 14.8	135.2 17.5	2.21	124.4 24.0	130.8 27.7	127.6 26.5	2.46	133.9 29.2	132.3 25.7	134.1 28.5	0.40
Med-Ant	206.5 21.0	204.5 20.9	203.9 18.4	-1.14	193.4 28.8	193.3 28.5	195.0 27.9	0.98	186.1 28.7	191.0 34.1	188.2 33.2	0.88	187.8 21.9	184.1 20.2	185.8 24.0	-1.13
Med-Post	189.2 15.1	187.9 13.9	187.8 14.6	-0.66	177.6 20.5	175.0 23.1	178.0 23.9	0.12	184.9 27.2	185.4 29.9	183.9 30.2	-0.72	176.3 14.8	174.3 14.9	174.9 13.9	-0.73
Post	155.2 21.7	156.3 22.0	154.2 22.5	-0.68	144.4 19.1	141.5 17.4	142.3 17.7	-1.26	142.3 21.7	141.3 22.6	140.9 22.1	-0.93	139.4 16.6	138.4 16.5	140.0 19.1	0.32
Lat-Post	129.7 20.7	130.9 17.9	127.6 20.9	-1.54	134.8 28.5	133.6 28.7	135.6 26.2	1.06	128.8 21.3	128.0 21.1	127.2 22.2	-1.27	126.4 15.8	128.2 16.9	130.2 23.0	2.74
All	164.8 15.8	164.7 15.7	162.6 16.2	-1.29	157.2 15.8	156.7 16.1	158.8 15.3	1.13	153.9 22.3	156.4 24.8	154.6 24.3	0.32	153.7 16.6	152.6 15.5	154.0 18.1	0.27

Table 7. Regional bone mineral content (mean, SD), mean changes, and p-value (LSD) where significant, 4%.

	<i>Control</i>				<i>Aerobic</i>				<i>Resistance</i>				<i>Combined</i>			
	<i>Pre</i>	<i>Mid</i>	<i>Post</i>	<i>Avg.Pre-Post % Change</i>	<i>Pre</i>	<i>Mid</i>	<i>Post</i>	<i>Avg.Pre-Post % Change</i>	<i>Pre</i>	<i>Mid</i>	<i>Post</i>	<i>Avg.Pre-Post % Change</i>	<i>Pre</i>	<i>Mid</i>	<i>Post</i>	<i>Avg.Pre-Post % Change</i>
<i>4% BMC</i>																
Lat-Ant	106.7 14.7	105.4 13.0	103.8 13.5	-2.57	99.1 17.9	99.6 16.6	103.2 16.0	4.63 (p=.0026)	102.5 22.9	105.7 26.4	104.1 25.4	1.13	98.8 13.1	99.0 13.5	99.1 14.7	0.15
Ant	86.3 12.6	86.8 13.0	85.0 12.5	-1.46	77.5 14.1	79.6 15.7	80.0 14.1	3.39	76.4 17.4	80.8 20.9	78.9 19.7	2.96	79.0 17.2	78.5 15.3	79.5 16.4	0.94
Med-Ant	122.9 7.9	121.5 9.9	120.4 8.3	-2.02	108.9 23.5	110.4 24.2	111.6 22.8	2.75 (p=.0381)	109.3 25.7	112.4 30.1	110.6 28.0	0.96	106.8 15.6	105.8 14.6	106.7 16.3	-0.15
Med-Post	123.5 13.6	122.7 13.2	122.8 12.8	-0.50	108.7 13.9	109.7 16.2	112.5 16.9	3.28	117.3 19.1	119.5 20.8	118.5 20.2	0.92	109.9 17.4	110.5 17.3	111.3 16.5	1.42
Post	102.4 16.7	102.8 16.3	101.6 17.2	-0.81	89.1 18.3	87.8 15.6	88.0 14.9	-0.51	94.4 18.1	93.2 18.1	93.4 19.3	-1.18	89.3 13.4	89.4 12.7	90.3 14.2	1.17
Lat-Post	86.6 19.2	87.9 16.6	85.7 17.2	-0.56	84.6 20.7	84.6 20.1	85.4 18.2	1.72	88.2 18.3	88.2 18.6	87.1 19.1	-1.35	82.4 12.4	84.7 13.1	85.4 15.8	3.55
All	104.7 10.6	104.5 10.2	103.2 10.3	-1.32	94.6 14.1	95.3 14.2	96.8 13.1	2.54 (p=.0069)	98.0 17.8	100.0 20.2	98.8 19.3	0.57	94.4 11.9	94.7 11.2	95.4 12.1	1.18

Table 8. Regional cortical density (mean, SD) and mean changes, 38%.

	<i>Control</i>				<i>Aerobic</i>				<i>Resistance</i>				<i>Combined</i>			
	<i>Pre</i>	<i>Mid</i>	<i>Post</i>	<i>Avg.Pre-Post %Change</i>	<i>Pre</i>	<i>Mid</i>	<i>Post</i>	<i>Avg.Pre-Post %Change</i>	<i>Pre</i>	<i>Mid</i>	<i>Post</i>	<i>Avg.Pre-Post %Change</i>	<i>Pre</i>	<i>Mid</i>	<i>Post</i>	<i>Avg.Pre-Post %Change</i>
<i>38% Ct.Dn</i>																
Lat-Ant	1197.8 17.1	1192.1 20.6	1195.8 17.5	-0.16	1210.5 22.2	1212.2 23.2	1211.1 23.5	0.06	1204.7 22.3	1205.3 25.7	1203.9 18.7	-0.05	1200.1 16.9	1201.5 16.3	1197.2 14.7	-0.23
Ant	1166.0 28.5	1165.4 29.5	1167.8 31.9	0.15	1177.4 32.2	1169.3 36.0	1174.4 31.7	-0.24	1179.3 27.0	1173.7 29.8	1181.2 22.9	0.17	1170.5 19.6	1166.7 21.0	1167.9 22.6	-0.22
Med-Ant	1209.9 26.0	1211.8 25.1	1210.3 23.9	0.04	1222.0 20.7	1227.0 21.7	1221.5 25.7	-0.03	1215.3 19.3	1219.3 27.6	1216.8 21.3	0.13	1217.4 20.3	1211.1 21.0	1216.6 19.5	-0.06
Med-Post	1224.1 24.2	1220.0 28.1	1222.6 27.0	-0.12	1228.6 17.0	1225.1 24.3	1224.8 20.6	-0.31	1224.5 19.5	1221.8 24.0	1221.5 25.5	-0.25	1225.2 17.6	1223.4 19.2	1218.8 16.7	-0.52
Post	1208.4 23.8	1204.1 23.5	1205.8 21.8	-0.21	1214.4 18.8	1213.9 14.7	1217.6 22.3	0.27	1209.6 20.3	1206.8 22.5	1206.9 22.7	-0.22	1211.5 20.3	1209.4 19.0	1211.1 21.8	-0.02
Lat-Post	1234.5 15.7	1232.9 19.5	1235.9 15.1	0.12	1246.0 18.5	1234.7 30.4	1239.3 20.8	-0.53	1241.8 24.0	1234.9 30.5	1238.1 21.2	-0.28	1235.2 20.3	1231.4 13.7	1235.7 15.9	0.05
All	1206.8 18.1	1204.4 18.4	1206.4 16.7	-0.03	1216.5 13.3	1213.7 14.7	1214.8 17.3	-0.13	1212.5 17.6	1210.3 18.0	1211.4 16.8	-0.08	1210.0 12.6	1207.3 12.3	1207.9 12.1	-0.17

Table 9. Regional cortical area (mean and SD) and mean changes, 38%.

	<i>Control</i>				<i>Aerobic</i>				<i>Resistance</i>				<i>Combined</i>			
	<i>Pre</i>	<i>Mid</i>	<i>Post</i>	<i>Avg.Pre-Post % Change</i>	<i>Pre</i>	<i>Mid</i>	<i>Post</i>	<i>Avg.Pre-Post % Change</i>	<i>Pre</i>	<i>Mid</i>	<i>Post</i>	<i>Avg.Pre-Post % Change</i>	<i>Pre</i>	<i>Mid</i>	<i>Post</i>	<i>Avg.Pre-Post % Change</i>
<i>38% Ct.Ar</i>																
Lat-Ant	29.1 6.0	29.2 5.9	29.1 5.8	0.36	27.5 3.6	27.6 3.7	26.7 3.8	-2.94	28.0 5.1	29.0 6.1	29.1 5.9	3.82	27.7 5.6	27.0 3.5	26.8 3.0	-1.75
Ant	65.3 8.2	66.3 8.8	66.2 8.0	1.37	58.4 7.8	59.5 7.8	59.7 7.2	2.36	62.0 11.7	62.3 10.2	61.8 10.3	0.24	61.9 9.1	62.6 8.7	62.6 9.9	0.93
Med-Ant	26.1 4.7	26.4 4.7	26.6 5.0	2.10	28.1 7.0	28.8 7.1	30.2 7.1	8.16	25.9 6.6	26.6 6.6	26.4 6.4	2.30	24.6 3.7	25.5 4.1	25.6 4.7	3.81
Med-Post	42.6 4.7	42.3 4.6	42.6 4.6	0.14	39.8 9.5	39.7 9.4	40.7 9.8	2.36	41.2 8.9	41.8 8.5	41.6 8.8	0.98	37.9 8.3	37.7 7.9	38.0 7.9	0.45
Post	42.2 6.4	43.7 6.6	42.4 6.8	0.45	39.1 8.7	39.7 9.4	38.8 10.0	-1.23	42.6 7.6	42.3 7.0	41.5 7.0	-2.41	40.5 7.2	40.5 7.5	40.2 7.5	-0.80
Lat-Post	34.8 7.3	35.2 7.5	35.1 7.1	0.91	35.0 7.8	34.6 7.1	33.8 8.0	-3.60	33.6 7.0	33.4 6.7	33.8 7.6	0.42	35.3 6.5	35.2 5.3	35.0 5.5	-0.25
All	40.0 4.3	40.5 4.3	40.3 4.1	0.89	38.0 4.3	38.3 4.2	38.3 4.3	0.85	38.9 6.3	39.2 6.1	39.0 6.0	0.89	38.0 4.3	38.1 3.2	38.0 3.6	0.40

Table 10. Regional bone mineral content (mean, SD) and mean changes, 38%.

	<i>Control</i>				<i>Aerobic</i>				<i>Resistance</i>				<i>Combined</i>			
	<i>Pre</i>	<i>Mid</i>	<i>Post</i>	<i>Avg.Pre-Post % Change</i>	<i>Pre</i>	<i>Mid</i>	<i>Post</i>	<i>Avg.Pre-Post % Change</i>	<i>Pre</i>	<i>Mid</i>	<i>Post</i>	<i>Avg.Pre-Post % Change</i>	<i>Pre</i>	<i>Mid</i>	<i>Post</i>	<i>Avg.Pre-Post % Change</i>
<i>38% BMC</i>																
Lat-Ant	76.8 16.2	76.6 15.6	76.7 15.6	0.20	73.3 9.4	73.6 9.8	71.1 10.3	-2.99	74.2 13.4	76.8 15.6	77.0 15.5	3.79	73.1 14.6	71.2 9.1	70.5 8.0	-1.99
Ant	167.6 20.8	169.8 21.9	169.8 19.6	1.51	151.2 19.3	152.9 20.3	154.1 17.9	2.12	160.4 28.4	160.6 25.6	160.5 25.5	0.39	159.4 23.2	160.4 20.6	160.6 24.5	0.67
Med-Ant	69.5 13.3	70.4 13.0	70.9 14.3	2.14	75.5 18.1	77.5 18.6	81.1 19.0	8.14	69.3 17.2	71.1 17.2	70.6 16.5	2.44	65.7 9.5	67.8 10.5	68.4 12.1	3.76
Med-Post	114.7 13.5	113.7 13.3	114.7 13.2	0.01	107.6 25.5	106.9 25.5	109.7 26.1	2.05	110.9 23.2	112.3 22.5	111.4 22.4	0.72	102.0 21.3	101.3 20.5	101.7 20.6	-0.05
Post	112.1 15.5	115.5 15.5	112.3 16.5	0.25	104.2 22.2	105.8 23.9	103.7 25.1	-1.00	113.2 19.4	112.2 18.2	110.0 17.7	-2.63	107.9 18.7	107.6 19.9	107.1 19.8	-0.87
Lat-Post	94.5 19.6	95.5 20.0	95.3 18.9	1.03	95.8 20.4	93.7 18.7	91.8 20.5	-4.10	91.5 18.1	90.4 17.2	91.8 19.7	0.15	95.8 17.5	95.2 13.7	95.0 14.2	-0.18
All	105.9 11.6	106.9 11.4	106.6 11.1	0.86	101.3 11.0	101.8 11.0	101.9 10.7	0.70	103.2 15.8	103.9 15.4	103.5 15.2	0.81	100.7 11.3	100.6 7.9	100.5 9.3	0.22

Table 11. Regional cortical density (mean, SD) and mean changes, 66%.

	<i>Control</i>				<i>Aerobic</i>				<i>Resistance</i>				<i>Combined</i>			
	<i>Pre</i>	<i>Mid</i>	<i>Post</i>	<i>Avg.Pre- Post % Change</i>	<i>Pre</i>	<i>Mid</i>	<i>Post</i>	<i>Avg.Pre- Post % Change</i>	<i>Pre</i>	<i>Mid</i>	<i>Post</i>	<i>Avg.Pre- Post % Change</i>	<i>Pre</i>	<i>Mid</i>	<i>Post</i>	<i>Avg.Pre- Post % Change</i>
66% Ct.Dn																
Lat-Ant	1147.9 18.2	1144.6 30.1	1148.3 13.6	0.05	1150.4 29.7	1156.0 22.3	1147.0 25.2	-0.24	1151.8 17.2	1155.3 24.1	1145.7 24.2	-0.52	1151.3 15.4	1147.8 19.3	1146.0 24.6	-0.45
Ant	1130.7 38.8	1130.7 31.0	1141.1 25.6	0.96	1147.2 29.4	1142.6 44.0	1150.4 34.8	0.28	1149.1 26.2	1148.5 24.0	1148.7 28.7	-0.02	1140.1 22.2	1139.8 18.5	1138.0 19.0	-0.17
Med-Ant	1190.0 33.5	1185.8 22.2	1179.9 20.5	-0.81	1201.1 34.0	1185.2 31.3	1190.0 22.8	-0.88	1193.7 20.5	1184.1 22.2	1186.0 19.2	-0.63	1194.7 19.4	1191.1 18.7	1188.3 18.0	-0.53
Med-Post	1208.4 19.8	1197.0 21.5	1201.1 16.3	-0.59	1213.6 16.2	1201.4 49.6	1209.5 38.2	-0.34	1214.4 17.5	1212.0 20.3	1212.7 25.6	-0.14	1208.9 23.7	1211.5 20.4	1212.9 16.3	0.36
Post	1197.5 19.7	1192.6 19.7	1190.2 16.6	-0.61	1190.5 23.5	1189.7 22.9	1187.2 23.4	-0.26	1194.6 18.1	1193.0 19.0	1188.5 17.1	-0.51	1196.9 16.6	1192.7 18.0	1193.3 18.0	-0.31
Lat-Post	1184.4 34.2	1175.4 49.2	1198.5 17.3	1.24	1192.4 25.7	1194.5 39.0	1204.3 15.6	1.04	1196.8 26.3	1197.0 31.9	1200.3 22.1	0.32	1190.7 15.6	1199.8 16.7	1196.6 14.5	0.51
All	1176.5 15.8	1171.0 17.8	1176.5 11.9	0.04	1182.5 15.5	1178.3 27.5	1181.4 20.1	-0.07	1183.4 16.0	1181.6 16.4	1180.3 14.9	-0.25	1180.4 16.6	1180.5 9.2	1179.2 9.8	-0.10

Table 12. Regional cortical area (mean, SD) and mean changes, 66%.

	<i>Control</i>				<i>Aerobic</i>				<i>Resistance</i>				<i>Combined</i>			
	<i>Pre</i>	<i>Mid</i>	<i>Post</i>	<i>Avg.Pre-Post % Change</i>	<i>Pre</i>	<i>Mid</i>	<i>Post</i>	<i>Avg.Pre-Post % Change</i>	<i>Pre</i>	<i>Mid</i>	<i>Post</i>	<i>Avg.Pre-Post % Change</i>	<i>Pre</i>	<i>Mid</i>	<i>Post</i>	<i>Avg.Pre-Post % Change</i>
66% Ct.Ar																
Lat-Ant	23.9 6.3	22.8 5.8	23.7 5.3	0.24	22.0 3.6	22.6 4.1	22.4 3.9	1.63	24.4 5.2	24.4 5.8	24.3 5.6	-0.28	22.5 3.5	22.3 4.4	22.0 4.2	-2.25
Ant	79.1 7.1	78.3 7.5	78.1 7.5	-1.36	72.6 9.4	71.8 10.0	72.3 9.6	-0.38	74.9 15.3	75.3 14.4	75.2 15.0	0.38	74.6 10.5	74.9 10.7	75.2 10.7	0.79
Med-Ant	27.8 5.0	27.3 5.2	27.7 5.5	-0.72	27.2 6.7	26.9 6.8	27.5 6.7	1.53	27.5 6.8	28.0 7.0	27.8 6.5	1.45	28.4 5.3	29.0 5.5	29.4 5.9	3.38
Med-Post	36.9 5.0	37.4 5.9	37.7 6.1	1.98	34.0 6.4	33.7 6.3	34.3 6.4	1.12	34.1 5.4	33.9 4.9	34.3 5.8	0.39	33.5 5.7	33.3 5.2	33.6 5.7	0.27
Post	56.8 6.3	57.4 6.6	56.3 6.5	-1.00	55.7 8.8	55.1 8.4	54.9 9.1	-1.59	61.5 8.7	61.6 8.5	61.1 8.4	-0.50	57.1 7.4	56.7 7.9	56.8 7.6	-0.57
Lat-Post	36.2 6.8	35.7 6.9	36.2 7.2	-0.26	35.4 7.2	34.5 6.6	34.9 8.1	-1.64	33.2 6.9	33.3 6.0	33.2 6.6	0.15	35.6 7.0	35.4 6.4	35.4 6.7	-0.42
All	43.5 4.6	43.1 4.6	43.3 5.0	-0.19	41.2 4.9	40.8 5.1	41.1 5.1	0.11	42.6 6.2	42.7 6.1	42.6 6.0	0.27	42.0 4.1	41.9 4.1	42.1 3.9	0.20

Table 13. Regional bone mineral content (mean, SD) and mean changes, 66%.

	<i>Control</i>				<i>Aerobic</i>				<i>Resistance</i>				<i>Combined</i>			
	<i>Pre</i>	<i>Mid</i>	<i>Post</i>	<i>Avg.Pre-Post % Change</i>	<i>Pre</i>	<i>Mid</i>	<i>Post</i>	<i>Avg.Pre-Post % Change</i>	<i>Pre</i>	<i>Mid</i>	<i>Post</i>	<i>Avg.Pre-Post % Change</i>	<i>Pre</i>	<i>Mid</i>	<i>Post</i>	<i>Avg.Pre-Post % Change</i>
66% BMC																
Lat-Ant	60.5 16.5	57.5 15.1	59.9 13.5	0.28	55.9 10.0	57.5 10.8	56.5 9.8	1.43	61.8 13.3	62.1 14.7	61.2 13.1	-0.80	56.9 9.0	56.4 11.5	55.5 11.1	-2.65
Ant	196.6 16.2	194.6 19.1	195.9 18.5	-0.42	183.1 23.3	180.4 25.5	182.8 22.8	-0.12	189.0 36.9	190.0 35.3	189.6 36.2	0.36	187.2 26.2	187.6 25.6	188.3 26.7	0.61
Med-Ant	73.0 14.4	71.4 14.3	71.9 14.9	-1.52	71.8 18.0	70.2 18.1	72.1 17.9	0.67	72.1 17.9	72.9 17.9	72.4 17.0	0.79	74.7 14.2	75.9 14.3	76.8 14.9	2.81
Med-Post	98.0 13.9	98.5 15.4	99.6 16.3	1.36	90.8 17.4	89.3 17.8	91.6 18.5	0.82	91.1 14.4	90.3 13.0	91.3 14.9	0.26	89.0 14.7	88.6 12.9	89.5 14.5	0.64
Post	149.7 16.5	150.5 17.6	147.3 16.9	-1.60	145.7 21.4	144.0 20.6	143.1 22.3	-1.86	161.4 21.6	161.4 21.2	159.6 21.3	-1.00	150.4 19.4	148.8 20.2	149.1 19.6	-0.87
Lat-Post	94.3 17.4	92.2 18.1	95.3 18.6	0.98	92.7 18.3	90.5 17.4	92.2 20.9	-0.58	87.4 17.4	87.7 15.3	87.6 16.8	0.47	93.2 18.5	93.4 16.8	93.2 18.0	0.09
All	112.0 12.2	110.8 12.2	111.7 13.2	-0.15	106.7 12.8	105.3 13.3	106.4 13.1	0.06	110.5 15.2	110.7 15.0	110.3 14.6	0.01	108.6 10.4	108.4 10.3	108.7 9.8	0.10

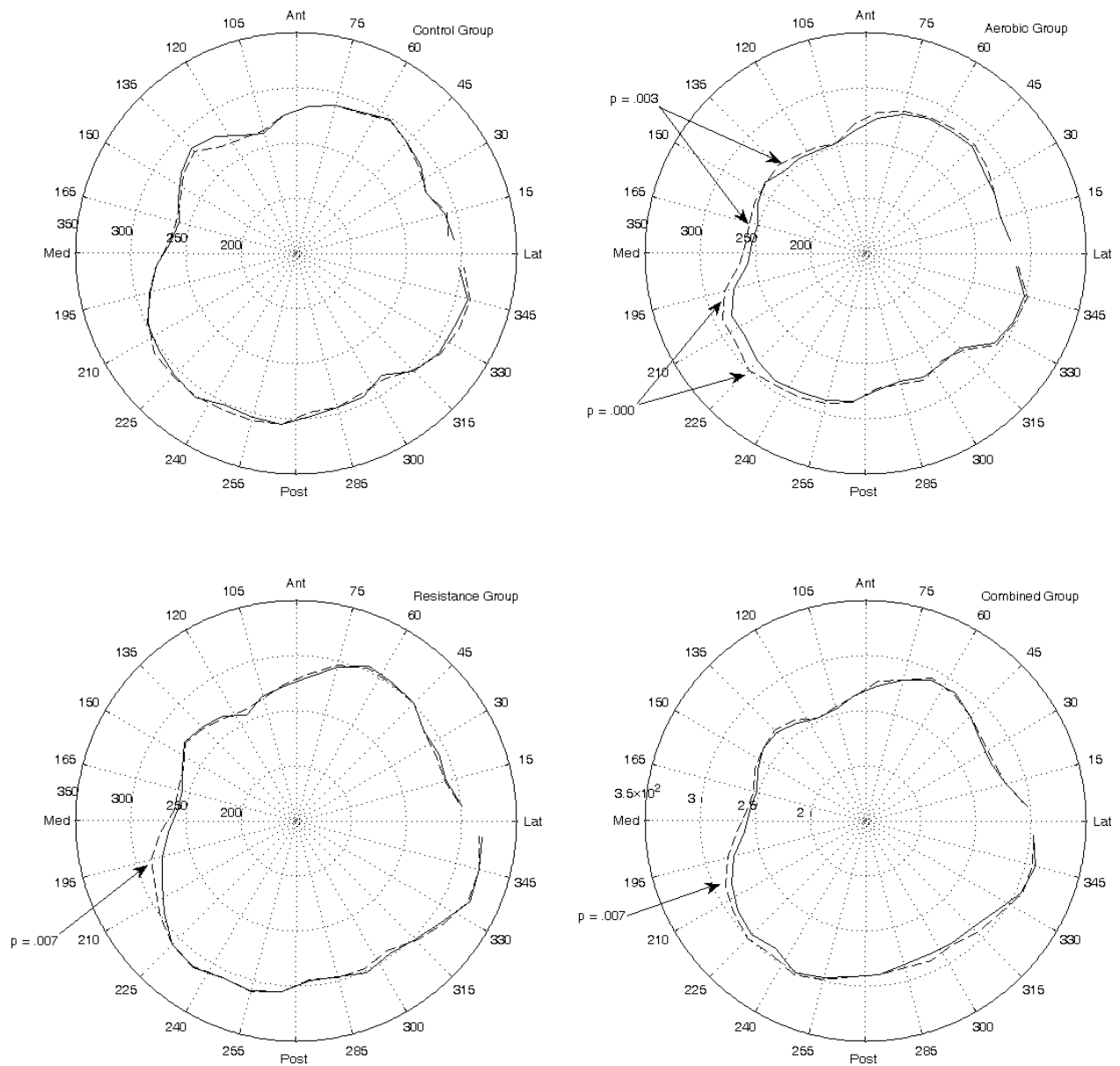


Figure 2. Average regional Tb.Dn, 4% (mg/cm³). Pre (solid), mid (dashed), and post (dotted) training.

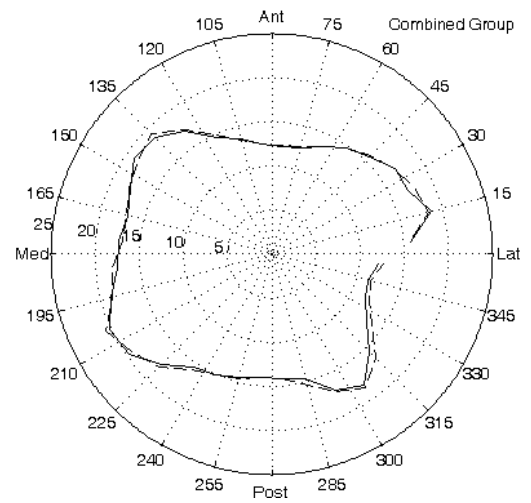
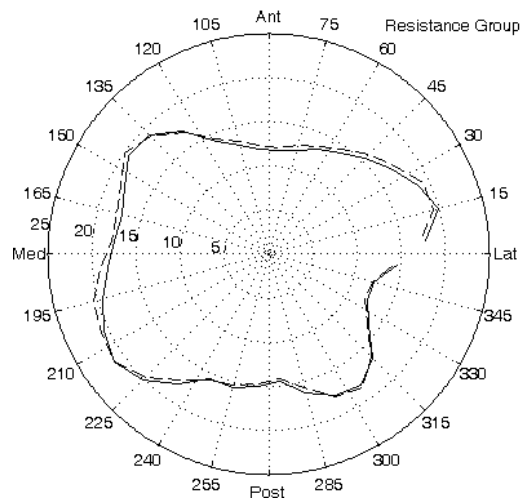
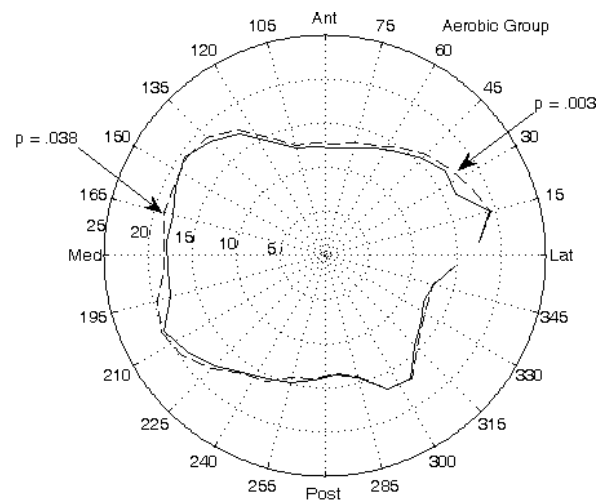
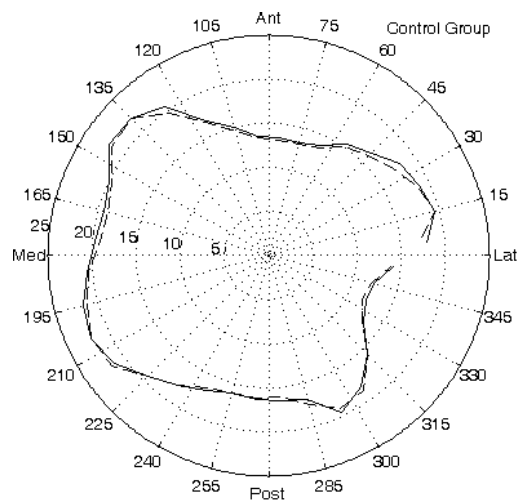


Figure 3. Average Regional Trabecular |BMC|, 4% (mg/mm). Pre(solid), mid (dashed), and post (dotted) training.

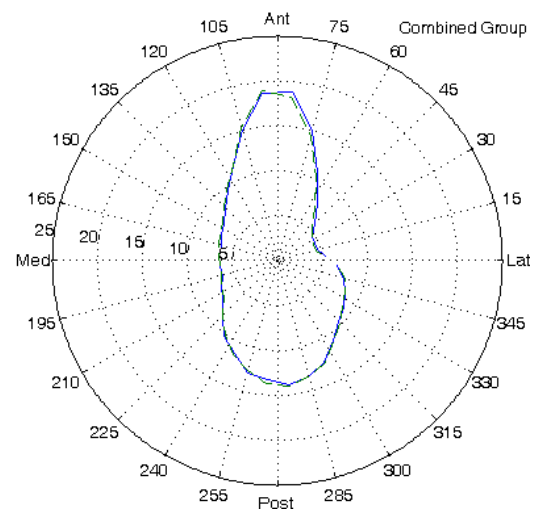
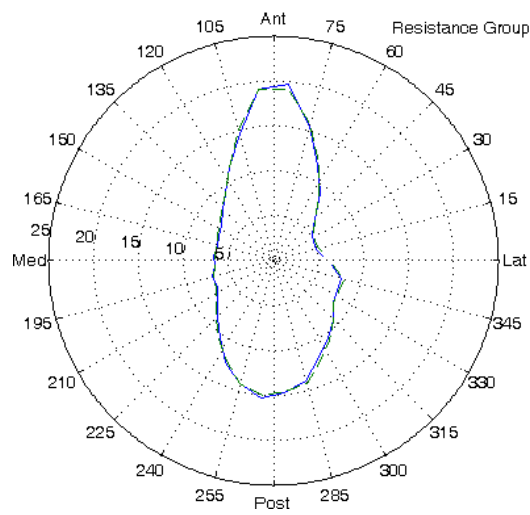
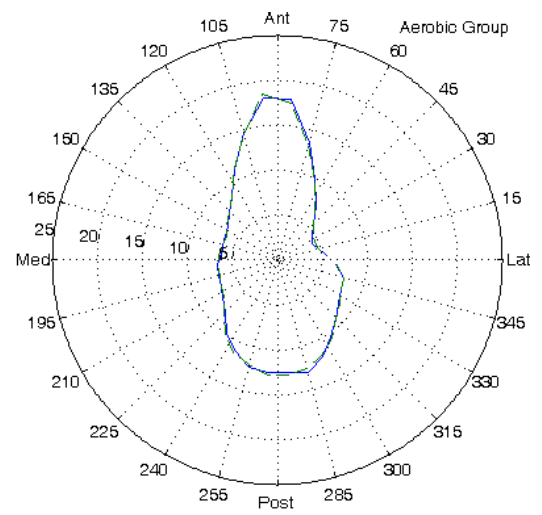
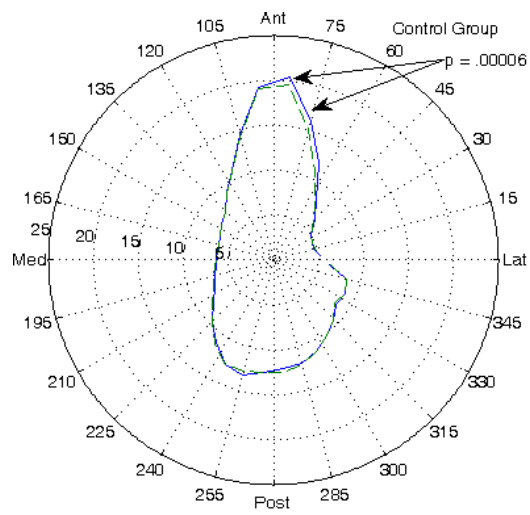


Figure 4. Cortical thickness, Ct.Th, 66%, mm. Pre (solid), and post (dashed) training.

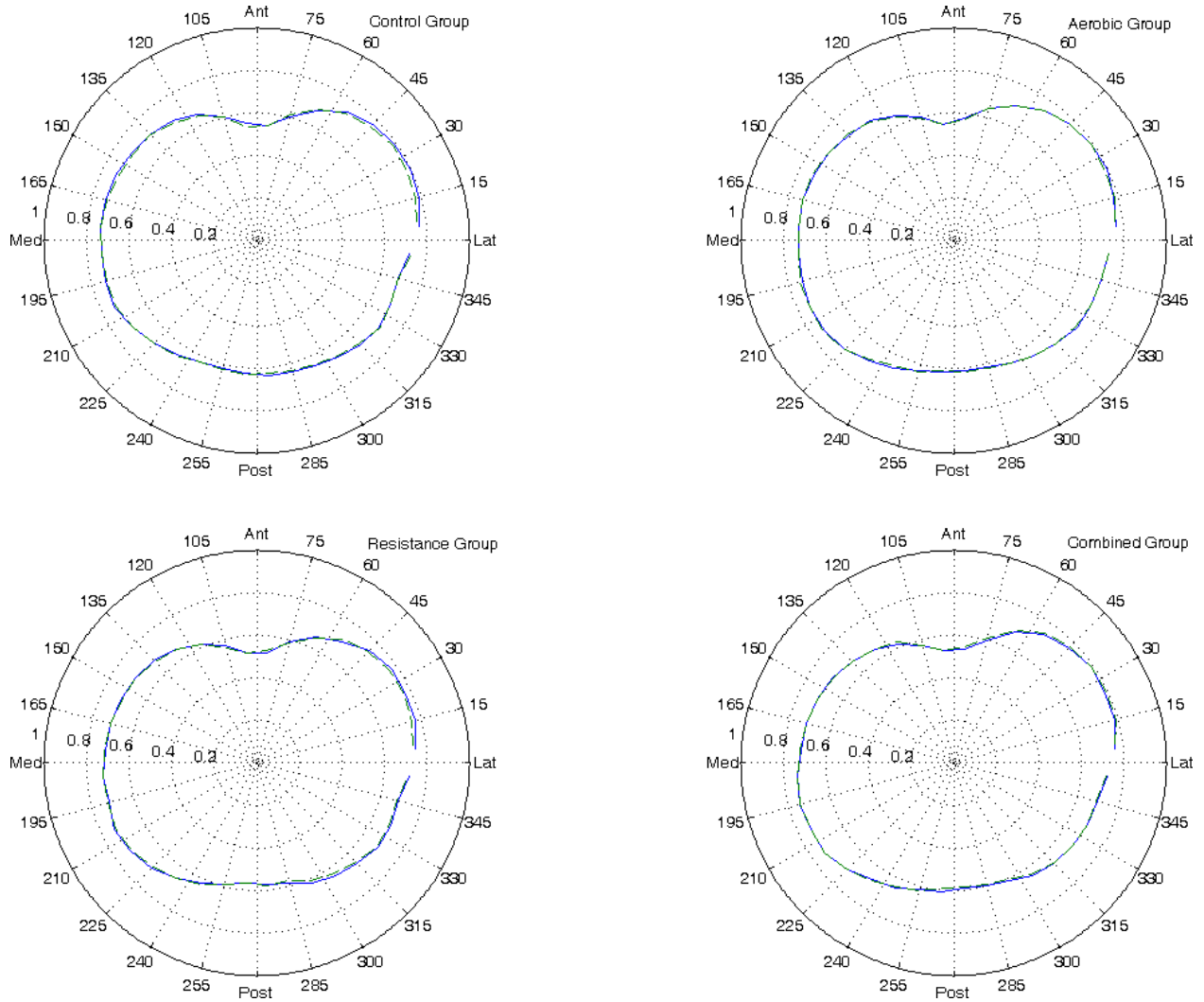


Figure 5. Normalized canal radius, Ca. |Rd|, 66%. Pre (solid), and post (dashed) training.

2.4 Discussion

In this study, trabecular density (Tb.Dn) in the ultra-distal tibia was the first measure to reflect bone changes brought on by increased physical activity. This agrees in principal with other studies that have used pQCT in some manner to monitor changes in bone. Findlay et al. (2002) found that pQCT of the distal tibia had the potential to be the most sensitive site for measuring morphological changes following tibial fracture. Similarly, Veitch et al. (2005) also found trabecular bone to be the best sentinel for measuring changes following fracture. This early trabecular modeling is consistent with his faster remodeling rate compared to cortical bone, a fact owed to it's greater surface area (Guo 2001).

It should be noted that the density changes noted at the 4% site are at the “apparent” level. That is, the average voxel intensity increased. Since each voxel bounded a volume

0.4 mm \times 0.4 mm \times 2.2 mm, and a typical trabeculae is 0.2 mm thick and 1 mm in length, this can mean that individual trabeculae could have, on average, increased in density, or more likely, that the trabecular latticework became more tightly packed through apposition to existing or growth of new trabeculae.

Our results further suggest that impact-producing aerobic exercises are the most effective at producing such changes. That aerobic exercise seems necessary to produce observable changes is not surprising giving the state of knowledge of bone cell mechanobiology. Dynamic loads are best at producing bone rates of strain of sufficient magnitude to produce the interstitial fluid flow that appears necessary to stimulate remodeling. On average, it seems that weight training, although capable of producing high bone strains, yields lower strain *rates* than aerobic exercises.

Observing changes in the diaphyseal region of the bone over a short time period is more difficult, as was evidenced by the lack of any significant changes in cortical density at either the 38% or 66% sites. It is possible that more intense exercise regimens might yield greater changes in bone density though with a concomitantly higher risk of injury. Cortical remodeling is necessarily slower and the changes in apparent density are more subtle than in trabecular bone. Based on the results of this study, we would expect any cortical changes to be first observable in the anterior sector where density is slightly less and more remodeling activity seems to occur. As with other researchers such as Lai et al. (2005a), we did find that the posterior cortex had a higher Ct.Dn than the anterior cortex, both at the 38% and 66% sites.

To explain the variation in the amount by which trabecular density increased at the 4% site (particularly in the aerobic exercise group) we sought to correlate those changes with moment of inertia (a diaphyseal measure of the mechanical efficiency in bending), slenderness index (a measure of the robustness of the bone relative to the body weight) and body weight. Changes in density did not correlate with any of these parameters. That they did not might either imply that our sample size was too small to detect the correlation, or that the 4% site is substantially invariant to these parameters.

There are other caveats when looking for short-term, exercise induced changes in bone. First, since the changes in morphology are subtle, it is important for pre and post images to be registered correctly, lest measurement errors obscure the changes. The main sources of error during image alignment are 1) having images taken at slightly different locations 2) movement of the subject during the image collection process which can induce noise and 3) improper alignment of pre and post images by the analysis software. If the first two issues are circumvented however (in other words, if “clean” images are collected from a subject at the same location) then the software alignment procedure is robust.

As documented elsewhere, pQCT does have limits to its utility (Ferretti 1997; Ferretti et al. 2002). pQCT measures volumetric bone mineral density, vBMD. That is, the amount of mineralized bone present within a voxel. It is not calibrated to measure collagen within the bone matrix. As collagen production precedes mineralization in new bone formation, this first step in functional adaptation and remodeling remains essentially transparent to pQCT measures. It is also susceptible to “partial volume effects” (Stratec Medizintechnik GmbH 2004). This is particularly true at the endosteal and periosteal boundaries of the diaphysis, and in the trabecular bone that dominates the epiphyses of long bones. These two sites are, of course, where changes in bone morphology are most likely to occur.

3. Israeli Defense Force Cohort Analysis

3.1 Introduction

The Matlab software which was originally written for the University of Connecticut study described in Chapter 2 was next used to conduct a preliminary analysis of data collected from a training cohort in the Israeli Defense Force.

The purpose of this study was to quantify basic geometric and morphological differences in men and women from the cohort. Stress fracture rates of women in the IDF have been found to be as high as 40%. By quantifying the differences between sexes, it may be possible to determine which parameters (e.g., cortical bone density, moment of inertia, trabecular area) have the largest disparities between men and women and consequently may be the best predictors for stress fracture.

3.2 Methods

From an original cohort of 143 subjects, images from 91 subjects, collected during induction to Basic Combat Training, were forwarded for analysis. Of these, 20 were male and 71 were female.

The images were collected by a research team from the IDF and USARIEM using a Stratec/Medizintechnik XCT 2000. Subjects were positioned on a chair with the nondominant leg extended through the scanning cylinder and were asked to maintain a convenient and stable position for the duration of the procedure (10-15 minutes). A scout scan was used to identify the distal end plate of the tibia. Scans of the tibia were taken using single axial slices 2.2 mm thick with voxel size 0.5 mm. These were collected at a translation speed of 20 mm/s at 4%, 38%, and 66% of tibial length.

Analysis of the images was done using the software written for the University of Connecticut study described in Chapter 2 with some modifications. The image registration process was improved, and the codes were modified to allow stand-alone analysis (in other words, no “pre” and “post” alignment was necessary). The essential Matlab codes are described in Appendix A.

As with the University of Connecticut study, the special-purpose codes written allowed for a detailed regional analysis of morphological parameters such as density and area. Each bone was divided into six sectors (see Figure 1 in Chapter 2 for sector definitions). In these sectors, density and area were averaged and compared between male and female recruits.

3.3 Results

3.3.1 Measures at 4% of Tibial Length

Male subjects had slightly higher volumetric density in all sectors at 4% with the greatest disparity being in the Anterior and Medial-Anterior sectors where it was on average 14.6% higher in men than women (Figure 6). Trabecular area was on average 27.5% less in women than in men with the largest discrepancy in the medial sectors (Figure 7).

3.3.2 Measures at 38% of Tibial Length

Women in this study had cortical bone density which was 3% higher than men on average, though their bone area was on average 32% less. Cortical density at 38% in men was 1159.5 ± 101.2 and in women it was found to be 1194.1 ± 103.5 . On average, men and women had proportionally similar cortical wall thicknesses. This is seen in Figure 10 which shows the radius of the intramedullary canal as a percentage of the radius to the periosteal bone boundary. Average cortical wall thickness in men was 4.77 mm and in women was 4.03 mm (Figure 11).

3.3.3 Measures at 66% of Tibial Length

The 66% site displayed the same inverse relationship between cortical density and area as at the 38% site. Men had an average cortical density of 1124.3 ± 144.4 compared to women who had average values of 1153.0 ± 116.6 (Figure 12). Cortical density values were 3% lower at the 66% site than the 38% site in men and 3.4% lower in women. Cortical area in women was roughly 30% less than that of men at the 66% site (Figure 13). The intramedullary canal is proportionally larger in men at the 66% site than in women (Figure 14) though cortical wall thickness was only marginally greater (Figure 15).

3.3.4 Geometric Measures

The moment of inertia (about the Medial-Lateral axis, Anterior-Posterior axis, or polar axis) was found to be twice as high among the male recruits as it was in women at both 38% and 66% (Figure 16 and Figure 17). The bone strength index (BSI) showed a concomitant relationship (Figure 18 and Figure 19). The higher moments of inertia in male recruits seems attributed to an average bone width which is about 25% higher than in women (Figure 20 and Figure 21).

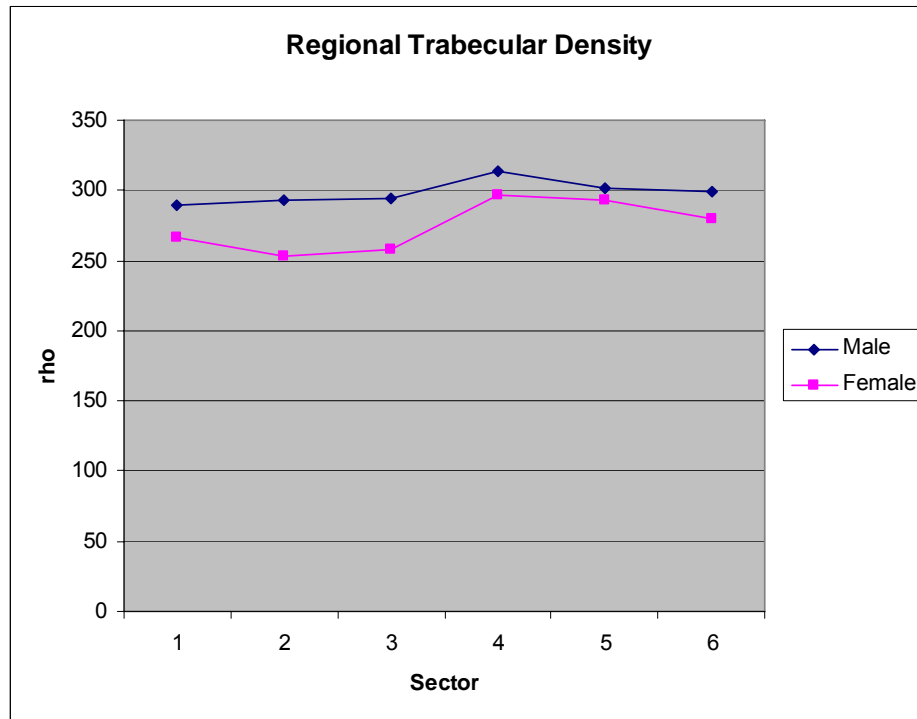


Figure 6. Regional Trabecular Density at 4% of tibial length.

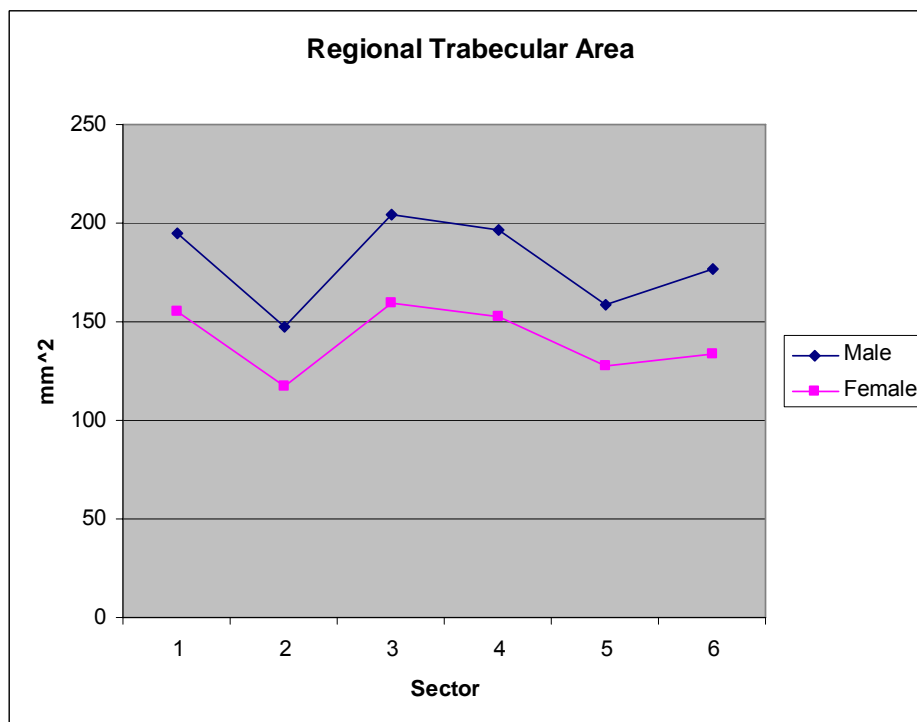


Figure 7. Regional Trabecular Area at 4% of tibial length.

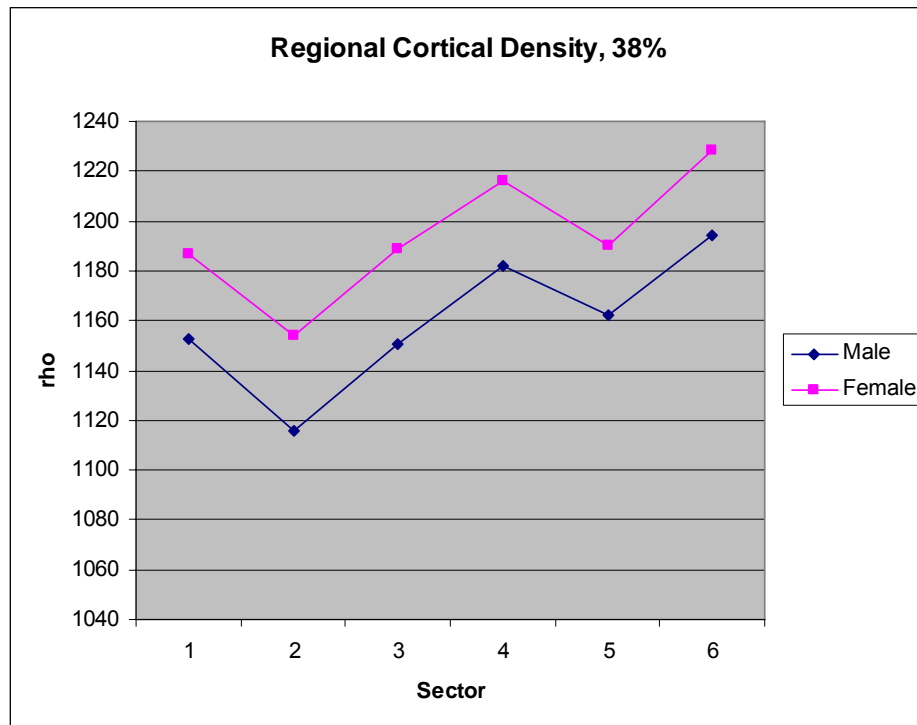


Figure 8. Regional Cortical Density at 38% of tibial length.

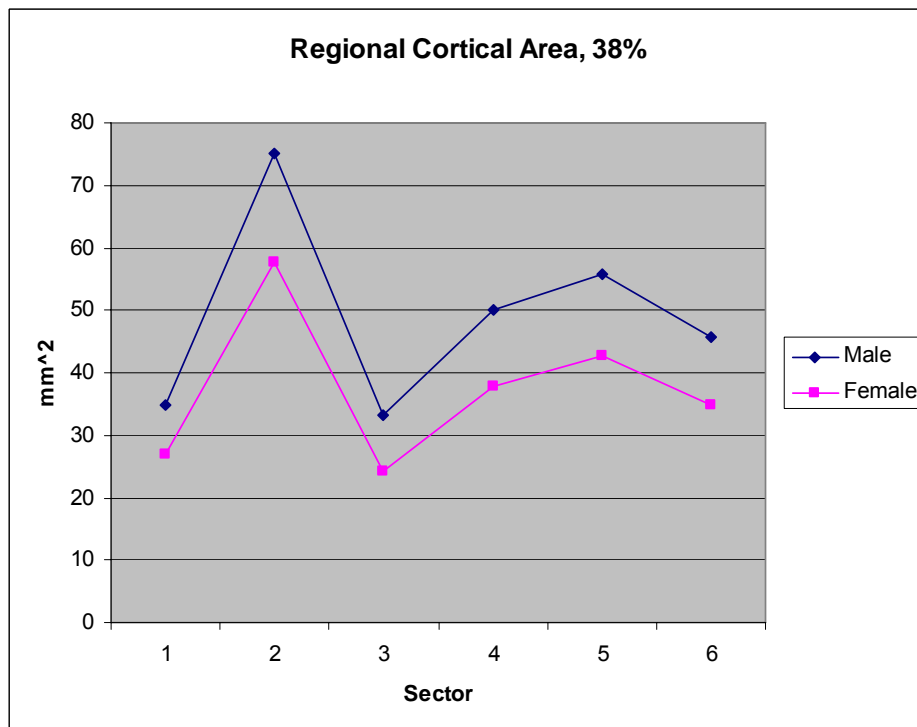


Figure 9. Regional Cortical Area at 38% of tibial length.

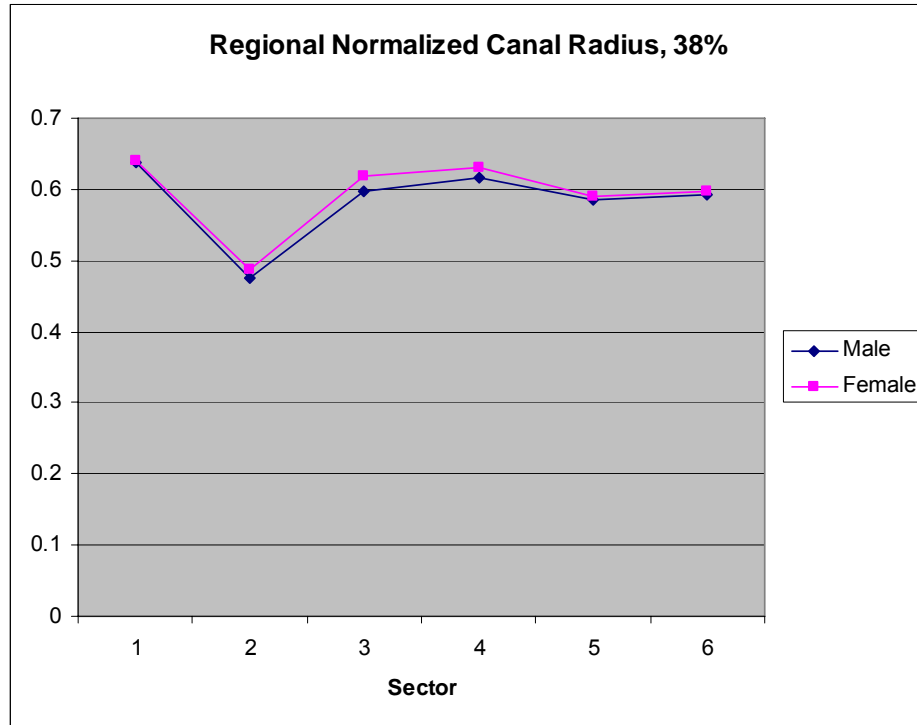


Figure 10. Regional Normalized Canal Radius at 38% of tibial length.

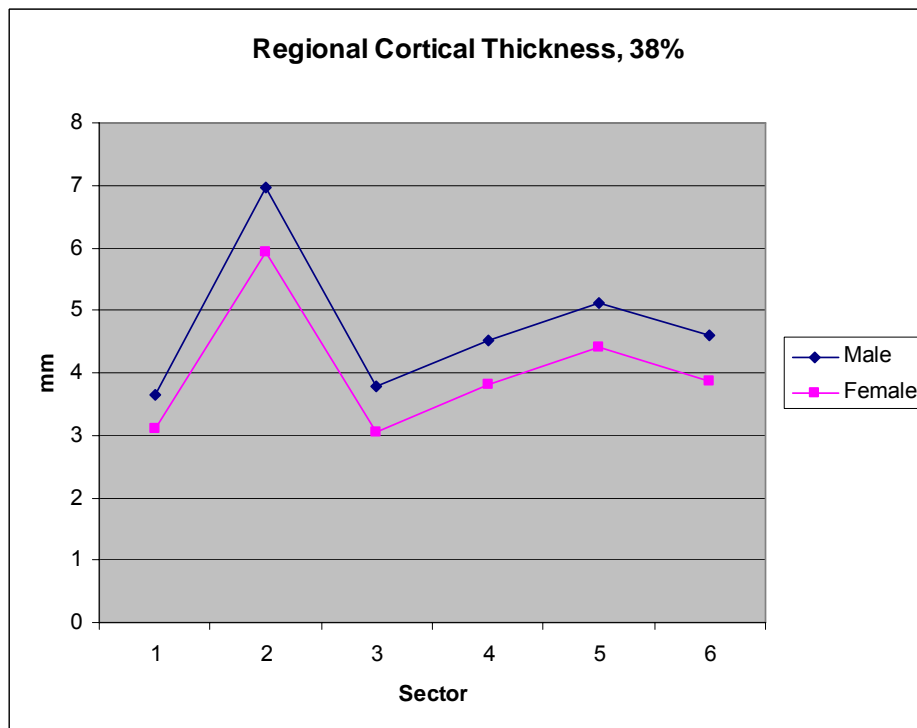


Figure 11. Regional Cortical Thickness at 38% of tibial length.

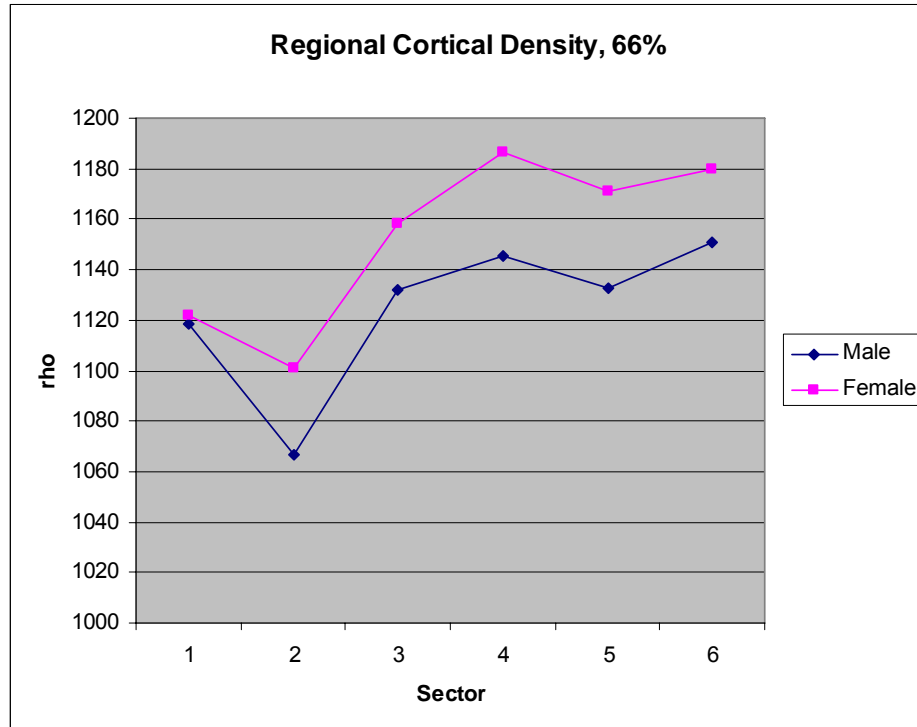


Figure 12. Regional Cortical Density at 66% of tibial length.

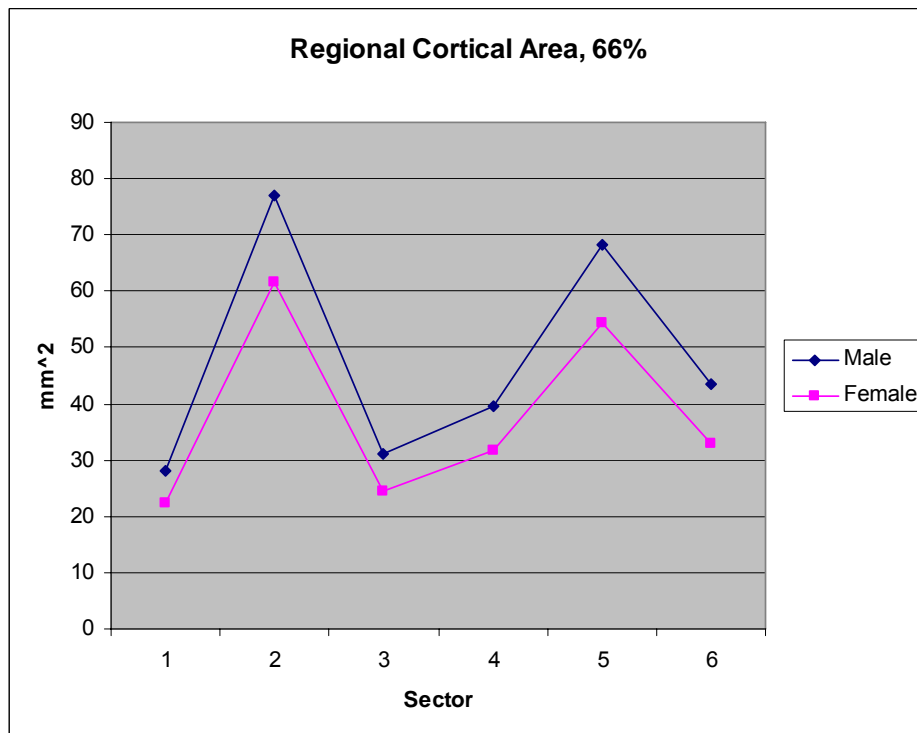


Figure 13. Regional Cortical Area at 66% of tibial length.

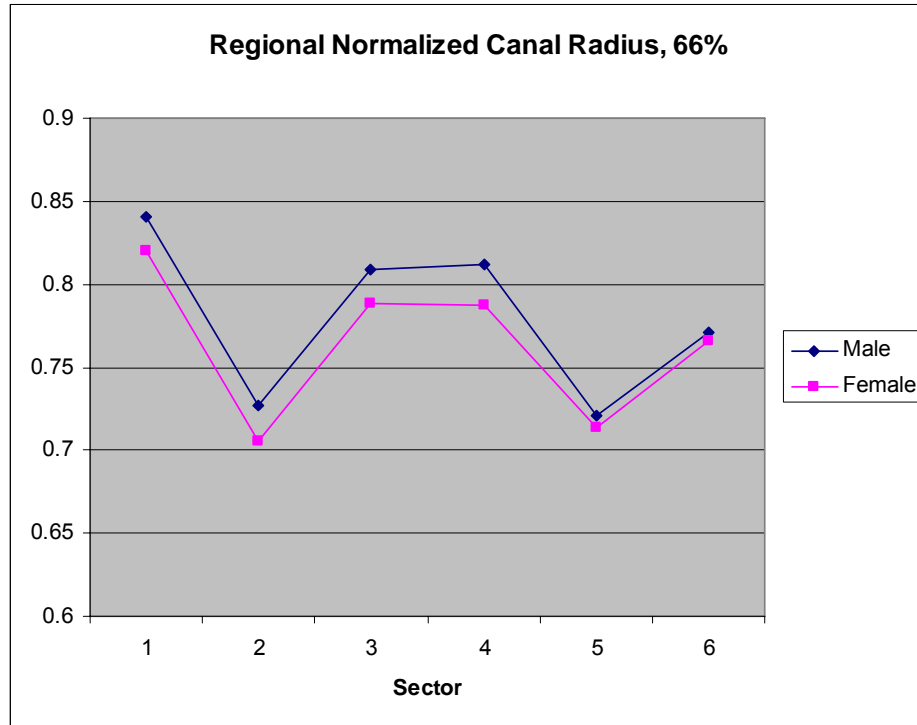


Figure 14. Regional Normalized Canal Radius at 66% of tibial length.

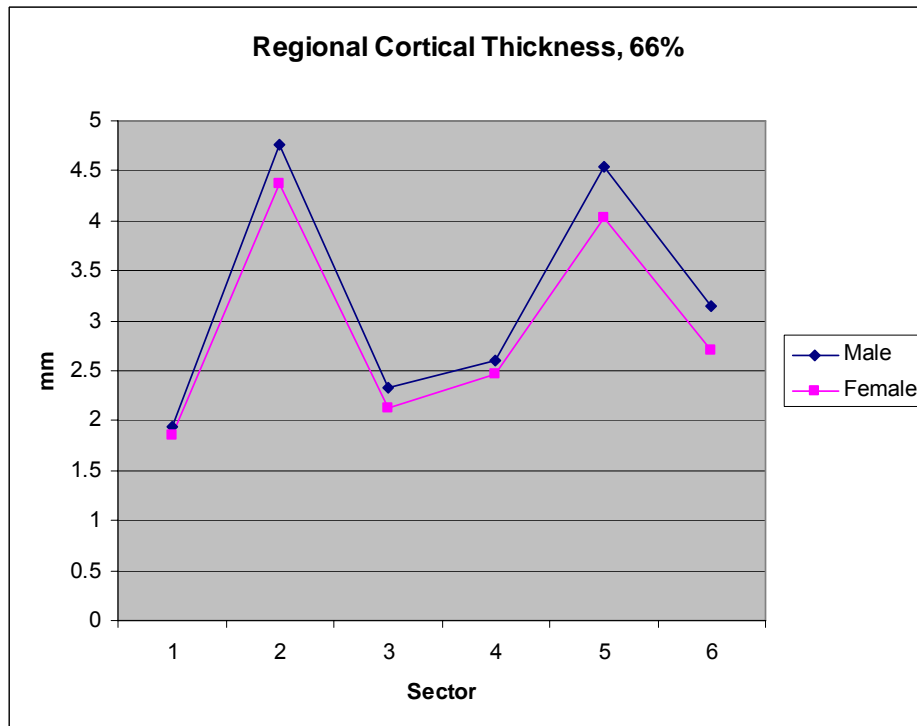


Figure 15. Regional Cortical Thickness at 66% of tibial length.

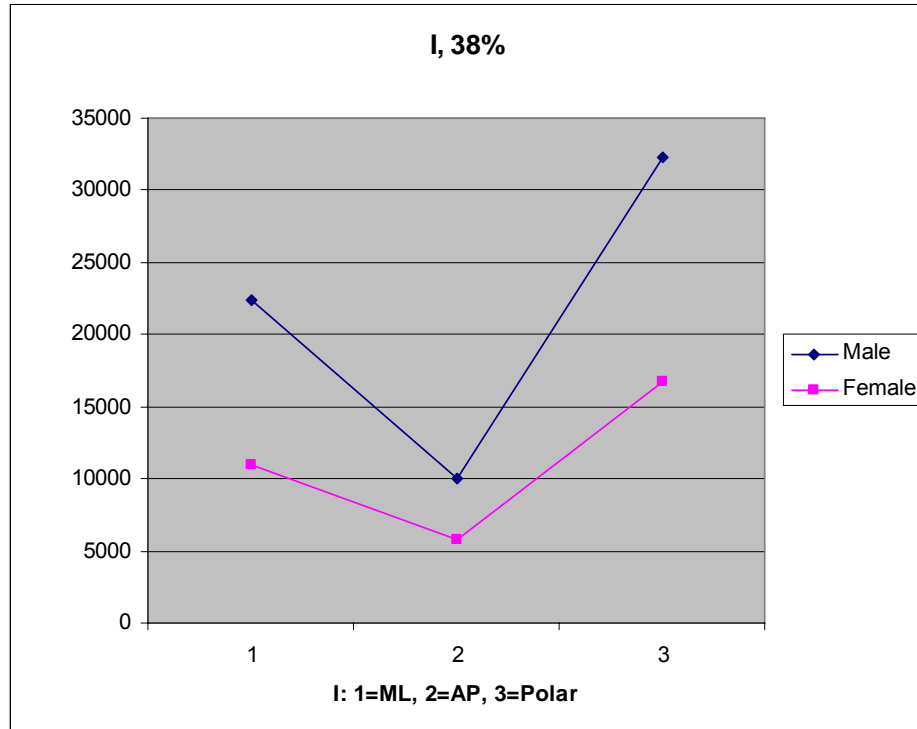


Figure 16. Cross Sectional Moments of Inertia measured about the Medial-Lateral (ML), Anterior-Posterior (AP), and Polar axes at 38% of tibial length.

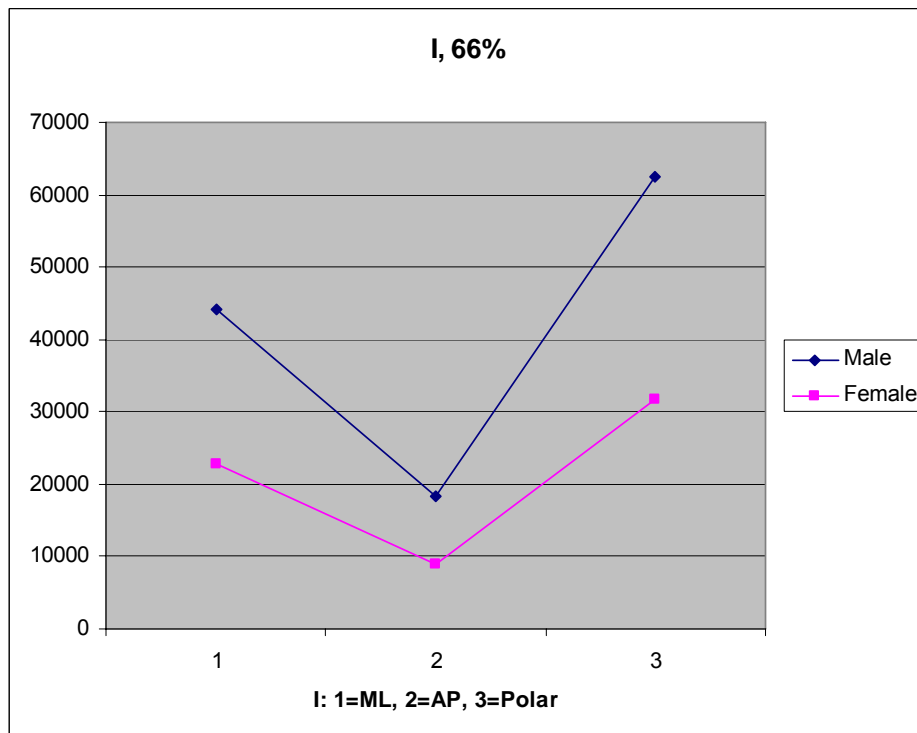


Figure 17. Cross Sectional Moments of Inertia measured about the Medial-Lateral (ML), Anterior-Posterior (AP), and Polar axes at 66% of tibial length.

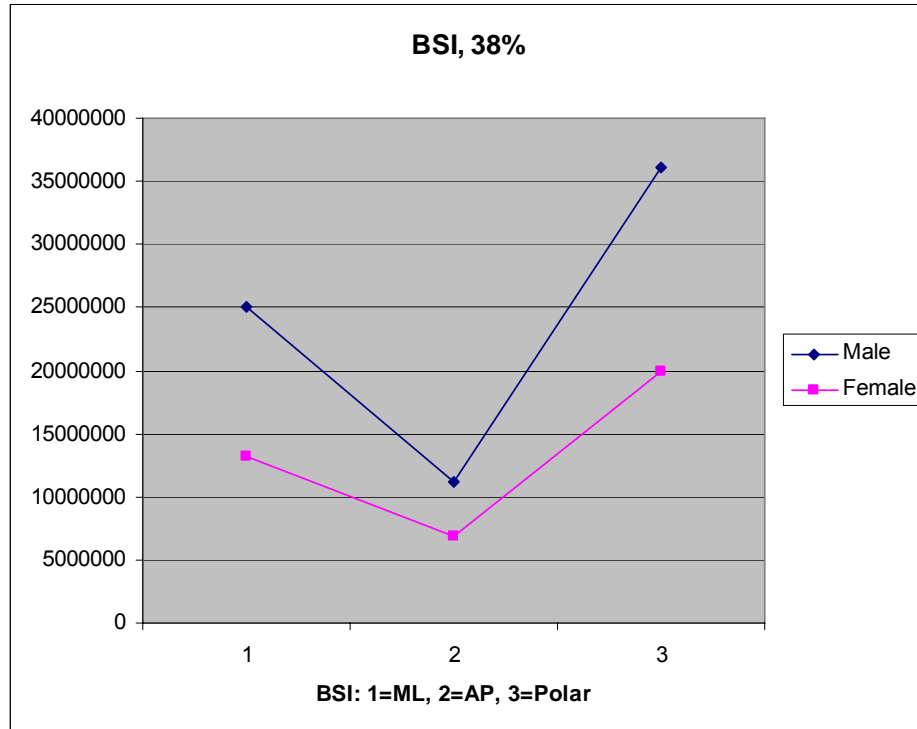


Figure 18. Bone Strength Index measured about the Medial-Lateral (ML), Anterior-Posterior (AP), and Polar axes at 38% of tibial length.

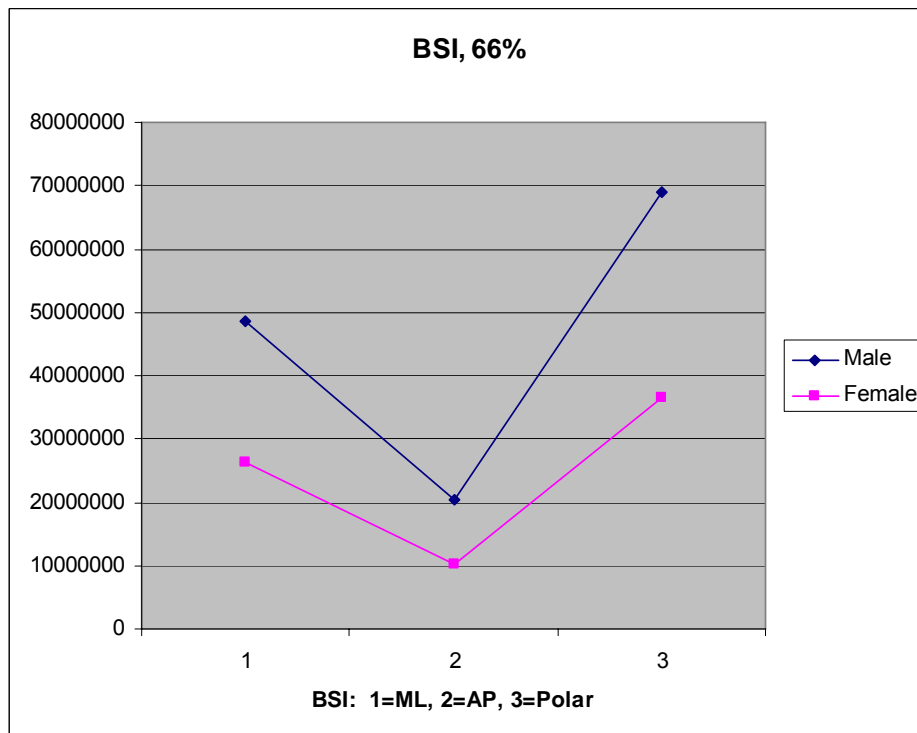


Figure 19. Bone Strength Index measured about the Medial-Lateral (ML), Anterior-Posterior (AP), and Polar axes at 66% of tibial length.

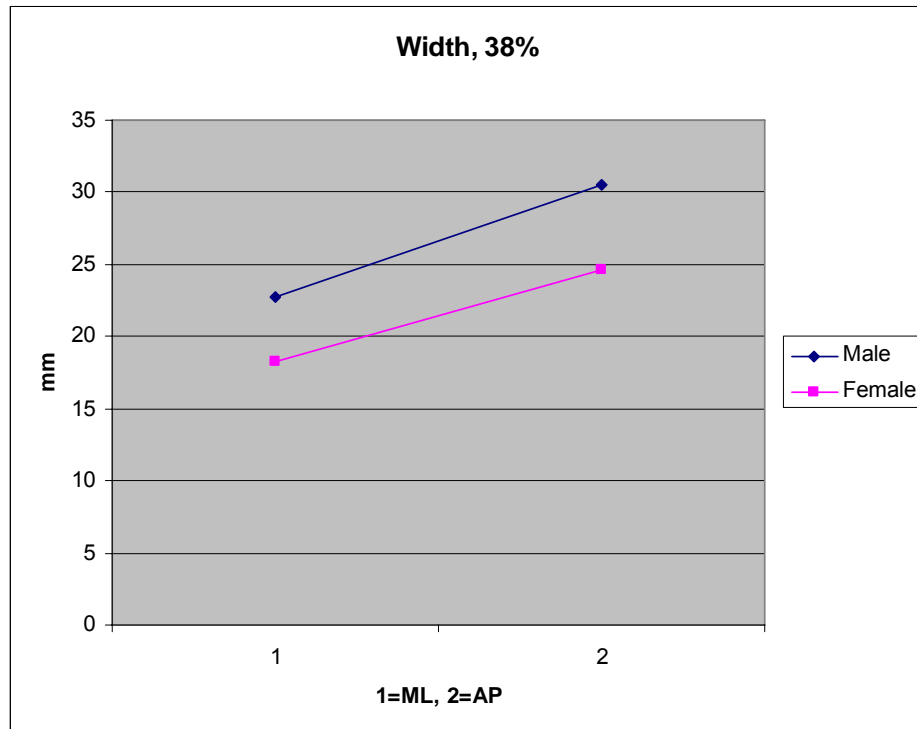


Figure 20. Diaphyseal width measured along the Medial-Lateral (ML) and Anterior-Posterior (AP) axes at 38% of tibial length.

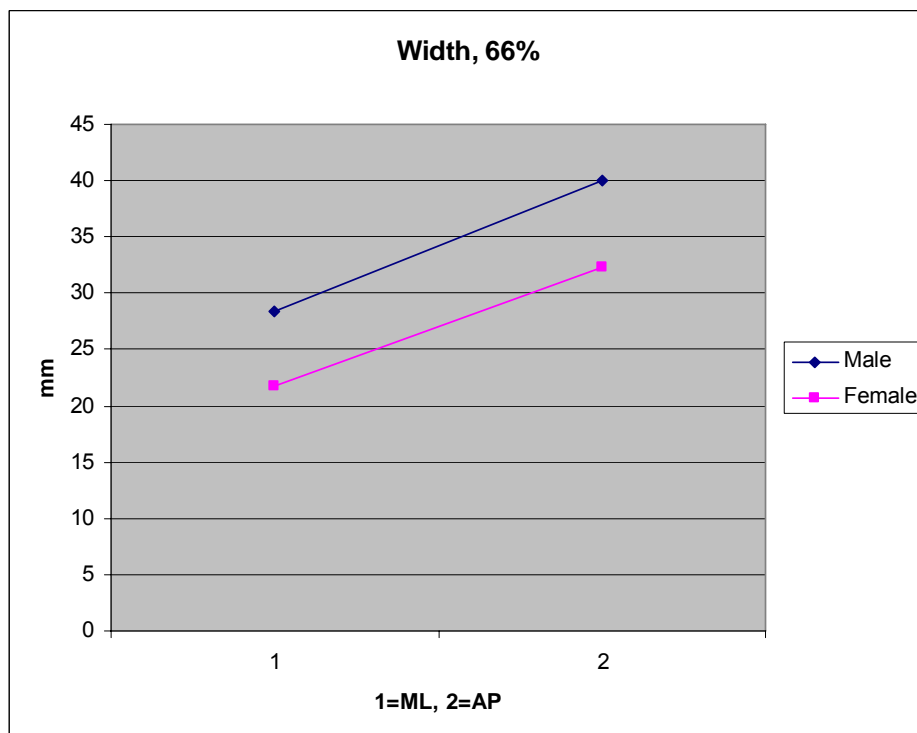


Figure 21. Diaphyseal width measured along the Medial-Lateral (ML) and Anterior-Posterior (AP) axes at 66% of tibial length.

3.4 Discussion

While the geometric differences in males and females highlighted in this preliminary study are not wholly unexpected, this study did illustrate two ways in which women are at higher risk of stress fracture than men. First, the female recruits in this study had cortical bone which was more highly mineralized. While a higher mineral content may contribute to bone strength, it is also more brittle and prone to damage accumulation.

The second reason is more an issue of mechanical efficiency. The cross section of the diaphysis of the tibia in women gives a moment of inertia roughly half of that of men. This implies that the bones of the female recruits are half as able to deal with bending stresses as their male counterparts. In light of this, it is not surprising the tibias of the female recruits have stiffened (via greater mineralization) to compensate for this fact. While it is true that women weigh, on average, significantly less than men, the resulting load on the tibia is generally not so much less (that is, it is not usually half of a typical male tibial load) as to make up for the difference in moment of inertia.

4. Patient Specific Stress Analysis

4.1 Background

Bone is a living tissue whose function and adaptation are mechanically mediated, and bone related diseases often have a mechanical pathogenesis. Effective diagnosis, intervention, and treatment of maladies such as stress fracture and age-related bone loss could greatly benefit from an understanding of the mechanical environment that results *in vivo* during normal and atypical physical activity. The mechanical stimulus is, however, both highly patient and location specific. The goal of this study is to research and develop a computational method with potential clinical practicality for assessing the stress distribution in long bones.

This Background section has three parts. In the first we will present the rationale for this project by briefly summarizing mechanobiology and its role in some bone related diseases. Next, we will describe the main difficulties in making patient-specific assessments of the mechanical state (such as stress or strain), specifically in the context of intervention of tibial stress fractures, which is the focus of the Bone Research portion of the Overuse Injury Modeling project. Finally, we will outline advanced computational modeling and solution techniques and some preliminary results that we have achieved.

4.1.1 Introduction: Mechanobiology in bone related diseases

Mechanobiology refers to the interdisciplinary study of the regulation of biological processes by mechanical stimuli (Carter et al. 1998). In bones, a change in the predominant ambient mechanical state has long been known to lead to adaptations in the overall shape and density distribution within a bone (Chamay and Tschantz 1972; Frost 1964; Wolff 1892). While mechanically induced stimuli are part of the normal function of healthy bone tissue (regulating processes such as mRNA protein synthesis, cell proliferation, differentiation, or apoptosis) abnormalities in stimulus can contribute to such bone related problems as stress fracture and osteoporosis.

Mechanotransduction is at the heart of bone remodeling and functional adaptation. Mechanotransduction is the ability of a cell to sense and respond to a mechanical stimulus such as stress or strain. A population of osteocytes residing in a region of bone tissue sense the mechanical demands placed on them, and respond by recruiting osteoclast and osteoblast precursors as needed. This seems to be done by some combination of chemical signaling, mRNA expression, and gap junction communication. While many insights have been gained into the signaling pathways that drive remodeling, it remains unclear exactly how the mechanical-to-electrochemical signal transduction occurs.

Both clinical and cell-level research has, however, implicated dynamic loads as being crucial for mechanotransduction. In long bones of the lower extremities, the strains which have been observed *in vitro* to stimulate a chemical response are far larger than those experienced by the bone organ *in vivo*. So how then, can these daily activities maintain healthy bones? The answer may lie in a process of strain amplification (Figure 22). Dynamic loads are known to produce fluid flow in the lacunar-canalicular system in which osteocytes reside (Knothe Tate et al. 1998). These osteocytes are tethered in place by a hair-like matrix between their cell processes and the canal walls. As fluid flows through this matrix, it results in a drag force which stretches the long, finger-like processes (You et al. 2002). The cell process strains generated during this stretching have been shown to be many times larger than organ level strains—large enough to elicit a cellular response (Han et al. 2004; Weinbaum et al. 2003). Thus, the mechanical stimulus most important for inducing remodeling activity may be the local *rate* of strain, and not simply the static stress or strain.

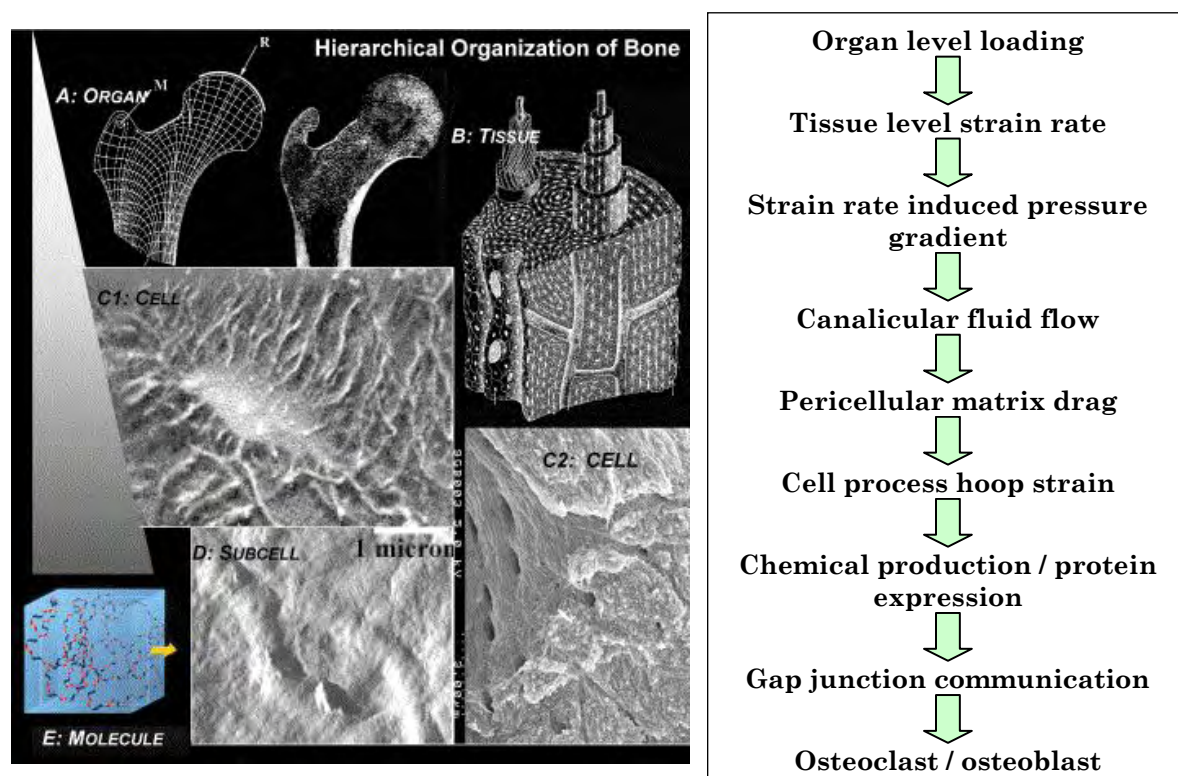


Figure 22. A model of strain amplification from the organ level (A) to tissue-level strain rate (B) to the osteocyte residing in the lacunar-canalicular system (C1, C2). Image courtesy of Melissa Knothe-Tate, Case Western Reserve University.

While the rate of loading may drive mechanotransduction, it is the peak values of static stress and strain which are responsible for the fatigue damage accumulation known

as stress fracture. Stress fractures result when the rate of extracellular matrix (ECM) microcracking generated by the repeated loading of a bone exceeds the rate at which new secondary osteons are created by basic multicellular units (BMUs). Eventually, microcracks coalesce and form a painful fatigue fracture. The remodeling process which is designed to clear damaged tissue may actually exacerbate the problem in some situations. Voids generated by osteoclastic removal of the damaged ECM may act as a stress attractor. Repeated stresses to the area following the induction of targeted remodeling have been observed to lead to fatigue fracture (Muir et al. 1999). Whether this remodeling is truly targeted or simply stochastic is unclear (Costa Gomez et al. 2005). So then, in answering the question of what causes stress fractures, it is first necessary to understand:

1. The character of bone in which microdamage is most likely to occur.
2. The level of mechanical stimulus likely to lead to microdamage.
3. The role of mechanotransduction in aiding or exacerbating fracture.

A few generalizations can be made regarding these issues. Microcracking seems more likely to occur in cortical bone which is more highly mineralized (Wasserman et al. 2005). The degree of mineralization appears to be a function of the predominant mechanical state in situ. Bone which is typically loaded in tension tends to have lower mineral density, and a higher amount of remodeling activity than bone whose ambient state is compressive (Bell et al. 1999; Skedros et al. 1994). Bone which is more highly mineralized will strain less under a given load than bone which is less mineralized, but it tends to be more brittle. Thus the magnitude of strain itself is not a good predictor of damage propensity (Donahue and Sharkey 1999). In the tibia (which will be the focus of this effort), the highest bone mineral density (BMD) tends to be found in the posterior region, with the anterior cortex having the lowest BMD (Lai et al. 2005a). The largest strains in the tibia are found in the anterior cortex which is primarily loaded in tension. The predominant state on the posterior side is compression.

The local mechanical stimulus affects the architecture of bone as well. In young adults, the amount of physical activity was associated with cortical bone size and trabecular bone density (Lorentzon et al. 2005). At the tissue level, the organic collagen fibers imbedded in cortical bone typically align transversely to the direction of compression. Bone tissue typically loaded in tension results in collagen fibers collinear with the load path (Riggs et al. 1993).

As bones age, the remodeling rate slows, and concern for fatigue damage-induced stress fractures gives way to a concern for instantaneous (and often catastrophic) fracture due to decreased mechanical competence. Even in older adults not diagnosed with osteoporosis, there is a marked decrease in bone strength that occurs during aging. Overall colla-

gen content decreases concomitantly with a decreased level of stress needed to induce fracture (Bailey et al. 1999). The porosity of cancellous bone increases, and the diaphyseal cortex thins from bone loss at the endosteal boundary, though this is sometimes accompanied by a slight gain in periosteal circumference. Thus, there is a double effect of increased brittleness with decrease in cortical thickness. The result is that daily activities produce higher stress in more fracture-prone material. This phenomenon is often exacerbated by decreased hormonal levels which are particularly acute in women following menopause.

The mechanical stimulus at the heart of all these phenomena (mechanotransduction, damage accumulation, and to a lesser degree, age-related bone loss) is a highly patient-specific interplay of anthropometrics, bone morphology, density distribution, and physical activity (see Figure 23, for example). And yet the ability to estimate stimuli such as stress and strain in a patient has not kept pace with mechanobiology research. Without research into techniques for a rapid, accurate assessment of a patient's relative bone strength, cellular research cannot fully make its way into the clinic and benefit the warfighter.

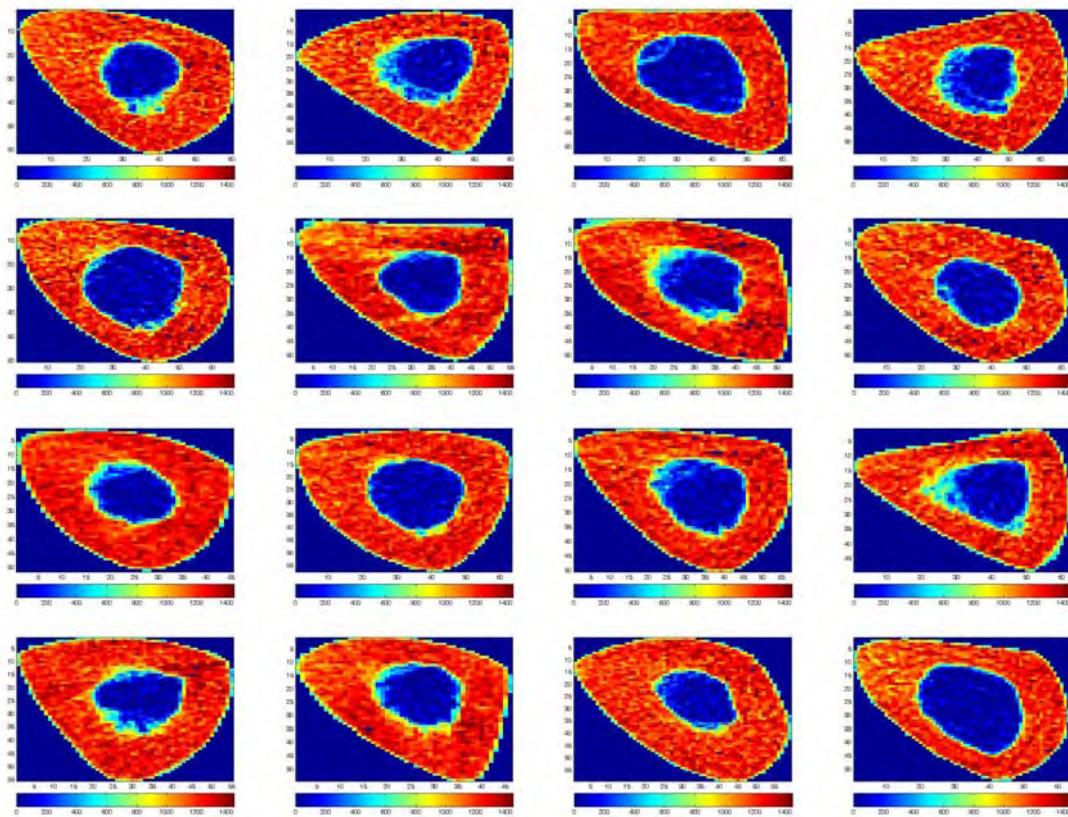


Figure 23. Variations in shape and density distribution from 16 female participants, age 18-35, of the University of Connecticut study (see Chapter 2). Images were taken by pQCT at 38% of tibial length. These morphological variations, combined with individual anthropometrics and physical activity, will lead to a highly patient and location specific stress/strain profile.

4.1.2 Current challenges to patient-specific computational modeling

While mechanobiological bone research begins at or below the cellular level, and has as its end goal improved patient care, the gap between is bridged by clinical data collection and computational mechanics. In the case of patient-specific stress assessment (for fatigue or brittle fracture intervention), there are three overarching challenges: *rapid model generation*, *rapid solution*, and extensive, well-documented *fracture morbidity data*. This study addresses the first two of these issues with the hope that fracture morbidity data can be collected after the rapid model generation/solution infrastructure has been developed.

Rapid model generation is the process of obtaining, with minimal time and measurement, a three dimensional representation of the bone of interest. Whole bone CT scans, for instance, are not feasible due to the excessive radiation exposure incurred from the many slices needed for 3D reconstruction. Peripheral Quantitative Computed Tomography (pQCT) scans allow for imaging of the extremities in less than three minutes per slice with a radiation exposure of less than 15 mRem per slice, and an image resolution of about 4mm. And yet the “virtual bone” needed in a 3D model must capture the overall shape of the bone as well as the internal density distribution within. Additionally, the bone model will be incomplete without patient-specific estimates of applied forces to the organ. These can include both joint contact loads and muscle forces.

A number of researchers have addressed the rapid modeling challenge using voxel-based finite element meshes. These convert individual voxels obtained from high-resolution CT directly into hexahedral or tetrahedral finite elements. The uniform size and shape of the elements usually, but not always, (Boyd and Muller 2005) produce a model with a jagged surface that one might get from building a model bone from stackable toy blocks. This approach remains impractical for whole bone modeling due to radiation exposure concerns.

Rapid solution refers specifically to a finite element analysis (FEA) of the bone. In mechanics, FEA is a computational technique for the discretization and solution of displacements, strains, and stresses within a (usually complex) structure under prescribed loads. Its use is ubiquitous in engineering design, and it has found widespread utility in biomechanical applications such as orthopedic implant design and generic bone remodeling simulations (Impelluso and Negus 2005). FEA is usually conducted using commercial software on desktop workstations. Conducting a FEA on a patient’s bone presents two principal challenges: using a sufficient number of elements to capture the complex geometry of the object and correctly representing the material properties. Both of these characteristics tend to slow the solution time dramatically.

If the strain and stress field can be estimated on a patient-by-patient basis, the logical next step is to ascertain what activities (defined by the stresses incurred and the corre-

sponding number of doses over a given period of time) will lead to fatigue damage. This step requires a unique and extensive *clinical stress fracture morbidity data* from a population of subjects, including a detailed activity log, images of their bone morphology, and specific documentation of those who incurred stress fracture. This data can be used as a means of “calibrating” stresses predicted computationally.

4.2 Our Approach to Patient Specific FE Modeling

In order to rapidly generate fully 3D models of an individual tibia from three pQCT scans, a number of codes were written in Matlab and C. These were used in conjunction with two proprietary software packages: TrueGrid (a 3D hex mesher) and SolidWorks (an engineering CAD package). Once the model was generated, solutions for this study were conducted using the Finite Element software, LS Dyna, though any static finite element software could be used. Solving for stresses and strains in models with a reasonable number of elements typically requires less than 15 minutes on a modern personal computer. A more detailed description of the modeling procedure follows.

4.2.1 pQCT to 3D Model procedure

While a detailed procedure is given in Appendix B, here is a summary.

1. Image registration. pQCT images are registered using a Matlab code called **regtool.m**. The center of the intramedullary canal is calculated at 66% and this location is defined as the origin. The 38% image and 4% images are shifted by the same amount.
2. Generic epiphyses, taken from the Standardized Tibia Project, are scaled in **SolidWorks** to match dimensions measured from the subject in the x, y, and z directions.
3. The bone boundary is extracted from the surrounding image. This is done using a Matlab utility called **boundwriter.m**. The transverse boundary of the diaphysis at 38% and 66% are imported into the CAD package SolidWorks. (See Figure 24). A lofted surface is generated in the missing diaphyseal section and the surface of the entire tibia is exported.
4. Utility file **tgShaft.m** calculates points on the surface of the bone needed as an intermediate step for generating a hex mesh in TrueGrid.
5. **tgWriter.m** writes a TrueGrid input file which will generate the tibial mesh.
6. **TrueGrid** is run and a hex mesh is automatically generated for the patient’s bone. (See Figure 25).

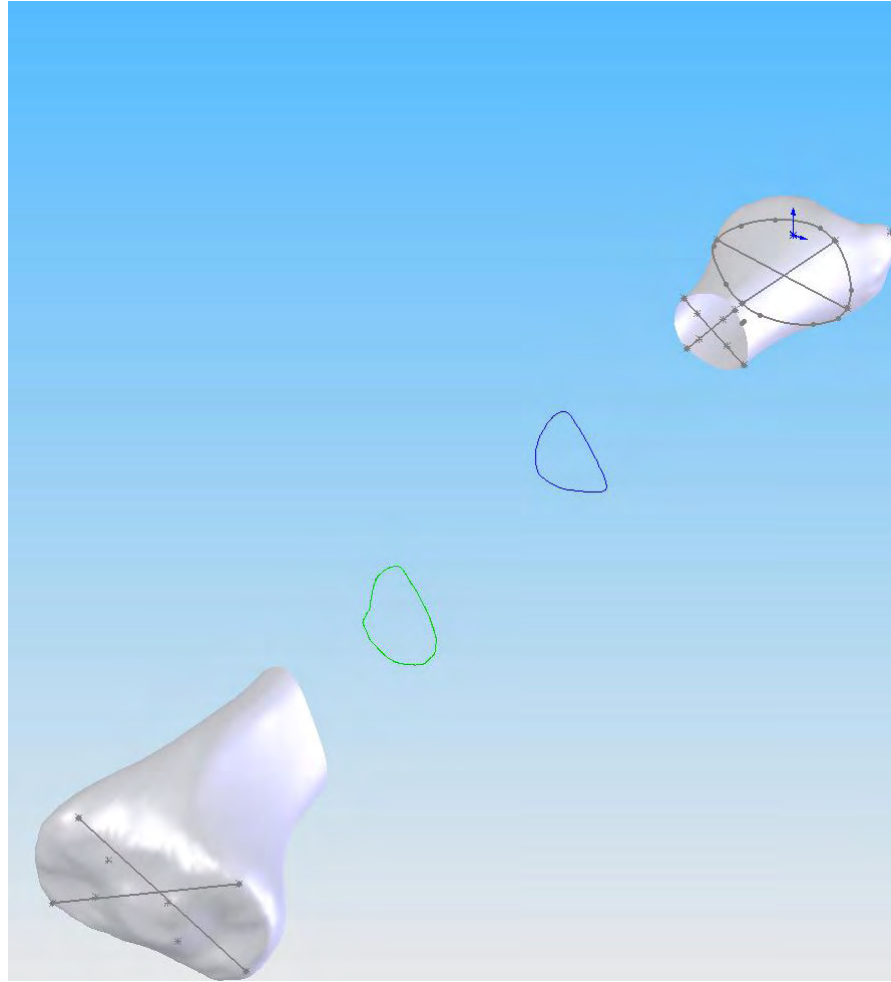


Figure 24. Diaphyseal boundaries (green and blue traces) imported into a generic tibial model of the epiphyses with the diaphysis missing. The patient's own pQCT images are used to model the high stress diaphyseal region.

7. The TrueGrid mesh file is read by an executable file (written in C) called **meshbouncer.c**. Meshbouncer identifies a list of nodes and elements which will correspond to the pQCT images. This is a necessary intermediate step prior to assigning bone density to every element of the finite element mesh.
8. The Matlab code **ct2mesh.m** reads the subjects pQCT files, and identifies which elements in the finite element mesh correspond to each pixel in the subjects 38% and 66% pQCT images.
9. Another C code, **matAssign.c**, maps bone density from the images to the finite element mesh at the epiphyses (using the 4% slice) and the elements located at 38% and 66%. Elements in between these mapped areas are assigned bone density based on interpolation from the transverse planes where the density is known.

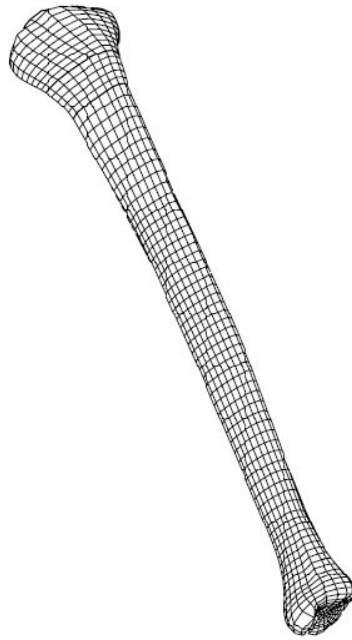


Figure 25. A finite element mesh of a tibia generated in TrueGrid.

10. A finite element model which captures the subject bone's shape and density distribution has now been generated (see Figure 26). A few other utilities may be used at this point such as **constrain.c** (used for assigning displacement and force boundary conditions to whole groups of nodes) or **dhr2dyn.c** (used for exporting the model for use with LS-Dyna).

Patient specific finite element models were generated for all 17 subjects in the Combined group from the University of Connecticut study (Chapter 2). Two load cases were developed: one in which a load of 3BW was applied to the proximal surface with the distal surface constrained, and another in which a static 1000N load was applied to the proximal end with the distal end again constrained. In each case, 60% of the load was applied to the medial side of the bone and 40% was applied to the lateral side.

By developing a pQCT-initiated rapid modeling and solution capability, it will be possible to conduct tibial stress analyses on every individual in the military cohort to estimate the individual stress and strain distribution resulting from a given activity. It will then be possible to compare stress distributions in subjects who incurred stress fracture with subjects who did not, and begin to evaluate the relationships between exercise regimens to tibial stresses to bone morphologies and anthropometrics.

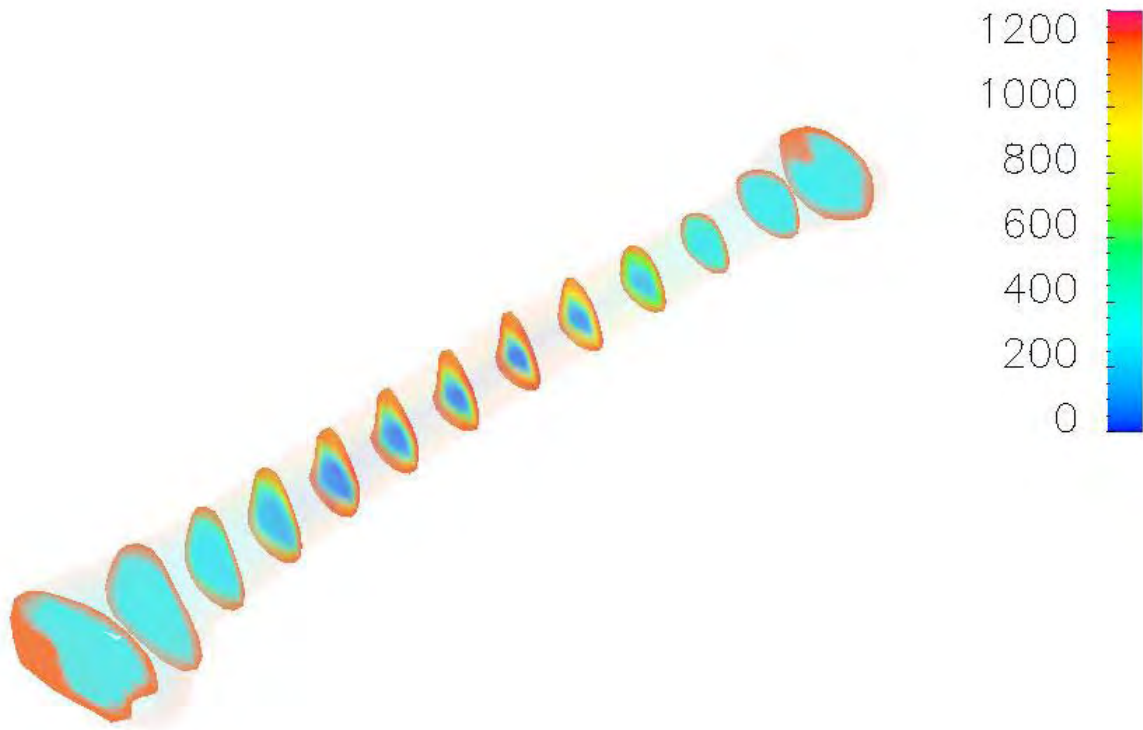


Figure 26. A semi-transparent view of the final finite element model of a subject. The exterior shape of the bone and the density distribution have been derived from three pQCT images taken from the subject.

4.3 Future Improvements

Having conducted this pilot study and proven that patient specific modeling is an achievable goal future improvements will focus on completely automating the process by skipping SolidWorks and TrueGrid altogether. This can be done by developing extensible interpolation algorithms to distribute element nodes. There are numerous ways to do this, including leveraging current research in statistical shape modeling (Rajamani et al. 2004). This would also further speed up model generation time. It would not be impractical to be able to acquire images from a subject, generate a 3D model based on those images, and conduct a patient-specific finite element model in under 30 minutes using a pQCT scanner and a personal computer. Such a capability would be a logical complement to current statistical methods of screening recruits at high risk for stress fracture (Figure 27).

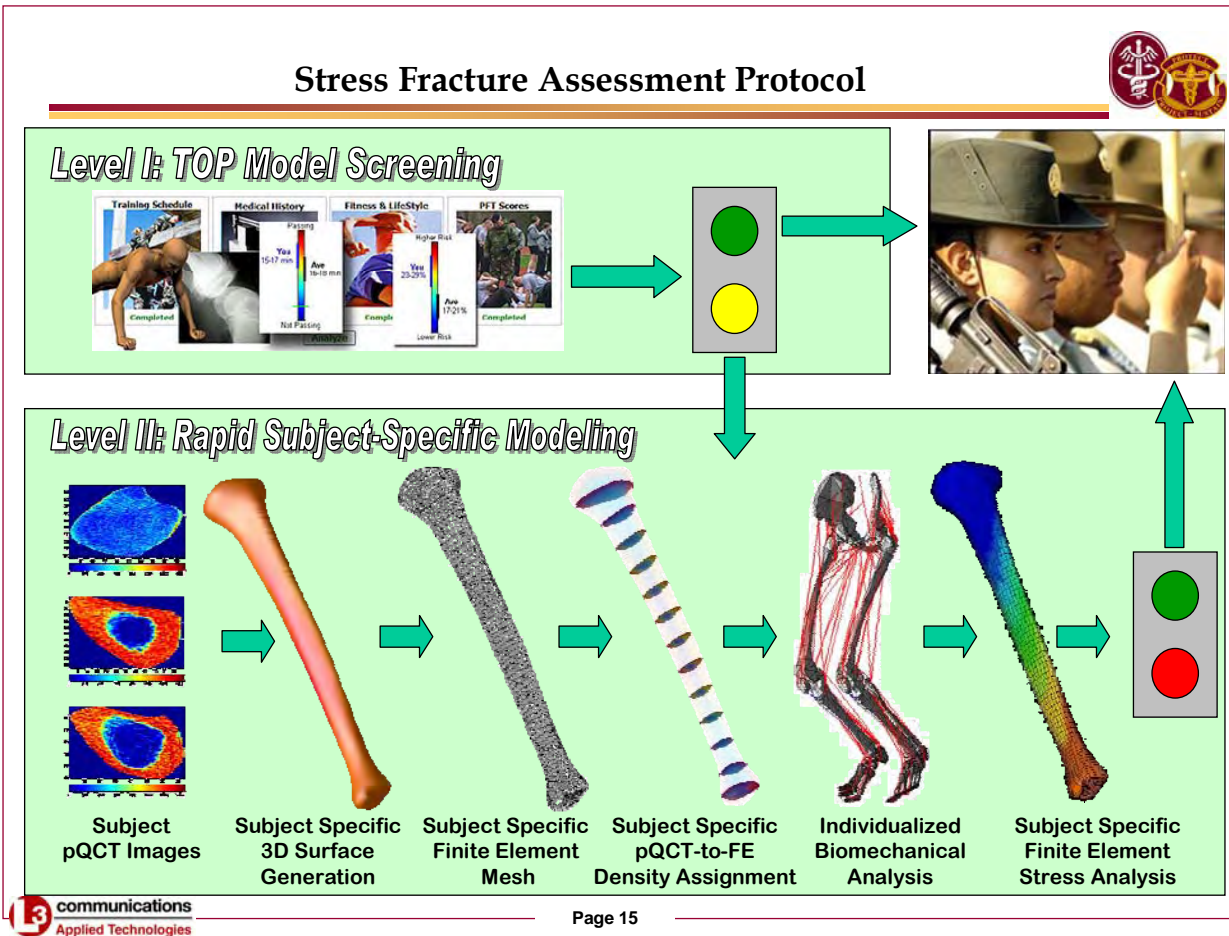


Figure 27. A two-level protocol for assessing stress fracture risk in recruits.

4.4 Summary

Stress fracture onset seems to be a probabilistic, material-fatigue type phenomenon in which damage (in the form of microcracks in the cortex) coalesce to eventually form a stress fracture. There are two variables related to this mechanical pathogenesis. First, one has to know the tibial stresses occurring during activities. Secondly, the number of cycles must be known. That is, the number of times the stress-inducing activity occurs is needed over a given time period.

Estimating the number of cycles of an activity is possible with little effort given accurate activity logs. The first variable however, tibial stress, is highly patient specific, with the same activity producing different stresses in different individuals. The procedure outlined here is a practical method for estimating these stresses on an individual basis using noninvasive diagnostic equipment and a personal computer.

5. References

- Bailey, A. J., Sims, T. J., Ebbesen, E. N., Mansell, J. P., Thomsen, J. S., & Mosekilde, L. (1999). "Age-related changes in the biochemical properties of human cancellous bone collagen: relationship to bone strength." Calcif Tissue Int **65**(3): 203-210.
- Bell, K. L., Loveridge, N., Power, J., Garrahan, N., Meggitt, B. F., & Reeve, J. (1999). "Regional differences in cortical porosity in the fractured femoral neck." Bone **24**(1): 57-64.
- Boyd, S. K. & Muller, R. (2005). "Smooth surface meshing for automated finite element model generation from 3D image data." J Biomech.
- Carter, D. R., Beaupre, G. S., Giori, N. J., & Helms, J. A. (1998). "Mechanobiology of skeletal regeneration." Clin Orthop(355 Suppl): 41-55.
- Chamay, A. & Tschantz, P. (1972). "Mechanical influences in bone remodeling. Experimental research on Wolff's law." J Biomech **5**(2): 173-80.
- Cheng, S., Sipila, S., Taaffe, D. R., Puolakka, J., & Suominen, H. (2002). "Change in bone mass distribution induced by hormone replacement therapy and high-impact physical exercise in post-menopausal women." Bone **31**(1): 126-135.
- Chilibeck, P. D., Sale, D. G., & Webber, C. E. (1995). "Exercise and bone mineral density." Sports Med **19**(2): 103-122.
- Costa Gomez, T. M., Barrett, J. G., Sample, S. J., Radtke, C. L., Kalscheur, V. L., Lu, Y., Markel, M. D., Santschi, E. M., Scollay, M. C., & Muir, P. (2005). "Up-regulation of site-specific remodeling without accumulation of microcracking and loss of osteocytes." Bone **37**(1): 16-24.
- Donahue, S. W. & Sharkey, N. A. (1999). "Strains in the metatarsals during the stance phase of gait: implications for stress fractures." J Bone Joint Surg Am **81**(9): 1236-44.
- Ferretti, J. L. 1997. "Noninvasive Assessment of Bone Architecture and Biomechanical Properties in Animals and Humans Employing pQCT Technology." J Jpn Soc Bone Morphom **7**, 115-125.
- Ferretti, J. L., Cointry, G. R., & Capozza, R. F. (2002). Noninvasive Analysis of Bone Mass, Structure, and Strength. In Orthopaedic Issues in Osteoporosis, ed. Yuehuei, H. CRC Press:pp. 145-167.
- Findlay, S. C., Eastell, R., & Ingle, B. M. (2002). "Measurement of bone adjacent to tibial shaft fracture." Osteoporos Int **13**(12): 980-989.
- Frost, H. M. (1964). The Laws of Bone Structure Charles C. Thomas.

- Fujita, T. (2002). "Volumetric and projective bone mineral density." J Musculoskelet Neuronal Interact **2**(4): 302-305.
- Guo, X. E. (2001). Mechanical properties of cortical bone and cancellous bone tissue. In Bone Mechanics Handbook, 2nd Edition, ed. Cowin, S. C. Boca Raton, FL, CRC Press:pp. 1-23.
- Han, Y., Cowin, S. C., Schaffler, M. B., & Weinbaum, S. (2004). "Mechanotransduction and strain amplification in osteocyte cell processes." Proc Natl Acad Sci U S A **101**(47): 16689-16694.
- Heinonen, A., Sievanen, H., Kannus, P., Oja, P., Pasanen, M., & Vuori, I. (2000). "High-impact exercise and bones of growing girls: a 9-month controlled trial." Osteoporos Int **11**(12): 1010-1017.
- Impelluso, T. & Negus, C. (2005). Biomechanics and the cyber-infrastructure: delivering the bone and other models to the surgeon. In Computational Modeling of Tissue Surgery, eds. Zeman, M. E. & Cerrolaza, M. Boston, WIT Press:pp. 235-268.
- Johannsen, N., Binkley, T., Englert, V., Neiderauer, G., & Specker, B. (2003). "Bone response to jumping is site-specific in children: a randomized trial." Bone **33**(4): 533-539.
- Judex, S. & Zernicke, R. F. (2000). "High-impact exercise and growing bone: relation between high strain rates and enhanced bone formation." J Appl Physiol **88**(6): 2183-2191.
- Knothe Tate, M. L., Knothe, U., & Niederer, P. (1998). "Experimental elucidation of mechanical load-induced fluid flow and its potential role in bone metabolism and functional adaptation." Am J Med Sci **316**(3): 189-195.
- Lai, Y. M., Qin, L., Hung, V. W., & Chan, K. M. (2005a). "Regional differences in cortical bone mineral density in the weight-bearing long bone shaft--a pQCT study." Bone **36**(3): 465-471.
- Lai, Y. M., Qin, L., Yeung, H. Y., Lee, K. K., & Chan, K. M. (2005b). "Regional differences in trabecular BMD and micro-architecture of weight-bearing bone under habitual gait loading--a pQCT and microCT study in human cadavers." Bone **37**(2): 274-282.
- Lorentzon, M., Mellstrom, D., & Ohlsson, C. (2005). "Association of Amount of Physical Activity With Cortical Bone Size and Trabecular Volumetric BMD in Young Adult Men:The GOOD Study." J Bone Miner Res **20**(11): 1936-1943.
- Macdonald, H. M., Kontulainen, S. A., Khan, K. M., & McKay, H. A. (2007). "Is a school-based physical activity intervention effective for increasing tibial bone strength in boys and girls?" J Bone Miner Res **22**(3): 434-446.
- Mosley, J. R. & Lanyon, L. E. (1998). "Strain rate as a controlling influence on adaptive modeling in response to dynamic loading of the ulna in growing male rats." Bone **23**(4): 313-318.

- Muir, P., Johnson, K. A., & Ruaux-Mason, C. P. (1999). "In vivo matrix microdamage in a naturally occurring canine fatigue fracture." Bone **25**(5): 571-576.
- Nonaka, K., Fukuda, S., Aoki, K., Yoshida, T., & Ohya, K. (2006). "Regional distinctions in cortical bone mineral density measured by pQCT can predict alterations in material property at the tibial diaphysis of the Cynomolgus monkey." Bone **38**(2): 265-272.
- Rajamani, K. T., Hug, J., Nolte, L.-P., & Styner, M. 2004. "Bone morphing with statistical shape models for enhanced visualization." Proc. SPIE. 5367[Medical Imaging], 122-130.
- Rautava, E., Lehtonen-Veromaa, M., Kautiainen, H., Kajander, S., Heinonen, O. J., Viikari, J., & Mottonen, T. (2007). "The reduction of physical activity reflects on the bone mass among young females: a follow-up study of 142 adolescent girls." Scand J Med Sci Sports **17**(2): 191.
- Riggs, C. M., Lanyon, L. E., & Boyde, A. (1993). "Functional associations between collagen fibre orientation and locomotor strain direction in cortical bone of the equine radius." Anat Embryol (Berl) **187**(3): 231-238.
- Robling, A. G., Hinant, F. M., Burr, D. B., & Turner, C. H. (2002). "Shorter, more frequent mechanical loading sessions enhance bone mass." Med Sci Sports Exerc **34**(2): 196-202.
- Rubin, C. T. & Lanyon, L. E. (1984). "Regulation of bone formation by applied dynamic loads." J Bone Joint Surg Am **66**(3): 397-402.
- Ruffing, J., Cosman, F., Zion, M., Tendy, S., Garrett, P., Lindsay, R., & Nieves, J. (2006). "Determinants of bone mass and bone size in a large cohort of physically active young adult men." Nutr Metab (Lond) **3**: 14.
- Schoutens, A., Laurent, E., & Poortmans, J. R. (1989). "Effects of inactivity and exercise on bone." Sports Med **7**(2): 71-81.
- Selker, F. & Carter, D. R. (1989). "Scaling of long bone fracture strength with animal mass." J Biomech **22**(11-12): 1175-83.
- Sievanen, H., Koskue, V., Rauhio, A., Kannus, P., Heinonen, A., & Vuori, I. (1998). "Peripheral quantitative computed tomography in human long bones: evaluation of in vitro and in vivo precision." J Bone Miner Res **13**(5): 871-882.
- Skedros, J. G., Bloebaum, R. D., Mason, M. W., & Bramble, D. M. (1994). "Analysis of a tension/compression skeletal system: possible strain-specific differences in the hierarchical organization of bone." Anat Rec **239**(4): 396-404.
- Specker, B. & Binkley, T. (2003). "Randomized trial of physical activity and calcium supplementation on bone mineral content in 3- to 5-year-old children." J Bone Miner Res **18**(5): 885-892.
- Stratec Medizintechnik GmbH 2004. "XCT 3000 Manual Software version 5.50." _

- Tobias, J. H., Steer, C. D., Mattocks, C. G., Riddoch, C., & Ness, A. R. (2007). "Habitual levels of physical activity influence bone mass in 11-year-old children from the United Kingdom: findings from a large population-based cohort." J Bone Miner Res **22**(1): 101-109.
- Tommasini, S. M., Nasser, P., Schaffler, M. B., & Jepsen, K. J. (2005). "Relationship between bone morphology and bone quality in male tibias: implications for stress fracture risk." J Bone Miner Res **20**(8): 1372-1380.
- Umemura, Y., Ishiko, T., Yamauchi, T., Kurono, M., & Mashiko, S. (1997). "Five jumps per day increase bone mass and breaking force in rats." J Bone Miner Res **12**(9): 1480-1485.
- Vainionpaa, A., Korpelainen, R., Sievanen, H., Vihriala, E., Leppaluoto, J., & Jamsa, T. (2007). "Effect of impact exercise and its intensity on bone geometry at weight-bearing tibia and femur." Bone **40**(3): 604-611.
- Veitch, S. W., Findlay, S. C., Hamer, A. J., Blumsohn, A., Eastell, R., & Ingle, B. M. (2005). "Changes in bone mass and bone turnover following tibial shaft fracture." Osteoporos Int.
- Wasserman, N., Yerramshetty, J., & Akkus, O. (2005). "Microcracks colocalize within highly mineralized regions of cortical bone tissue." Eur J Morphol **42**(1-2): 43-51.
- Weinbaum, S., Zhang, X., Han, Y., Vink, H., & Cowin, S. C. (2003). "Mechanotransduction and flow across the endothelial glycocalyx." Proc Natl Acad Sci U S A **100**(13): 7988-7995.
- Wolff, I., van Croonenborg, J. J., Kemper, H. C., Kostense, P. J., & Twisk, J. W. (1999). "The effect of exercise training programs on bone mass: a meta-analysis of published controlled trials in pre- and postmenopausal women." Osteoporos Int **9**(1): 1-12.
- Wolff, J. (1892). Das Gesetz der Transformation der Knochen Berlin, A. Hirschwald.
- You, L. D., Weinbaum, S., Cowin, C., & Schaffler, M. B. 2002. "A new understanding of osteocyte process ultrastructure." .589-590. Houston, TX, USA, IEEE.

Appendix A. pQCT Image Analysis Utilities

Below is a description of the Matlab utility programs (in their current form) written first for the University of Connecticut study and then for the IDF pQCT study.

In general, the results predicted from these codes will be a function of

- Density calibration formula
 - o Example: $\rho(\text{mg/cc}) = 1484 \cdot (I/1000.0) - 337.3$
- Thresholds used
 - o What intensity values are trabecular?
 - o What intensity values are cortical?
- Pixel resolution (0.4mm vs. 0.5mm)
- Image rotation
 - o Where is the Anterior direction?
- Image alignment
 - o How do you place a “mid” or “post” image on top of the “pre” image?

I. SubjectReader.m

- A. Reads a set of binary images corresponding to one subject.
- B. An image set is made up of Image Times and Slices
 1. UCONN:
 - a. 3 Times (Pre, Mid, Post)
 - b. 3 Slices (4, 38, 66)
 - c. 9 images
 2. IDF:
 - a. 2 Times (Pre, Post)
 - b. 3 Slices (4, 38, 66)
 - c. 6 images
- C. Extracts the tibia from the rest of the image using various pixel intensity threshold rules (**tibRead.m**).
 1. Images from the right tibia are “flipped” to make them into a left tibia.
- D. Measure the relative location between the centroids of each slice
 1. Identify 32 registration points around the tibial boundaries at each slice
 2. Calculate the centroid
 3. Measure the differences in (x,y) centroid locations
- E. Align “Mid” and/or “Post” images to the “Pre” images
 1. This is now (11/30/06) an automatic process
 - a. “Mid” and/or “Post” images are shifted and rotated until the difference in their boundaries is minimized
- F. Define a “Master Slice”
 1. Typically the “Pre 66%” image
- G. Re-Center the Master Slice image on canal (not the tibial boundary)
 1. Measure the amount that the Master Slice has been shifted and shift all other images in the set by the same amount
- H. Shift all “Slave Slices” (4%, 38%) so that their location relative to the Master Slice is correct.

- I. Rotate all images
- J. Rotation is determined by the “Master Slice”
 - 1. The cusp (the Anterior crest) of 66% is rotated to be at 90° (Anterior direction).
 - 2. This is also now automatic
 - a. Some individuals with “blunt crests” have to be rotated manually.
- K. Write output to a binary file for later processing
 - 1. All images have been rotated and aligned, and had their inner and outer boundaries identified.
- II. **GeomAnalysis.m**
 - A. Can read individual subjects or groups from a batch file
 - B. Measure A-P width and M-L width
 - 1. (Max – Min)*mm/pixel
 - C. Measure Moments of Inertia (I)
 - 1. Find all tibial pixels in the cortical range (threshold dependent)
 - 2. Also dependent on mm/pixel
 - 3. I-ML and I-AP depend on definition of the M-L and A-P axis
 - D. Cortical Area
 - 1. Look at each pixel in the tibia image
 - a. If it falls within the cortical thresholds (800-1500 mg/cc) count it
 - b. Sum the cortical pixels, convert pixels to mm²
 - E. Trabecular Area
 - 1. Look at each pixel in the tibia image
 - a. If it falls within the trabecular thresholds (100-600 mg/cc) count it
 - b. Sum the trabecular pixels, convert pixels to mm²
 - F. Density
 - 1. For each sector of each image, identify all pixels in a given threshold range (100-600mg/cc for trabecular, 800-1500mg/cc for cortical)
 - 2. Average all the densities of all relevant pixels.
 - G. BSI
 - 1. $BSI = I * \text{Average Cortical Density}$
 - H. SI (Slenderness Index)
 - 1. Can calculate if we have the tibial length L, and body weight.
 - I. Average Thickness
 - 1. For each sector, calculate the average difference in radius between the endosteal boundary and the periosteal boundary.
 - J. Average Radius
 - 1. This is the canal radius as a percentage of total radius. (As cortical wall thins, the average radius approaches 1.)
 - 2. For each sector, divide the average outer (periosteal) radius by the average inner (endosteal) radius.

Appendix B. Sample Patient Specific FEA Results

boundWriter.m

1. Read three image files (*.M01, *.M02, *.M03)
2. Align and rotate images
3. Define boundary (Outbound, OutboundPol)
4. Smooth this boundary by averaging nearby values. using **boundarySmoother.m**
5. Write **tibia38.sldcrv**, **tibial66.sldcrv** containing boundary points of the 38% and 66% levels.
6. Calculate diaphyseal widths
 - a. ML1 = 38% Med-Lat width
 - b. AP1 = 38% Ant-Post width
 - c. ML2 = 66% Med-Lat width
 - d. AP2 = 66% Ant-Post width
7. Calculate the x and y scaling factors using widths from the Standardized Tibia
 - a. 20.0 = 38% Med-Lat width
 - b. 21.5 = 66% Med-Lat width
 - c. 27.0 = 38% Ant-Post width
 - d. 33.3 = 66% Ant-Post width
8. Write the **tibia.info** file with the following
 - a. Tibial length (read from **pQCTData\DataTables\SubjectData.txt**)
 - b. The “D-Plane” (15% of Tibial length)
 - c. The “38-Plane”
 - d. The “66-Plane”
 - e. The “A-Plane” (85% of Tibial Length)
 - f. The X-Scale factor
 - g. The Y-Scale factor
 - h. The Z-Scale factor (using a Standardized Tibia length of 354.0mm)

SolidWorks

1. Scale epiphyses
2. Import the 38% and 66% curves
3. Construct guide curves prior to making lofted surfaces
4. Generate the lofted surfaces between sections
5. Export as IGS file

tgShaft.m

1. Read three image files (*.M01, *.M02, *.M03)
2. Align and rotate images
3. Define boundary (Outbound, OutboundPol)
4. Smooth this boundary by averaging nearby values. using **boundarySmoother.m**
5. Identify coordinates at four angular locations around the 38% boundary: 60, 135, 225, 270. These are points
 - a. [Point1X, Point1Y]
 - b. [Point2X, Point2Y]

- c. [Point3X, Point3Y]
 - d. [Point4X, Point4Y]
6. Points 5 through 8 are interior to the boundary (see 10/31/06 journal entry)
 - a. Points 5 and 7 lie between points 1 and 3
 - b. Points 6 and 8 lie between points 2 and 4
7. Convert the coordinates into XY. Voxel-mm conversion is hardcoded.
8. Repeat this for the 66%
9. TGShaftPoints.txt writes a total of 16 points

tgWriter.m

1. Read the tibial length and plane locations from **tibia.info**.
2. Read the Scale factors from **tibia.info** and write them into a “scaling matrix”.
3. Begin writing **TrueGrid (tg)** file.

TrueGrid

1. Generate a mesh in Marc format.

tg2dhr.c

1. Convert file format to DHR format

meshbouncer.c

1. Read **dhr** file
 - a. material
 - b. connectivity
 - c. coordinates
 - d. fixity conditions
 - e. post proc data
2. Read **tibia.info** file
 - a. tibLength
 - b. D-Plane (zD)
 - c. 38-Plane (z38)
 - d. 66-Plane (z66)
 - e. A-Plane (zA)
3. Determine which nodes are on the surface with **SurfaceNodes** (in **utility/utills.h**).
 - a. Send the surface nodes to **layerNodes**.
 - i. Determine the surface nodes at z38
 - ii. write the z38 surface nodes to ***.38s**
 - iii. Determine the surface nodes at z66
 - iv. write the z66 surface nodes to ***.66s**
4. Determine which nodes are on the interior of each plane:
 - a. Send all nodes to layerNodes, pick out the ones on z38
 - i. Write output to ***.38n**
 - b. Send all nodes to layerNodes, pick out the ones on z66
 - i. Write output to ***.66n**
 - c. Send all nodes to layerNodes, pick out the ones on zA
 - i. Write output to ***.An**
 - d. Send all nodes to layerNodes, pick out the ones on zD

- i. Write output to ***.Dn**
5. Determine which elements abut each layer
 - a. Send all nodes/connectivity to layerElements, pick out the ones on z38
 - i. Write output to ***.38c**
 - b. Send all nodes/connectivity to layerElements, pick out the ones on z66
 - i. Write output to ***.66c**
 - c. Send all nodes/connectivity to layerElements, pick out the ones on zA
 - i. Write output to ***.Ac**
 - d. Send all nodes/connectivity to layerElements, pick out the ones on zD
 - i. Write output to ***.Dc**

ct2mesh.m

1. Read the mesh boundary files
 - a. ***.38s, *.38n, *.38c**
 - b. ***.66s, *.66n, *.66c**
2. Read the Tibia image
3. Create the image boundary
4. Scale the coordinates
5. Re-center the image and boundary
6. Convert the mesh, image, and boundaries into Polar
7. Rotate the images
8. Look through the connectivity arrays for each element
 - a. Identify the four nodes making up the element
 - i. **Node1**
 - ii. **Node2**
 - iii. **Node3**
 - iv. **Node4**
 - b. Read the coordinates of the each node making up an element
 - i. **A(x,y)**
 - ii. **B(x,y)**
 - iii. **C(x,y)**
 - iv. **D(x,y)**
 - c. Cycle through each pixel and determine if it falls within the bounds of the connected nodes
 - i. Calculate the vectors making up the element (**quadVec**)
 - ii. Calculate vectors from a pixel to a vertex.
 - iii. Calculate cross-products as needed.
 - d. Average all pixel values falling within the element

matAssign.c

1. Read dhr file
 - a. Material data
 - b. Connectivity
 - c. Coordinates
 - d. Fixity Conditions
2. Open the connectivity files for the four planes (A, 38, 66, D)
3. Open the material files
 - a. **material.038**

- b. **material.066**
- 4. Interpolate from 66 to 38 along element stacks with **elementInterpolator**.
- 5. Assign densities to the epiphyses
 - a. Assign trabecular density to all elements in the interior of the epiphyses.
 - b. Assign cortical density to the shell
- 6. For all elements
 - a. Assign engineering constants to each element
 - b. Align principal directions with the z-axis

constrain.c

- 1. Apply directional displacements to a specified plane

dhr2dyn.c

- 1. Convert input file to LS-Dyna format

Post Processing Utilities

ContourPlotter.m

- 1. Reads files called "Countour.txt" for each member of a group
 - a. File contains nodal values from three adjacent "strands" of nodes
 - b. At each element level, these values are averaged.
 - c. For each level:
 - i. SigmaI is avg of the three SigmaI's
 - ii. SigmaVM
 - iii. SigmaZ
 - iv. TauMax
- 2. Plots 1st Principal, Von Mises, Z, and Maximum Shear stress (separate traces for each member) for a stack of element values

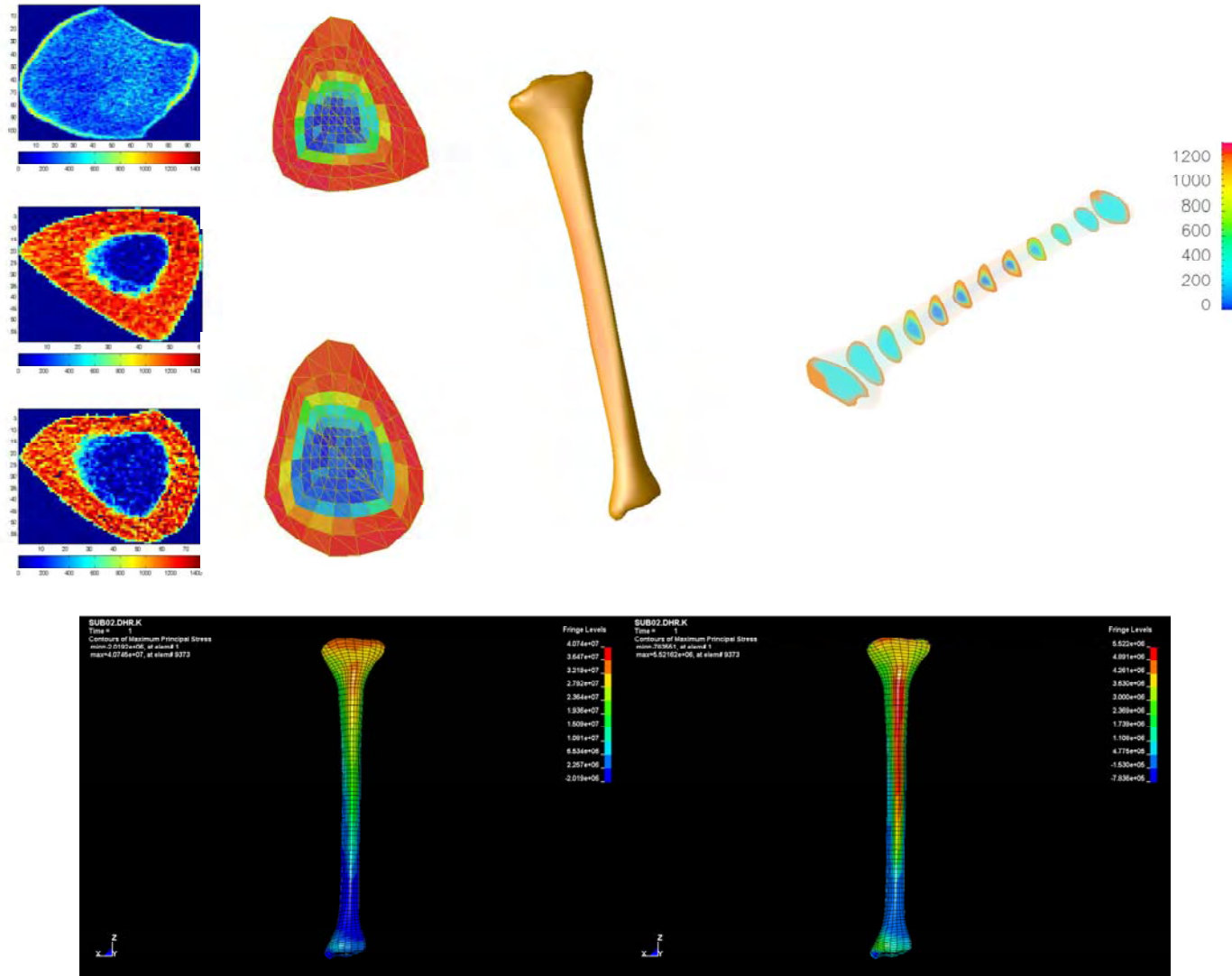


Figure 28. Subject 02: Top (from Left): pQCT Images, FEA model at 38% (above) and 66% (below), predicted 3D geometry, predicted 3D density. Bottom (from Left): Predicted principal stress distribution for a 3BW load, predicted principal stress distribution for a 1000N load.

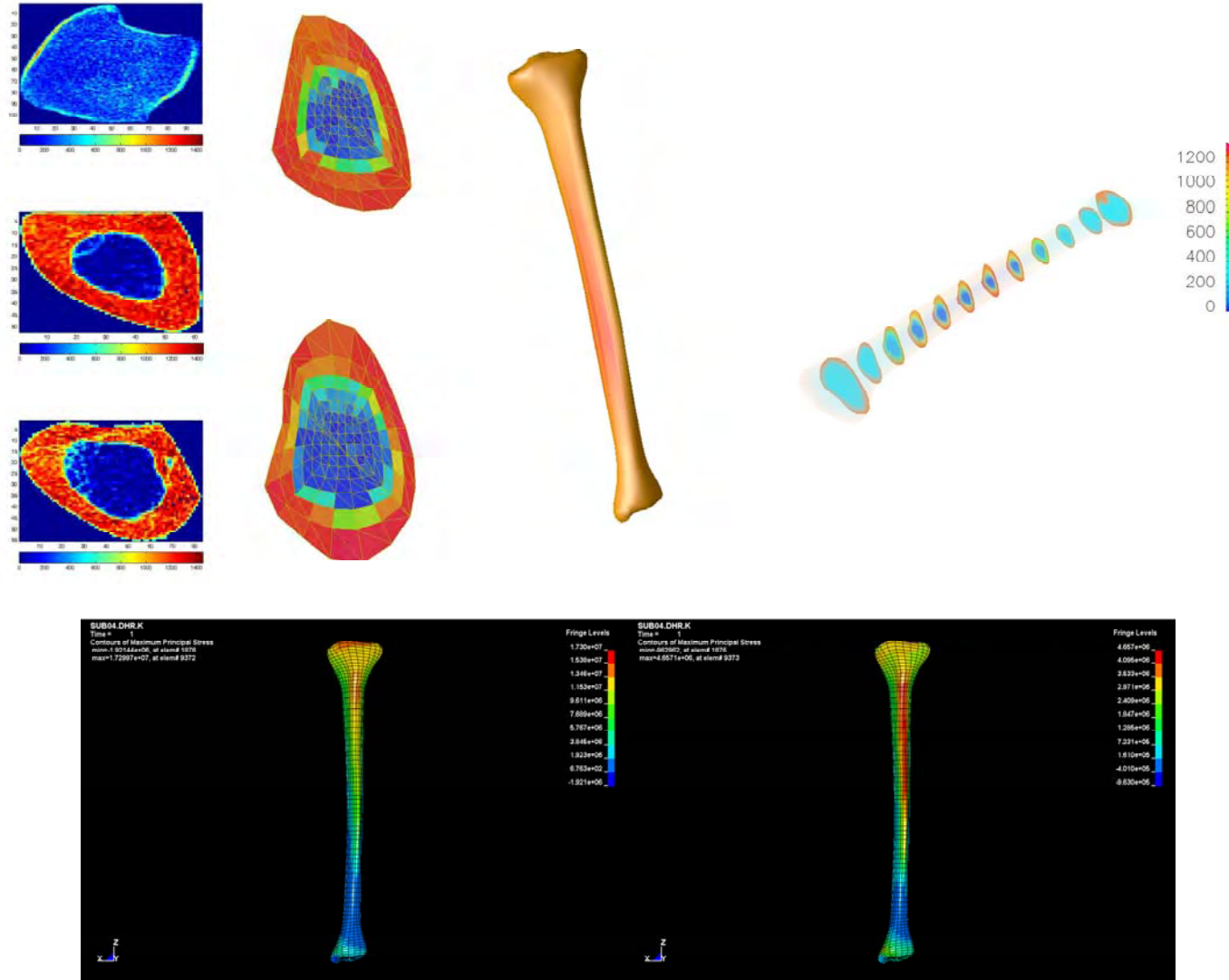


Figure 29. Subject 04: Top (from Left): pQCT Images, FEA model at 38% (above) and 66% (below), predicted 3D geometry, predicted 3D density. Bottom (from Left): Predicted principal stress distribution for a 3BW load, predicted principal stress distribution for a 1000N load.

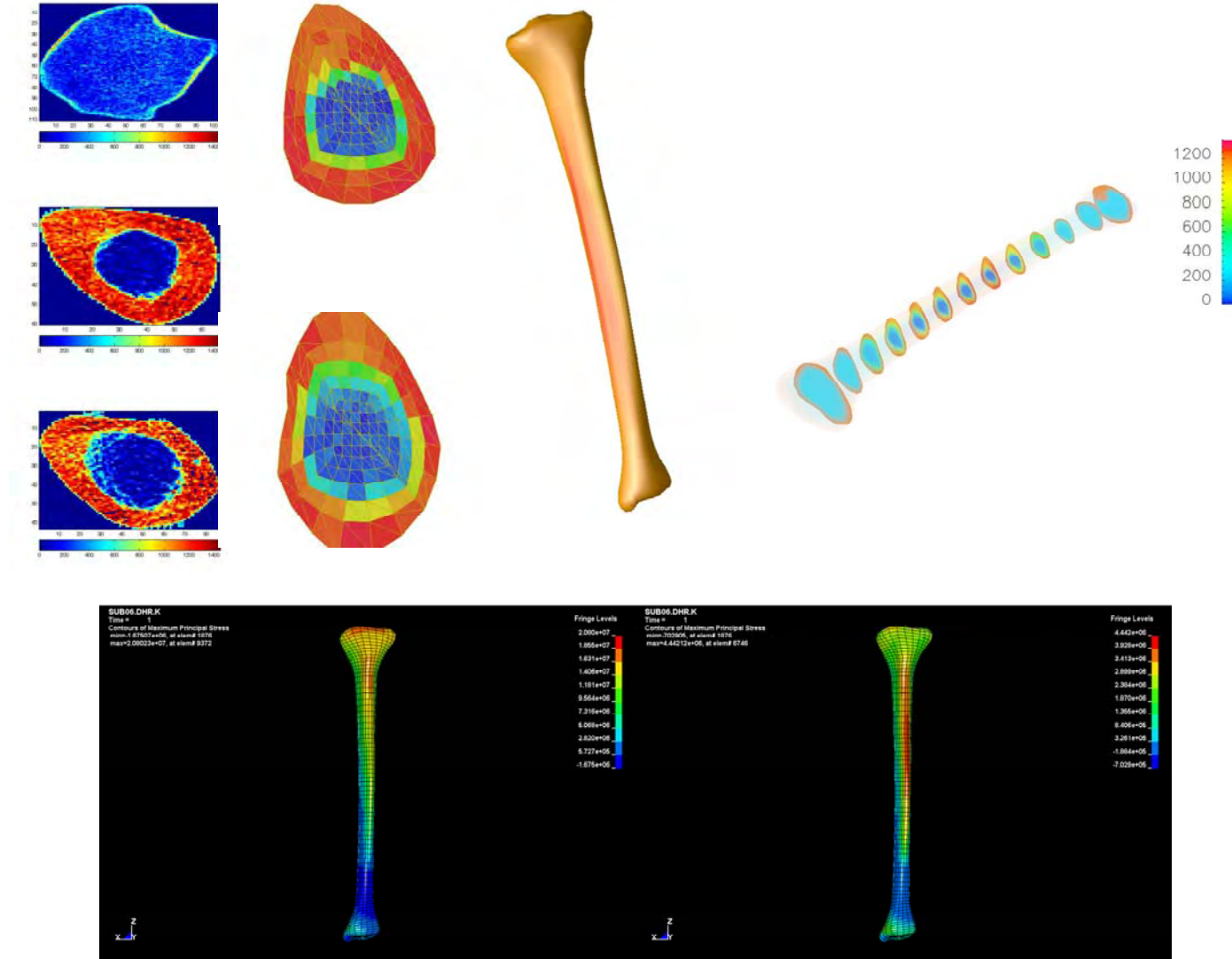


Figure 30. Subject 06: Top (from Left): pQCT Images, FEA model at 38% (above) and 66% (below), predicted 3D geometry, predicted 3D density. Bottom (from Left): Predicted principal stress distribution for a 3BW load, predicted principal stress distribution for a 1000N load.

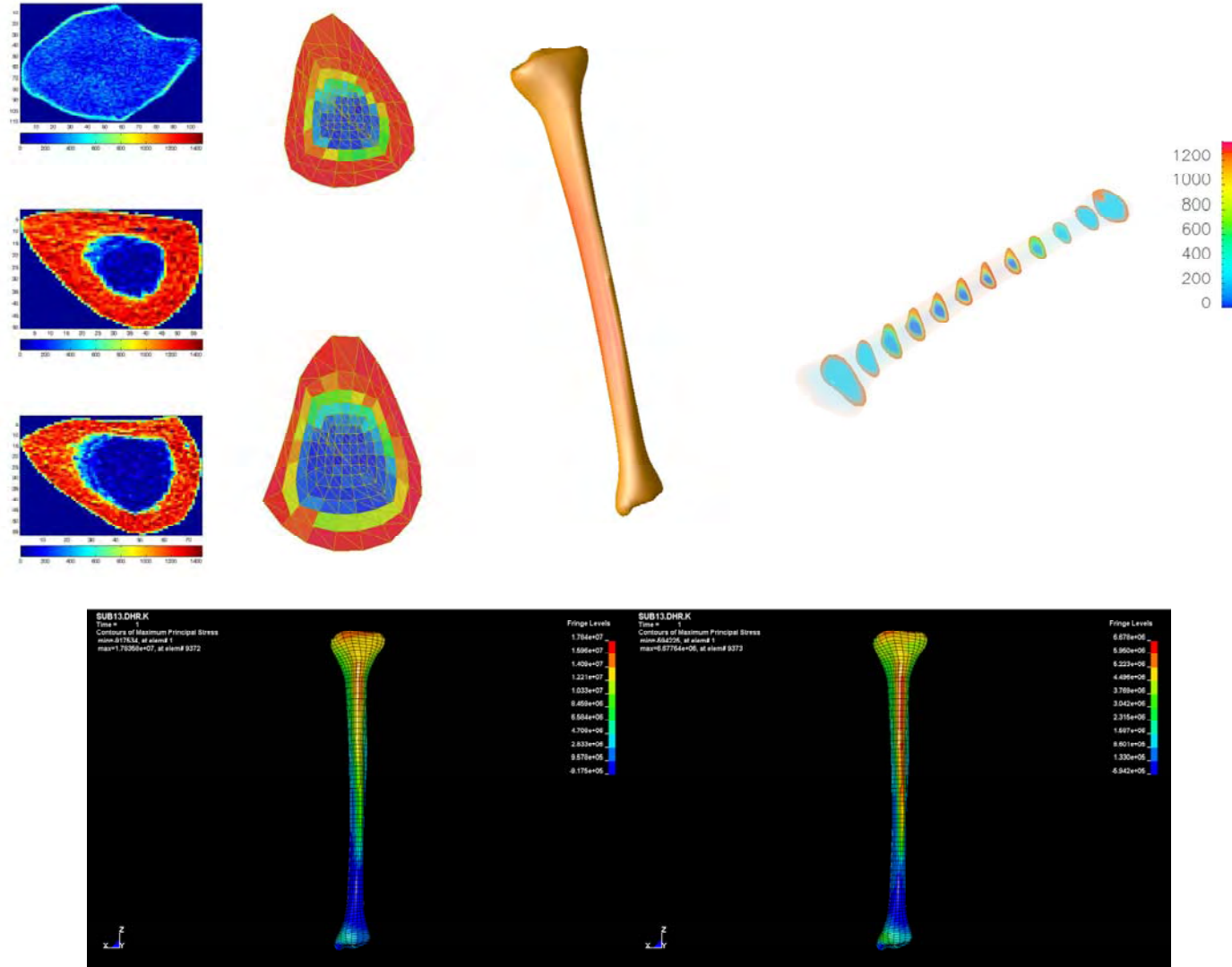


Figure 31. Subject 13: Top (from Left): pQCT Images, FEA model at 38% (above) and 66% (below), predicted 3D geometry, predicted 3D density. Bottom (from Left): Predicted principal stress distribution for a 3BW load, predicted principal stress distribution for a 1000N load.

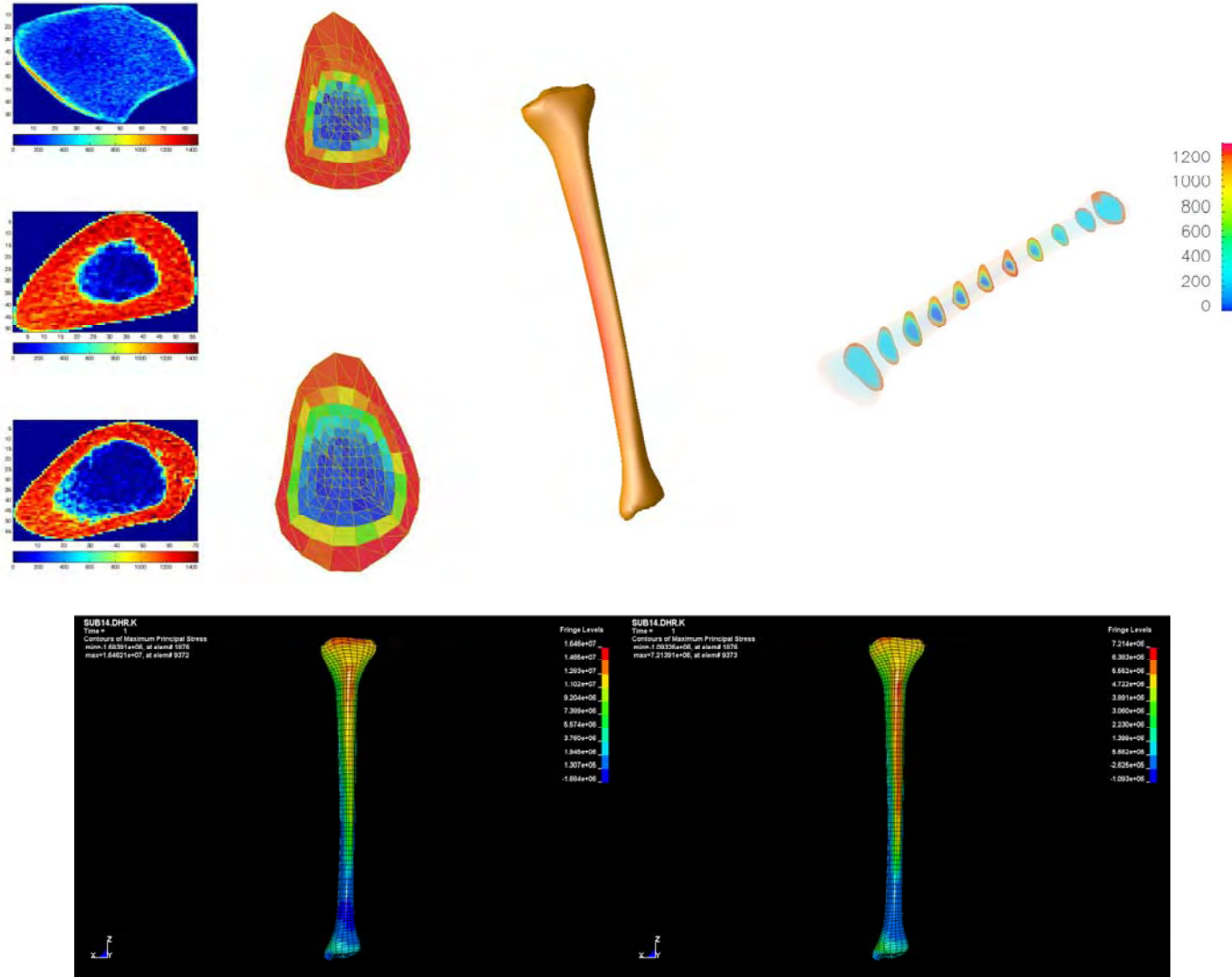


Figure 32. Subject 14: Top (from Left): pQCT Images, FEA model at 38% (above) and 66% (below), predicted 3D geometry, predicted 3D density. Bottom (from Left): Predicted principal stress distribution for a 3BW load, predicted principal stress distribution for a 1000N load.

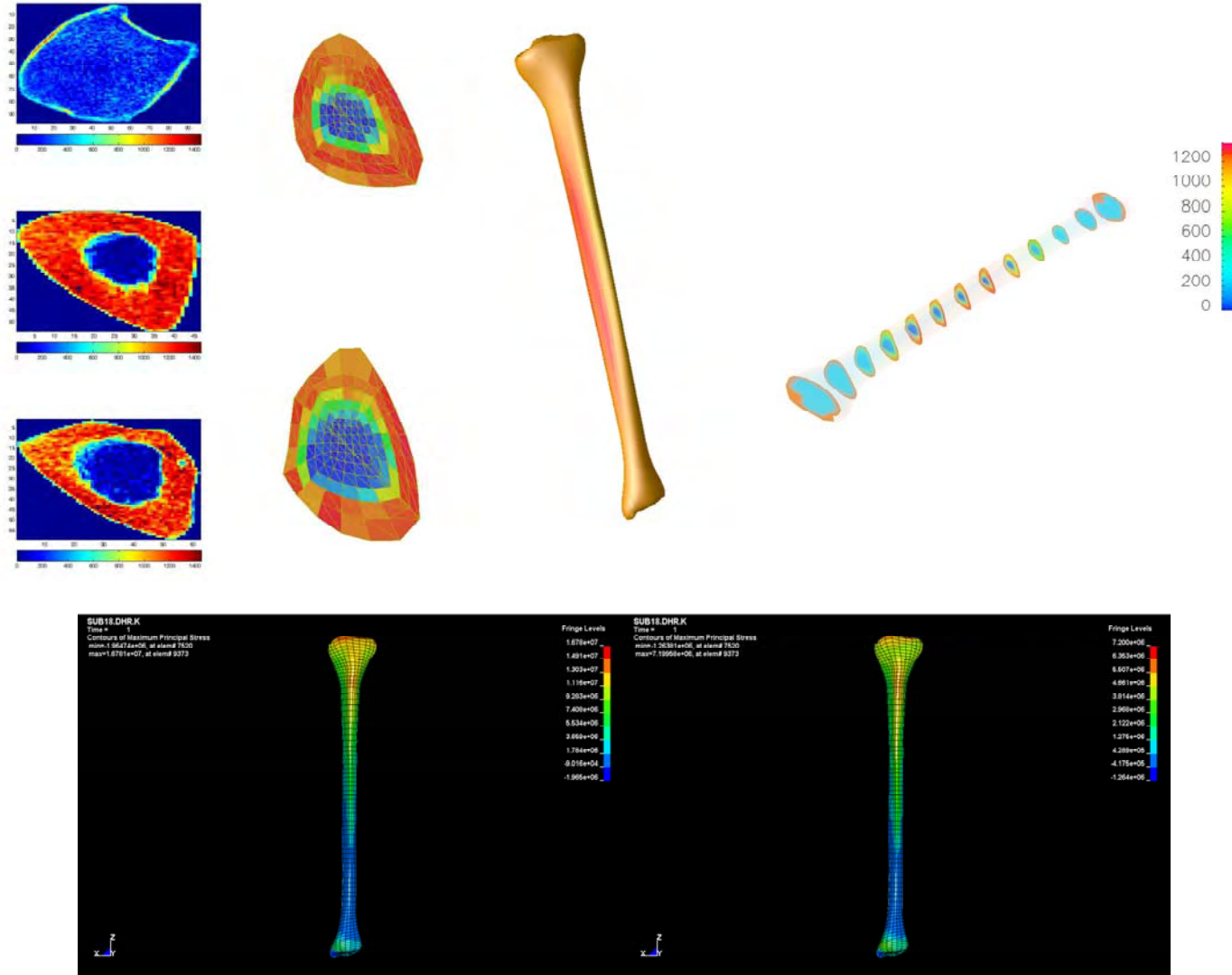


Figure 33. Subject 18: Top (from Left): pQCT Images, FEA model at 38% (above) and 66% (below), predicted 3D geometry, predicted 3D density. Bottom (from Left): Predicted principal stress distribution for a 3BW load, predicted principal stress distribution for a 1000N load.

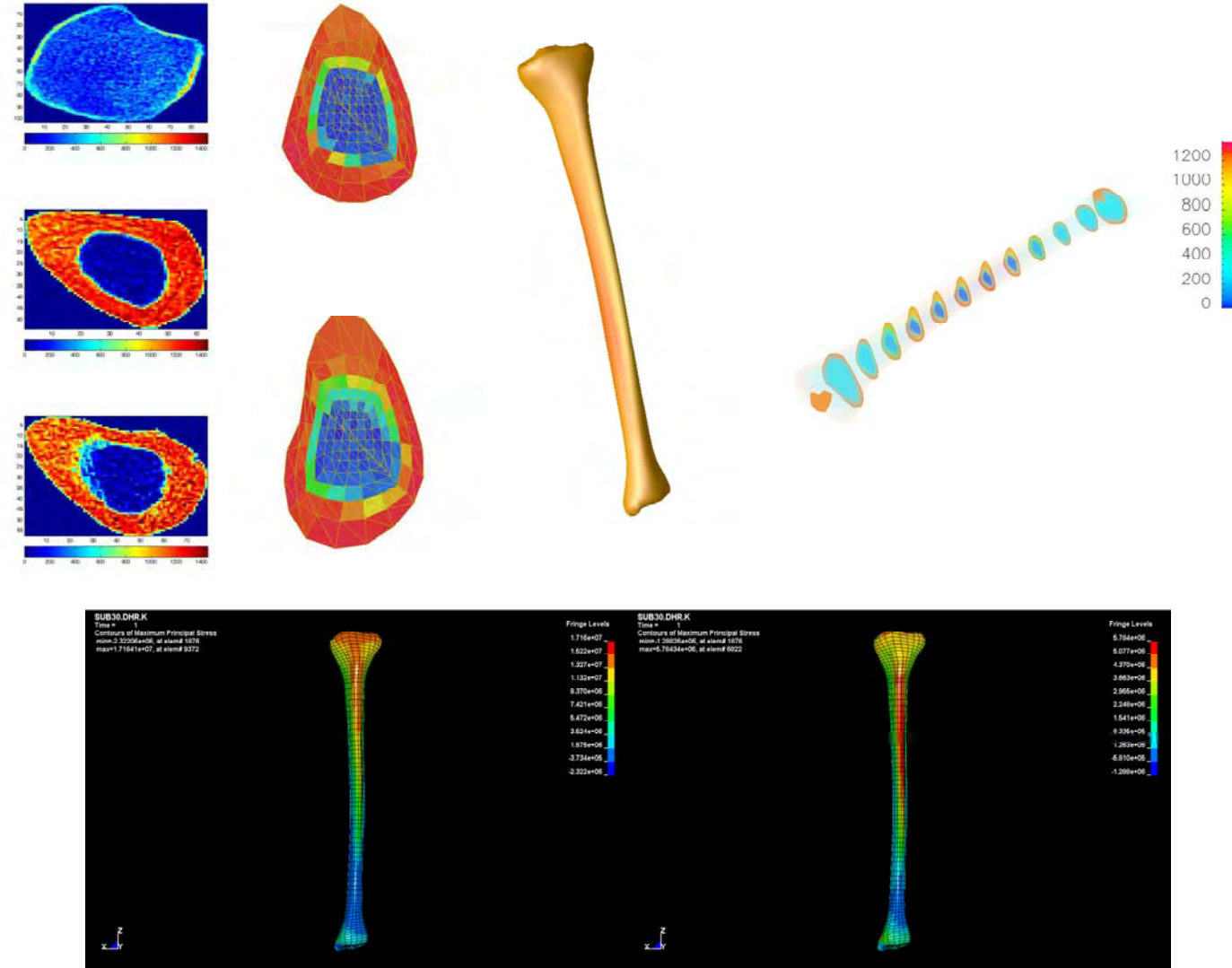


Figure 34. Subject 30: Top (from Left): pQCT Images, FEA model at 38% (above) and 66% (below), predicted 3D geometry, predicted 3D density. Bottom (from Left): Predicted principal stress distribution for a 3BW load, predicted principal stress distribution for a 1000N load.

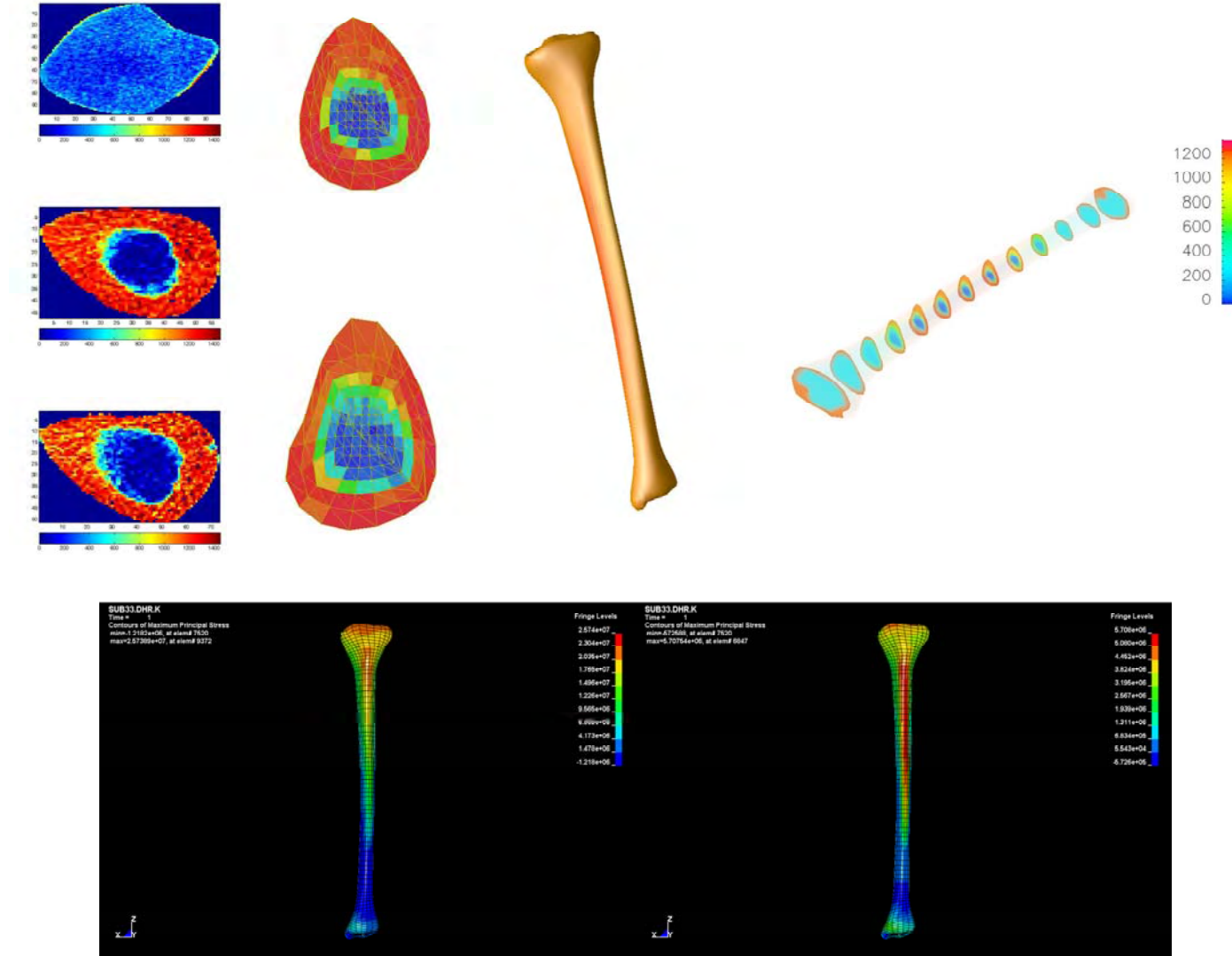


Figure 35. Subject 33: Top (from Left): pQCT Images, FEA model at 38% (above) and 66% (below), predicted 3D geometry, predicted 3D density. Bottom (from Left): Predicted principal stress distribution for a 3BW load, predicted principal stress distribution for a 1000N load.

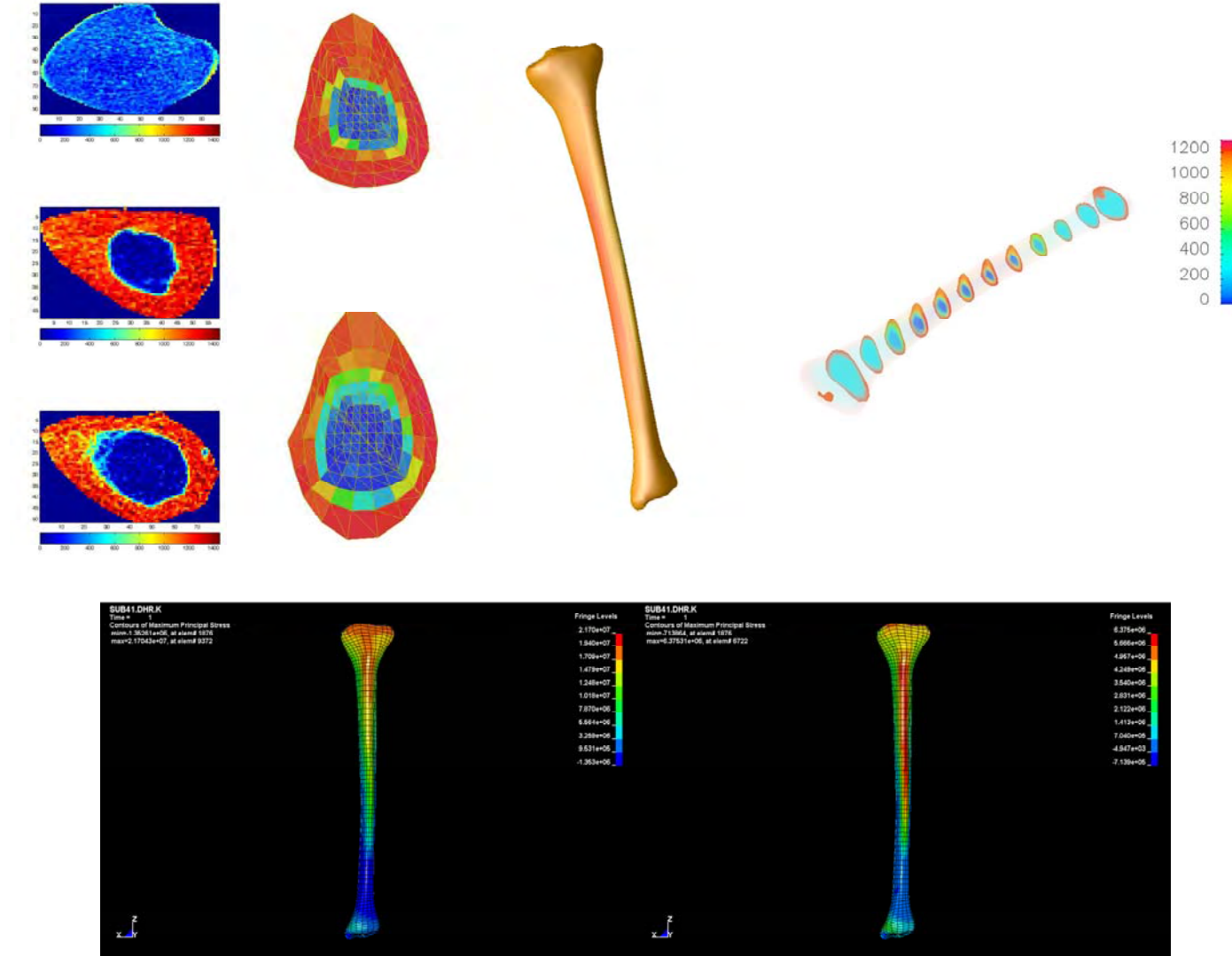


Figure 36. Subject 41: Top (from Left): pQCT Images, FEA model at 38% (above) and 66% (below), predicted 3D geometry, predicted 3D density. Bottom (from Left): Predicted principal stress distribution for a 3BW load, predicted principal stress distribution for a 1000N load.

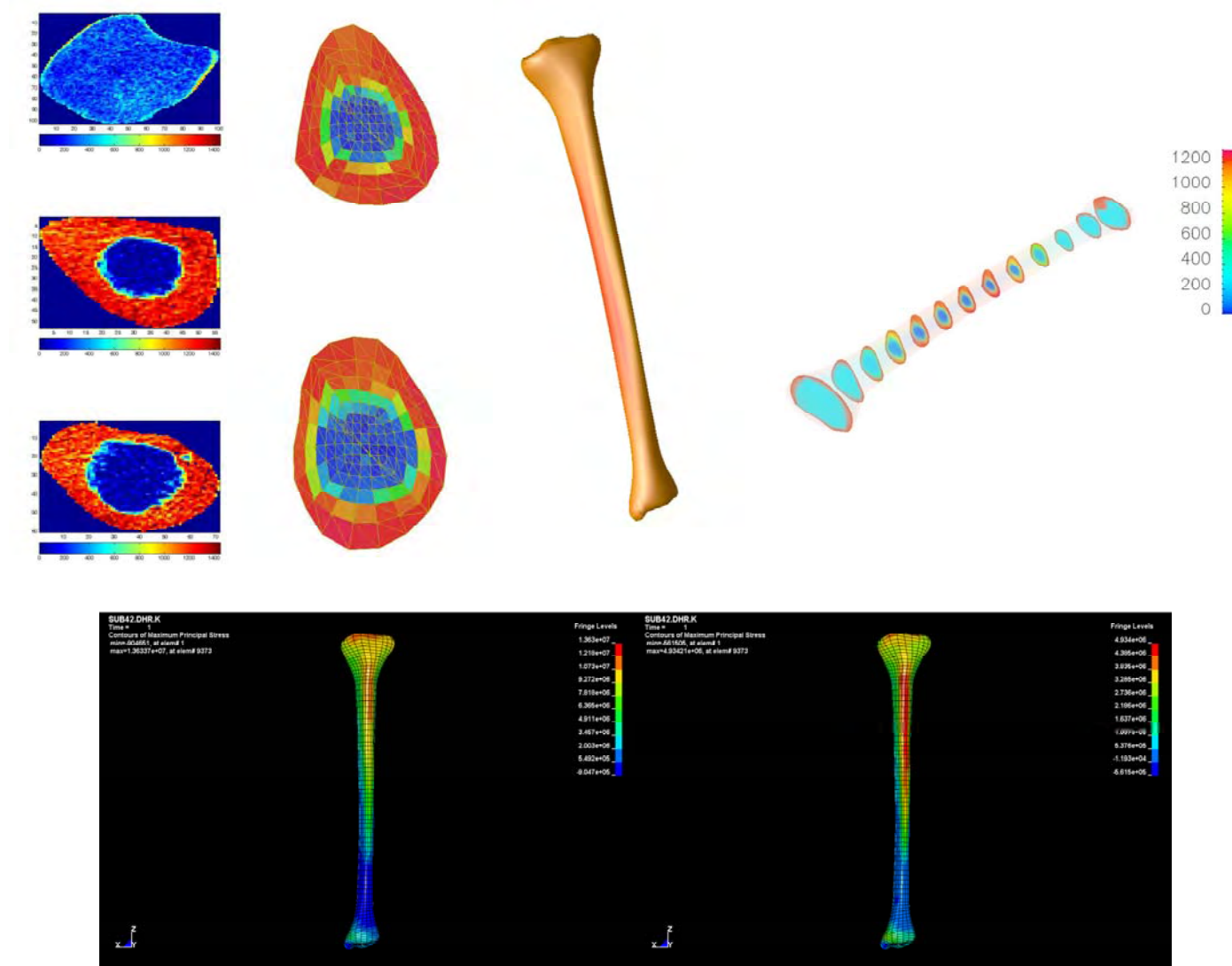


Figure 37. Subject 42: Top (from Left): pQCT Images, FEA model at 38% (above) and 66% (below), predicted 3D geometry, predicted 3D density. Bottom (from Left): Predicted principal stress distribution for a 3BW load, predicted principal stress distribution for a 1000N load.

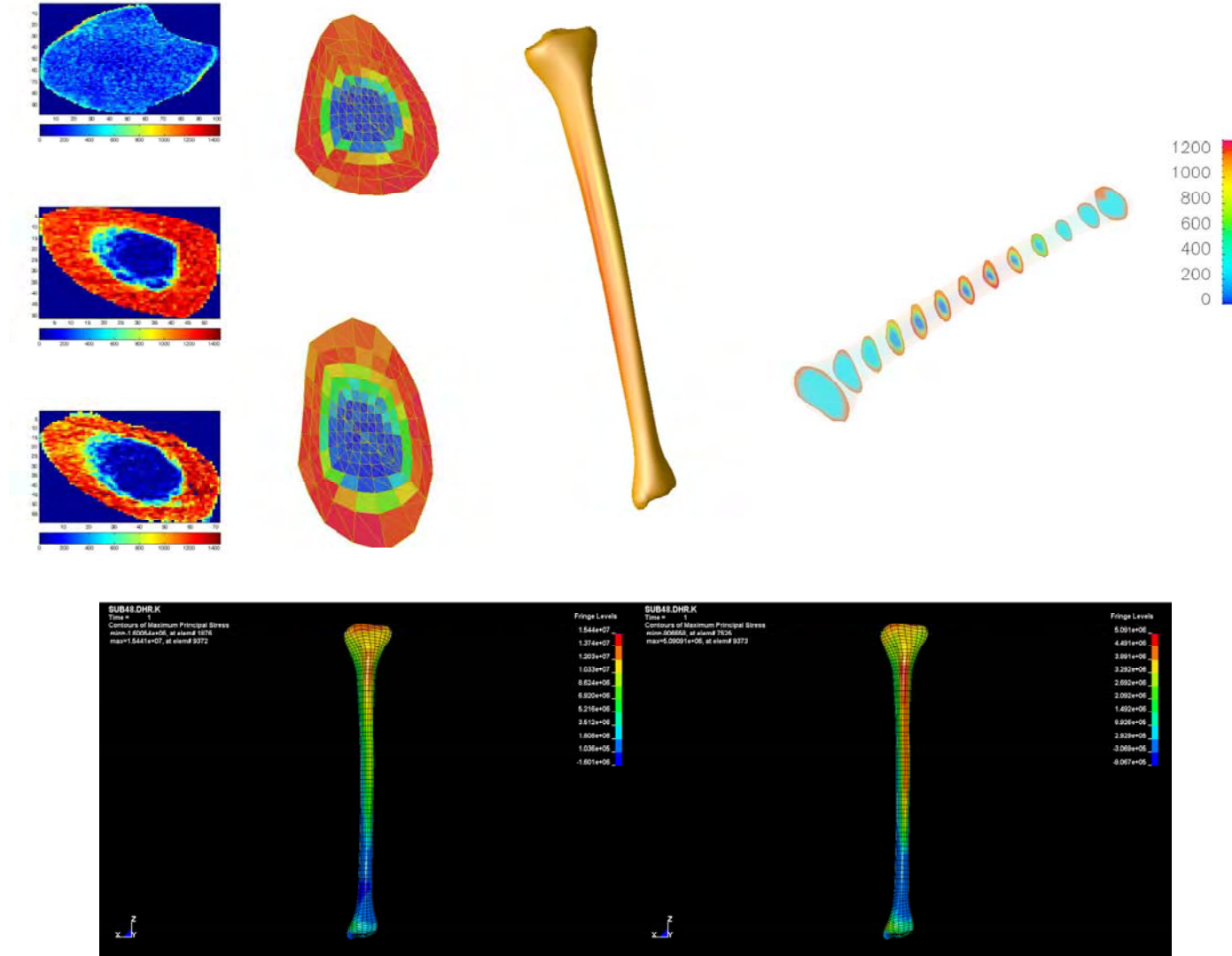


Figure 38. Subject 48: Top (from Left): pQCT Images, FEA model at 38% (above) and 66% (below), predicted 3D geometry, predicted 3D density. Bottom (from Left): Predicted principal stress distribution for a 3BW load, predicted principal stress distribution for a 1000N load.

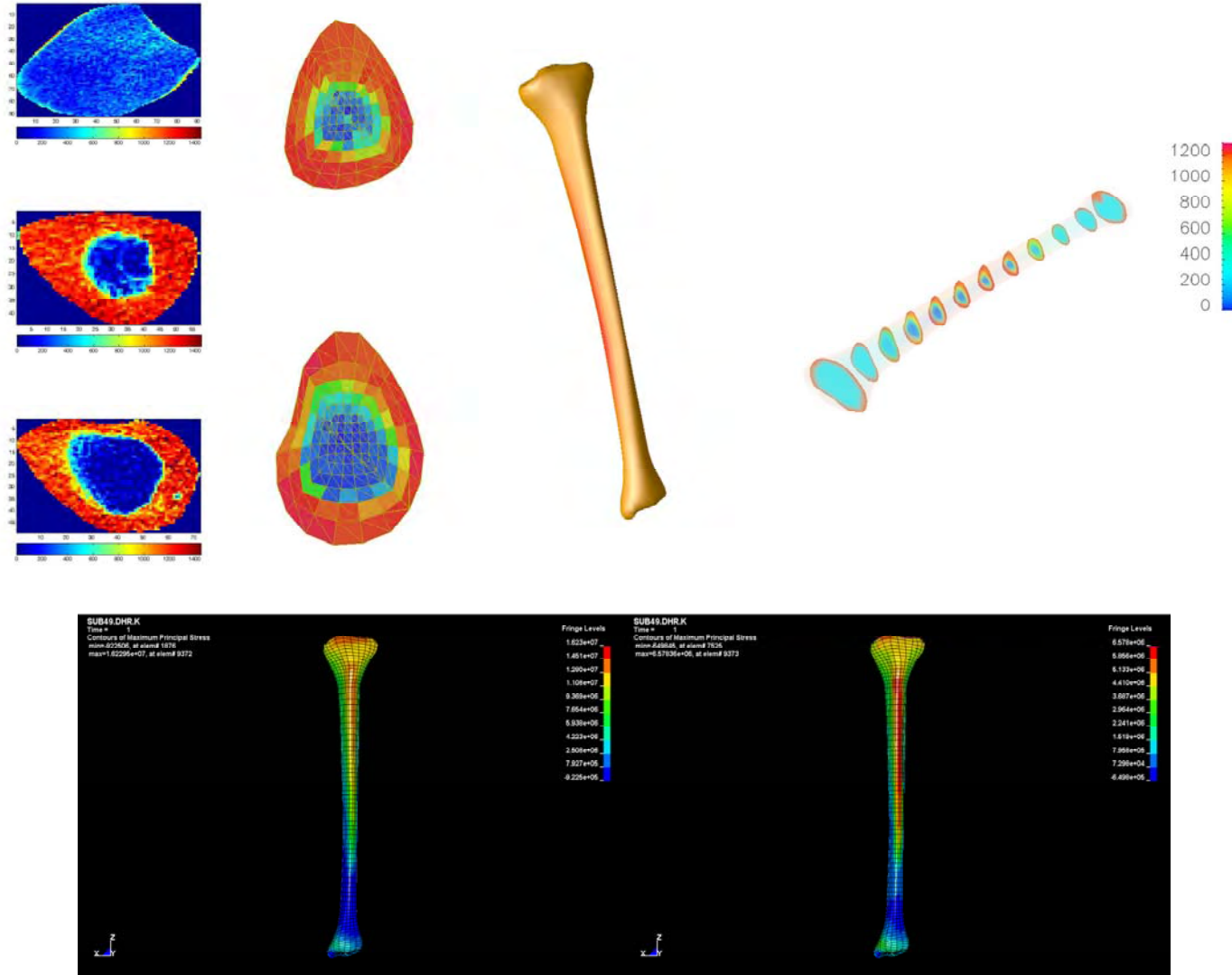


Figure 39. Subject 49: Top (from Left): pQCT Images, FEA model at 38% (above) and 66% (below), predicted 3D geometry, predicted 3D density. Bottom (from Left): Predicted principal stress distribution for a 3BW load, predicted principal stress distribution for a 1000N load.

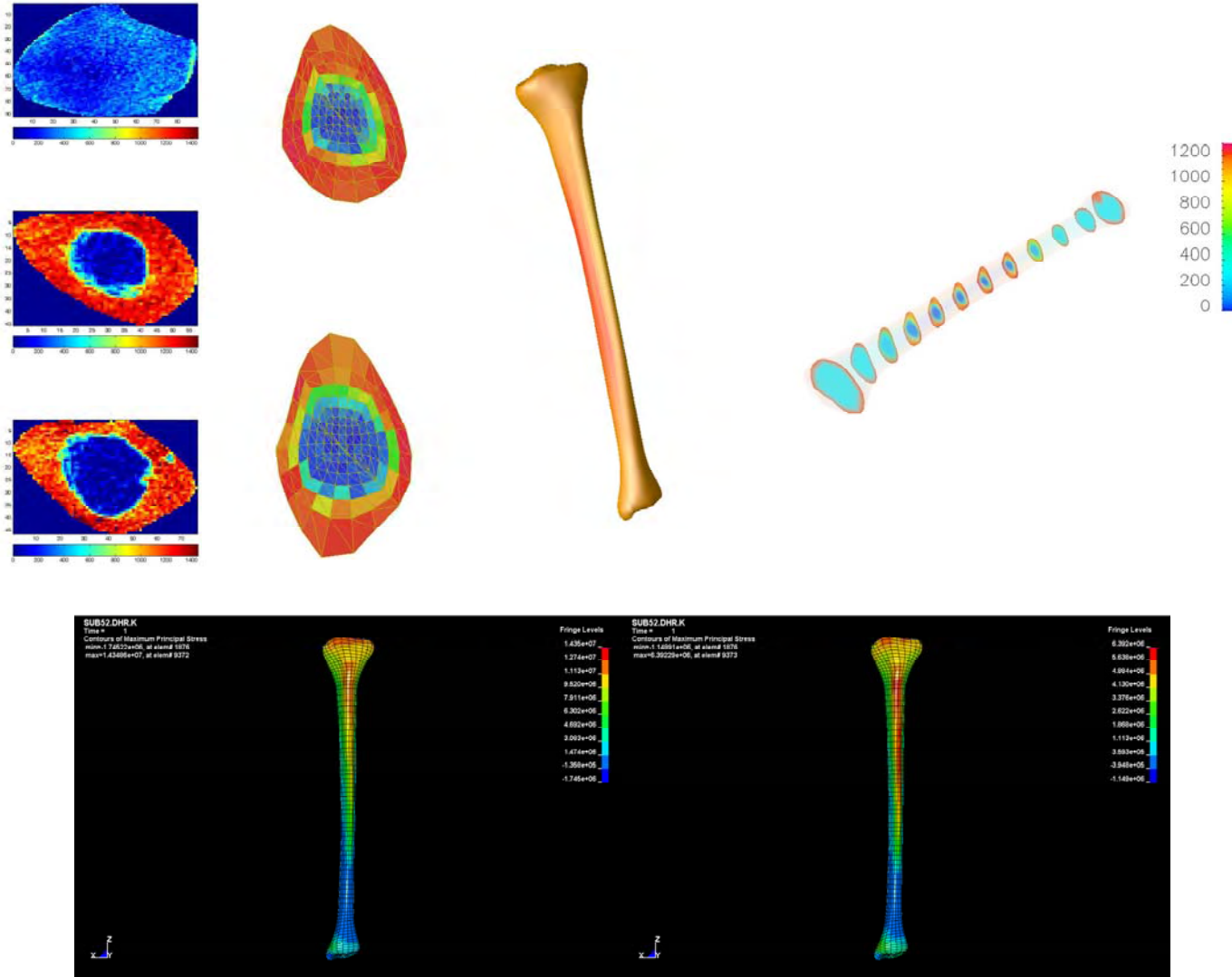


Figure 40. Subject 52: Top (from Left): pQCT Images, FEA model at 38% (above) and 66% (below), predicted 3D geometry, predicted 3D density. Bottom (from Left): Predicted principal stress distribution for a 3BW load, predicted principal stress distribution for a 1000N load.

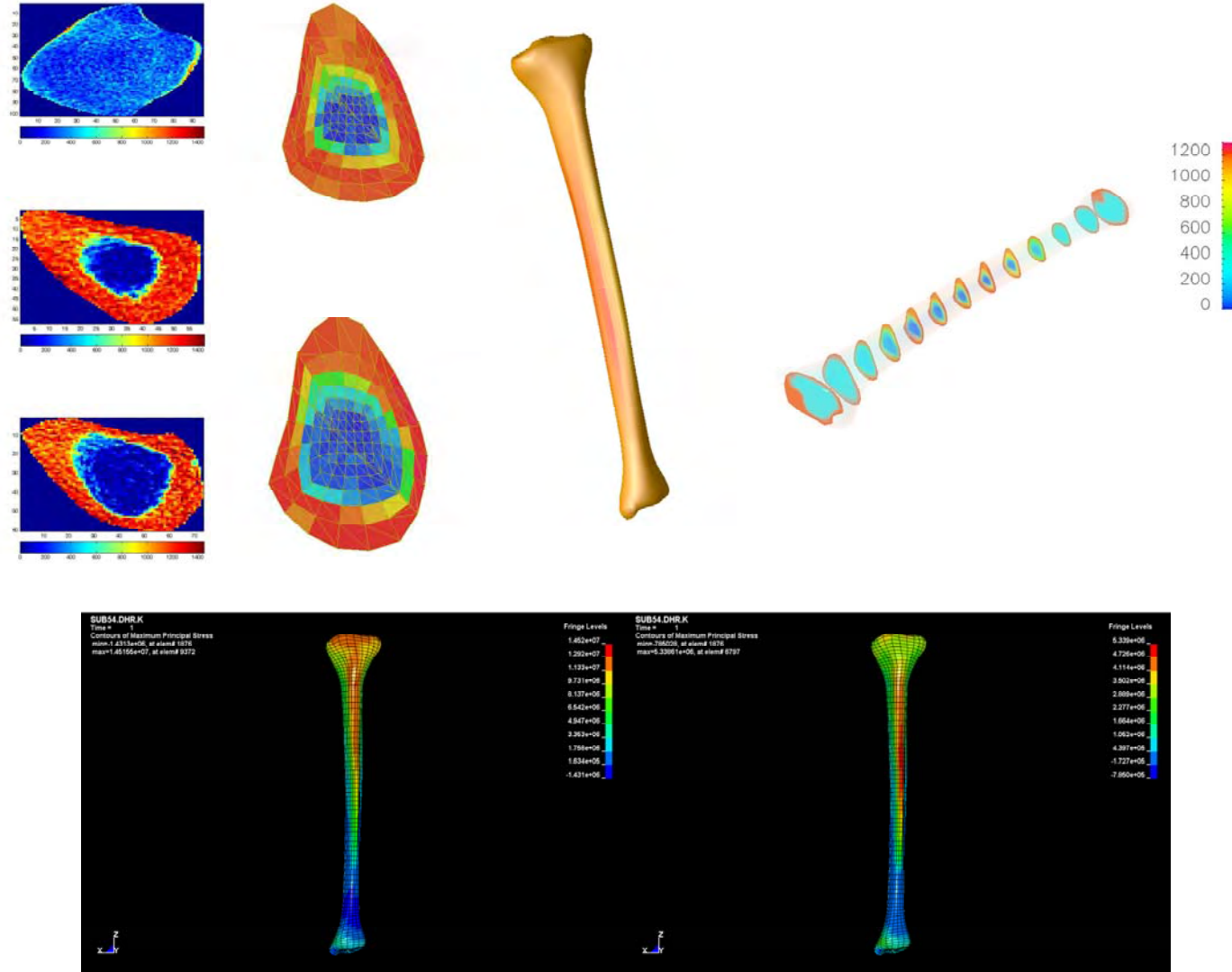


Figure 41. Subject 54: Top (from Left): pQCT Images, FEA model at 38% (above) and 66% (below), predicted 3D geometry, predicted 3D density. Bottom (from Left): Predicted principal stress distribution for a 3BW load, predicted principal stress distribution for a 1000N load.

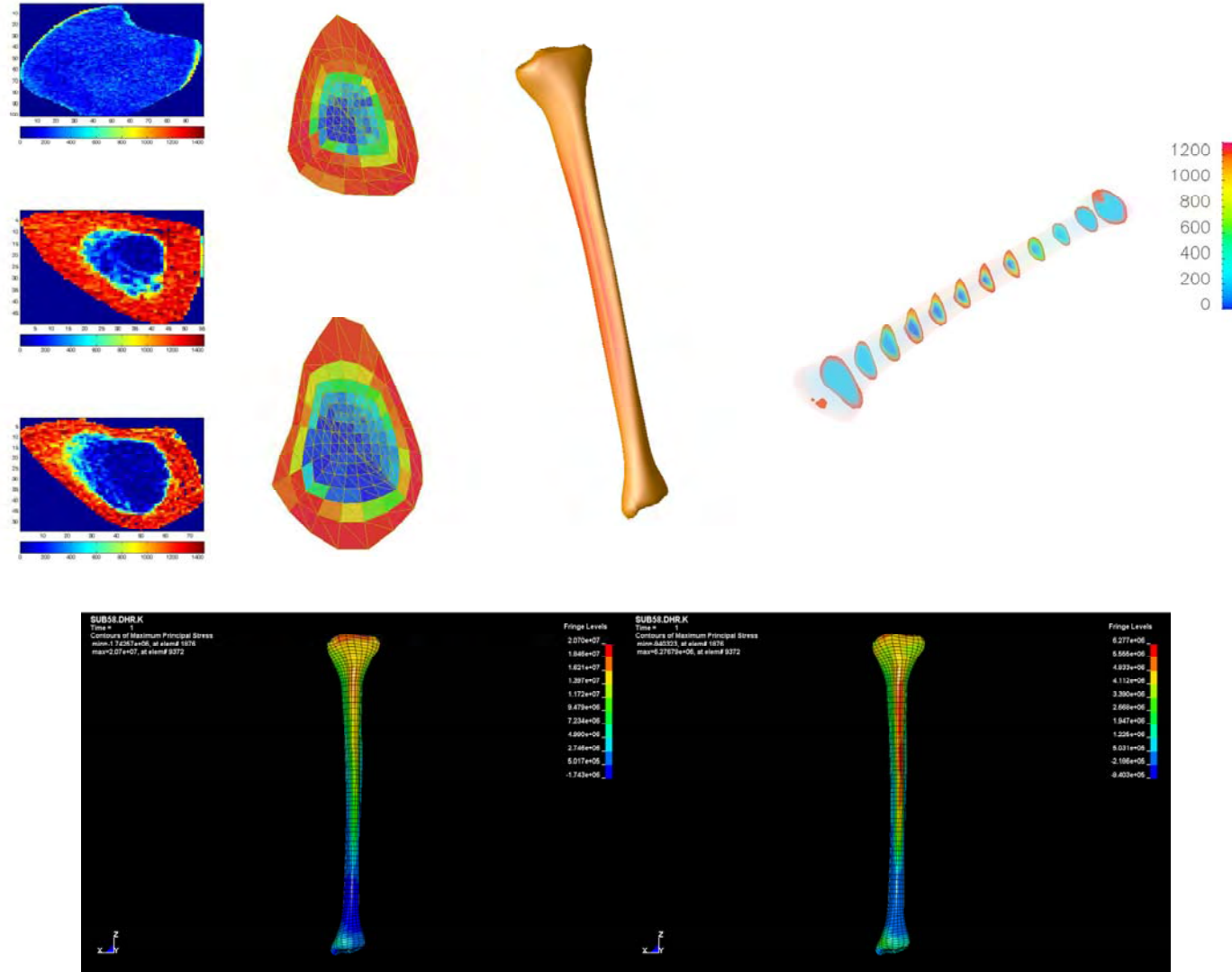


Figure 42. Subject 58: Top (from Left): pQCT Images, FEA model at 38% (above) and 66% (below), predicted 3D geometry, predicted 3D density. Bottom (from Left): Predicted principal stress distribution for a 3BW load, predicted principal stress distribution for a 1000N load.

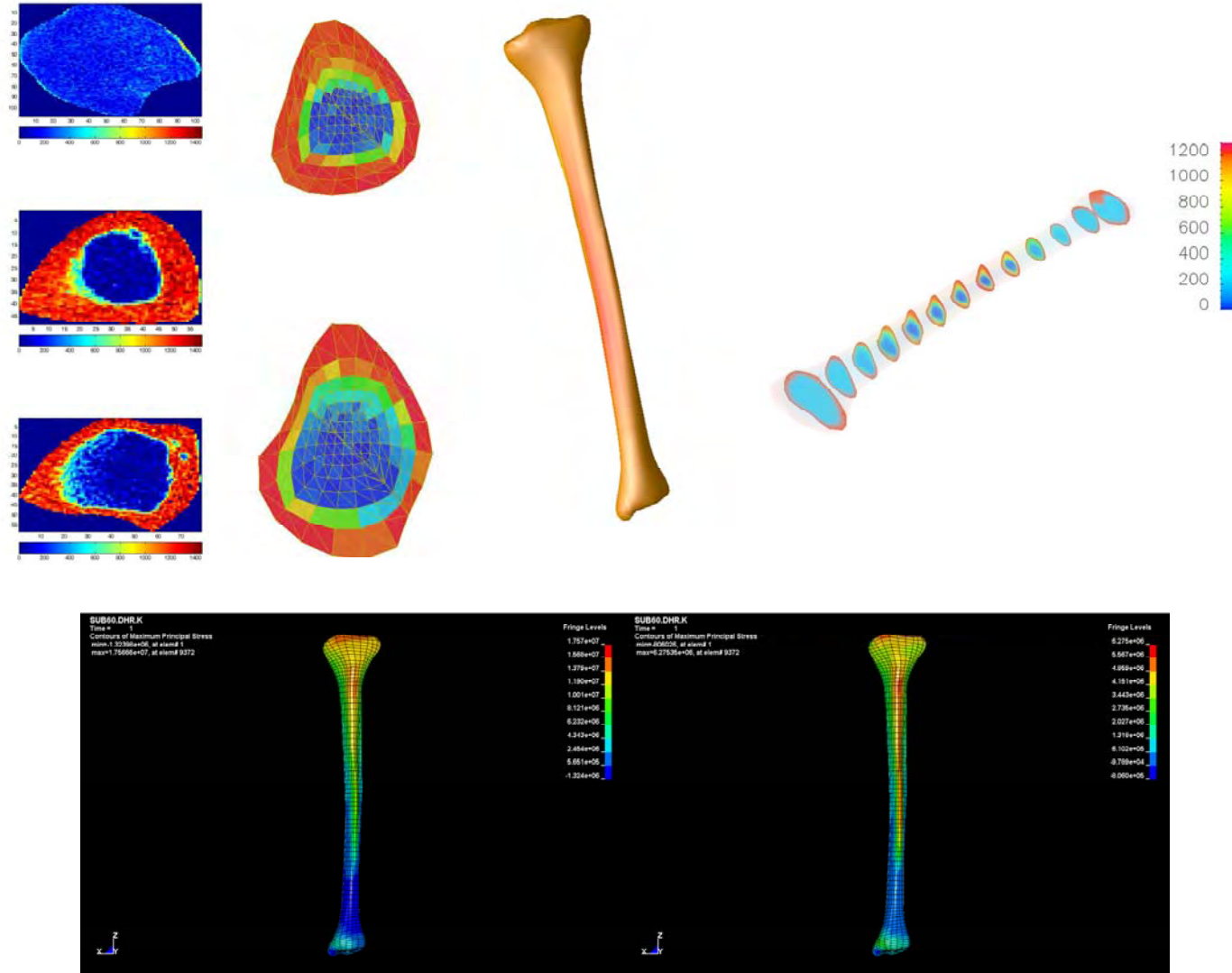


Figure 43. Subject 60: Top (from Left): pQCT Images, FEA model at 38% (above) and 66% (below), predicted 3D geometry, predicted 3D density. Bottom (from Left): Predicted principal stress distribution for a 3BW load, predicted principal stress distribution for a 1000N load.

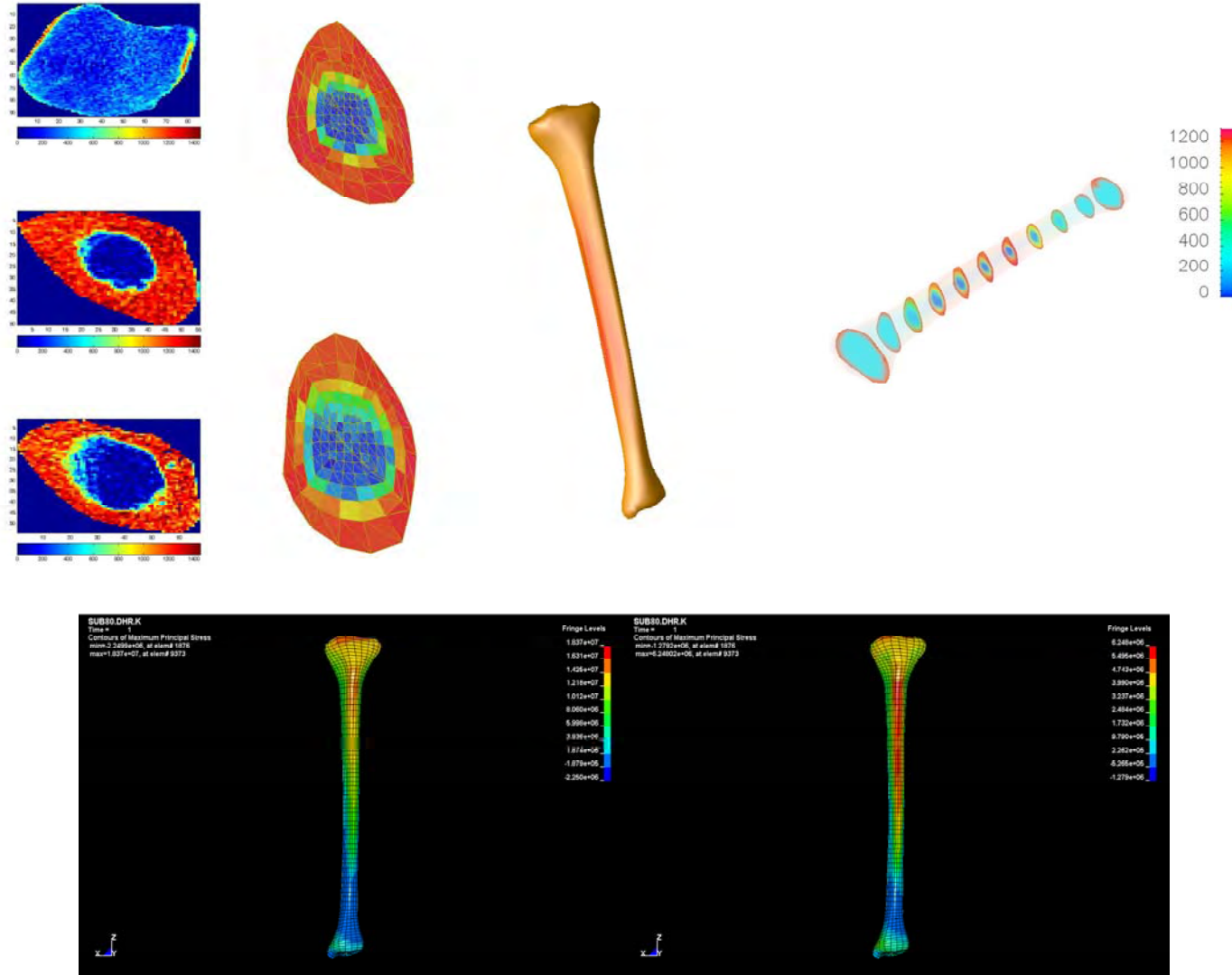


Figure 44. Subject 80: Top (from Left): pQCT Images, FEA model at 38% (above) and 66% (below), predicted 3D geometry, predicted 3D density. Bottom (from Left): Predicted principal stress distribution for a 3BW load, predicted principal stress distribution for a 1000N load.



communications

Applied Technologies

OVERUSE INJURY ASSESSMENT MODEL

Part IV: NMS-Dynamics

FINAL REPORT

Report No. J3181-07-338
for period February 22, 2002 – February 21, 2007
under Contract No. DAMD17-02-C-0073

Prepared by:

Kofi Amankwah, Ph.D.
Weixin Shen, Ph.D.

L-3 Communications/Jaycor
3394 Carmel Mountain Road
San Diego, California 92121-1002

Prepared for:

Commander
U.S. Army Medical Research and Materiel Command
504 Scott Street
Fort Detrick, Maryland 21702-5012

August 2007

REPORT DOCUMENTATION PAGE				Form Approved OMB No. 0704-0188	
Public reporting burden for this collection of information is estimated to average 1 hour per response, including the time for reviewing instructions, searching existing data sources, gathering and maintaining the data needed, and completing and reviewing this collection of information. Send comments regarding this burden estimate or any other aspect of this collection of information, including suggestions for reducing this burden to Department of Defense, Washington Headquarters Services, Directorate for Information Operations and Reports (0704-0188), 1215 Jefferson Davis Highway, Suite 1204, Arlington, VA 22202-4302. Respondents should be aware that notwithstanding any other provision of law, no person shall be subject to any penalty for failing to comply with a collection of information if it does not display a currently valid OMB control number. PLEASE DO NOT RETURN YOUR FORM TO THE ABOVE ADDRESS.					
1. REPORT DATE (DD-MM-YYYY) 08-20-2007		2. REPORT TYPE Final Report		3. DATES COVERED (From - To) Feb. 2002 - Feb. 2007	
4. TITLE AND SUBTITLE Overuse Injury Assessment Model, Part IV: NMS-Dynamics				5a. CONTRACT NUMBER DAMD17-02-C0073	
				5b. GRANT NUMBER	
				5c. PROGRAM ELEMENT NUMBER	
6. AUTHOR(S) Kofi Amankwah Weixin Shen				5d. PROJECT NUMBER 3181	
				5e. TASK NUMBER	
				5f. WORK UNIT NUMBER	
7. PERFORMING ORGANIZATION NAME(S) AND ADDRESS(ES) L-3 Communications/Jaycor 3394 Carmel Mountain Road San Diego, CA 92121				8. PERFORMING ORGANIZATION REPORT NUMBER J3181-07-338	
9. SPONSORING / MONITORING AGENCY NAME(S) AND ADDRESS(ES) U.S. Army Medical Research Acquisition Activity Director 820 Chandler Street Fort Detrick, MD 21702-5014				10. SPONSOR/MONITOR'S ACRONYM(S) USAMRAA	
				11. SPONSOR/MONITOR'S REPORT NUMBER(S)	
12. DISTRIBUTION / AVAILABILITY STATEMENT					
13. SUPPLEMENTARY NOTES					
14. ABSTRACT The human body is a complex, highly nonlinear system. Biomechanical modeling has become an important tool in understanding the neuromuscular and skeletal components of this system. The object of this work has been to develop a flexible suite of modeling components that can be assembled rapidly to address a majority of biomechanical questions. The NMS-Dynamics toolbox provides the basic components needed to build biomechanical models. Models can be built to solve kinematic, inverse and forward analysis problems. Models built with the toolbox were also deployed as standalone applications, and a method to scale the data of one subject to other subjects was implemented.					
15. SUBJECT TERMS biomechanics, lower extremity model, modeling software, NMS-Dynamics, head and neck model, inverse dynamics, forward dynamics					
16. SECURITY CLASSIFICATION OF:			17. LIMITATION OF ABSTRACT	18. NUMBER OF PAGES	19a. NAME OF RESPONSIBLE PERSON
a. REPORT UNCLASSIFIED	b. ABSTRACT UNCLASSIFIED	c. THIS PAGE UNCLASSIFIED			Blossom Widder
			UNLIMITED	37	19b. TELEPHONE NUMBER (include area code) (301) 619-7143

Executive Summary

The human body is a complex, highly nonlinear system. Biomechanical modeling has become an important tool in understanding the neuromuscular and skeletal components of this system. The object of this work has been to develop a flexible suite of modeling components that can be assembled rapidly to address a majority of biomechanical questions. The NMS-Dynamics toolbox provides the basic components needed to build biomechanical models. Models can be built to solve kinematic, inverse and forward analysis problems. Models built with toolbox were also deployed as standalone applications, and a method to scale the data of one subject to other subjects was implemented.

Contents

	<u>Page</u>
1. INTRODUCTION	1
1.1 BACKGROUND	1
1.2 OBJECTIVES	2
1.3 NMS-DYNAMICS TOOLBOX	2
1.4 DEPLOY THE MODELS IN STANDALONE SOFTWARE.....	4
2. MODEL DEVELOPMENT	5
2.1 BIOMECHANICAL MODELING ENGINE.....	5
2.2 MODEL COMPONENTS	5
2.3 MODEL BUILDING.....	6
2.4 CUSTOMIZING MODELS	6
2.5 IMPROVEMENTS TO MODEL DEVELOPMENT PROCESS	7
3. APPLICATIONS	9
3.1 BACKGROUND	9
3.1.1 Inverse Dynamic Analysis.....	9
3.1.2 Forward Dynamic Analysis	9
3.2 HEAD-NECK MODEL: INVERSE PROBLEM.....	10
3.2.1 Summary of Previous Work	10
3.3 HEAD-NECK MODEL: FORWARD PROBLEM	14
3.3.1 Summary of Previous Work	14
3.4 LOWER EXTREMITY MODEL: INVERSE PROBLEM	18
3.4.1 Model Building	18
3.4.2 Scaling Subject Data.....	20
4. DEVELOPMENT OF APPLICATION INTERFACES	22
4.1 OBJECTIVE.....	23
4.2 LAYOUT AND DEVELOPMENT	23
4.3 USER INTERFACE	23
5. SUMMARY	29
5.1 CURRENT YEAR PROGRESS.....	29
5.2 ACCOMPLISHMENTS.....	29
6. REFERENCES	31
APPENDIX A. NMS-DYNAMICS MODEL COMPONENTS	33

Illustrations

	<u>Page</u>
1-1. Example of a biomechanical model built with the NMS-Dynamics toolbox.....	3
2-1. Model customization. Steps involved in customizing a model for a specific subject and scenario.	7
3-1. Head-neck model for inverse analysis	11
3-2. Inverse analysis of head-neck model.	14
3-3. Head-neck model for forward analysis.	15
3-4. Calculated joint trajectories.	17
3-5. Reaction forces at the ankle.	19
3-6. Foot forces. Ground reaction force at the foot, reaction force at the ankle, and gravitational force on the foot.	19
3-7. Example of scaling kinematic data.	21
3-8. Example of scaling ground reaction force data.	22
4-1. Outline of steps involved with the NSM-Dynamics Analysis application.....	23
4-2. Welcome screen.....	24
4-3. Project configuration screen	25
4-4. Model specific screen to set parameters	26
4-5. Model specific screen to display results	27
A-1. Rigid body.	33
A-2. Planar joint.....	33
A-3. Parallel spring and damper (1 DOF).....	34
A-4. Parallel spring and damper (3 DOF).....	34
A-5. Series spring and damper (1 DOF).	34
A-6. Muscle.	35

Tables

	<u>Page</u>
3-1. Kinematic Input to Model.....	13
3-2. Force and Moment Inputs to the Model.....	17

1. Introduction

As an overview to this project, the Introduction will provide a brief description of biomechanical modeling and its importance to biomedical research. Then an outline of project objectives and specifically the current year objectives will be given. Following the Introduction, the sections will further detail the progress accomplished in developing biomechanical modeling software and applying that software to solve specific biomechanical problems.

1.1 Background

The modeling, simulating, and analyzing of the human neuromuscular system have become an increasingly important area of research. This has been driven by two factors: the basic desire to understand the fundamental mechanisms of the neuromuscular system, and by the increasing desire to improve health and reduce injuries to humans. For the military, the desire to improve health and reduce injuries is a continual challenge. Military researchers face challenges to develop better equipment, improve physical training regimens, and design better methods to assess the health status of soldiers.

To address these challenges, one approach is to perform only experiments or field observations and then analyze the measurements. From the analysis, conclusions are made about how the equipment or training regimen could be improved. This experimental approach, however, suffers several limitations. The human body is a complex and highly nonlinear system; therefore significant variations in intra-subject and inter-subject measurements can be expected. Consequently large numbers of subjects are required to obtain statistically significant results. However, even with statistically significant results, the underlying mechanisms remain unknown due to the empirical nature of statistics. These results can only answer the question posed by the experiment. In addition, human experimental work requires large amounts of resources, is difficult to control with large numbers of subjects over long periods of time, and has ethical limitations.

More recently, biomechanical modeling has become an important part of understanding the human neuromuscular and skeletal systems. With modeling, the human body is represented with sets of mathematical relationships and related parameters. Utilizing computer simulations, the model can simulate various scenarios to examine their effects on the health and performance of the body. In addition, by varying the model parameters during a simulation a better understanding can be gained of the underlying mechanisms of the neuromuscular system, and the influence of those mechanisms on the health and performance of the body. The advantages of modeling are that many more tests can be performed rapidly, with fewer resources, and with no need for concerns about subject

safety. Biomechanical models however, must be developed and validated with experimental data to ensure their results are credible.

The construction of an accurate model begins with experimentation, but through development and utilization of the model further lines of research are discovered. Modeling helps the researcher understand which mechanisms are most influential. Therefore, a combination of experimentation, analysis, modeling and simulation are needed to confront the complexity of the neuromuscular and skeletal systems of the human body.

1.2 Objectives

Once a biomechanical model is developed it can be a very powerful tool for analysis. However developing a model can be a time consuming process due to the validation process. Consequently, various modeling applications have been developed to ease model development. These modeling applications, however, are targeted at a specific type of biomechanical problem, do not allow for rapid development, or do not allow for easy integration with other analysis software. Therefore our objective during this project was to develop a neuromuscular and skeletal modeling application that provided a flexible suite of modeling tools which could be assembled rapidly to address a majority of biomechanical questions.

1.3 NMS-Dynamics Toolbox

The resulting product is the NeuroMuscular and Skeletal Dynamics (NMS-Dynamics) Toolbox. NMS-Dynamics is a block programming language that allows users to develop biomechanical models by connecting blocks representing bones, joints, muscles, and passive tissues (Figure 1-1). These models can be utilized to analyze experimental data and to simulate novel scenarios.

Key features of the toolbox include:

- *Efficient:* Models can be assembled from standardized components through a graphical interface; therefore, users are spared from basic programming and can concentrate on the advanced aspects of the model
- *Consistent:* Developing models in a systematic way will make the comparison of results easier
- *Flexible:* The toolbox components are modular so that model assembly and component improvements are easily accomplished
- *Manageable:* Simulation results can be stored in a systematic and easily retrievable manner
- *Powerful:* The Matlab and Simulink platforms by Mathworks (www.mathworks.com) form the software engine
- *Reliable:* The components and algorithms will be rigorously developed and tested
- *Open:* The toolbox allows for the addition of new algorithms and components

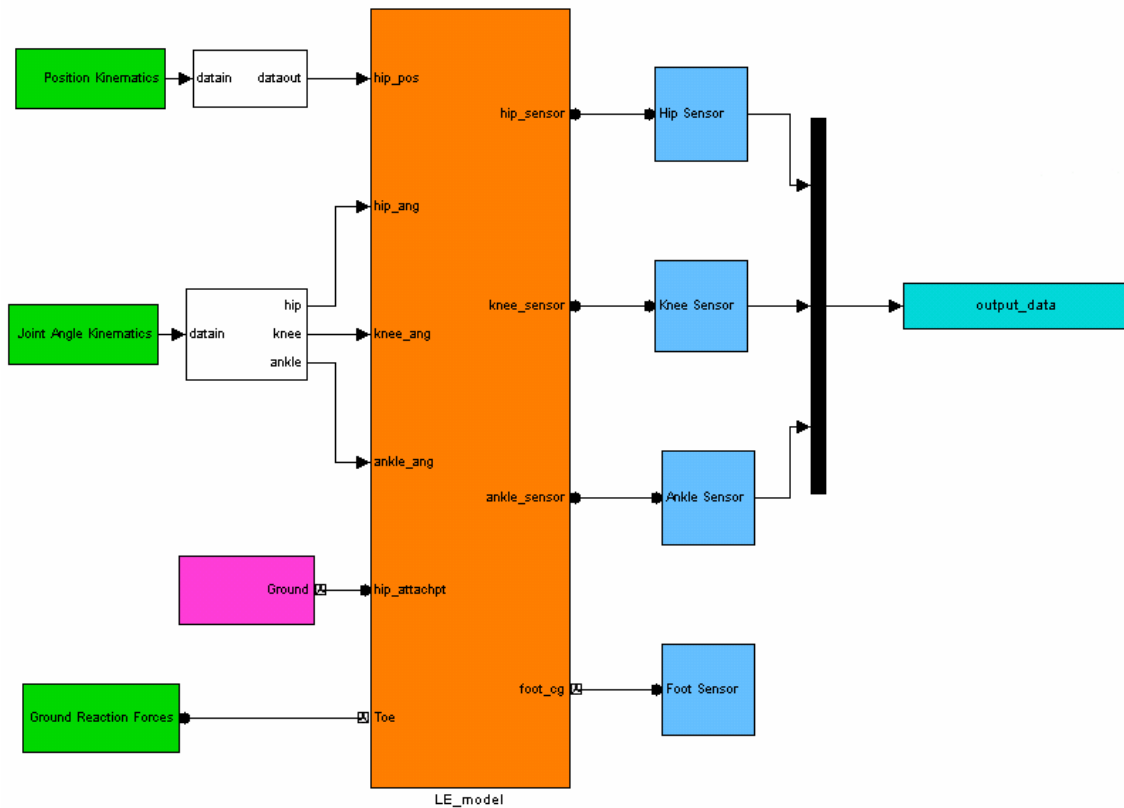


Figure 1-1. Example of a biomechanical model built with the NMS-Dynamics toolbox.

The toolbox can be applied in two manners. The toolbox can be utilized by individuals developing their own models. These individuals can specify the block parameters and simulate their model under various conditions such as walking or running. This rapid development and simulation of biomechanical models enables the user to focus their time on answering their biomechanical questions and spend less time developing the model needed to answer their question.

The second way the toolbox can be employed is during the development of custom applications for a customer. The developer can use the toolbox to build the underlying model for their customer and then build an interface for the customer to easily interact with the model. As a result, the customer does not need to spend time building the application to do their analysis or simulation. The model and interface are built for them so that they can focus on utilizing this tool to answer their particular question.

1.4 Deploy the Models in Standalone Software

The other objectives of the effort also included:

- Developing the ability to deploy a NMS-Dynamics model as a standalone application
- Developing a method to scale kinematic and ground reaction force data from one subject to another subject of different height or weight
- Improving the flexibility of the model building code (e.g. removing hard coded values and special case programming)

Enabling a model to be deployed and improving the model building process are described in the next section. The steps involved in building a model will be explained and then the improvements made to the building process will be discussed. Following that section, example applications will be presented to demonstrate the types of problems that can be addressed with the toolbox along with a method developed to scale data between subjects. In the fourth section, developing user interfaces for the models will be described. In the last section, the project accomplishments will be summarized.

2. Model Development

This section describes the process of building and customizing a model using the NMS-Dynamics toolbox. Building a model requires connecting the appropriate segment and joint blocks together and setting their parameters. The ability to adjust the model parameters quickly provides the user flexibility when customizing the model.

2.1 Biomechanical Modeling Engine

Matlab® and Simulink® (MathWorks, www.mathworks.com) form the basis of the mathematical engine underlying this neuromuscular and skeletal modeling application. Matlab is a high-level computer language that provides users with a robust set of functions and algorithms to perform computationally intensive calculations. Simulink is a platform developed for model-based design. It consists of a graphical interface where models are built by connecting blocks representing mathematical operations, signal processing functions, and control system components. With this platform, models can be developed rapidly and solved with the algorithms included in the platform. Simulink also contains a toolbox called SimMechanics that contains specific blocks such as masses, springs, dampers, and joints for solving rigid body dynamics problems.

The advantages of using Matlab are the power of its included functions and algorithms, and that the high-level language allows for easy programming. The graphical interface of Simulink provides a rapid means for building models without typing code, and SimMechanics provides the functions necessary to solve static and dynamic rigid body problems. The basic rigid body, force, and joint components of SimMechanics allow for custom blocks representing biomechanical components such as bones, muscles, and ligaments to be built.

2.2 Model Components

NMS-Dynamics is a rigid body toolbox for biomechanical analysis. It includes rigid bodies that can be customized to represent specific bones by changing the inertia matrix and mass of the body. The toolbox also has the ability to connect the bodies with many types of joints including: revolute, transverse, and universal. The toolbox includes elements to model the passive and active characteristics of ligaments and muscles. For ligaments, spring and damper blocks can be customized to model linear and nonlinear systems. For muscles, musculotendon models have been developed to include both the passive and active (force-length and force-velocity) properties. The flexibility of the toolbox allows for many different musculotendon models to be developed and utilized. A description of the currently developed blocks is included in Appendix A.

2.3 Model Building

For any biomechanical model, the basic components include:

- Rigid body segment blocks, which represent bones
- Joint blocks, which describe how the bones move relative to each other
- Passive element blocks, which represent passive biological tissues
- Active element blocks, which represent active muscles

By combining these blocks in an appropriate manner, biomechanical models of the whole body or portions of the body can be developed.

In addition to the model being developed, the simulation environment must be developed. Environmental parameters include the location and orientation of the model with respect to the inertial reference frame, the direction and magnitude of the gravitational frame, and the inputs and outputs to the model. Depending on the type of problem being addressed, the inputs to the model can include ground reaction forces, joint kinematics, and muscle activations. For system outputs, the metrics most relevant for addressing the problem will be measured or calculated, and passed out of the model.

With all of the necessary blocks added and connected appropriately, the block parameters must be set to properly describe the properties of a particular subject. For example, the bone length in the model is set by measuring the bone length of the subject. However if the model needs to be applied to several different subjects, manually changing the block parameters will be a slow process. Consequently, routines were developed to automate the process.

2.4 Customizing Models

For each subject, their specific model parameters are stored in a parameter file. To customize the model to a particular subject, the customization routines read the appropriate parameter file and apply those values to the model. Consequently, the model can easily be adjusted to reflect the properties of a new subject by creating a parameter file for that subject and then running the customization routines.

The routines divide the customization process into 3 steps (Figure 2-1). Step 1 involves configuring the environmental parameters including: gravity, the type of analysis (i.e. forward or inverse dynamic analysis) and the numerical solver to utilize. Then the model blocks are customized. The segment masses, moments of inertias, and dimensions are set. The axes of rotation of the joints are specified. The elasticity and viscosity parameters of the passive properties and the active muscle properties are configured. The last step includes setting the input files to load and setting the location for saving the calculated outputs.

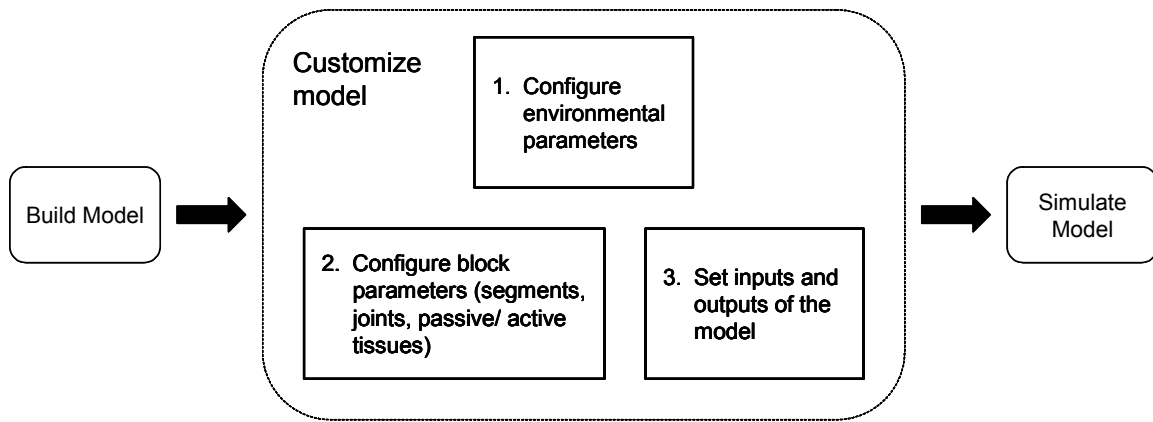


Figure 2-1. Model customization. Steps involved in customizing a model for a specific subject and scenario.

The initially developed routines had some limitations. Not all segment blocks or types of joint blocks were compatible with the routines. The routines hard coded values into the model, so that for each new subject the model had to be recompiled before it was deployable. Although the routines had automated a majority of the process, there were more efficiencies that could be added

2.5 Improvements to Model Development Process

One of the objectives of the effort was to make the model deployable as a standalone application. To accomplish this goal, the model needed to be compiled into an executable file. Consequently, improvements in the modeling process needed to be accomplished so that the models could be quickly and efficiently built, and once compiled could be adjusted to reflect the properties of different subjects and scenarios.

Initial improvements to the customization process included an increase in the number of joint types that could be configured automatically. Previously only planar joints could be configured. Now joints including hinge, planar, prismatic, universal, and 6 degree of freedom (DOF) can be configured. Improved customization routines enabled variable names to be set as parameter values. This allowed the flexibility of customizing the model after it had been compiled, thereby removing the need to recompile the model every time after customization. Improved error checking during the development process also ensured that the compiled model would execute without errors.

The model compiling process was improved with routines that automatically produced the parameter files, such as the segment parameters for each subject, needed by the compiled model. Also, in the initial version, the input signals such as the ground reaction forces to the model were hard coded. Currently, this limitation has been eliminated and now different inputs can be read and utilized by the model without the need to recompile the model.

Through these many improvements, the robustness of the development process was enhanced. The speed of configuring models to particular subjects or scenarios was increased, and the compiling process was further automated.

3. Applications

To illustrate the capabilities and improvements to the NMS-Dynamics toolbox, a head-neck model and a lower extremity model were developed. For the head-neck model an inverse and a forward analysis were performed. For the lower extremity model, an inverse analysis was completed. The following subsections will explain inverse and forward dynamic analysis. Then each model and its corresponding analysis will be discussed.

3.1 Background

3.1.1 *Inverse Dynamic Analysis*

For an inverse dynamic analysis, the goal is to calculate the joint forces and moments needed for a specific system configuration. To achieve this goal, the necessary data are the kinematics of the system and the external forces applied to the system. With the data and the equations of motion of the system, a solution can then be computed.

For a biomechanical problem, the necessary kinematic data can be measured from accelerometers mounted on body segments or from a motion capture system. With accelerometers, the acceleration data can be integrated to get the required velocities and displacements. With a motion capture system, the displacement data can be differentiated to obtain velocities and accelerations.

The externally applied forces in a biomechanical analysis of human systems are usually ground reaction forces. Force plates can measure these reaction forces. For other applied forces such as the impact during a vehicle crash, a human surrogate with force transducers is initially used to measure the applied force.

For the equations of motion of the system, the inertial properties of the body segments must be known. These properties can be obtained through direct measurement on the subject. There are also regression equations to calculate these values based on a number of anthropometric measurements such as body weight, stature and specific geometric dimensions of individual segments. Solving the equations of motion gives the joint reaction forces and moments. A major advantage of utilizing NMS-Dynamics is its power to develop and solve the equations of motion for the user.

3.1.2 *Forward Dynamic Analysis*

A forward dynamics problem is the opposite of the inverse problem. For this problem, the goal is to determine the motion of the system due to forces and moments being applied to the system. To calculate the solution, the necessary data are the joint forces and moments at each degree of freedom, and all externally applied forces.

The joint forces and moments are generated by the actuators that cross the joint. For biomechanical analysis, muscles, tendons, and ligaments are the actuators of the system. Tendons and ligaments are passive elements that produce force based on their length or velocity. Muscle is an active element. The neuronal input to muscle determines the level of activation and therefore the force generated by the muscle.

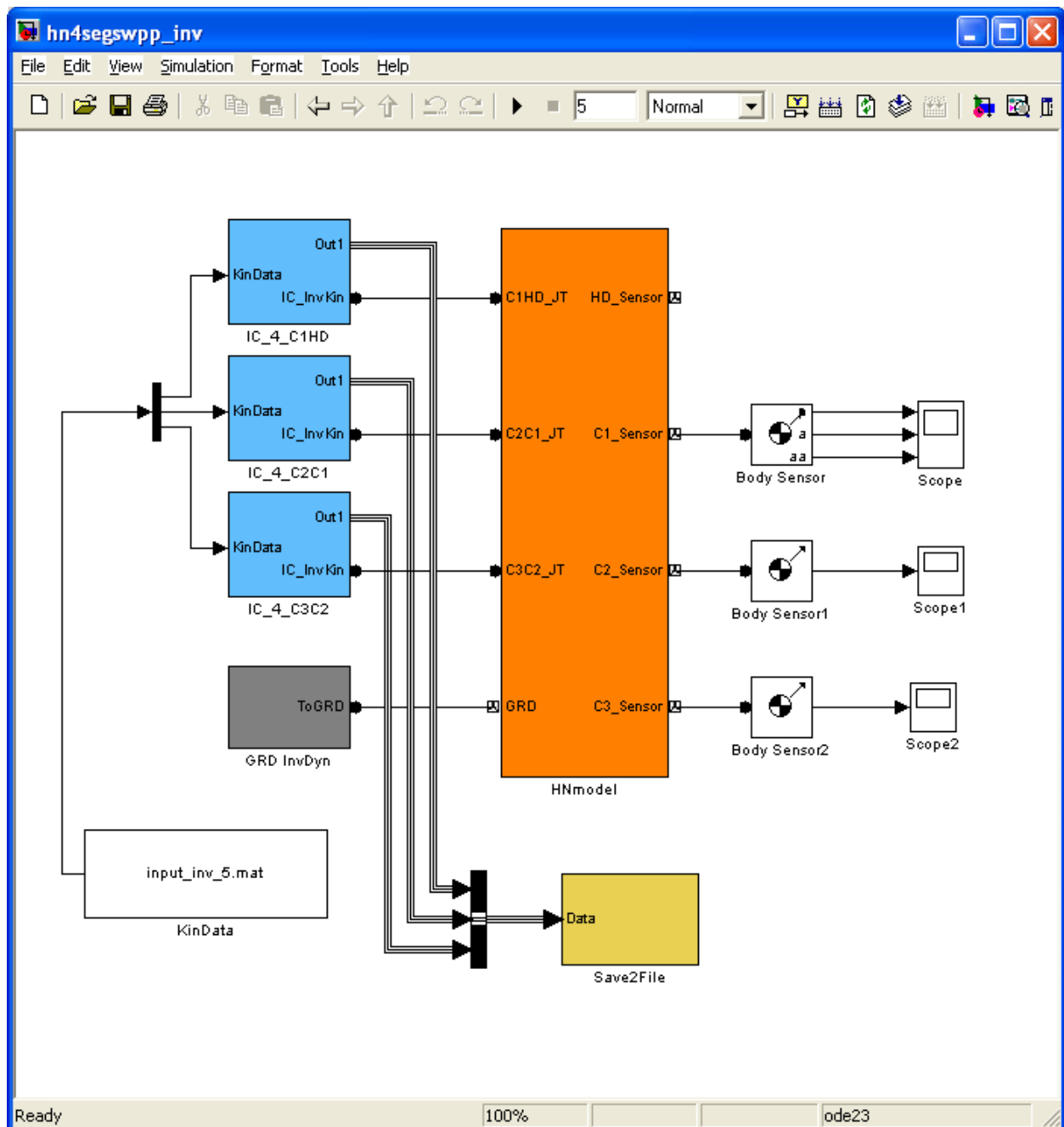
To solve a forward dynamics problem the inertial properties of the body segments must also be known. If muscles are included the activation levels of each muscle as a function of time must be included. If no muscles are included, the joint torques as functions of time must be specified. In addition, any externally applied forces must be specified. Integrating the equations of motion through time gives the motion at each degree of freedom of the model. The advantage of utilizing NMS-Dynamics is its ability to develop and integrate the equations of motion for the user.

3.2 Head-Neck Model: Inverse Problem

3.2.1 *Summary of Previous Work*

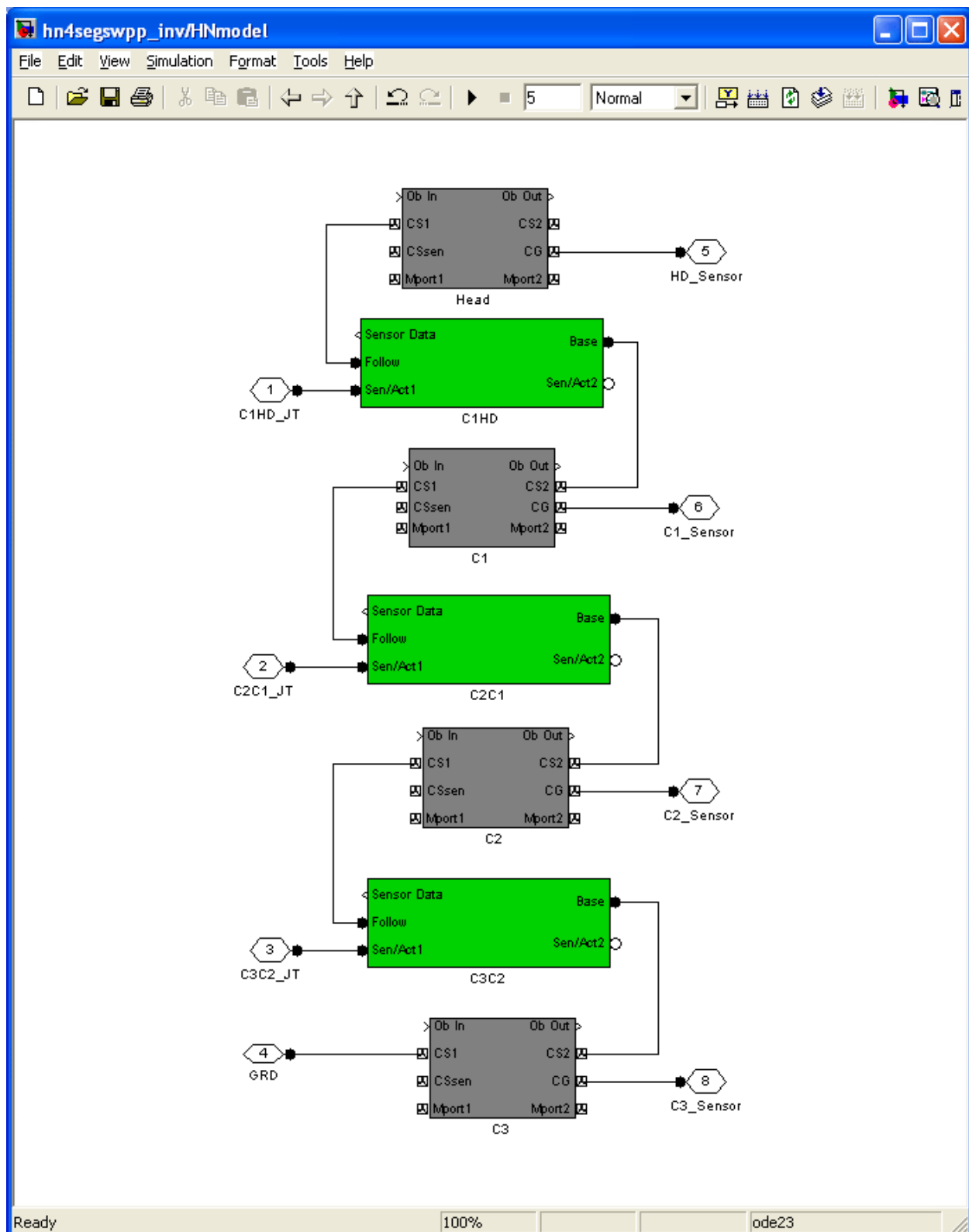
The head-neck model (Figure 3-1) contains rigid bodies representing the head, and the spinal vertebrae of C1, C2, and C3. The joints between each of these segments are planar joints, which allow translation along the X (forward direction) and Y (upward vertical direction) axis, and rotation about the Z (lateral direction) axis. Passive elements at each of the joints provide joint elasticity and viscosity. No muscles are included in this example model, and gravity acts in the $-Y$ direction.

Other elements needed for a complete model include an inertial ground block, blocks to prescribe the motion of each degree of freedom, and a block to save the output data. The model via the C3 segment is connected to the ground block with an in-plane joint, which allows translation along the X and Y axes. For each joint, a motion block (e.g. IC_4_C1HD) prescribes the kinematics for each degree of freedom of the joint. During the simulation, the kinematic data is loaded from a file. The data from the simulation is saved to a file with the aid of the Save2File block. Additionally, sensor blocks are attached to the head-neck model to view the results during the simulation.



(a) HNmodel and related blocks needed to form a complete Head-neck model

Figure 3-1. Head-neck model for inverse analysis



(b) Subcomponents of HNmodel

Figure 3-1. Cont'd

The model parameters are defined in a `passdata.dat` and `segdata.dat` files. The `segdata.dat` file defines the mass, moment of inertia, and the location and rotation of each rigid body relative to the proximally connected body. The `passdata.dat` file defines the equations relating the elastic and viscous properties to the position and velocity for each degree of freedom. The equations can be linear or nonlinear. As the last step before simulating the model, these parameter values from the `.dat` files are loaded and applied to the model.

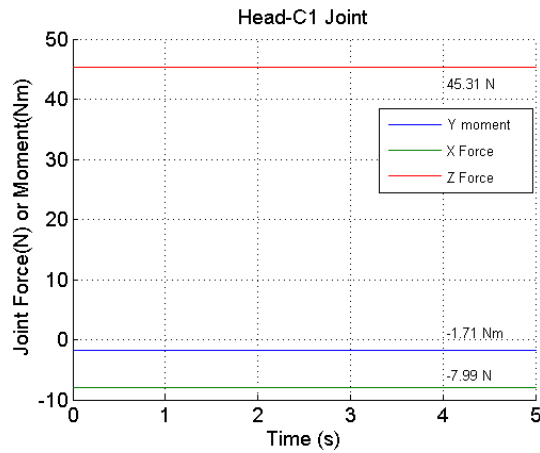
For this inverse dynamics example, the model was simulated while positioned in a static posture. During the simulation, the forces and torques needed at each degree of freedom were calculated so that the model maintained its posture (Table 3-1). The calculated results (Figure 3-2) were then saved to an output file.

Table 3-1. Kinematic Input to Model.

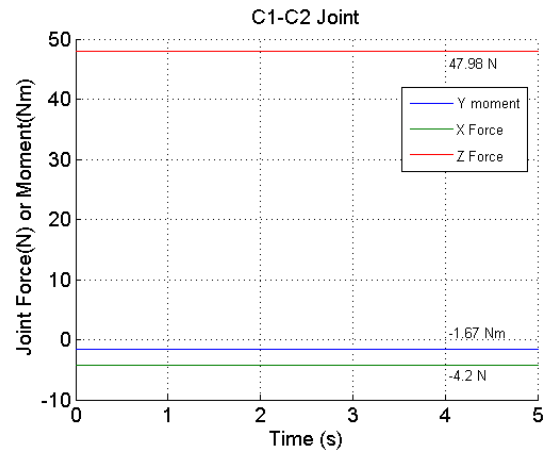
Joint	Rotation about Y-axis Angle (°)	X Position (m)	Z Position (m)
C1 – HD	5	0	0
C2 – C1	5	0	0
C3 – C2	5	0	0

The velocities and accelerations were all set to zero.

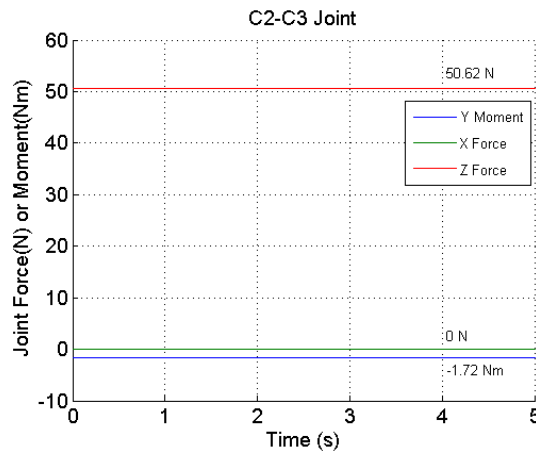
Using NMS-Dynamics, a user is able to rapidly build and simulate models without the need to derive the equations of motion. Through this inverse simulation example, a four segment model was built and simulated. The simulation was able to calculate the necessary forces and moments for the model to hold a static posture.



(a) Head-C1 Joint



(b) C1-C2 Joint



(c) C2-C3 Joint

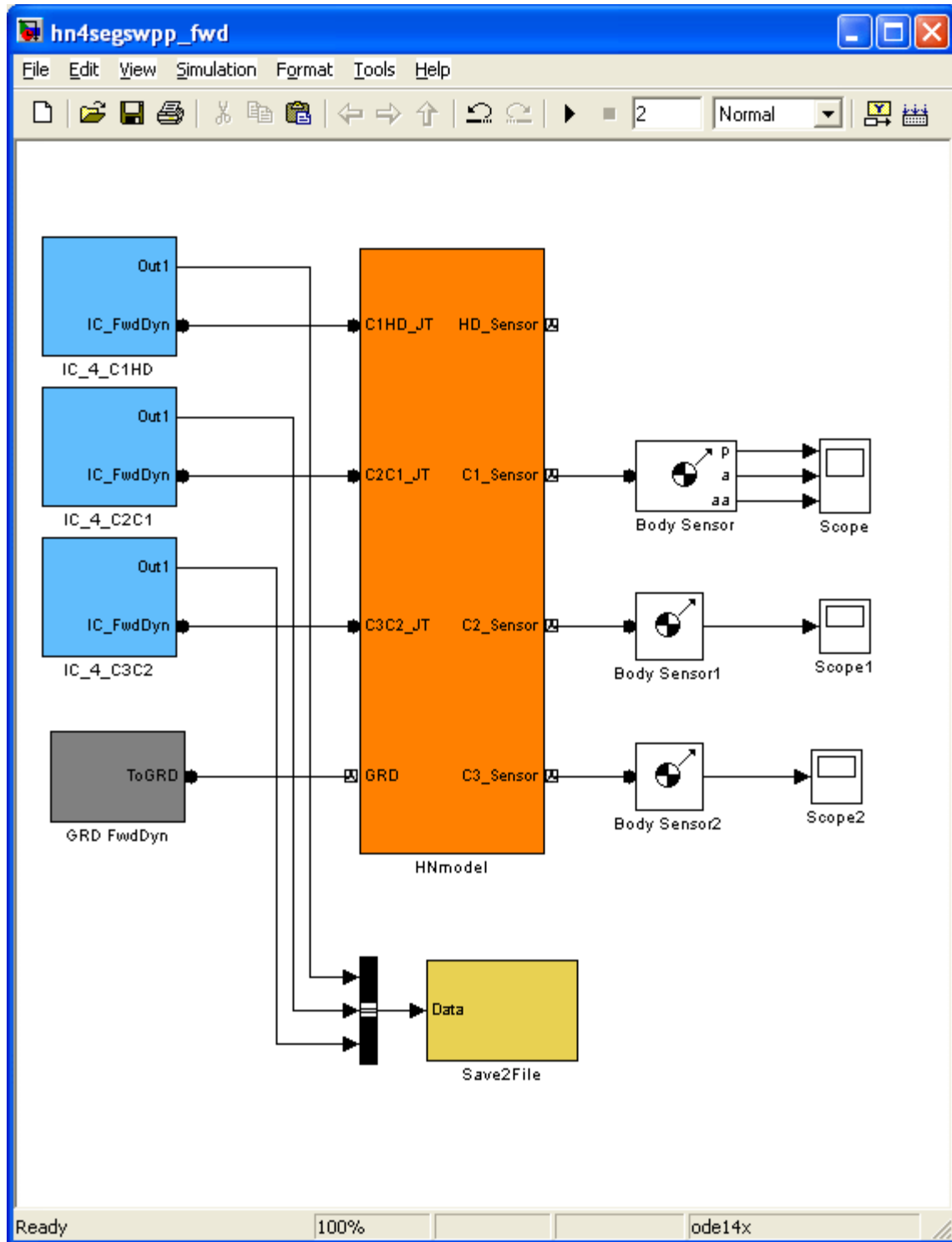
Figure 3-2. Inverse analysis of head-neck model.

Calculated joint forces and moments required to maintain the static posture of the model

3.3 Head-Neck Model: Forward Problem

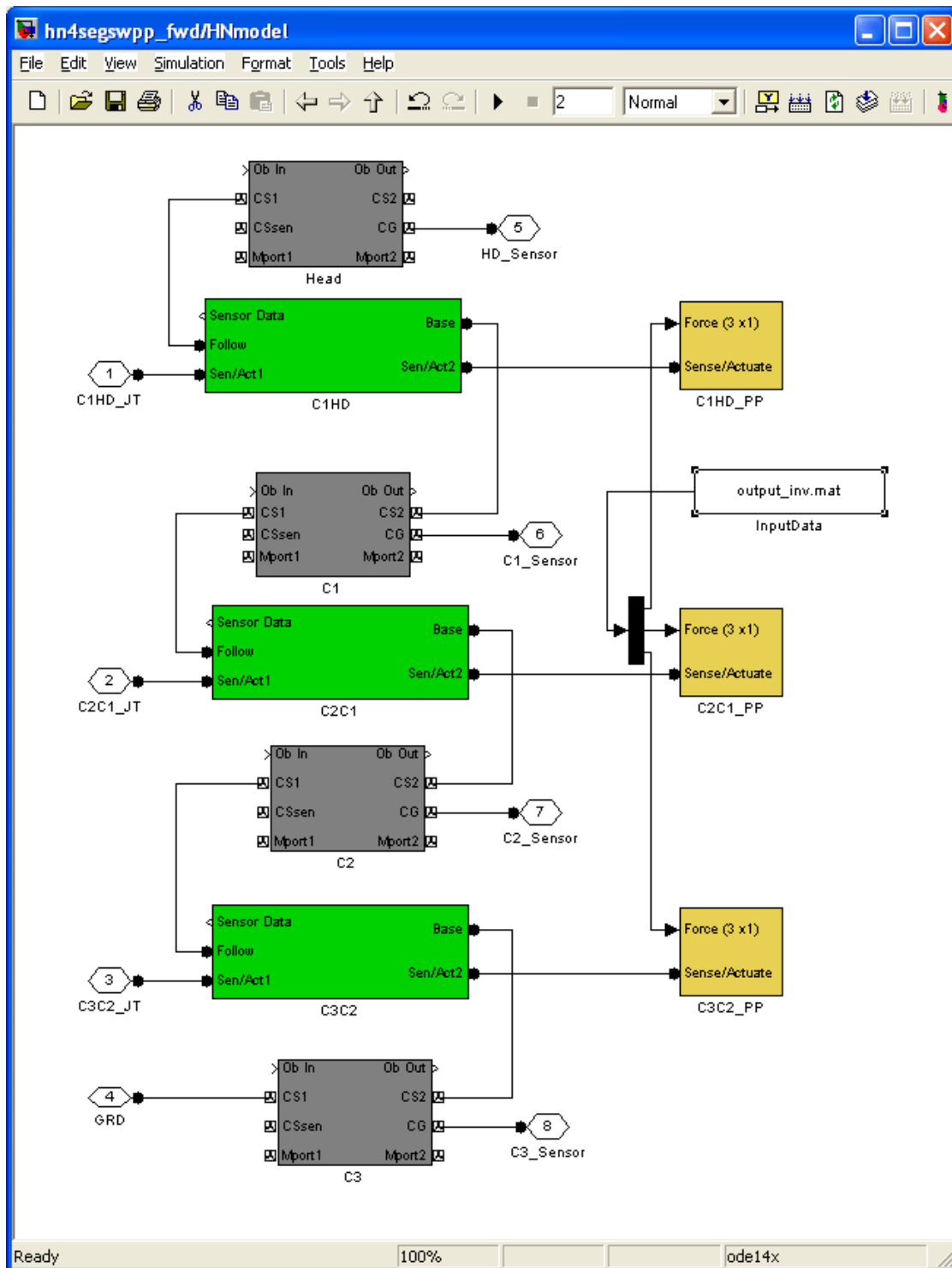
3.3.1 Summary of Previous Work

As with the model described for the inverse analysis, the head-neck model for the forward analysis (Figure 3-3) contains rigid bodies representing the head, and the spinal vertebrae of C1, C2, and C3. The joints between each of these segments are planar joints. Passive elements at each of the joints provide joint elasticity and viscosity and no muscles are included.



(a) HNmodel and related blocks needed to form a complete Head-neck model

Figure 3-3. Head-neck model for forward analysis.



(b) Subcomponents of HNmodel

Figure 3-3. Cont'd

Similar to the inverse analysis model, an inertial ground block and a block to save the output data are included. The difference with the forward model is that the blocks which prescribed the joint motions have been removed. Those blocks have been replaced with blocks (e.g. IC_4_C1HD) which prescribe the joint forces and moments.

To initialize the model parameters and prepare the model for simulation, a function is executed to load the parameter values from the appropriate .dat files and apply them to the model. The applied joint forces and moments are used by the simulation at each time step to determine the joint angle and position trajectories.

For the forward dynamics example, the model was simulated with constant joint forces and moments (Table 3-2). During the simulation, the resulting joint trajectories were calculated (Figure 3-4) are then saved to an output file.

Table 3-2. Force and Moment Inputs to the Model

Joint	Y Moment (Nm)	X Force (N)	Z Force (N)
C1 – HD	-1.71	-7.99	45.31
C2 – C1	-1.67	-4.20	47.98
C3 – C2	-1.72	0.00	50.62

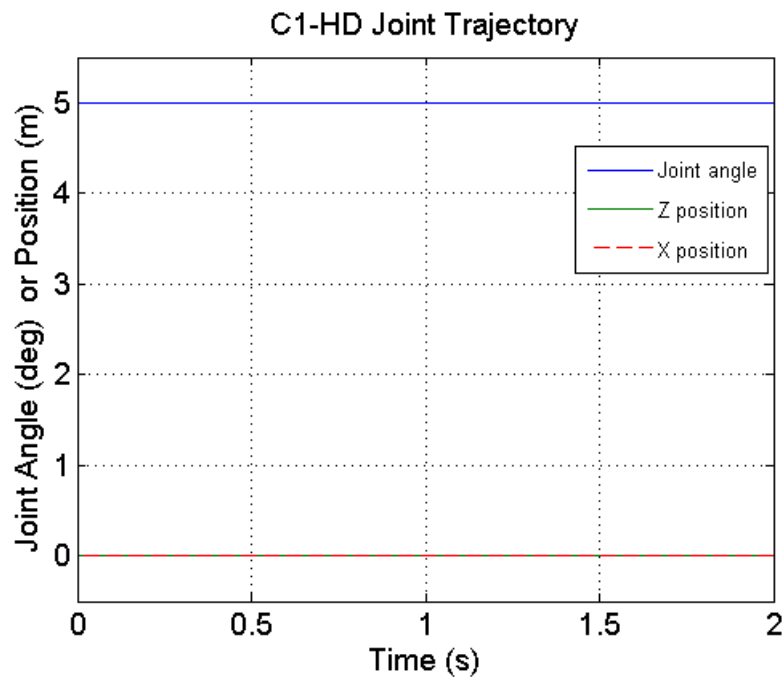


Figure 3-4. Calculated joint trajectories.

The initial position of the model was the same as the inverse problem example. Therefore if the same forces and moments calculated from the inverse problem were applied in the forward problem the model should remain stationary, which the results show. This illustrates how the NMS-Dynamics toolbox can solve a forward dynamics problem to determine the trajectory of a model across time.

3.4 Lower Extremity Model: Inverse Problem

3.4.1 Model Building

During the current year, a lower extremity model was developed, which included the thigh, shank, and foot segments of a single leg. At the hip joint a 5 DOF joint was employed (3 DOF for linear movements, 1 DOF for flexion and extension, and 1 DOF for adduction and abduction). The knee was a hinge joint with 1 DOF for flexion and extension. The ankle had 1 DOF for plantar flexion and dorsiflexion. The input signals to the model included the ground reaction forces applied to the foot, joint angle kinematics applied at each joint and planar kinematics applied at the hip joint. The outputs calculated included the reaction forces and moments at each joint.

The data for the ground reaction forces (GRFs) and joint kinematics were measured during an experiment that involved subjects wearing different types of boots and loads on their back while walking. The ground reaction forces were measured by a force platform. Markers placed on the subject provided the joint kinematics. The measurements contained information for one walking stride.

Once the model was built, the toolbox engine determined the equations of motion and solved them during the simulation. Some of the results from simulating the model are included in the figures below (Figure 3-5 and Figure 3-6). The first figure (Figure 3-5) shows the reaction forces at the ankle joint (+x, forward direction; +y, lateral direction; +z, upward direction). The largest force is in the z-direction which corresponds to the force needed to support the body weight. The second largest force is in the x-direction which corresponds to the breaking and propulsion of the body as it moves forward. Lastly, the y-direction has the smallest force values, because the body acceleration in this direction while walking forward is the smallest.

The second figure (Figure 3-6) shows the ground reaction force in the upward vertical direction (+z-direction) along with the reaction force at the ankle in the z-direction and the force of gravity on the foot. Since the foot is a rigid body between the ankle and the ground, the reaction force at the ankle can be calculated with the following equation:

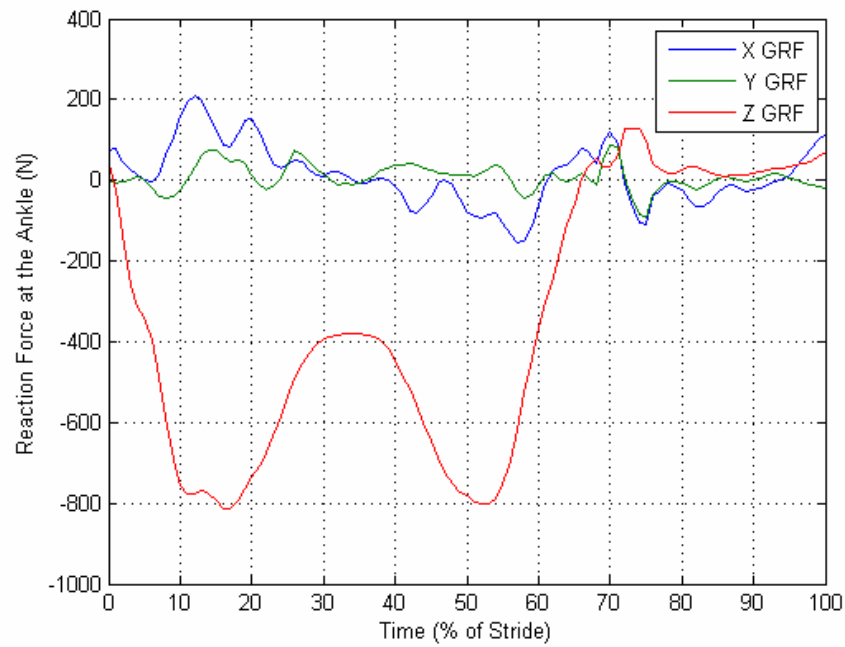


Figure 3-5. Reaction forces at the ankle.

The +x-direction is forward, +y-direction is lateral, and +z-direction is upward.

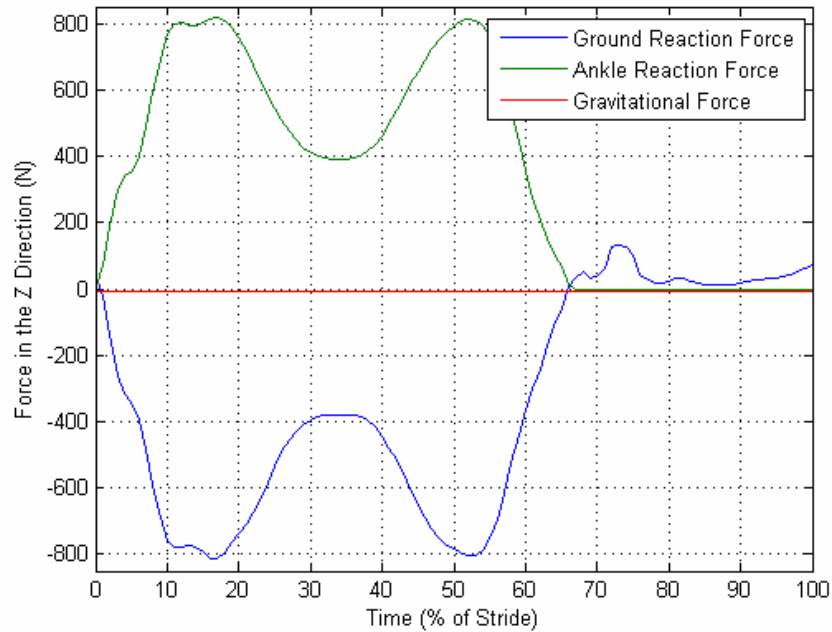


Figure 3-6. Foot forces. Ground reaction force at the foot, reaction force at the ankle, and gravitational force on the foot.

Forces shown are in the z-direction.

$$F_{grf} + F_{ankle} + F_{gravity} = m_{foot} \times a_{foot}$$

where F_{grf} = ground reaction force at the foot (N)
 F_{ankle} = reaction force at the ankle (N)
 $F_{gravity}$ = force of gravity due to mass of the foot (N)
 m_{foot} = mass of the foot (kg)
 a_{foot} = acceleration of foot COM (m/s²)

Therefore as a simple check of the model setup, the GRF, the ankle joint reaction force, and the force of gravity on the foot were added and the sum divided by the acceleration of the foot. The result was equal to the mass of the foot, which indicates the model was setup properly and was calculating the reaction force correctly.

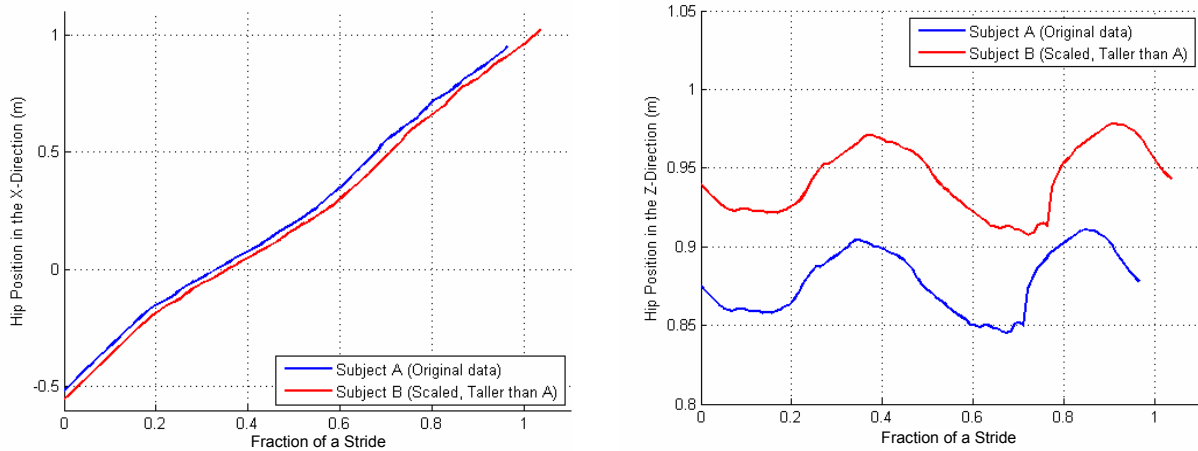
3.4.2 *Scaling Subject Data*

By being able to scale the kinematic and GRF data by the subject's anthropometry and the properties of the movement, estimates about joint forces and moments can be computed without putting the individual through a laboratory protocol. This ability is very advantageous because recruiting subjects is always a difficult task. Additionally, with a good model many more simulated experiments can be performed, and experiments not possible in the laboratory or ethically feasible can be simulated.

For scaling data from one subject to another subject, it was assumed that the subject anthropometry fell within the 50th percentile male. Scaling data from one subject (Subject A) to another subject (Subject B) was based on the anthropometry of the two subjects. Segment lengths and masses were calculated based on tables from the literature (Contini, 1972; Dempster, 1955). Kinematic data were scaled based on the height ratio of the subjects, and the ground reaction force data were scaled based on the height and body weight ratios of the two subjects.

To scale kinematic data, a scaling factor was first determined by dividing the height of Subject B by the height of Subject A. For the linear kinematic data of the hip, the velocity of Subject B needed to be equal to the velocity of Subject A for any given point within a stride. However with a height difference between the subjects, the stride length of Subject B would be longer or shorter depending on whether Subject B was taller or shorter than Subject A. Therefore to maintain the same velocity, the length of time needed to complete a stride for Subject B also needed to change. The time per stride for Subject A was multiplied by the scaling factor to determine the time per stride for Subject B. Similarly the position data for Subject A were multiplied by the scaling factor to determine the position data for

subject B (Figure 3-7). Since the velocity magnitudes were the same between subjects, the acceleration magnitudes also remained the same. The only change for the velocity and acceleration curves was the amount of time between data points, which changed by the scaling factor multiple.



(a) Scaling of hip position data (x-direction) (b) Scaling of hip position data (z-direction)

Figure 3-7. Example of scaling kinematic data.

Data for Subject B was calculated by scaling the data of Subject A.
Subject B is taller and heavier than Subject A.

For the angular kinematic data, the scaling process was similar, however the angular position data needed to remain equal between the Subject A (the given subject) and Subject B (the scaled subject). The angular velocities of Subject B were determined by multiplying the angular velocities of Subject A by one over the scaling factor; therefore if subject B was taller than Subject A, the angular velocities of Subject B would be smaller than those of Subject A. Consequently, subject B would have a longer stride, but a lower stride frequency so that the overall horizontal velocity of the subjects would be equal.

To scale the ground reaction forces, equations from the literature (Borghese et al., 1996; Cavanagh and Williams, 1979; Dufek et al., 1990; Hamill et al., 1984; Hamill and Bense, 1996; Himann et al., 1988; Kinoshita, 1985; Martin and Marsh, 1992; McCrory et al., 2001; Nilsson and Thorstensson, 1989; Powers et al., 1999; Simpson and Jiang, 1999; White et al., 1998; Woodmansee et al., 2004) were utilized. The equations calculate the peak braking and propulsion forces (X-direction), and the two peak vertical forces (Z-direction). These equations calculate the forces based on the velocity of movement and the body weight of the subject. Therefore to calculate the scaled ground reaction force data, the ground reaction force curves from Subject A were scaled so that the peaks of the vertical

forces, and the propulsion and braking forces matched the forces calculated by the equations. In addition the curves were stretched or compressed in time to match the new scaled time per stride (Figure 3-8).

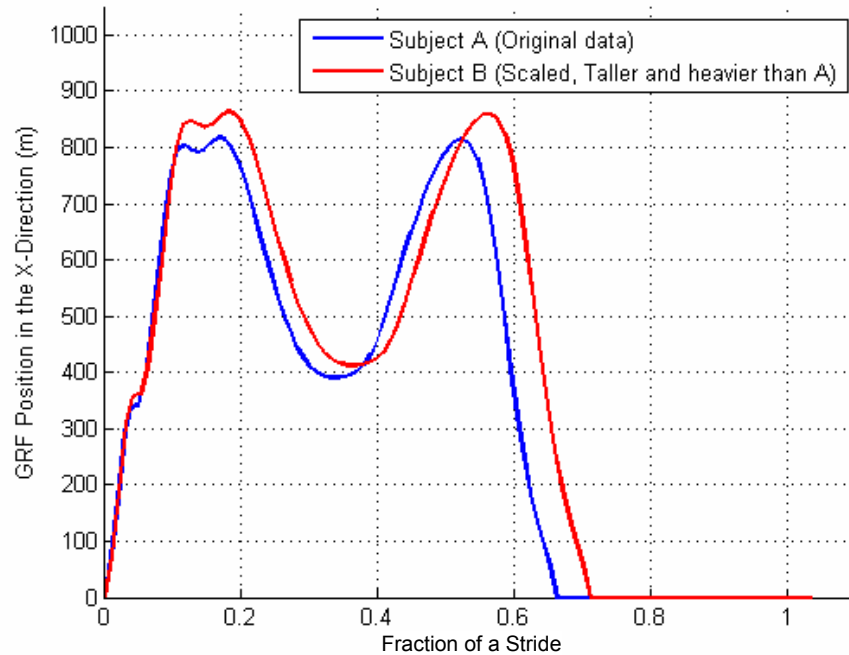


Figure 3-8. Example of scaling ground reaction force data.

Subject B data was calculated by scaling Subject A data.
Subject B is taller and heavier than Subject A.

Being able to scale the model and associated data was a significant improvement to the capabilities of the toolbox. With this ability, researchers will be able to simulate many more subjects and many more scenarios than they could perform through traditional experimental protocols in a laboratory.

4. Development of Application Interfaces

The previous section described the process used to build models for inverse and forward analysis. In this section, developing a graphical user interface (GUI) for the model will be explained. Utilizing the lower extremity and head-neck models discussed in the above sections, the objective of developing the interface, the interface layout, and an example of stepping through the interface will be described.

4.1 Objective

A desktop application was developed for accessing the models developed with the NMS-Dynamics toolbox. The objective of the application was twofold. First the application would provide an interface to the lower extremity and head-neck models for simulating various scenarios. Secondly, the application interface would provide a user-friendly way to access the models.

4.2 Layout and Development

For the application, a simple layout which stepped the user through the program was designed (Figure 4-1). The layout is divided into a number of steps. Initially the user is given the choice of loading a previous simulation project or starting a new one. For a new project, the next step is for the user to decide which model to use, and the file name and location for their simulation project. The user can also provide a project description for later reference. Then the user moves to the next step where the specific model parameters are set and the simulation is started. In the final step the user can graphically plot results from the simulation.

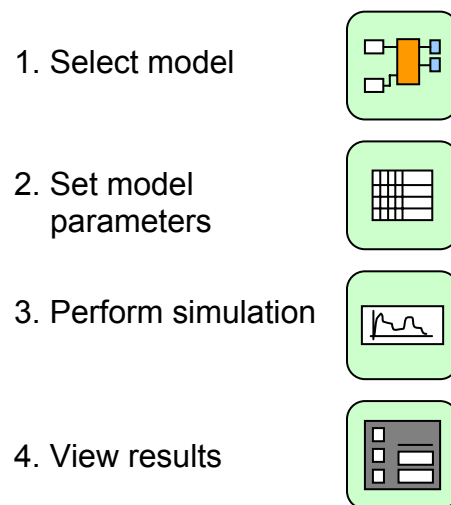


Figure 4-1. Outline of steps involved with the NSM-Dynamics Analysis application

The application interface was developed to provide the user a quick and easy method for running simulations. The ability to save simulation projects allows the user to perform and compare different simulation scenarios. The step-by-step process helps the user setup the simulation properly, and the plots give the user immediate feedback about the results.

4.3 User Interface

Illustrations of the application interface are presented to show its current standing. The first figure (Figure 4-2) shows the welcome screen to the NMS-Dynamics Analysis 1.0

application. On the welcome screen, a description of the application and its capabilities are given. From this screen a user can exit the program, load a previous project, or start a new project.

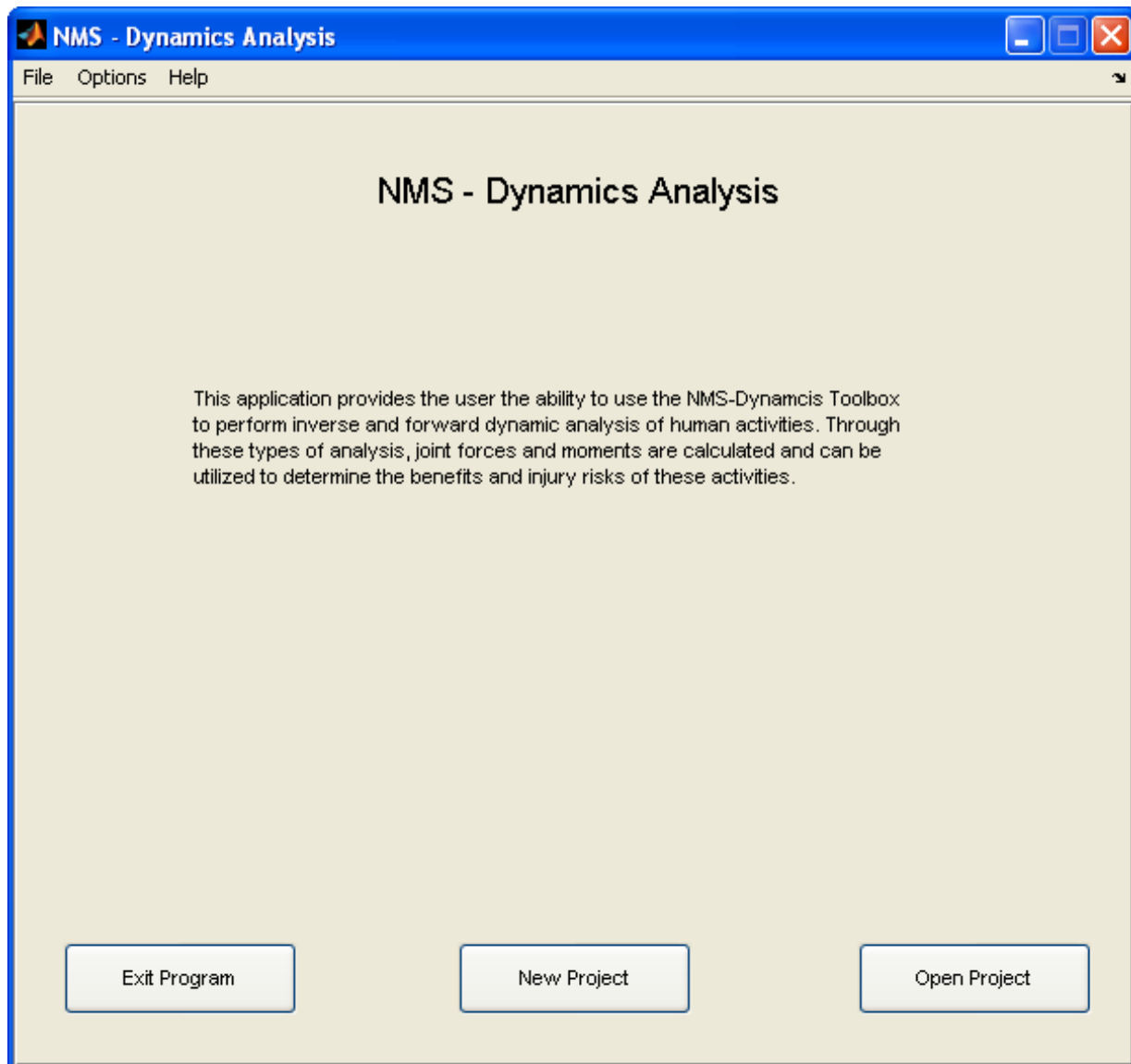


Figure 4-2. Welcome screen

When a new project is selected, the user is taken to a screen (Figure 4-3) where they select the model to simulate, determine the name of the project, and set the location for saving the results. A project description box is provided so that the user can describe their project for future reference.

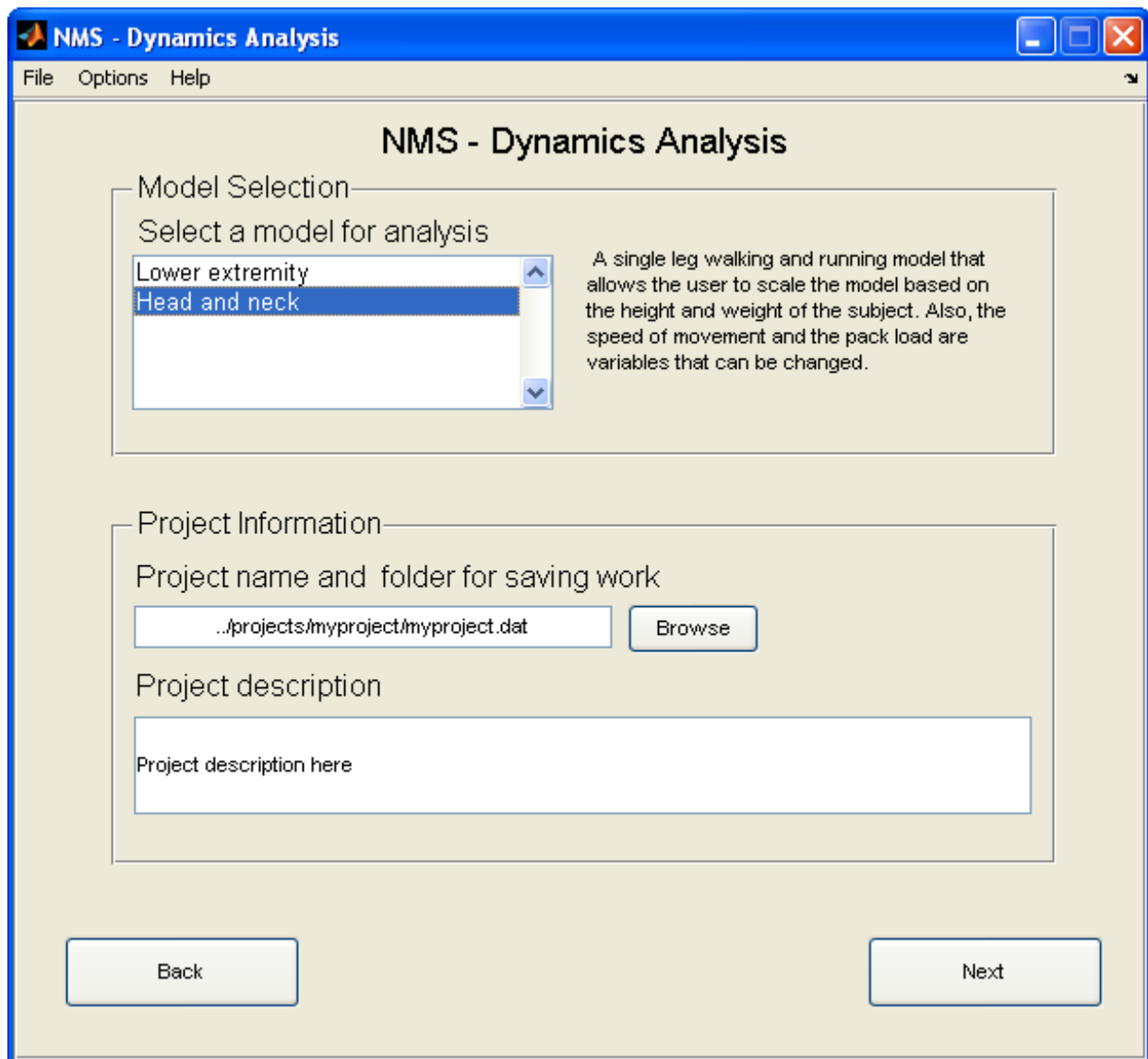


Figure 4-3. Project configuration screen

After selecting the model and setting the file and directory information the user is moved to the next screen to specify the model parameters (Figure 4-4). At the top of the screen, the project file name is displayed along with the project description. Below that information, parameters specific to the model are presented for tuning. For example, the helmet mass for the subject can be set for the head-neck model. The simulation begins when the Run Analysis button is pressed.

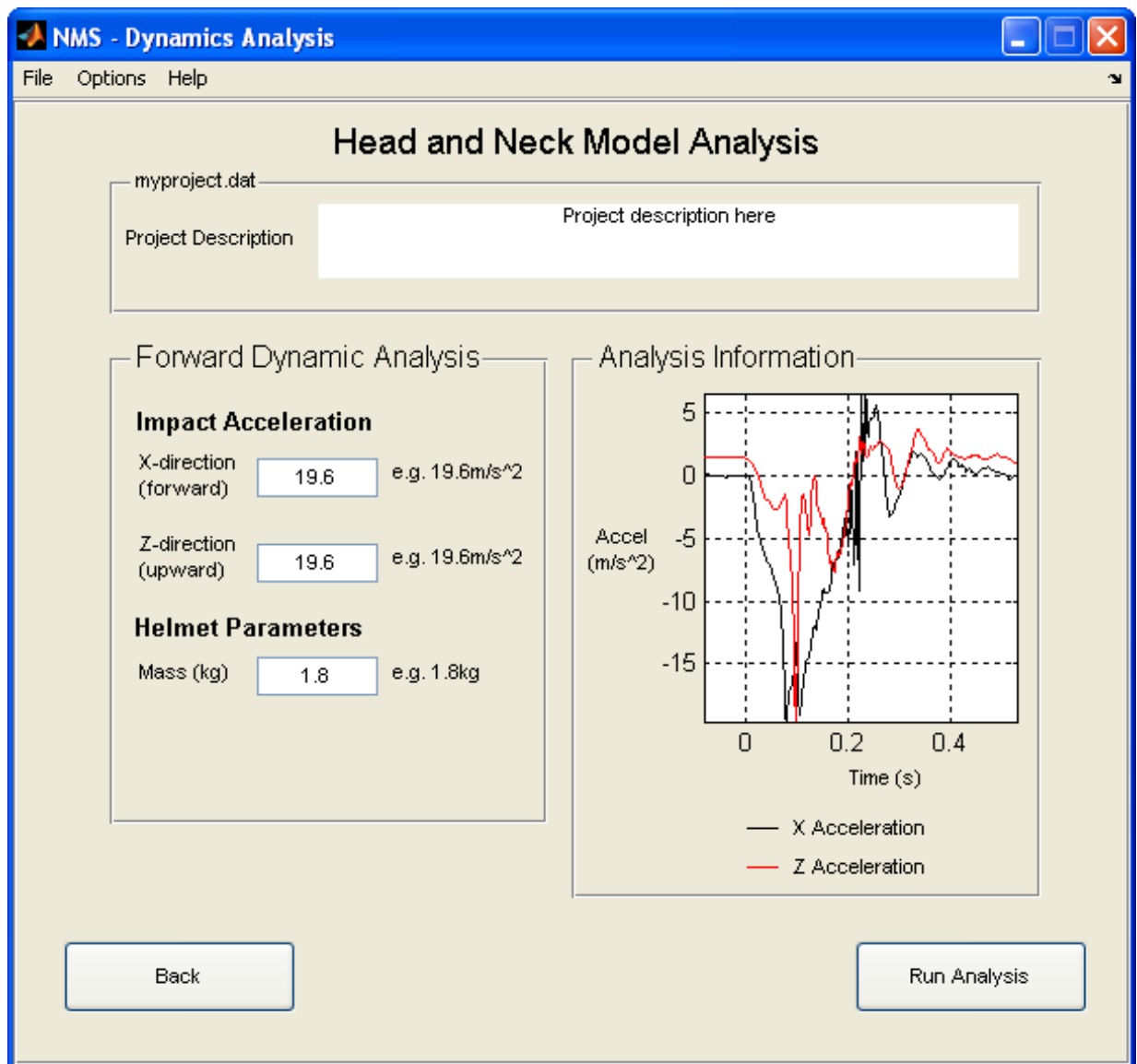


Figure 4-4. Model specific screen to set parameters

When the simulation is complete the results screen specific to the model is shown (Figure 4-5). The user can use this screen to generate some basic plots of the results. The results are saved to the folder designated earlier by the user so that the data can be further examined by the user.

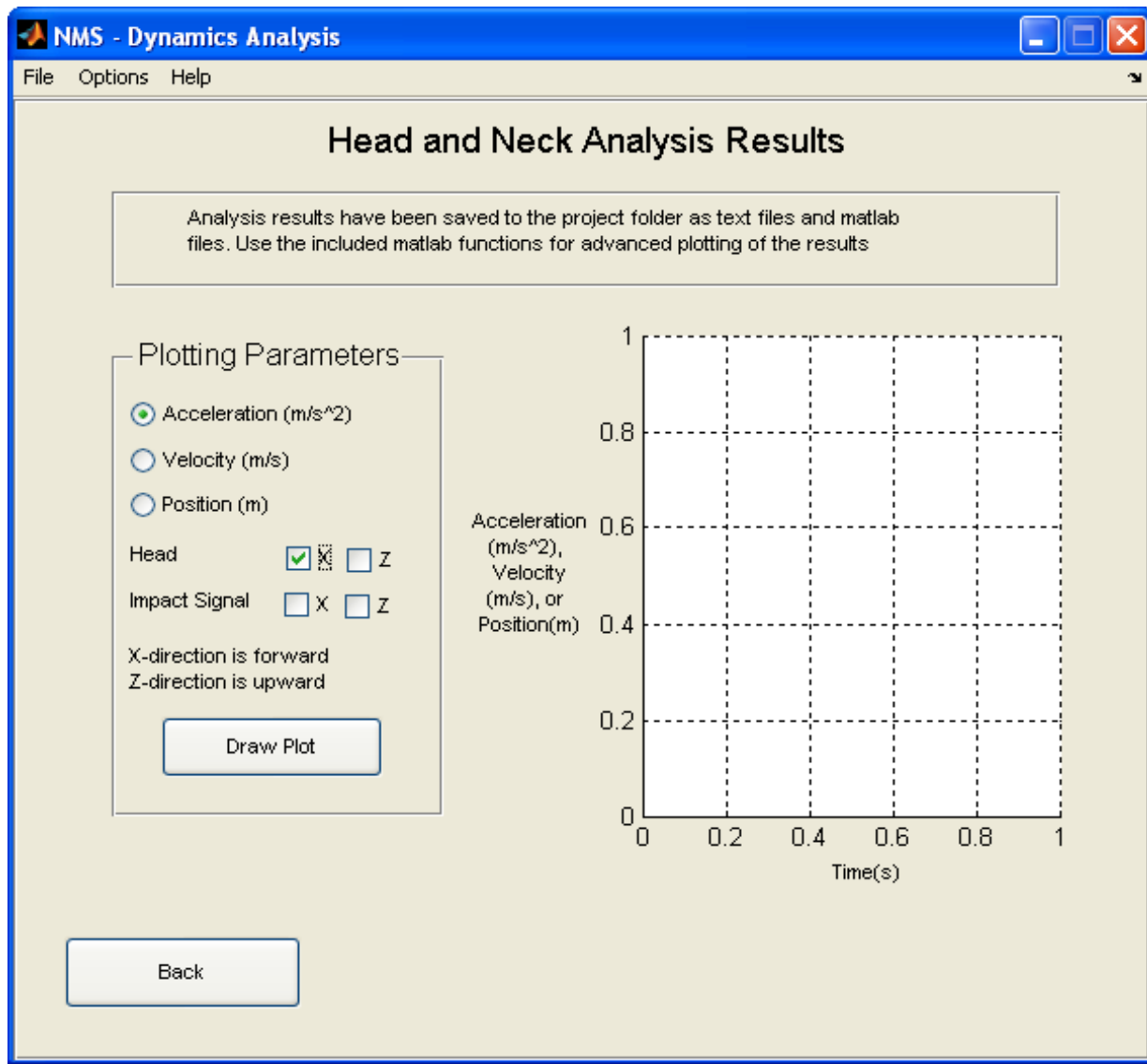


Figure 4-5. Model specific screen to display results

Additional features of the application include a file menu at the top of the screen. This menu allows the user to easily exit the program, open projects, and start a new project. Under the options menu, the default save directory for the result data can also be set.

5. Summary

5.1 Current Year Progress

In the Introduction section, the objectives for the current year were outlined. The first objective was to develop the ability to deploy a model as a standalone application. This objective was accomplished by compiling the model into an executable program and developing a graphical user interface to interact with the program. The second objective entailed developing a scaling method to estimate the kinematic and ground reaction force data of a subject based on that data from another subject. To scale the data needed for the calculations, regression equations from the literature were employed. The last objective was to improve the flexibility of the model building code by removing hard coded values and special case programming. The model building process was streamlined and is now a more efficient and robust process.

5.2 Accomplishments

The objective of this current version of the NMS-Dynamics toolbox was to develop a set of basic tools that would allow one to rapidly build biomechanical models. To do this we have developed a basic set of elements to accomplish this task. The elements include a rigid body, a planar joint, viscoelastic joint properties, and a muscle model (Appendix A). Through the examples it was shown that the toolbox can solve inverse and forward analysis problems.

6. References

- Borghese, N. A., Bianchi, L., Lacquaniti, F., (1996). Kinematic determinants of human locomotion. *Journal of Physiology* 494, 863-79.
- Cavanagh, P. R., Williams, K. R., (1979). A comparison of ground reaction forces during walking barefoot and in shoes. *Biomechanics VII*. University Park Press, Baltimore, pp. 151-156.
- Contini, R., (1972). Body Segment Parameters, Part II. *Artificial Limbs* 16, 1-19.
- Dempster, W. T., (1955). *Space Requirements of the Seated Operator*. US Air Force, Wright-Patterson Air Force Base, OH.
- Dufek, J., Schot, P., Bates, B., (1990). Dynamic lower extremity evaluation of males and females during walking and running. *Journal of Human Movement Studies* 18, 159-175.
- Hamill, J., Bates, B. T., Knutzen, K. M., (1984). Ground reaction force symmetry during walking and running. *Research Quarterly For Exercise and Sport* 55, 289-293.
- Hamill, J., Bense, C. K., (1996). *Biomechanical Analysis of Military Boots: Phase II Volume II Human User Testing of Military and Commercial Footwear*. University of Massachusetts at Amherst, Amherst, MA.
- Himann, J. E., Cunningham, D. A., Rechnitzer, P. A., Paterson, D. H., (1988). Age-related changes in speed of walking. *Medicine and Science in Sports and Exercise* 20, 161-6.
- Kinoshita, H., (1985). Effects of different loads and carrying systems on selected biomechanical parameters describing walking gait. *Ergonomics* 28, 1347-62.
- Martin, P. E., Marsh, A. P., (1992). Step length and frequency effects on ground reaction forces during walking. *Journal of Biomechanics* 25, 1237-9.
- McCrory, J. L., White, S. C., Lifeso, R. M., (2001). Vertical ground reaction forces: objective measures of gait following hip arthroplasty. *Gait and Posture* 14, 104-9.
- Nilsson, J., Thorstensson, A., (1989). Ground reaction forces at different speeds of human walking and running. *Acta Physiologica Scandinavica* 136, 217-27.
- Powers, C. M., Heino, J. G., Rao, S., Perry, J., (1999). The influence of patellofemoral pain on lower limb loading during gait. *Clinical Biomechanics (Bristol, Avon)* 14, 722-8.
- Simpson, K. J., Jiang, P., (1999). Foot landing position during gait influences ground reaction forces. *Clinical Biomechanics (Bristol, Avon)* 14, 396-402.
- White, S. C., Yack, H. J., Tucker, C. A., Lin, H. Y., (1998). Comparison of vertical ground reaction forces during overground and treadmill walking. *Medicine and Science in Sports and Exercise* 30, 1537-42.
- Woodmansee, M. W., Sih, B. L., Shen, W., Niu, E., (2004). *Bone Overuse Injury Assessment Model: Annual Report*. Simulation, Engineering, and Testing Group, Jaycor Inc., San Diego, CA

Appendix A. NMS-Dynamics Model Components

A.1 Segments

The rigid body block (Figure A-1) can be used to represent a body such as a bone. The block contains a mass and inertia parameter. Each segment also has two muscle ports (MPort1 and MPort2) for attaching muscles. More muscles can be attached thorough the use of a mechanical branching bar. The segment can be connected to a joint block through the CS1 and CS2 ports. CS1 is a coordinate system with its location defined relative to the adjoining segment. CG is the center of gravity of the segment with its location defined relative to CS1. CS2 is another coordinate system with is location defined with respect to CS1. CSsen, which can be used for attaching a body sensor, is another coordinate system with its location defined with respect to CS1. To ensure muscles wrap over the segments properly, obstacle points can be input to the block and then passed through to the attached muscle.

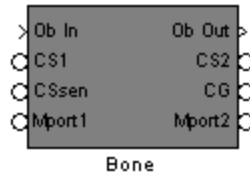


Figure A-1. Rigid body.

A.2 Joints

The planar joint block (Figure A-2) allows for rotation about one axis and translations along the other two axes. The user can specify which axis rotates and which axes translate. The joint has two Sensor/Actuator ports which allow measuring or applying moments/forces or rotations/displacements to the joint. Sensor data including position, velocity, and reaction force/moment are output through the Sensor Data port.



Figure A-2. Planar joint.

A.3 Passive Elements

A.3.1 Spring and Damper Parallel (1 DOF)

The Parallel Spring and Damper block (Figure A-3) models a single elastic element in parallel with a single viscous element. Therefore it only outputs a force/moment signal for 1 degree of freedom (DOF). The equation for each element is defined by the user and can be nonlinear. This block attaches to the Sensor/Actuator port of a joint block which provides the joint position and velocity information needed for the calculation.

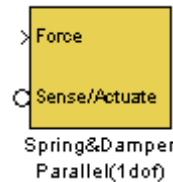


Figure A-3. Parallel spring and damper (1 DOF).

A.3.2 Spring and Damper Parallel (3 DOF)

This block (Figure A-4) contains 3 sets of parallel elastic and viscous elements. This allows one to add passive properties to the Planar Joint block without combining 3 single DOF blocks. It attaches to the Sensor/Actuator port.

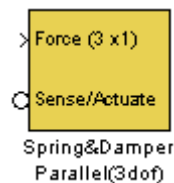


Figure A-4. Parallel spring and damper (3 DOF).

A.3.3 Spring and Damper Series (1 DOF)

The spring and damper in series block (Figure A-5) has a single elastic element in series with a viscous element. Consequently it only provides force/moment data for 1 DOF. The equation for each element is linear and is defined by the user. It attaches to the Sensor/Actuator port on a joint block.

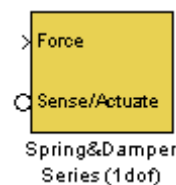


Figure A-5. Series spring and damper (1 DOF).

A.4 Active Elements

The muscle block (Figure A-6) calculates the force generated by the muscle for a given length and activation. It then applies that force to the two segments connected by the muscle. The Base and Follower ports connect to the Muscle ports of two segments. The musculotendon force and length are outputted for debugging purposes. This muscle block also has the ability to wrap itself over one cylindrical obstacle. The location, orientation, and reference frame of the obstacle are input through the Ob data port.

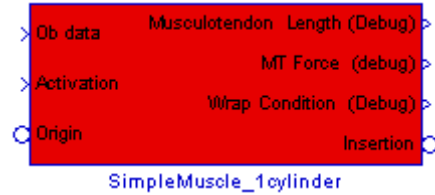


Figure A-6. Muscle.



communications

Applied Technologies

OVERUSE INJURY ASSESSMENT MODEL

Part V: Mobile Biomechanical Measuring System

FINAL REPORT

Report No. J3181-07-339
for period February 22, 2002 – February 21, 2007
under Contract No. DAMD17-02-C-0073

Prepared by:

Weixin Shen, Ph.D.
Kofi Amankwah, Ph.D.
Eugene Niu, Ph.D.
Jonathan Zhang.
L-3 Communications/Jaycor
3394 Carmel Mountain Road
San Diego, California 92121-1002

Prepared for:

Commander
U.S. Army Medical Research and Materiel Command
504 Scott Street
Fort Detrick, Maryland 21702-5012

August 2007

REPORT DOCUMENTATION PAGE				Form Approved OMB No. 0704-0188	
Public reporting burden for this collection of information is estimated to average 1 hour per response, including the time for reviewing instructions, searching existing data sources, gathering and maintaining the data needed, and completing and reviewing this collection of information. Send comments regarding this burden estimate or any other aspect of this collection of information, including suggestions for reducing this burden to Department of Defense, Washington Headquarters Services, Directorate for Information Operations and Reports (0704-0188), 1215 Jefferson Davis Highway, Suite 1204, Arlington, VA 22202-4302. Respondents should be aware that notwithstanding any other provision of law, no person shall be subject to any penalty for failing to comply with a collection of information if it does not display a currently valid OMB control number. PLEASE DO NOT RETURN YOUR FORM TO THE ABOVE ADDRESS.					
1. REPORT DATE (DD-MM-YYYY) 08-20-2007		2. REPORT TYPE Final Report		3. DATES COVERED (From - To) Feb. 2002 - Feb. 2007	
4. TITLE AND SUBTITLE Overuse Injury Assessment Model, Part V: Mobile Biomechanical Measuring System				5a. CONTRACT NUMBER DAMD17-02-C0073	
				5b. GRANT NUMBER	
				5c. PROGRAM ELEMENT NUMBER	
6. AUTHOR(S) Weixin Shen Kofi Amankwah				5d. PROJECT NUMBER 3181	
				5e. TASK NUMBER	
				5f. WORK UNIT NUMBER	
7. PERFORMING ORGANIZATION NAME(S) AND ADDRESS(ES) L-3 Communications/Jaycor 3394 Carmel Mountain Road San Diego, CA 92121				8. PERFORMING ORGANIZATION REPORT NUMBER J3181-07-339	
9. SPONSORING / MONITORING AGENCY NAME(S) AND ADDRESS(ES) U.S. Army Medical Research Acquisition Activity Director 820 Chandler Street Fort Detrick, MD 21702-5014				10. SPONSOR/MONITOR'S ACRONYM(S) USAMRAA	
				11. SPONSOR/MONITOR'S REPORT NUMBER(S)	
12. DISTRIBUTION / AVAILABILITY STATEMENT					
13. SUPPLEMENTARY NOTES					
14. ABSTRACT We developed a prototype M-TES DataLogger system that integrated accelerometers and force sensors onto a commercial off-the-shelf (COTS) wireless sensor network (WSN) platform and implemented onboard data compression and fusing codes to record biomechanical data on a wearable data logger. Analysis algorithms were developed and implemented in companion M-TES Analyzer software that determines from measurements the biomechanical parameters for walking, running, and jumping activities. These products could provide accurate logging of training regime and intensity that in turn would significantly improve the prediction accuracy of performance and injury outcomes of military physical training.					
15. SUBJECT TERMS biomechanical measurements, wireless sensors, data logger, gait analysis					
16. SECURITY CLASSIFICATION OF:			17. LIMITATION OF ABSTRACT UNLIMITED	18. NUMBER OF PAGES 63	19a. NAME OF RESPONSIBLE PERSON Blossom Widder
a. REPORT UNCLASSIFIED	b. ABSTRACT UNCLASSIFIED	c. THIS PAGE UNCLASSIFIED			19b. TELEPHONE NUMBER (include area code) (301) 619-7143

Executive Summary

The predictive accuracy of training outcomes is significantly limited by the lack of accuracy in field data, especially the accurate logging of training regime and intensity. This issue needs to be addressed by providing ambulatory, unobtrusive instruments that are capable of acquiring biomechanical measurements at a resolution sufficient enough for distinguishing different exercise modality and changes in locomotion patterns due to individual variations or changes in individual physical status. In this research, we developed a prototype instrument M-TES DataLogger system that integrated accelerometers and force sensors onto a commercial off-the-shelf (COTS) wireless sensor network (WSN) platform and implemented onboard data compression and fusing codes to record biomechanical data on a wearable data logger. Analysis algorithms were implemented in companion software, M-TES Analyzer, which estimates from the measurements the biomechanical parameters for walking, running, and jumping activities.

Contents

	<u>Page</u>
EXECUTIVE SUMMARY	ES-1
1. INTRODUCTION	1
2. M-TES 1.0 SYSTEM	3
2.1 M-TES 1.0 SYSTEM CONFIGURATION	3
2.1.1 Overview	3
2.1.2 Challenges	3
2.2 M-TES HARDWARE: SENSORS AND BASE STATION	4
2.2.1 Motes and Wireless Sensor Network.....	4
2.2.2 Accelerometers and Force Sensors.....	6
2.2.3 Base Station	7
2.3 M-TES SOFTWARE: ANALYZER 1.0.....	8
2.3.1 Data Storage.....	8
2.3.2 Activity classifications	9
3. SAMPLE RESULTS	13
3.1 DESCRIPTION OF TESTS (WALK, RUN, JUMP).....	13
3.2 TIME TRACE MEASUREMENTS	13
3.3 ACCURACY IN BIOMECHANICAL PARAMETERS	14
3.3.1 Activity characterization – how to determine walk/run/jump	14
3.3.2 Parameters determination (step length, velocity, jump height, ...).....	14
4. SUMMARY	17
5. REFERENCE.....	19

Illustrations

	<u>Page</u>
2-1. DIAGRAM OF M-TES SETUP.....	3
2-2. MICA2DOT AND MICA2 MOTES.....	5
2-3. NESC PROGRAMMING ELEMENTS.....	6
2-4. ANALOG DEVICES ADXL210AE ACCELEROMETER.....	7
2-5. FLEXIFORCE A201 SENSOR.....	7
2-6. STARGATE PLATFORM (PROCESSOR BOARD AND CONNECTIVITY BOARD).....	8
2-7. EXAMPLE OF RAW AND FILTERED DATA. (A) FOR THE WALKING DATA, THE ACCELERATION PEAKS AND TROUGHS ARE OUT OF PHASE. (B) FOR THE JUMPING DATA THE ACCELERATIONS ARE IN PHASE AS THE JUMP BEGINS.	11
3-1. FLEXIFORCE FORCE MEASUREMENTS. (A) FORCE PLATE MEASUREMENT UNDER ONE FOOT FROM HEEL STRIKE TO TOE OFF (B) 3 FULL CYCLES OF FLEXIFORCE MEASUREMENTS.....	13
3-2. DETERMINATION OF TRANSITION POINTS WITHIN A WALKING STEP.....	14

1. Introduction

Military physical training programs involve a number of activities to improve the health and performance of the soldier. A constant challenge is designing programs to maximize the individual's performance while minimizing the risk of a training injury. Therefore to properly evaluate a training program, it is necessary to know the details of the program. These details include: type of activity performed, duration of the activity, and intensity of the training. Currently some information about training regimens is manually recorded. However the inconsistency of these records and the insufficient information at the level of the individual make it difficult to accurately model the effects of a training regimen on an individual. Therefore to develop models that will predict the performance ability and improvements of an individual it is necessary to have a method of measuring and recording the training regimen that an individual experiences. A mobile biomechanical measurement device would provide a method to address this necessity.

Through this project, a prototype device was developed to wirelessly measure the biomechanics of an individual during walking, running, and jumping. The Mobile Training and Exercise System (M-TES) consists of two ankle sensors and a data logging base station that are worn by the user. The system measures the activities of the user via the sensors and records the data to the memory on the base station. To examine the activities of the user, the data is downloaded from the base station to a computer and analyzed with the M-TES Analyzer software.

Within a gait laboratory, a researcher can measure many aspects of the individual, including: kinematics via an optical tracking system, ground reaction forces via force plates, and energy expenditure via a metabolic gas analysis system. These types of systems allow for very accurate measurements of the user during an activity, but they also restrict the activity to an idealized form. For example, a cyclist on a training bicycle in a laboratory does not have all of the external influences such as hills, wind dynamics, other cyclists, and spectators. Consequently, a challenge with biomechanical measurements is performing these measurements under realistic conditions.

Previous studies have demonstrated the feasibility of portable biomechanical measurements devices (Cardon and DeBourdeaudhuij, 2007; Esliger *et al.*, 2007a; Karantonis *et al.*, 2006c; Lau and Tong, 2007b; Tanaka *et al.*, 2007). These devices have traditionally employed accelerometry to measure the activity of the individual. Basic systems utilized the accelerometers to quantify the activity level of the user (Esliger *et al.*, 2007b). For example, at low accelerations, the user is classified as inactive, at small accelerations the user is at a low activity level, at medium accelerations the user is at a

medium activity level, and at high accelerations the user is considered to be at a high activity level. This method provides a general description of the activity intensity level of the individual, but provides little information about the type of activity or the characteristics of the activity.

A better system utilizes the accelerometer data to classify the activity and calculate an intensity level for the activity (Karantonis *et al.*, 2006b). With this type of system, activities such as walking, running, and jumping can be distinguished from each other, and whether the individual was running with low, medium, or high intensity can be determined. This system is very good for logging the activities of an individual and providing some information about their intensity level. However, details about their biomechanics are still lost. There is no means of reconstructing the elements of the movement needed for a detailed biomechanical analysis.

Consequently, a goal of the system developed was to retain sufficient information so that important elements of the movement could be reconstructed. Knowing these elements and how they differ between activities, the movement could be classified, the intensity level quantified, and biomechanical characteristics of the activity analyzed. For example, knowing the elements of each step during walking would allow for calculations of step length and walking velocity. Having acceleration measurements at heel strike and toe off could be used to estimate ground reaction forces.

The goal of developing the M-TES is to provide the ability to measure and record the activities of an individual in the field. The activities would include walking and running over different terrains and elevations, and jumping over obstacles. Some of the technical challenges for the hardware components included sampling the sensors sufficiently fast, having adequate bandwidth for transmitting data to the base station, and providing scalability so that more or different sensors could be added to the system. For the software components, the challenges were storing the data in an efficient manner and analyzing the data to properly reconstruct and classify the activities.

The requirements and challenges of the device will be further addressed in the following section. Then the specifications of the hardware and software components will be discussed. In the third section, data will be presented to illustrate the ability of the system to classify and reconstruct different types of movements. In the last section, a summary description of the device, its capabilities, and the future direction for development will be presented.

2. M-TES 1.0 System

2.1 M-TES 1.0 System Configuration

2.1.1 Overview

The M-TES system consists of two sensor units, a data logging base station, and a software program to analyze the recorded data (Figure 2-1). The two sensor units are worn on the ankles and each contains a biaxial accelerometer which measures accelerations in the vertical and forward directions. A force sensor is also attached to the sensor unit to measure the force under the heel of the foot. The data recorded by the sensor units are transmitted to the base station where they are stored. The base station employs flash memory to store the data until the data can be downloaded to a computer for analysis. The M-TES Analyzer program uses the data to reconstruct and classify the movements of the user, and calculate biomechanical metrics such as speed and stride length.

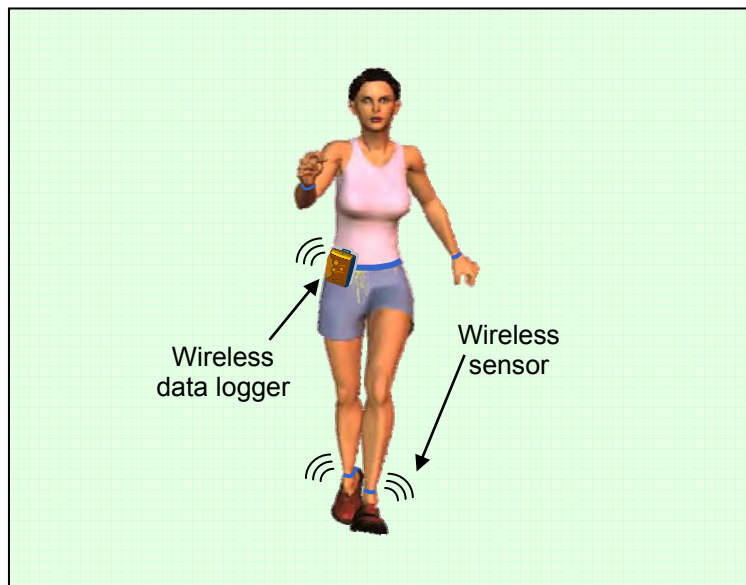


Figure 2-1. Diagram of M-TES setup.

2.1.2 Challenges

The technical requirements for a device with the above features include:

- 1) *Sample rate:* A majority of human movements have frequency components below 20 Hz, therefore the sample frequency of the sensors would need to be at least 40 Hz to ensure the measured signal was not aliased.
- 2) *Communication protocol:* Because the sensor data needs to be transmitted wirelessly to the base station, the sensor units need a radio transmitter with a short range for transmission but be capable of high data throughput.

- 3) *Data logging base station:* The base station needs to communicate wirelessly with the sensor units, store the data it receives, and communicate with a computer to download the stored data.
- 4) *Classification algorithm:* The algorithm is required to distinguish walking, running and jumping.
- 5) *Data storage:* Recording data for hours at sampling frequencies above 40 Hz leads to very large amounts of data (i.e., on the order of megabytes). Consequently a method for efficiently storing the data is necessary.
- 6) *Commercial off-the-self (COTS) components:* The components need to be commercially available to reduce the cost of the device and to allow for flexibility of component substitutions.

Consequently, the challenge was finding the components and developing the algorithms to meet all of these requirements, while ensuring everything was integratable and that the cost of the device was reasonable. The final selection for the device components and the algorithm developed were able to address these requirements and in the following sections details about each component and the analysis software will be discussed.

2.2 M-TES Hardware: Sensors and Base Station

2.2.1 Motes and Wireless Sensor Network

Motes are small wireless sensors that receive and transmit various sensor data while using a minimal amount of power. They contain a microprocessor, A/D converters, sensors (type depends on the application), and a radio for wireless communications (Figure 2-2). Typically motes are deployed in remote areas to measure a signal where access is difficult or inconvenient.

Motes can communicate with other motes. Therefore when a number of motes are deployed over an area, each one can communicate with its neighbors. As a result a wireless sensor network (WSN) is formed that allows messages to be relayed between the motes. For example, a base station (typically a mote directly connected to a computer) at one end of this WSN can send a message to any one mote by having the intermediate motes relay the message. For the M-TES, Mica2Dot (Crossbow Technologies, www.xbow.com) motes were used for each sensor unit as the platform for attaching the accelerometers and the force sensor. The base station also contained a mote (Mica2, Crossbow technologies, www.xbow.com) for receiving and transferring the sensor data to the data logger for storage.

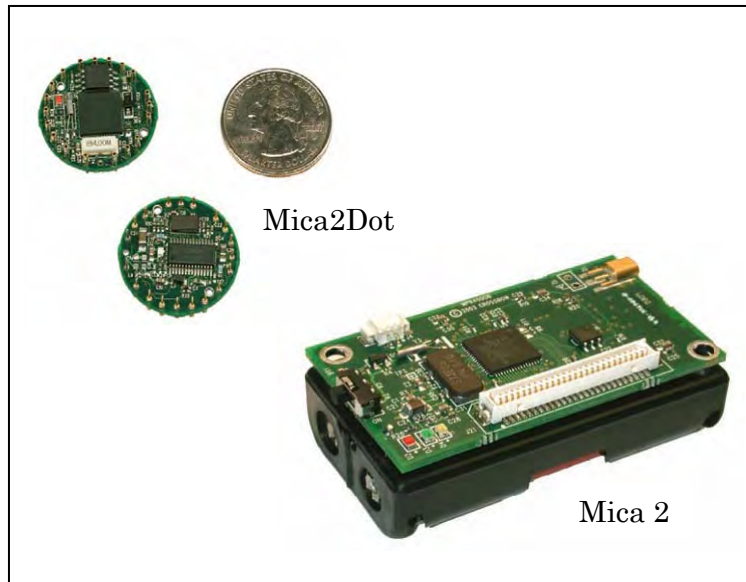


Figure 2-2. Mica2Dot and Mica2 motes.

For communication, the Mica2Dot motes used a radio frequency of 433 MHz, provided a 19.2 Kbaud data rate, and used the IEEE 802.15.4 standard for the communication protocol. The communication range of these motes in the outdoors is ideally 1000 ft and during transmission the mote draws 25 mA.

Each mote contains a microprocessor with the TinyOS operating system, which allows a developer to program small applications that can run autonomously on the mote. The development language for these applications is nesC which has similar syntax to the C programming language, but is a structured component-based language. An application in nesC consists of a number of components which are linked together (Figure 2-3) and the application flow is more event driven than sequential.

TinyOS/nesc Concept	Description
Application	A TinyOS/nesc application consists of one or more components, linked ("wired") together to form a run-time executable
Component	Components are the basic building blocks for nesc applications. There are two types of components: <i>modules</i> and <i>configurations</i> . A TinyOS component can provide and use interfaces.
Module	A component that <i>implements</i> one or more interfaces.
Configuration	A component that <i>wires</i> other components together, connecting interfaces used by components to interfaces provided by others. (This is called wiring .) The idea is that a developer can build an application as a set of modules, wiring together those modules by providing a configuration. Furthermore, every nesc application is described by a top-level configuration that specifies the components in the application and how they invoke one another.
Interface	An interface is used to provide an abstract definition of the interaction of two components. This concept is similar to Java in that an interface should not contain code or wiring. It simply declares a set of functions that the interface's provider must implement—commands—and another set of functions the interfaces' requirer must implement—events. In this way it is different than Java interfaces which specify one direction of call. Nesc interfaces are bi-directional. For a component to call the commands in an interface it must implement the events of that interface. A single component may require or provide multiple interfaces and multiple instances of the same interface. These interfaces are the <i>only</i> point of access to the component.

Figure 2-3. nesc programming elements.

Description of concepts involved with a structured component-based language, taken from *Getting Started Guide, Rev. A*, Crossbow Technologies Inc.

For the M-TES system, a nesc program for the sensor units was developed to sample the sensors at a specified frequency and then transfer the data to the base station when the data buffer on the mote was filled. For the base station mica2 mote, a nesc program was developed to receive the messages from the sensor units and to transfer the data to the data logger for storage.

2.2.2 Accelerometers and Force Sensors

A biaxial accelerometer was attached to the mote to measure forward and vertical accelerations; and a force sensor was attached to measure the force applied by the foot to the ground. The accelerometer chosen was the Analog Devices ADXL210AE (Figure 2-4). It has a measurement range of ± 10 g and a resolution of 2 mg at 60 Hz, which is sufficient to capture the accelerations during walking, running, and jumping. It also has a form factor and power requirements that allow easy integration with the Mica2Dot data acquisition board.

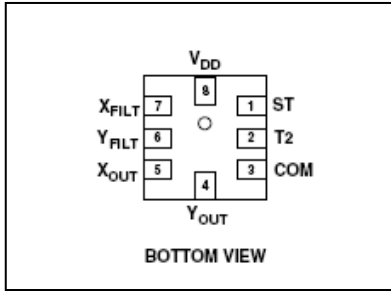


Figure 2-4. Analog Devices ADXL210AE accelerometer.

The force sensor implemented was the FlexiForce A201 sensor (Figure 2-5). This sensor has a sensing area of 0.71 cm², a response time of <5 microseconds, and a measurement range of 0-4.4 N. Attaching this sensor to the mote required an amplifier circuit. By tuning this circuit appropriately, the measurement range of the sensor was also modified to ensure the forces encountered during walking, running, or jumping would not saturate the sensor readings.



Figure 2-5. FlexiForce A201 sensor.

2.2.3 Base Station

The base station for the M-TES is the Stargate (Crossbow Technologies, www.xbow.com), a single board computer with an Intel 400 MHz Xscale processor (Figure 2-6). The main goal of the base station was to provide storage for the data being received from the sensor units, and a means to download the data to a desktop computer for further analysis. The Stargate has a small form factor, 8.9 cm by 6.4 cm. This is roughly the size of a PDA, so the unit could easily be worn by the user without interfering much with their mobility. For communication with the sensor motes, a Mica2 mote is attached to the Stargate to receive and send signals to the motes. The Mica2 mote is essentially the same as the Mica2Dot mote, but with a larger form factor. For storage, the Stargate has 64 MB of SDRAM, but it also contains a compact flash slot for increased storage capacity. With the compact flash slot more than 2 GB of storage capacity could be added. The Stargate also has an Ethernet port for communicating via a network with desktop computers. This communication option allows for data to be downloaded to a computer that is located at a distance from the actual base station.

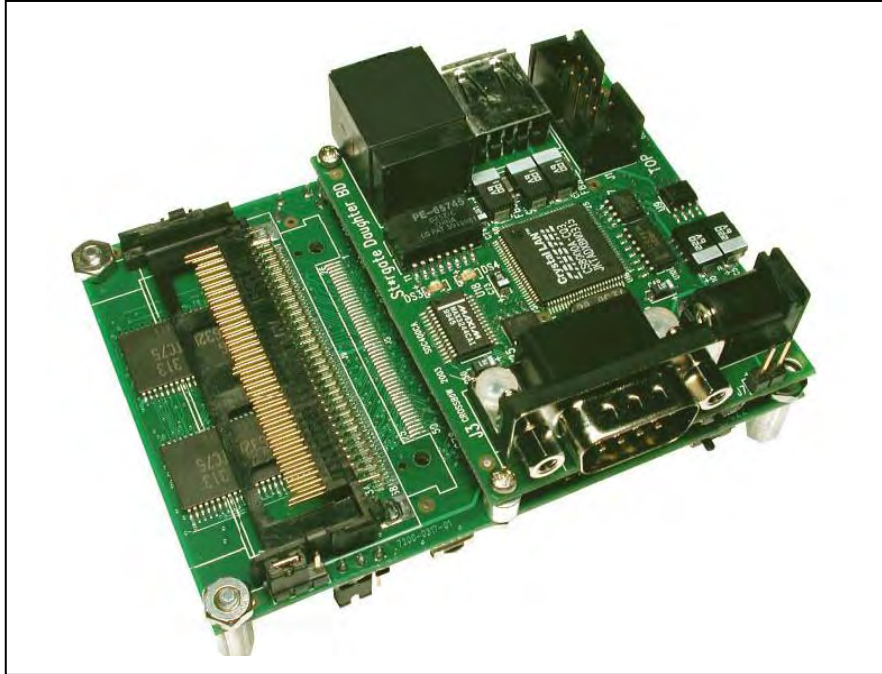


Figure 2-6. Stargate platform (processor board and connectivity board)

The operating system on the Stargate is Linux based which allows for c/c++ programs to be easily compiled and run on the platform. The current system has an application that receives the data from the sensor units and stores the data to the compact flash card for later downloading.

2.3 M-TES Software: Analyzer 1.0

2.3.1 Data Storage

As a result of the high sample rate, the amount of data acquired over an hour of exercise can be extensive. Past developers overcame this obstacle by calculating and storing average values. For example, if a device was sampling biaxial acceleration data at a sample frequency of 50 Hz then for each second the device would need to store $2 \times 50 = 100$ pieces of data. However, if the device first calculated the desired metric (e.g., walking speed) and then averaged those values over 1 second, then for each second the device would need to store only one piece of data. This method reduces the amount of storage needed, but it also loses some of the information obtained. For the M-TES, a goal was to retain the majority of data so that more advanced biomechanical analysis could be performed offline. Consequently, taking averages of the data or calculated metrics was not a viable option for reducing the data storage requirements. Therefore, it was necessary to find a data compression method for storing the entire signal.

The Fourier transform (FT) was the method utilized with the M-TES to provide data compression. The transform is typically used to determine the dominant frequency components of a signal. By examining the transformed signal, the frequencies with the most power are the dominant ones and the frequencies with little power can be mostly ignored. A Fourier transformed signal is the same length as the original signal, and is symmetric about its middle. Also, the original signal can be regained by performing an inverse Fourier transform (IFT) on the transformed signal.

For the M-TES, the properties of the FT and knowledge about the frequency components of walking, running, and jumping were utilized to compress the data. The first step in the compression method entailed low pass filtering of the signal. Previous research (Karantonis *et al.*, 2006a; Lau and Tong, 2007a) has found the frequency components of walking, running, and jumping to be below 20 Hz. Therefore the raw signal was initially low passed filtered at this cutoff frequency. The next step involved performing a FT on the signal. Because the FT signal is symmetric only the first half of the signal needed to be stored; and this reduced the required storage capacity by half. Additionally, the low power frequency components in the frequency ranges above the dominant frequencies could be ignored with only minor effects when the IFT was performed. Therefore a threshold frequency was determined for these higher frequencies and the FT values above this threshold level were effectively set to zero. By setting them to zero these data points could also be removed and replaced with a number indicating how many zeros were needed when reconstructing the full FT signal. Depending on the frequency components of the signal, this second reduction could reduce the storage capacity by another half. Therefore the storage capacity of the original signal would be reduced to a quarter of its original requirements. To regain the original data, the FT signal would be reconstructed by adding the necessary zeros and then adding in the symmetrical half of the signal. Performing an IFT on this reconstructed FT signal would result in a signal that was very close to the original signal, and with the regained signal advanced biomechanical analysis could be performed.

2.3.2 Activity Classifications

Activity classification is an essential function of this system. Through classification algorithms, the M-TES did not only determine periods of activity from inactivity, but it also determined what activity was performed and the intensity of the performance. To analyze the recorded data, a 1 second window was employed. Therefore during each second of data the algorithms:

- 1) Determined if the user was active or inactive
- 2) If active, characterized the type of activity (e.g., walking, running, jumping)
- 3) Calculated activity metrics, (e.g., time of heel strike, walking velocity)

To separate activity from inactivity the algorithms calculated the magnitude of the acceleration vector and then took its derivative. If the slope was nonzero, then the user was active, otherwise the user was classified as inactive. A derivative method was used over a simple threshold method due to the effects of gravity and the changing orientation of the ankle worn sensors. Because the X and Y axes of the accelerometers rotated with the leg within the gravitational field, the angle between gravity and the axes was constantly changing. Therefore, at any static leg position the acceleration magnitude would be nonzero. Consequently a threshold for determining activity (the method commonly used for waist worn accelerometers) would not be proper, so a method using the derivative of the signal was developed.

With activity separated from inactivity, the next step was to classify the activities. The Fourier transform was used again to determine the frequency components of the signal. The signal was further filter-based on the frequency components determined by the FT. This smoother curve was initially used to determine if the user was jumping. For jumping the accelerations for the x and y directions tended to move in the same direction (i.e., both increasing or both decreasing), while for walking they moved in opposite directions (i.e., one increasing while the other is decreasing). With this knowledge the activity was separated into jumping or not jumping. To distinguish between walking and running, a threshold for the frequency of the movement was employed (Figure 2-7).

Knowing the activity, metrics about the activity could be calculated. For example, given the user was walking with a certain frequency and knowing the height of the user, the walking speed of the user could be determined. Similarly, using the times of toe off and heel strike, the amount of time in the air could be calculated and the height of the jump estimated. Because of ever improving classification and metric algorithms, the advantage of storing the complete data signal allows these types of analysis as well as future developed analyses to be performed without recollecting the data.

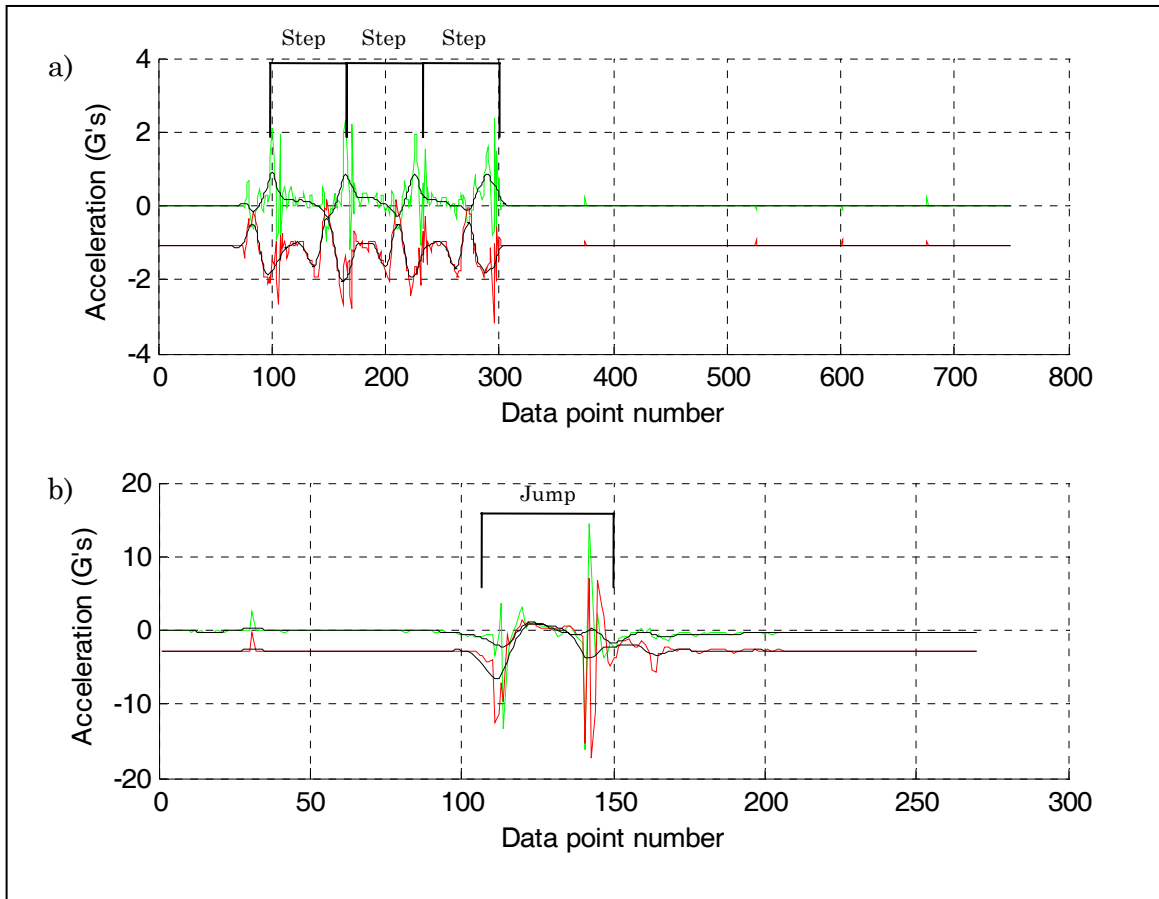


Figure 2-7. Example of raw and filtered data. (a) For the walking data, the acceleration peaks and troughs are out of phase. (b) For the jumping data the accelerations are in phase as the jump begins.

3. Sample Results

3.1 Description of Tests (Walk, Run, Jump)

To investigate the performance of the M-TES a protocol was developed. The protocol consisted of separate walk, run and jump tests. The separate activity tests were used to develop the classification algorithms and calculate activity metrics. Two subjects performed the experiments and the results will be described in the sections below.

3.2 Time Trace Measurements

In Figure 3-1 an example of a force measurement from the FlexiForce sensor is compared against the force measurements of a force platform. The FlexiForce sensor was placed under the heel of the subject, so it measures the points between heel strike and heel off. The force plate measured the force under the right foot of the subject throughout the entire stance phase. The FlexiForce data was able to signal heel strike. However, the measurements were not consistent in magnitude and the response time varied due to variations in heel strike between steps and damping caused by the cushioning of the shoe. As a result, the FlexiForce was measuring no zero forces during the swing phase of gait. Consequently, the accelerometers are a better choice for determining gait parameters.

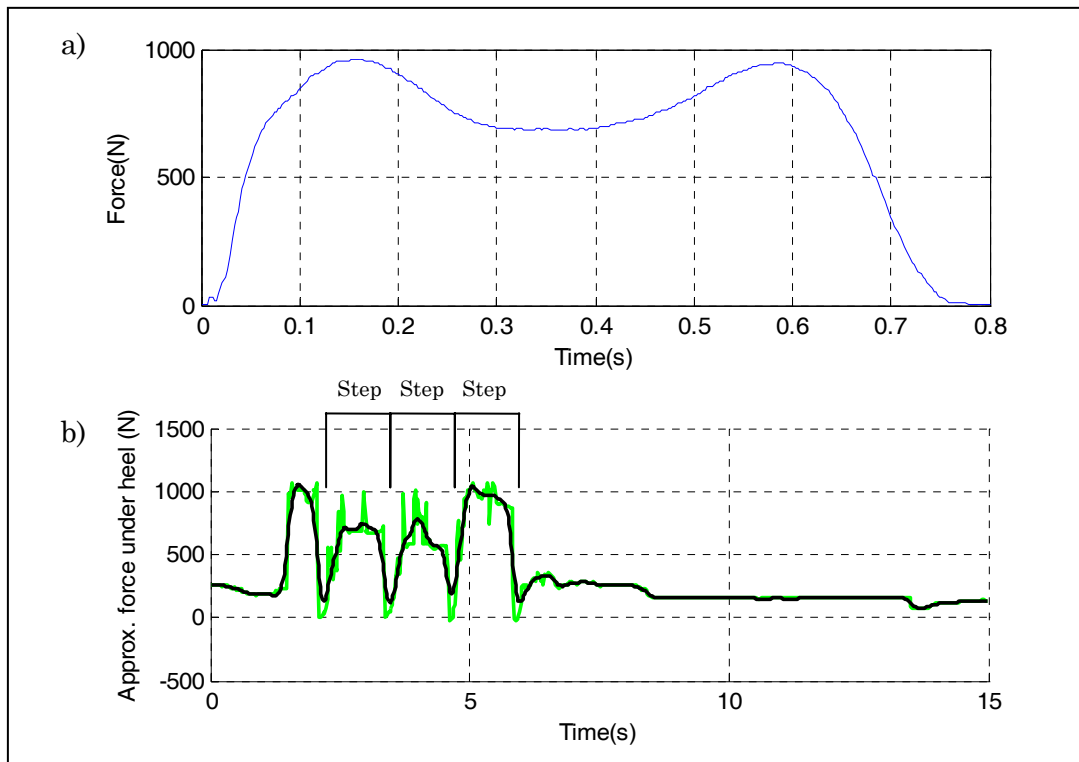


Figure 3-1. FlexiForce force measurements. (a) force plate measurement under one foot from heel strike to toe off (b) 3 full cycles of FlexiForce measurements

3.3 Accuracy in Biomechanical Parameters

3.3.1 Activity Classification

In this section, data from a walking test is displayed along with the results from the classification algorithm (Figure 3-2). From these preliminary results, the algorithm did a satisfactory job at distinguishing the activity and key points (i.e., heel strike and toe off) for the activity. However, more experiments with an increased number of subjects would need to be performed to fully evaluate the robustness of the algorithm.

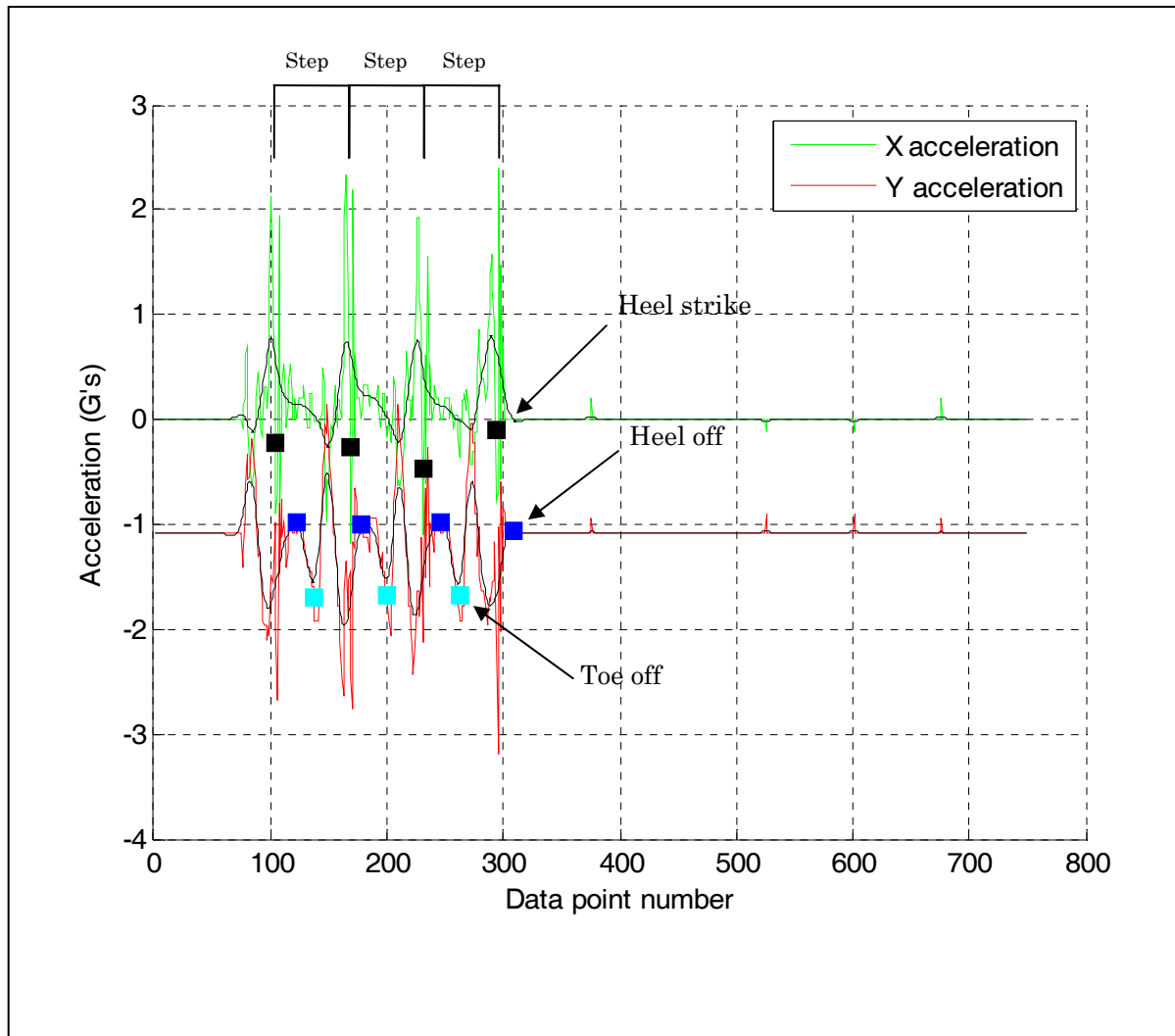


Figure 3-2. Determination of transition points within a walking step

3.3.2 Calculating Activity Metrics

For walking and running, the average speed of the subject was calculated as the distance from their starting point to the force platform divided by the time needed to reach the platform. The analyzer program calculated the velocity utilizing the acceleration during

stance phase and the leg length of the subject. By calculating the angular acceleration when the leg was vertical and double integrating, an angle of rotation could be determined. Using this angle and the length of the leg, a horizontal distance of movement could be calculated. By dividing this result by the time taken and multiplying by a scaling factor the horizontal velocity of the center of mass could be estimated. The average speed of the subject during the experiment was measured to be 1.26 m/s. The results from the analyzer program were 1.12, 1.39, 1.09 and 1.3 m/s for each of the 1 second windows. The average of these numbers was 1.23 m/s, which is close to the true value. With more testing, the robustness of the algorithm will be tested and improved.

For jumping, the time in the air was calculated as the time between toe off and heel strike. These values were then compared against the toe off and heel strike times of the force platform for accuracy. The measured time in the air was 0.462 seconds. The calculated time was 0.44 seconds. In addition, if desired, the jump height could be estimated assuming the acceleration profile of the subject was not affected by any external factors beyond gravity.

4. Summary

The goal of this project was to develop a measurement system that could be worn in the field for measuring an individual's activity without interfering with the mobility of the user. The prototype system developed was the M-TES (Mobile Training and Exercise System). The current system consists of a data logging base station and two ankle sensors that are worn by the user. In addition to the devices, a software program was developed to analyze the data. The M-TES Analyzer program classified the activities of the user and calculated various activity metrics.

Through this initial development effort, it was shown that the M-TES is capable of recording, storing, and analyzing biomechanical data. Future efforts will increase the robustness of the device and the algorithms so that the M-TES can truly be utilized in the field. In addition, several more experiments will be performed to statistically demonstrate that the M-TES device and software are accurate and reliable.

5. References

- Cardon,G. and DeBourdeaudhuij,I. (2007) Comparison of pedometer and accelerometer measures of physical activity in preschool children, *Pediatr.Exerc.Sci.* **19**, 205-214.
- Esliger,D.W., Probert,A., Gorber,S.C., Bryan,S., Laviolette,M., and Tremblay,M.S. (2007b) Validity of the Actical accelerometer step-count function. *Med Sci.Sports Exerc.* **39**, 1200-1204.
- Karantonis,D.M., Narayanan,M.R., Mathie,M., Lovell,N.H., and Celler,B.G. (2006a) Implementation of a real-time human movement classifier using a triaxial accelerometer for ambulatory monitoring, *IEEE Trans.Inf.Technol.Biomed.* **10**, 156-167.
- Lau,H. and Tong,K. (2007b) The reliability of using accelerometer and gyroscope for gait event identification on persons with dropped foot. *Gait.Posture.*
- Tanaka,C., Tanaka,S., Kawahara,J., and Midorikawa,T. (2007) Triaxial accelerometry for assessment of physical activity in young children. *Obesity.(Silver.Spring)* **15**, 1233-1241.



Training, Overuse injury, and Performance Model

TOP

Version 1.1

User's Guide

Bryant L. Sih
L-3 Communications/Jaycor
3394 Carmel Mountain Road
San Diego, California 92121-1002

August 2007

Contents

- OVERVIEW.....1**
 - BASIC USER.....1
 - MID-LEVEL USER.....1
- BASIC USER.....2**
 - LOGIN.....2
 - PROGRAM SETUP.....3
 - RESULTS.....5
 - Body Fat Standard*.....5
 - Physical Fitness*.....5
 - Overuse Injury*.....5
- MID-LEVEL USER.....9**
 - LOGIN.....9
 - PROGRAM SETUP.....9
 - Groups*.....9
 - Regimen*.....9
 - Analysis*.....10
 - RESULTS.....11
 - Body Fat Standards*.....11
 - Performance*.....11
 - Overuse Injury*.....11

Overview

The Training, Overuse Injury, and Performance (TOP) Model is a software framework for assessing the effects of physical training on performance and injury. Because it is web-based, only an internet connection and web-browser are required. No software installation is needed. This software will:

- Predict individual Army Physical Fitness Test (APFT) scores
- Identify individuals who are at “high risk” of injury for a given training regimen
- Recommend modified training regimens for individuals who are at high risk for injury
- Compare training regimens for differences in both performance and injury outcomes

The software interface is designed to allow users with different functional objectives to manage the program and acquire the results they desire in an efficient and user-friendly manner. Two different user types have been developed. Depending on the type of user, different levels of software functionality are available. The users have been divided in the following manner:

Basic User

Interested in comparing their individual performance progress and injury likelihood during BCT to their peers. The output displays their individual scores and the average scores of their peers. This user can not change the training regimen, but can enter and modify their anthropometric data and physical fitness test (PFT) scores. Likely Basic Users are individual soldiers.

Mid-Level User

Focused with the performance and injury outcomes of a small group of individuals (2-30) involved in a training regimen. The output identifies individuals at high risk for performance failure or injury. This user can modify the properties of the individuals in the group and the training regimen. Likely Mid-Level Users are Drill Sergeants and fitness advisors.

Basic User

Login

To access TOP 1.1, point your web browser to the TOP 1.1 website, whose address is available from your commander. Enter your Username and Password in the appropriate fields and click on the *Submit* button. If an account does not exist, you can create one by clicking on *Create User* (Figure 1).

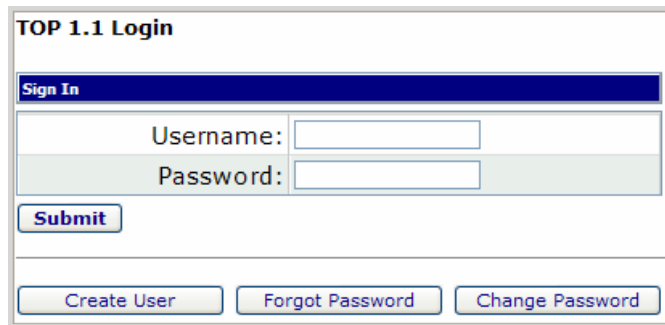


Figure 1. The TOP 1.1 login window.

To create a user, the following information is required: User Name, Password (length should be between 3 and 10 characters and not contain any symbols), First Name, Last Name, User Type (Basic User), Group ID, and Start Date. Group ID and Start Data are required and available from your commanding officer or equivalent. First and Last Names should be between 1 and 50 characters and should not contain any symbols. See Figure 2.

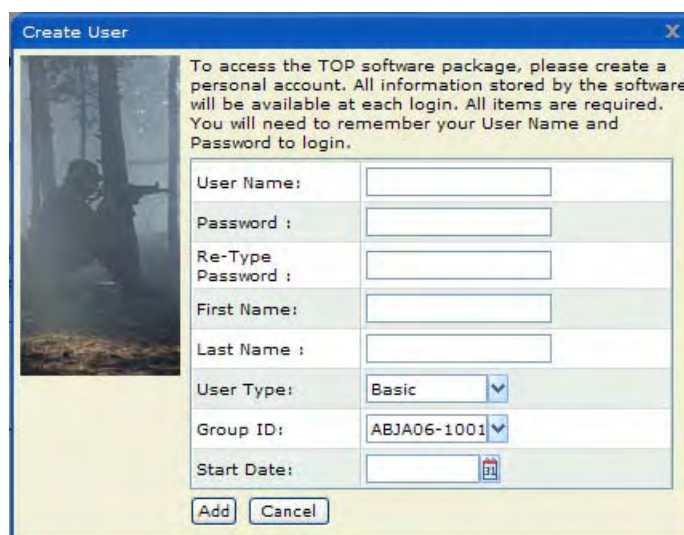


Figure 2. The Create User pop-up window.

Program Setup


After logging in, each of the 4 buttons in the main section leads to a window most of which require additional information. All buttons must be marked “Completed” before a training analysis can be performed. The analysis will predict your final physical fitness test (PFT) score and the likelihood of injury. The data required for the analysis is shown in Table 1. After all four sections are marked “Completed,” click on the *Analyze* button.

Table 1. The following information is needed to create a Basic User.

Medical History	
Age	Years
Gender	Male or female
Height	Inches
Weight	Pounds
Abdomen (males only)	Measure in inches the abdominal circumference against the skin at the navel (belly button), level and parallel to the floor.
Neck	Measure in inches the neck circumference at a point just below the larynx (Adam's Apple).
Hip (females only)	Measure in inches the hip circumference by placing the tape around the hips so that it passes over the greatest protrusion of the gluteal muscles (buttocks) as viewed from the side.
Forearm (females only)	Measure in inches the forearm circumference by placing the tape around the forearm so that it passes over the thickest portion of the forearm.
Wrist (females only)	Measure in inches the wrist circumference by placing the tape around the area that is the thinnest.
Fitness and Lifestyle Background	
How do you rate your current physical fitness compared to other individuals of your gender and age?	Select Excellent, Very Good, Fair, or Poor
During the 2 months prior to military training, what was the average number of times per week you exercised, played sports, or participated in strenuous labor?	Select Never, Once or less, 2 times, 3 times, 4 times, 5 times, 6 times, or 7 times or more.
Have you ever taken diet pills to lose weight?	Select Yes or No
Have you ever used laxatives to lose weight?	Select Yes or No
Have you ever caused yourself to vomit to lose weight?	Select Yes or No

Physical Fitness Scores	
Date	The date of the PFT
Run Time	The time of the PFT run in min:sec formula
# SU	The number of sit-ups or crunches done in the time allowed
# PU	The number of push-ups or pull-ups done in the time allowed
PFT Type	Select the type of PFT performed (IST, PFT, or Final PFT). Only an IST PFT is required.

Physical Fitness Scores
Finished
Cancel



Instructions
Record your Physical Fitness Test (PFT) results in the table below.

Date: The date of the PFT
Run Time: The time of the PFT run in min:sec formula
SU: The number of sit-ups or crunches done in the time allowed
PU: The number of push-ups or pull-ups done in the time allowed
Total Score: Your PFT score
PFT Type: Select the type of PFT performed

☐ clears the PFT results.

Recorded Physical Fitness Scores

Initial PFT

Date	Run Time	#SU	#PU	Total Score		
2006-08-09	00:20:20	50	48	229		

PFT

Date	Run Time	#SU	#PU	Total Score

Final PFT

Date	Run Time	#SU	#PU	Total Score

Enter additional PFT results:

Date:
PFT Type: Select One

Run Time (hh:mm:ss):
Situps:

Pushups:

Run Score
Situps Score

Pushups Score
Total Score

Figure 3. Basic User's enter Physical Fitness Test (PFT) results in the above pop-up window. Scores are automatically calculated.

Instructions

Each of the 4 buttons below leads to a window most of which require additional information. All buttons must be marked **Completed** before a training analysis can be performed.

The analysis will predict your final physical fitness test (PFT) score and the likelihood of injury.



Figure 4. After completing the four sections, click “Analyze” to run the TOP 1.1 simulation.

Results

The results of the program are broken into three sections: Body Fat Standard, Physical Fitness, and Overuse Injury & Stress Fracture. Clicking on *PDF Report* generates a 2 page printable sheet that contains the results of the simulation and a FAQ section.

Body Fat Standard

This test uses current standards and calculation formulas to estimate weight and body fat (% fat) compliance (U.S. Army 600-9). “Estimated” is your estimated values, “Allowed” is the values you must be below to be in compliance, and “Difference” is calculated by subtracting the Allowed from the Estimated values. A positive difference means not in compliance.

Physical Fitness

Your predicted performance on each of the final test events (Run, Sit-ups, and Push-ups) is based on your initial fitness test results (IST), planned training regimen, and fitness profile. Your overall “Outlook” for each test is given. Possible values are Good, Medium or Poor and are also shown graphically. “Predicted Value and Score” are the model predictions. “Pass Requirement and Score” are also presented for convenience.

Overuse Injury

The graphs in this section show your likelihood of sustaining a lower body (legs and hip) overuse injury and stress fracture over the course of the training regimen specified. An overuse injury is an injury caused by repetitive motion. Common examples are tendonitis/bursitis/fasciitis, pain, and non-acute strains/sprains. A stress fracture is an overuse injury of the bone, caused by training harder than the bone is capable of handling. The most common stress fracture bone is the tibia calf bone. The percent likelihood of a typical (average) individual being injured from this training regimen is specified in black.



Figure 5. The Basic User Results page showing Body Fat Standard compliance, Physical Fitness predictions, and Injury likelihood.

TOP 1 1

Training, Overuse Injury & Performance Modeling

Analysis Report for:
Name: Smith, Joe
Username: Male1
GroupID: ABJA06-1001

Date: 06/29/2007

BASIC INFORMATION

Age (yrs): 22 Height (in): 67 Training Type: Army Basic Combat Training
Gender: Male Weight (lbs): 150 Location: Ft. Jackson, SC
Start Date: 2006-08-08

BODY FAT STANDARD

	Estimated	Allowed	Difference	Result
%Fat	17	22	5	IN COMPLIANCE
Weight	150	169	19	IN COMPLIANCE

PHYSICAL FITNESS

Final Physical Fitness Test

Your predicted performance on each of the final test events is based on your initial physical fitness test results (IPFT), planned training regimen, and fitness profile.

Final PFT Predictions	Run	Sit-Ups	Push-Ups
Out look	Good	Good	Good
Predicted	14:04-16:01	100-116	96-115
Predicted Score	88-66	100	100
Pass Requirement	17:25	43	31
Passing Score	50	50	50

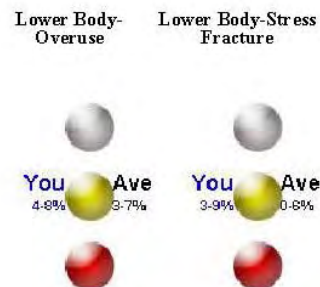


OVERUSE & STRESS FRACTURE INJURY

An overuse injury is an injury caused by repetitive motion. Common examples are tendonitis/bursitis/fasciitis, pain, and non-acute strains/sprains. A stress fracture is also an overuse injury but is considered separately.

Your chance of sustaining a lower body (legs & hip) overuse injury over the course of the planned training regimen. The percent likelihood of a typical (average) individual being injured from this training regimen is specified on the right.

A stress fracture is an overuse injury of the bone, caused by training harder than the bone is capable of handling. The most common stress fracture bone is the tibia or calf bone.



These results are based on the average response of individuals similar to you undergoing the planned regimen. Your results may differ.

TOP 1.1

Training, Overuse Injury & Performance Modeling

FREQUENTLY ASKED QUESTIONS

OVERVIEW

What is TOP 1.1?

TOP 1.1 is a tool designed to predict performance and injuries from training regimens or schedules.

How does it work?

TOP 1.1 uses your basic health information (height, weight, fitness level, etc.) in a computer simulation of your training plan. Using equations derived from scientific researchers, the program predicts your chances of injury and changes to your performance level.

PHYSICAL FITNESS

What is the Final Physical Fitness Test or Final PFT?

The Final PFT is the physical fitness test you must pass before graduating from training. The test is a three-event physical performance test used to assess muscular endurance and cardiorespiratory fitness. The three events are usually running, sit-ups, and push-ups. Passing scores are determined by your age, gender, and training program (basic combat training or an advanced training program).

What do the 'Final PFT Prediction' table results mean?

For each of the three events (and overall), a GOOD, BORDERLINE, or POOR grade is given. GOOD means you scored better than 95% of those in your age group. BORDERLINE is 50% and POOR is 5%. In addition, TOP 1.1 cannot predict your exact score for an event but gives a range for your likely scores.

What can I do to improve?

The regimen currently planned in order for you to pass the Final PFT may need to be modified. However, overtraining can lead to injuries and additional training should only be attempted with the guidance of a physical fitness advisor. Your fitness advisor can specify a different training program to be analyzed in TOP 1.1.

BODY FAT STANDARD

What is the Body Fat Standard?

The standard is a requirement that all enlisted personnel must meet in order to insure that everyone's fitness and percent body fat level meets acceptable standards. The criteria for compliance depend on the military branch.

What does 'Not In Compliance' mean?

In general, it means that your weight or percent body fat is too high. Dieting and exercise in a controlled manner is usually needed to bring your body fat standard measures back into compliance.

How is percent body fat estimated?

Key measurements such as height, weight, and neck circumference are used, comparing your values to similar individuals whose percent body fat is known.

Disclaimer

Exercise is not without its risks and this or any other exercise program may result in injury. To reduce the risk of injury in your case, consult a doctor before beginning this exercise program. The analysis presented is in no way intended as a substitute for medical consultation. As with any exercise program, if at any point during your workout you begin to feel faint, dizzy, or have physical discomfort, you should stop immediately and consult a physician.

Mid-Level User

Login

To access TOP 1.1, point your web browser to the TOP 1.1 website, whose address is available from your commander. Enter your Username and Password in the appropriate fields and click on the Submit button. If an account does not exist, contact your commander to create a Mid-Level User.

Program Setup

This software will allow you to view and analyze the predicted effects of different training regimens on performance and injury of a small group of individuals. To use this software, choose (1) a group of subjects, (2) a training regimen, and (3) items to analyze. Click on each of the grey section bars to make your selections. Additional instructions are given when each section is accessed.

Groups

Select a group of individuals based on their Group ID. Individual performance and injury history can also be viewed and edited by clicking on the Subject Details button. The View/Edit button allows the Mid-Level User to modify the military branch, training type, training location, start date, and special group ID code.

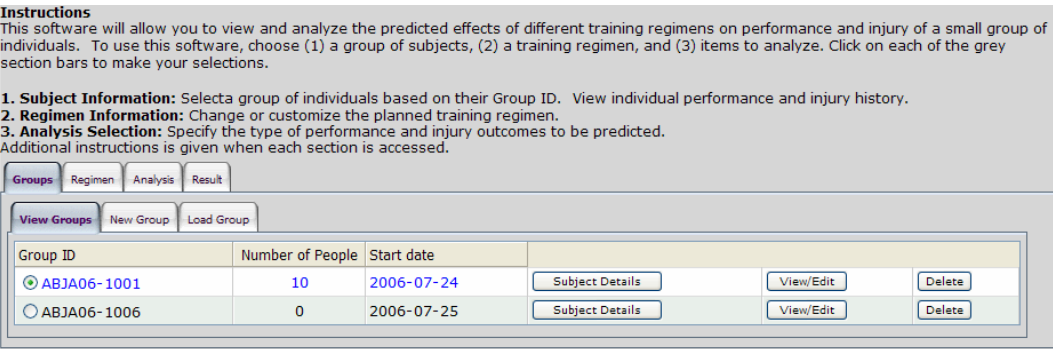


Figure 6. The Mid-Level Group tab is used to select different groups of subjects for analysis. Individual subject details can also be viewed and edited by clicking on the “Subject Details” button.

Regimen

Change or customize the planned training regimen. Clicking on the *Modify* button gives training regimen details where the amount of march, run, and conditioning drills can be adjusted. Adjustments are made as a percentage of a normal U.S. Army Basic Combat Training regimen on a weekly basis via sliders. *Conform Modified Values* saves changes and incorporates them into the prediction scheme.

Instructions

This software will allow you to view and analyze the predicted effects of different training regimens on performance and injury of a small group of individuals. To use this software, choose (1) a group of subjects, (2) a training regimen, and (3) items to analyze. Click on each of the grey section bars to make your selections.

1. Subject Information: Select a group of individuals based on their Group ID. View individual performance and injury history.

2. Regimen Information: Change or customize the planned training regimen.

3. Analysis Selection: Specify the type of performance and injury outcomes to be predicted. Additional instructions is given when each section is accessed.

Groups **Regimen** Analysis Result

Select Regimen New Regimen Load Regimen

Name Start date
Jan Regimen 2006-07-26 Modify Edit Delete

Regimen Details

Week	March Mileage(%)	Run Mileage(%)	Conditioning Drills(%)
week1	100	100	100
week2	100	100	100
week3	100	100	100
week4	100	100	100
week5	100	100	100
week6	100	100	100
week7	100	100	100
week8	100	100	100
week9	100	100	100

Confirm Modified Values Reset Values Cancel Save as regimen Variation

Figure 7. The Mid-Level User Regimen tab is used to select different training regimens and make changes to the weekly amount of training.

Analysis

Specify the type of performance and injury outcomes to be predicted. There are three performance tests and two overuse injury outcomes that can be predicted. See Figure 8. Specific subjects (or all) can be selected for analysis. An analysis name can also be entered.

Instructions
This software will allow you to view and analyze the predicted effects of different training regimens on performance and injury of a small group of individuals. To use this software, choose (1) a group of subjects, (2) a training regimen, and (3) items to analyze. Click on each of the grey section bars to make your selections.

1. Subject Information: Select a group of individuals based on their Group ID. View individual performance and injury history.
2. Regimen Information: Change or customize the planned training regimen.
3. Analysis Selection: Specify the type of performance and injury outcomes to be predicted.
Additional instructions are given when each section is accessed.

Groups Regimen **Analysis** Result

Performance		Overuse Injury	
<input type="checkbox"/> FPFT Run		<input type="checkbox"/> Lower Body	
<input type="checkbox"/> FPFT Push-ups		<input type="checkbox"/> Leg Stress Fracture	
<input type="checkbox"/> FPFT Sit-ups			
<input type="checkbox"/> Select All			

Subjects			
<input type="checkbox"/> Smith,Joe	<input type="checkbox"/> Joe,GI	<input type="checkbox"/> Doe,John	<input type="checkbox"/> Bob,Billy
<input type="checkbox"/> Simpson,Bart	<input type="checkbox"/> Smith,Jane	<input type="checkbox"/> Jane,GI	<input type="checkbox"/> Doe,Jane
<input type="checkbox"/> Jane,Mary	<input type="checkbox"/> Simpson,Lisa		
<input type="checkbox"/> Select All			

Analysis Name:

Figure 8. The Mid-Level User Analysis tab is where performance and injury models can be selected for use as well as specific individuals individuals.

Results

The results of the program are broken into three sections: Body Fat Standards, Performance, and Overuse Injury.

Body Fat Standards

This test uses current standards and calculation formulas to estimate weight and body fat (% fat) compliance (U.S. Army 600-9).

Performance

The predicted performance on each of the final test events (Run, Sit-ups, and Push-ups) is based on initial fitness test results (IST), planned training regimen, and fitness profile for each individual.

Overuse Injury

This section shows the likelihood of sustaining a lower body (legs and hip) overuse injury and stress fracture over the course of the training regimen specified. An overuse injury is an injury caused by repetitive motion. Common examples are tendonitis/bursitis/fasciitis, pain, and non-acute strains/sprains. A stress fracture is an overuse injury of the bone, caused by training harder than the bone is capable of handling. The most common stress fracture bone is the tibia or calf bone.

Each results section contains a main summary line and a detailed tab section that is broken into 5 areas: Main Poor/High Risk, Borderline/Medium Risk, Poor/Low Risk, and Info N/A. The main summary line shows a green, yellow, or red color to indicate the average performance of all subjects in the analyzed group as well as the group's average \pm standard deviation. The Main tabbed section gives a brief description of the exercise or injury and the number of people that fall into each category. The remaining tabs list the specific individuals of the category and their predicted scores.

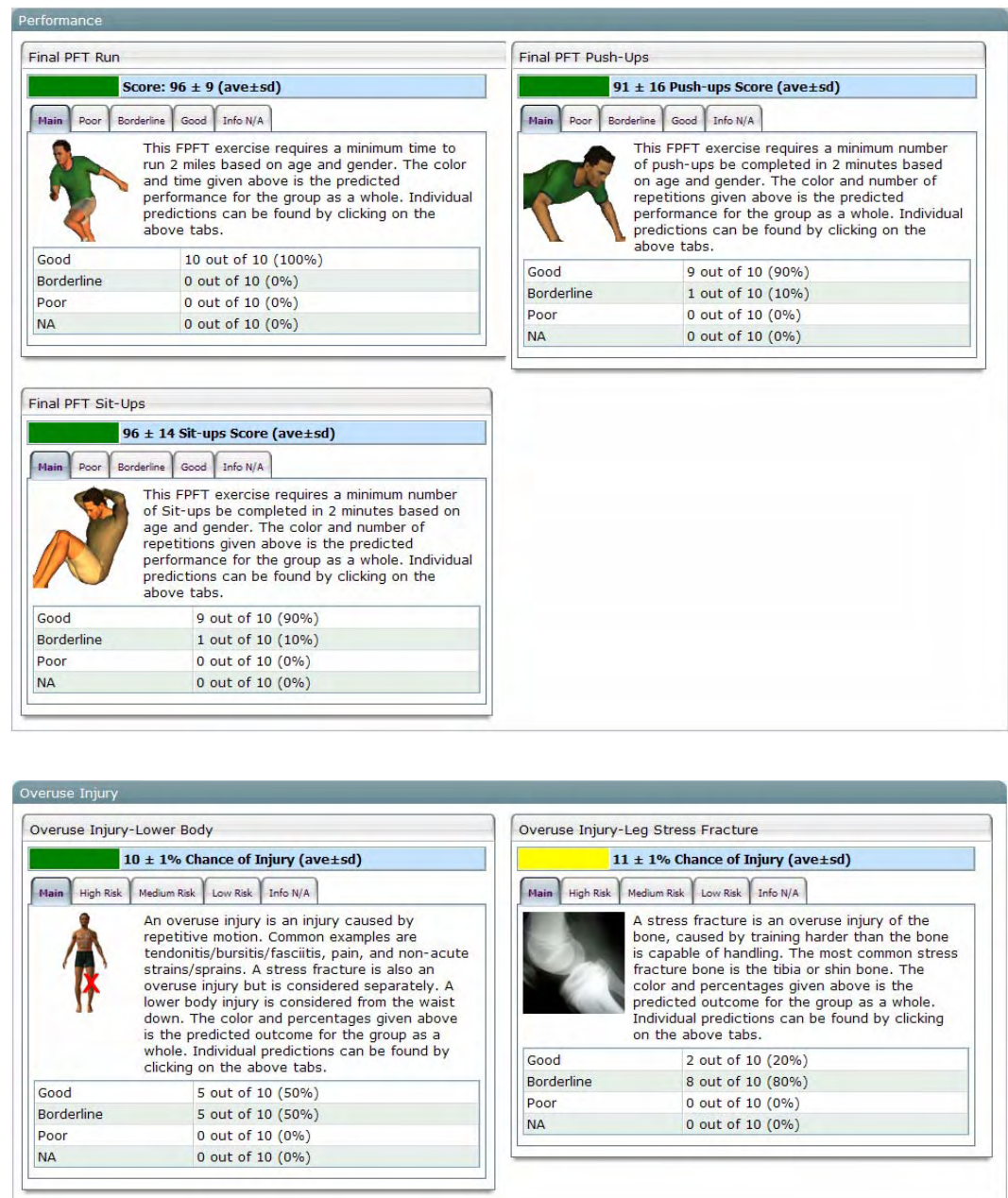


Figure 9. The Mid-Level User results tab contains different sections for each model.



communications

Applied Technologies

Assessment of Health Risk Behavior Measures from the U.S. Army Recruit Assessment Program (RAP) Dataset for Inclusion in the TOP Model Framework

SUPPLEMENTAL REPORT J3181-07-340

to

Overuse Injury Assessment Model

Part II: Training, Overuse Injury, and Performance Modeling

Report No. J3181-07-336

Prepared by:

Bryant L. Sih, Ph.D.

L-3 Communications/Jaycor

3394 Carmel Mountain Road

San Diego, California 92121-1002

Stephen C. Allison, PT, Ph.D.

Bruce Cohen, Ph.D.

**U.S. Army Medical Research and
Material Command**

Kansas Street, Building 42

Natick, Massachusetts 01760

Prepared for:

Commander

U.S. Army Medical Research and Materiel Command

504 Scott Street

Fort Detrick, Maryland 21702-5012

under Contract No. DAMD17-02-C-0073

August 2007

9Executive Summary

Data from trainees in basic combat training shared by investigators at the U.S. Army Center for Health Promotion and Preventive Medicine were analyzed to determine whether health risk behavior variables might improve the predictive accuracy of the Training, Overuse Injury, and Performance (TOP) models. Composite and single items from the U.S. Army Recruit Assessment Program (RAP) questionnaire were assessed. Test item cluster (TIC) analysis was performed with and without RAP variables so that prognostic accuracy from a traditional statistical method could be compared for prediction of injuries and physical performance deficits among trainees. Injuries considered include stress fracture, lower-body nonstress fracture overuse injury, and general nonacute training injuries. Physical performance was determined by the Army Physical Fitness Test (APFT).

Overall prognostic accuracy was not markedly improved when select RAP variables were included in the predictive models. Accuracy was >90% for predicting failure of APFT elements and for predicting stress fractures in females. Accuracy was about 85% for males and about 65% for females when predicting lower body overuse injuries (excluding stress fractures). Accuracy was about 55% for predicting general nonacute injuries in females. For all outcomes listed above, accuracy with models including RAP variables was not better than with models excluding RAP variable predictors. However, for predicting general nonacute injuries in males, prognostic accuracy was 76% without RAP variables and increased to 81% when the composite health risk factor of cigarette use was added to the model.

It appears from these analyses that health risk behavior variables may not meaningfully increase prognostic accuracy in the TOP models. However, a smoking predictor has the potential to improve predictive accuracy in the nonstress fracture overuse injury TOP model. Inclusion of smoking in the TOP model is therefore warranted. These analyses had a very limited purpose; findings should not be generalized beyond this purpose. The potential value of health risk behavior variables in predicting injury or other undesirable outcomes remains to be fully explored.

9Contents

	<u>Page</u>
1. INTRODUCTION	1
2. METHODS	2
3. RESULTS	7
3.1 FINAL APFT SIT-UPS	11
3.2 FINAL APFT RUN	13
3.3 STRESS FRACTURES	15
3.4 LOWER-BODY OVERUSE INJURIES (NONSTRESS FRACTURES)	17
3.5 GENERAL NONACUTE INJURIES	20
4. DISCUSSION	22
5. LITERATURE	23

9 Tables

	<u>Page</u>
1. Health Risk Behavior factor categories, the RAP questions used, and the scoring system. (From Chervak 2006).	3
2. Select RAP survey items analyzed for significance in predicting performance and injury during BCT.	4
3. ICD-9 Codes used to classify types of injuries sustained in BCT.	6
4. The logistic regression screening results for Health Risk Behavior factors and select RAP variables that are predictive of failing the final APFT Push-up event.	7
5. The TIC analysis results for predicting failing the final APFT Push-up event for males.	8
6. The TIC analysis results for predicting failing the final APFT Push-up event for females.	9
7. Cutoff values determined to maximize accuracy for the APFT Push-up event TIC analysis.	10
8. The logistic regression screening results for Health Risk Behavior factors and select RAP variables that are predictive of failing the final APFT Sit-up event.	11
9. The TIC analysis results for predicting failing the final APFT Sit-up event for females.	12
10. Cutoff values determined to maximize accuracy for the APFT Sit-up event TIC analysis.	12
11. The logistic regression screening results for Health Risk Behavior factors and select RAP variables that are predictive of failing the final APFT 2-mile run event.	13
12. The TIC analysis results for predicting failing the final APFT 2-mile run event for males.	14
13. Cutoff values determined to maximize accuracy for the APFT 2-mile run exercise TIC analysis.	14
14. The logistic regression screening results for Health Risk Behavior factors and select RAP variables that are predictive of sustaining a stress fracture during BCT.	15
15. The TIC analysis results for predicting a stress fracture during BCT for females.	15
16. Cutoff values determined to maximize accuracy for the stress fracture TIC analysis.	16
17. The logistic regression screening results for Health Risk Behavior factors and select RAP variables that are predictive of sustaining a lower-body nonstress fracture overuse injury during BCT.	17
18. The TIC analysis results for predicting a lower-body nonstress fracture overuse injury during BCT for males.	18
19. The TIC analysis results for predicting a lower-body nonstress fracture overuse injury during BCT for females.	18
20. Cutoff values determined to maximize accuracy for the lower-body nonstress fracture overuse injury TIC analysis.	19
21. The logistic regression screening results for Health Risk Behavior factors and select RAP variables that are predictive of sustaining a nonacute injury during BCT.	20

9 22.	The TIC analysis results for predicting a general nonacute injury during BCT for males.	20
23.	The TIC analysis results for predicting a general nonacute injury during BCT for females.	21
24.	Cutoff values determined to maximize accuracy for the general nonacute injury TIC analysis.	21

1. Introduction

The U.S. Army Recruit Assessment Program (RAP) Pilot Study at Fort Jackson, South Carolina obtained health risk behavior data via a questionnaire completed by men and women entering basic combat training (BCT) between October 2002 and May 2004. Data collected included demographic information, work history, medical history, and measures of psychosocial attributes and health behaviors. Although over 35,000 trainees completed the RAP, we obtained linked RAP data, APFT data, and injury data only for 3 battalions. In those battalions, 1,156 males and 746 females completed at least part of the 215 question survey. Data in these battalions were collected between 21 Mar and 28 Aug 2003. Linkage among BCT injury data, Army Physical Fitness Test (APFT) data, and RAP data was accomplished by investigators at the U.S. Army Center for Health Promotion and Preventive Medicine (USACHPPM) for subsequent analysis.

Previous use of the linked RAP dataset included an investigation of the association between health risk behavior and injury during BCT (Chervak 2006). Chervak used multivariate factor analysis and survival analysis to derive five individual health risk behavior indices (cigarette use, smokeless tobacco use, alcohol use, weight control practices, and diet/lifestyle choices) associated with injury. It was found that for males, those with a high or low combined index score had a greater chance of sustaining a BCT-related injury. Those with a high cigarette use score also were more likely to be injured. For females, cigarette and diet/lifestyle risks were associated with injury. The results suggest that behavioral risk factors contribute to the chances of injury during BCT.

While the previous study linked behavioral risk factors to injury, the definition of injury and analysis method were different than that used in the development of the TOP models. Also, the association between the APFT and behavior was not explored in the previous analysis. Thus, the purpose of this analysis was to determine if the five health risk behavior factors or other individual questionnaire items showed sufficient predictive power to warrant inclusion in the TOP model framework.

2. Methods

To determine the usefulness of the RAP questionnaire, we subjected the dataset to the same analysis as that which was used to develop the TOP models. A logistic regression was used as an initial screening tool to eliminate those measures that have no observed predictive value and reduce the chances of a Type I error (determining an association when none exists). Screening logistic regression models were developed using RAP variables alone without including other demographic or baseline performance variables. Two different sets of input/independent variables were used for the logistic regression models—the *Health Risk Behavior* indices derived by Chervak (2006) using multivariate factor analysis methods (Table 1) and a select group of individual items from the RAP questionnaire that previous experience suggests would most directly be associated with performance and injury outcomes in BCT (Table 2).

To assess goodness-of-fit for the initial logistic regression screening, the Observed Response test was used. The test involves comparing the model's predicted outcome versus the actual response. Each subject's outcome and the model's prediction are paired with another subject and the predictions are compared. A *concordant pair* is when both subjects are predicted correctly, a *discordant pair* occurs when both are predicted incorrectly, and a *tie* is when only one is correct. A model with a high percentage of concordant pairs and few discordant pairs is considered accurate and we assumed that if the number of concordant pairs was greater than discordant pairs, then the variables showed predictive value and were worth further consideration.

Table 1. Health Risk Behavior indices, the RAP questions used, and the scoring system.
(From Chervak 2006).

Index	Question/item	Specific item responses associated each risk category		
		Score=0	Score=1	Score=2
Cigarette use¹	Age at first use	Never smoked regularly	≥ 21 years old	<21 years old
	Years smoked	Never smoked regularly	1 year or less	2 or more years
	Packs smoked	Never smoked regularly	1/2 pack or less/day	1 pack or more/day
Smokeless tobacco use²	Number of cans/packs used	Never used regularly	1/2 can or less/day	1 can or more/day
	Years used	Never used regularly	1 year or less	2 or more years
Alcohol use³	Age at first drink	Have never had a drink	21 yrs or older	9-20 yrs old
	Years been drinking	Have never had a drink	Just tried a few times, 1 year or less	2 or more years
	Drinking and driving	Never	--	Yes
	CAGE score	0	--	1-4
	AUDIT-C score	0-4	--	5-12
Diet/lifestyle choices³	Hours of TV viewing	None	1 to 3 hrs/day	4+ hrs/day
	Caffeinated beverages	None - 3	4 to 5	6+/day
	Fast food consumption	None-2 to 3 times/wk	4-7 times/week	8+ times/wk
	Breakfast	5-7 mornings	1-4 mornings	Never
	Seat belt use	Always	Usually, Sometimes	Never
Weight control practices¹	Diet pill use	No	(none)	Yes
	Laxative use	No	(none)	Yes
	Vomiting	No	(none)	Yes

¹ Multiplied by a factor of 10 to standardize to a 60-point scale

² Multiplied by a factor of 15 to standardize to a 60-point scale

³ Multiplied by a factor of 6 to standardize to a 60-point scale

Table 2. Selected RAP survey items analyzed for significance in predicting performance and injury during BCT.

Gen4	Highest education
Gen5	Marital status
Smkever	Smoked more than 100 cigarettes in entire life
Smkpacks	Number of packs smoked daily when you smoked regularly
Alclstyr	How often did you consume alcohol during the year before entering the military
Alcabuse	During the past year, how often did you consume 6 or more alcohol drinks in one sitting
Eas24	Hours you sleep on most nights
Eas28	Number of times each week you eat breakfast
Seatbelt	Do you wear a seatbelt when driving/riding in a car?
Gen56	Has your physical health/emotional problems interfered with your social activities in the last year
Gen63	Problems keeping your attention on any activity for long
Gen68b	Did your physical health limit you in any kind of work or other daily activities
Gen69a	Did your emotional health cause you to accomplish less than you would have liked

Logistic regression modeling was followed by Test Item Cluster (TIC) analyses to determine the most predictive and parsimonious sets of predictive variables with associated cut-off scores. Cut-off scores were chosen using receiver-operator curve analysis, which attempts to minimize the proportion of false positives by selecting a cut score with high specificity and high positive likelihood ratio. Additional details of this method can be found in Allison et al. (2006). Note that if the initial logistic regression found no significant measures, a TIC analysis was not performed. For the TIC analysis, those RAP variables that were found significant through the logistic regression screening process were added to those previously considered for the TIC from other datasets (height, weight, BMI, age, initial APFT results, self-reported activity level, and self-reported fitness level; see Table 3) to determine if the RAP variables were of greater significance compared to other readily available measures.

Table 3. Additional data items considered for inclusion that were used in previous TIC analyses in predicting performance and injury during BCT.

Height	Stature (m)
Weight	Total body weight (kg)
BMI	Body mass index (kg/m ²)
Age	Age (years)
IST Push-up Total	Number of push-ups performed during the initial AFPT
IST Sit-up Total	Number of sit-ups performed during the initial APFT
IST Run Total	Run time (sec) performed during the initial APFT
PreAerobicDays	Number of days/week participated in a sport/activity with sweating for 20 minutes or more
PreActLevel	Self-rated fitness/health level

For this analysis, performance was defined as passing the final APFT for push-ups, sit-ups, and the 2-mile run. Three definitions of injury were used: stress fracture, lower-body nonstress fracture overuse injury, and general nonacute training injury. See Table 4 for ICD-9 codes used to categorize the injuries. Males and females were analyzed separately.

In addition, a separate TIC analysis was performed without the RAP measures to assess the effectiveness of the RAP measures by showing the amount of improvement in the TIC accuracy from these measures.

Table 4. ICD-9 Codes used to classify types of injuries sustained in BCT.

717	719.05	722.2	727.2	734	846.3
717.1	719.06	722.71	727.3	840	846.8
717.2	719.07	723.1	<i>727.62</i>	841	846.9
717.3	719.08	723.4	<i>727.65</i>	842	847
717.4	719.09	724.2	<i>727.66</i>	843	847.1
717.5	719.4	724.3	<i>727.67</i>	843.1	847.2
717.6	719.41	724.4	<i>727.68</i>	843.8	847.3
717.7	719.42	724.5	728.71	843.9	847.4
717.8	719.43	724.9	729.1	844	847.9
717.9	719.44	726.1	729.2	844.1	848
719	719.45	726.2	733.1	844.2	848.5
719.01	719.46	726.3	733.14	844.3	848.8
719.02	719.47	726.4	733.15	844.8	848.9
719.03	719.48	726.5	733.16	844.9	953.1
719.05	719.49	726.6	733.19	845	953.2
719.06	720.2	726.7	<i>733.93</i>	846	953.3
719.07	722	726.8	<i>733.94</i>	846.1	
719.03	722.1	726.9	<i>733.95</i>	846.2	

All numbers in the table were used to specify general nonacute BCT injury. *Italicized* numbers correspond to stress fractures and **bold** numbers are nonstress fracture overuse injuries.

3. Results

The following tables describe the results of the analysis, including the logistic regression screen processes, the TIC analysis, and the cutoff values for the TIC-identified variables that maximize the predictive accuracy of the TIC model for the injury and performance outcomes. Note that the number of subjects (N) differed for each analysis because of incomplete questionnaires (subjects with missing data for a given analysis were discarded), which results in small changes in prevalence.

For the TIC result tables, Sens = sensitivity, Spec = specificity, PLR = positive likelihood ratio, NLR = negative likelihood ratio, Prev = prevalence, PpostTP = positive test post-test probability, NpostTP = negative test post-test probability, Table2x2 = contingency table, Prog_accuracy = prognostic accuracy.

3.1 Final APFT Push-ups

Table 5. The logistic regression screening results for Health Risk Behavior factors and select RAP variables that are predictive of failing the final APFT Push-up event.

		Ntotal	Npos	Nneg	Significant Factors*	Prev	Concord	Tie	Discord
Health Risk Behavior Factors	M	889	62	827	WeightCntrl, Cigarettes, Alcohol	7%	86%	13%	0.50%
	F	519	31	488	LifeStyle	6%	88%	11%	0.40%
Select RAP Variables	M	723	49	674	gen4, eas24, gen5	7%	87%	13%	0.40%
	F	431	26	405	None	6%			

*See Table 1 and Table 2 for definitions.

Table 6. The TIC analysis results for predicting failing the final APFT Push-up event for males.

	Males		
Name	Health Risk Behavior Factors	Select RAP Variables	
Sig. Factors*	Push-up Total IST, Sit-up Total IST, Age, Run Total IST, WeightCntrl	Push-up Total IST, Sit-up Total IST, Age, Run Total IST, PreAerobicDays, Height (No RAP variables found predictive)	
Num of Factors	Any 2 or more	Any 2 or more	Any 3 or more
Sens	0.194	0.468	0.065
Spec	0.967	0.769	0.987
PLR	5.82	2.02	4.90
NLR	0.83	0.69	0.95
Prev	0.07	0.07	0.07
PpostTP	0.3	0.13	0.27
NpostTP	0.06	0.05	0.07
Table2x2	13 30 54 870	29 193 33 642	4 11 58 824
Prog_accuracy	0.9131	0.7480	0.9231

*See Table 1 and Table 3 for definitions.

Table 7. The TIC analysis results for predicting failing the final APFT Push-up event for females.

	Females	
Name	Health Risk Behavior Factors	
Sig. Factors*	Height, Push-up Total IST, Sit-up Total IST (No Health Risk Behavior Factors found predictive)	
Num of Factors	Any 2 or more	Any 3 or more
Sens	0.179	0.063
Spec	0.985	0.999
PLR	12.05	67.25
NLR	0.83	0.94
Prev	0.07	0.07
PpostTP	0.47	0.83
NpostTP	0.06	0.07
Table2x2	7 8 32 529	2 0 37 537
Prog_accuracy	0.9306	0.9358

*See Table 3 for definitions.

Table 8. Cutoff values determined to maximize accuracy for the APFT Push-up event TIC analysis.

Name*	Cutoff
<u>Males</u>	
Push-up Total IST	< 0.5 reps
Sit-up Total IST	< 9.5 reps
Age	< 18.5 yrs
Run Total IST	> 570 sec
WeightCntrl	> 39.5 points
PreAerobicDays	< 4.5 days/week
Height	> 1.98 m
<u>Females</u>	
Height	> 1.78 m
Push-up Total IST	< 1.5 reps
Sit-up Total IST	< 0.5 reps

*See Table 1 and Table 3 for definitions.

3.2 Final APFT Sit-ups

Table 9. The logistic regression screening results for Health Risk Behavior factors and select RAP variables that are predictive of failing the final APFT Sit-up event.

		Ntotal	Npos	Nneg	Significant Factors*	Prev	Concord	Tie	Discord
Health Risk Behavior Factors	M	889	16	873	None	98%			
	F	519	34	485	None	93%			
Select RAP Variables	M	723	14	709	None	98%			
	F	431	22	409	smkpacks	95%	90%	10%	0.20%

*See Table 2 for definition.

Table 10. The TIC analysis results for predicting failing the final APFT Sit-up event for females.

	Females
Name	Select RAP Variables
Sig. Factors*	Sit-up Total IST, BMI (No RAP variables found predictive)
Num of Factors	Any 1 or more
Sens	0.421
Spec	0.979
PLR	20.52
NLR	0.59
Prev	0.07
PpostTP	0.59
NpostTP	0.04
Table2x2	16 11 22 525
Prog_accuracy	0.9425

*See Table 3 for definitions.

Table 11. Cutoff values determined to maximize accuracy for the APFT Sit-up event TIC analysis.

Name*	Cutoff
<u>Females</u>	
Sit-up Total IST	< 7.5 reps
BMI	> 31 kg/m ²

*See Table 3 for definitions.

3.3 Final APFT Run

Table 12. The logistic regression screening results for Health Risk Behavior factors and select RAP variables that are predictive of failing the final APFT 2-mile run event.

		Ntotal	Npos	Nneg	Significant Factors*	Prev	Concord	Tie	Discord
Health Risk Behavior Factors	M	888	49	839	WeightCntrl	6%	89%	10%	0.30%
	F	517	50	467	None	10%			
Select RAP Variables	M	723	40	683	None	6%			
	F	429	43	386	None	10%			

*See Table 1 for definition.

Table 13. The TIC analysis results for predicting failing the final APFT 2-mile run event for males.

	Males	
Name	Health Risk Behavior Factors	
Sig. Factors*	Weight, Age, PreAerobicDays, Push-up Total IST, Run Total IST (No Health Risk Behavior Factors found predictive)	
Num of Factors	Any 2 or more	Any 3 or more
Sens	0.152	0.043
Spec	0.956	0.998
PLR	3.5	18.48
NLR	0.89	0.96
Prev	0.05	0.05
PpostTP	0.16	0.5
NpostTP	0.05	0.05
Table2x2	7 37 39 813	2 2 44 848
Prog_accuracy	0.9152	0.9487

*See Table 3 for definitions.

Table 14. Cutoff values determined to maximize accuracy for the APFT 2-mile run exercise TIC analysis.

Name*	Cutoff
<u>Males</u>	
Weight	> 113 kg
Age	< 19.5 yrs
PreAerobicDays	< 1.5 days/week
Push-up Total IST	< 9.5 reps
Run Total IST	> 790 sec

*See Table 3 for definitions.

3.4 Stress Fractures

Table 15. The logistic regression screening results for Health Risk Behavior factors and select RAP variables that are predictive of sustaining a stress fracture during BCT.

		Ntotal	Npos	Nneg	Significant Factors*	Prev	Concord	Tie	Discord
Health Risk Behavior Factors	M	979	12	967	None	1%			
	F	637	38	599	None	6%			
Select RAP Variables	M	794	7	787	None	1%			
	F	531	34	497	gen5,gen4	6%	88%	12%	0.40%

*See Table 2 for definitions.

Table 16. The TIC analysis results for predicting a stress fracture during BCT for females.

	Females			
Name	Select RAP Variables		Omitted Select RAP Variables	
Sig. Factors*	Push-up Total IST, Run Total IST, gen5		Push-up Total IST, Run Total IST	
Num of Factors	Any 2 or more		Any 1 or more	Any 2 or more
Sens	0.075		0.625	0.025
Spec	0.989		0.698	0.998
PLR	7.14		2.07	16.65
NLR	0.93		0.54	0.98
Prev	0.06		0.06	0.06
PpostTP	0.3		0.11	0.50
NpostTP	0.05		0.03	0.06
Table2x2	3 37	7 659	25 15 201 465	1 39 1 665
Prog_accuracy	0.9377		0.6941	0.9433

*See Table 2 and Table 3 for definitions.

Table 17. Cutoff values determined to maximize accuracy for the stress fracture TIC analysis.

Name*	Cutoff
<u>Females</u>	
Push-up Total IST	< 3.5 reps
Run Total IST	> 1500 sec
Gen5	5 (Divorced)

*See Table 2 and Table 3 for definitions.

3.5 Lower-body Overuse Injuries (Nonstress fractures)

Table 18. The logistic regression screening results for Health Risk Behavior factors and select RAP variables that are predictive of sustaining a lower-body nonstress fracture overuse injury during BCT.

		Ntotal	Npos	Nneg	Significant Factors*	Prev	Concord	Tie	Discord
Health Risk Behavior Factors	M	979	136	843	Cigarettes	14%	74%	24%	2.00%
	F	637	226	411	None	35%			
Select RAP Variables	M	794	109	685	gen5, alcabuse, eas28	14%	74%	24%	2.00%
	F	531	191	340	smkpacks	36%	41%	46%	13.00%

*See Table 1 and Table 2 for definitions.

Table 19. The TIC analysis results for predicting a lower-body nonstress fracture overuse injury during BCT for males.

	Males		
Name	Health Risk Behavior Factors	Select RAP Variables	Omitted Health Risk Behavior Factors
Sig. Factors*	Age, Push-ups Total IST, Cigarettes	Alcabuse, gen5, RunTotIST	Age, Push-ups Total IST
Num of Factors	Any 1 or more	Any 1 or more	Any 1 or more
Sens	0.51	0.125	0.047
Spec	0.631	0.962	0.964
PLR	1.39	3.3	1.29
NLR	0.77	0.91	0.99
Prev	0.14	0.14	0.13
PpostTP	0.18	0.34	0.17
NpostTP	0.11	0.12	0.13
Table2x2	76 343 72 587	17 33 119 837	7 35 143 936
Prog_accuracy	0.6150	0.8489	0.8412

*See Table 1, Table 2, and Table 3 for definitions.

Table 20. The TIC analysis results for predicting a lower-body nonstress fracture overuse injury during BCT for females.

	Females	
Name	Select RAP Variables	Omitted Select RAP Variables
Sig. Factors*	Run Total IST, smkpacks	RunTotal IST
Num of Factors	Any 1 or more	Any 1 or more
Sens	0.09	0.009
Spec	0.961	0.999
PLR	2.3	8.66
NLR	0.95	0.99
Prev	0.36	0.37
PpostTP	0.56	0.83
NpostTP	0.35	0.36
Table2x2	22 17 222 416	2 0 261 456
Prog_accuracy	0.6470	0.6370

*See Table 2 and Table 3 for definitions.

Table 21. Cutoff values determined to maximize accuracy for the lower-body nonstress fracture overuse injury TIC analysis.

Name*	Cutoff
<u>Males</u>	
Age	> 36.5 yrs
Push-up Total IST	< 7.5 reps
Cigarettes	> 39.5 points
Alcabuse	6 (Daily)
Gen5	4 (Married but separated)
Run Total IST	> 685 sec
<u>Females</u>	
Run Total IST	> 1135 sec
Smkpacks	> 1 pack/day

*See Table 1, Table 2, and Table 3 for definitions.

3.6 General Nonacute Injuries

Table 22. The logistic regression screening results for Health Risk Behavior factors and select RAP variables that are predictive of sustaining a nonacute injury during BCT.

		Ntotal	Npos	Nneg	Significant Factors*	Prev	Concord	Tie	Discord
Health Risk Behavior Factors	M	979	186	793	Cigarettes	19%	66%	31%	4.00%
	F	637	286	351	Cigarettes	45%	32%	49%	19.00%
Select RAP Variables	M	794	172	622	gen5, alcabuse	22%	61%	34%	5.00%
	F	531	251	280	smkpacks, gen5, gen4	47%	34%	49%	18.00%

*See Table 1 and Table 2 for definitions.

Table 23. The TIC analysis results for predicting a general nonacute injury during BCT for males.

	Males					
Name	Health Risk Behavior Factors		Select RAP Variables		Omitted RAP Factors or Variables	
Sig. Factors*	Age, Run Total IST, Cigarettes		Run Total IST, alcabuse, Age		Age, Run Total IST	
Num of Factors	Any 2 or more		Any 1 or more		Any 1 or more	
Sens	0.07		0.214		0.17	
Spec	0.982		0.897		0.911	
PLR	3.80		2.07		1.92	
NLR	0.95		0.88		0.91	
Prev	0.19		0.21		0.21	
PpostTP	0.47		0.36		0.34	
NpostTP	0.18		0.19		0.20	
Table2x2	14 187	16 856	46 169	83 720	40 195	78 803
Prog_accuracy	0.8108		0.7525		0.7554	

*See Table 1, Table 2, and Table 3 for definitions.

Table 24. The TIC analysis results for predicting a general nonacute injury during BCT for females.

	Females			
Name	Health Risk Behavior Factors	Select RAP Variables	Omitted RAP Factors or Variables	
Sig. Factors*	Sit-up Total IST, Run Total IST, Cigarettes	Run Total IST, smkpacks	Sit-up Total IST, Run Total IST	
Num of Factors	Any 2 or more	Any 1 or more	Any 1 or more	Any 2 or more
Sens	0.094	0.014	0.238	0.004
Spec	0.944	0.999	0.853	0.999
PLR	1.69	9.86	1.62	3.25
NLR	0.96	0.99	0.89	1.00
Prev	0.45	0.48	0.48	0.48
PpostTP	0.58	0.90	0.60	0.75
NpostTP	0.44	0.47	0.45	0.48
Table2x2	29 21 279 355	4 0 319 354	85 55 263 319	1 0 344 374
Prog_accuracy	0.5614	0.5288	0.5577	0.5216

*See Table 1, Table 2, and Table 3 for definitions.

Table 25. Cutoff values determined to maximize accuracy for the general nonacute injury TIC analysis.

Name*	Cutoff
<u>Males</u>	
Age	> 27.5 yrs
Run Total IST	> 685 sec
Cigarettes	> 59.5 points
Alcabuse	6 (Daily)
<u>Females</u>	
Sit-up Total IST	< 17.5 reps
Run Total IST	> 1500 sec
Cigarettes	> 49.5 points
Smkpacks	2 packs or more

*See Table 1, Table 2, and Table 3 for definitions.

4. Discussion

The TIC analysis revealed that for performance measures (APFT Push-up, Sit-up, and 2-mile run), the inclusion of either the Health Risk Behavior factors or the selected RAP variables did not substantially increase prognostic accuracy. Thus, it is unlikely that these factors will be of use in the TOP performance models.

There is little evidence from these analyses that health risk behavior measures will meaningfully improve prognostic accuracy beyond that of existing models predicting injury or poor physical performance except for predicting general nonacute injuries for males. In this case (Table 23), there is a change in prognostic accuracy from 76% to 81% with the inclusion of the Cigarette Health Behavior Risk factor. There are several potential explanations for this finding. For males, the high use of cigarettes may be reflective of a more aggressive subject who is willing to take more risks with their health than the average recruit. Heavy smokers are also more prone to physiological ailments, including reduced bone strength, lung capacity, etc. Because cigarette use and other smoking measures were not significant predictors for the more specific injury categories (stress fractures and lower-body nonstress fracture overuse injury), this suggests that smoking may be a more important factor for injuries to the upper-body and back regions, areas where aggressive recruits might be more apt to overtrain and injure themselves. While additional analyses could support this theory, none of the current TOP models address these types of injuries. In addition, it should be noted that the association may be a Type I error; subsequent datasets may not support the use of the factor. Results from these preliminary TIC derivations have not been validated in any independent data set.

These analyses had a very limited purpose; findings should not be generalized beyond this purpose. The potential value of health risk behavior variables in predicting injury or other undesirable outcomes remains to be fully explored.

Despite the inconclusive findings, smoking was identified in the initial screening process for all nonstress fracture related injuries. This suggests that a smoking factor has the potential to improve predictive accuracy in the nonstress fracture overuse injury TOP model. Thus, while the increase in accuracy may not be great, we conclude that the inclusion of smoking in the TOP model is warranted. We will continue to look at other datasets for additional guidance.

5. Literature

- Allison, S. C., Knapik, J., & Sharp, M. A. (2006). "Preliminary Derivation of Test Item Clusters for Predicting Injuries, Poor Physical Performance, and Overall Attrition in Basic Combat Training." US Army Medical Research and Materiel Command, Fort Detrick, Frederick, MD. T07-06.
- Chervak, M. C. (2006). "The Association of Health Risk Behaviors and Occupational Injury among U.S. Army Basic Trainees." Johns Hopkins University, Baltimore, Maryland.